Proton and Metal Ion Binding to Humic Substances

Han de Wit

J.C.M . de Wit

Proton and Metal Ion Binding to Humic Substances

Proefschrift

ter verkrijging van de graad van doctor

in de landbouw- en milieuwetenschappen

op gezag van de rector magnificus

dr. H.C. van der Plas

in het openbaar te verdedigen

op woensdag 23 december 1992

des namiddags te vier uur in de Aula

van de Landbouwuniversiteit te Wageningen.

Stellingen

Toen zond de Here God hem weg uit de hof van Eden
om de aardbodem te bewerken, waaruit hij genomen was.
(Genesis 3 vers 23).

1. Uit Genesis 3 vers 23 kan geconcludeerd worden dat humus de bron is van het menselijk leven.

2. Het extraheren en zuiveren van humeuze verbindingen uit de bodem leidt tot veel kleinere moleculen dan die in het natuurlijk milieu voorkomen.

3. Gezuiverde humeuze verbindingen zijn oligo-electrolieten.
   Bartschat et al, Environ. Sci. Technol. 1992 26:284-294, dit proefschrift

4. Deze oligo-electrolieten kunnen beschouwd worden als de bouwstenen van de humeuze verbindingen die in het natuurlijk milieu voorkomen.

5. Hoewel gezuiverde humeuze verbindingen polydisperse mengsels zijn van verschillende moleculen kan het effect van de variabele lading op ionbinding goed beschreven worden met een model waarin ze beschouwd worden als rigide bollen of cylinders die gekarakteriseerd worden door één bepaalde gemiddelde straal.
   Dit proefschrift.

6. De protonaffiniteitsverdelingen van verschillende humeuze verbindingen zijn sterk vergelijkbaar.
   Dit proefschrift.

7. De binding van protonen en metaalionen wordt in belangrijke mate door het variabele ladingskarakter van de humus- en fulvozuren bepaald.
   Dit proefschrift.

8. Onder een aantal goed gedefinieerde omstandigheden kunnen multi-component vergelijkingen versimpelen tot lineaire en Freundlich vergelijkingen. De constanten van deze vergelijkingen zijn gecompliceerde parameters.
   Dit proefschrift.

9. De binding van "trace metals" aan arme zandige bodems kan meestal beschreven kan worden met een pH afhankelijke Freundlich vergelijking.

10. In zure en/of calcium rijke bodems valt de competitie tussen verschillende "trace metals" voor de beschikbare bindingsplaatsen te verwaarlozen.

11. Een extra uitspoeling van "trace metals" als gevolg van adsorptie aan de opgeloste bodem organische stof valt meestal te verwaarlozen.

12. Wetenschappers vinden hun eigen onderzoek science, dat van anderen fiction.

13. 90 % van de wetenschappelijke artikelen zijn overbodig en dragen niet bij aan de voortgang van de wetenschap.

14. Iemand die voor 90 % gelijk heeft wordt eerder geloofd dan iemand die 100 % gelijk heeft.

15. Leden van de promotiecommissie die veel vragen stellen over de stellingen hebben het proefschrift meestal slecht gelezen.

16. Beter dan docenten zijn studenten in staat de kwaliteit van het onderwijs te beoordelen.

17. Het, als jonge onderzoeker, verkrijgen van een vaste positie aan een universiteit, is even moeilijk als het ontslaan van een niet functionerende universitair docent of hoogleraar.

18. De grote aandacht voor vrouwelijke wetenschappers tijdens congressen wekt de indruk dat vrouwen eminente wetenschappers zijn.

19. Het wordt nooit meer zoals het vroeger ook niet was.
   (vrij naar Lany Slobbe)

20. Wie het gemak niet zoekt is lui.
   (Jan Oudkerk)

21. De kunst van wetenschap is het weglaten.

Abstract

Wit, J.C.M. de, **Proton and Metal Ion Binding to Humic Substances.**
Doctoral thesis, Wageningen Agricultural University, The Netherlands. 255
pages.

Humic substances are polydisperse mixtures of organic molecules
which at least to some extent determine the mobility and bioavailability of
heavy metals in soils, sediments and aquatic systems. In order to make a
sound risk assessment of the fate of trace metals a good conception and
preferably a sound description is essential. In this thesis mechanistic
models are presented that explicitely take into account the dominant
factors that determine metal ion binding. These factors are the chemical
heterogeneity of the humic substances, the variable charge character, and
competitive binding of ions.

The description of the proton binding behaviour, in absence of metal
ions, forms the basis of the metal ion binding model. The proton binding
is described with analytical expressions for continuous heterogeneous
ligands in combination with a double layer model to account for the
electrostatic effects. The parameters for the proton description are obtained
from the analysis of proton titration with the so called mastercurve
procedure.

In order to describe metal ion binding an approximate binding
stoichiometry is assumed, in which upon the binding of one metal ion, x
protons are released in solution. With respect to site competition two
different limiting cases have been considered. In the fully coupled case it
is assumed that the different ions bind to the same sites and that the shape
of the affinity distribution is the same for all ions. In the uncoupled case
each ion has its own binding sites and the affinity distribution may differ
for different ions. Both models are capable of describing competitive ion
binding. The uncoupled model has the advantage of a lower number of
parameters that have to be specified.

Additional index words: humic acids, fulvic acids, metal ion adsorption,
chemical heterogeneity, affinity distribution, speciation

voor mijn oma:

Gerarda Prinsenberg - de Frankrijker

(zij had er graag bijgeweest)

Voorwoord

Hoewel mijn naam als enige op de kaft staat is dit proefschrift het resultaat van een goede samenwerking. Eenieder die aan de totstandkoming van dit proefschrift heeft bijgedragen wil ik bij deze bedanken.

Als eerste wil ik mijn promotoren Willem van Riemsdijk en Luuk Koopal bedanken. Het is prettig begeleiders te hebben die elkaar volledig aanvullen en de tijd nemen voor uitputtende discussies. Willem en Luuk, vaak leverde ik 's middag tegen vijven een nogal lijvig concept in. Ondanks drukke werkzaamheden en wat gesteun en gekreun, hadden jullie het de volgende dag reeds bekeken. Hoewel ik me realiseer dat dit ten koste ging van andere zaken (o.a. sectie, burostoelen voor de aio's van fysko, vrije tijd, familie) heb ik het zeer op prijs gesteld.

Gelukkig hoefde ik door de aanwezigheid van lot- en kamergenoot Maarten Nederlof de wetenschappelijke honger van de begeleiders niet in mijn eentje te stillen. Maarten, ik heb met veel plezier de afgelopen jaren een kamer met je gedeeld. Het was prettig om onder het genot van vele koppen koffie de voortgang van ons onderzoek te bespreken.

Dit onderzoek maakte deel uit van een door de EEG gefinancierd onderzoeksproject waarin werd samengewerkt met David Kinniburgh en Chris Milne van de British Geological Survey in Wallingford. David and Chris, I thank you for the comprehensive and high quality dataset you have collected, for the warm welcome in England and for the good cooperation over the last 5 years.

Naast Jaap Dijt, Marion Bloem, Yde Hamstra, Stefan Gruijters, Mari Marinussen, Christel Verhulst, Karin Ordelman, Wendela Schlebaum en David van den Burg die in het kader van een afstudeervak aan dit onderzoek hebben meegewerkt, bedank ik de medewerkers van de vakgroep Bodemkunde en Plantevoeding, en met name de bende van Frans (de sectie bodemhygiëne), het secretariaat en Kees Koenders, voor een prettige sfeer op de vakgroep (en daarbuiten).

Mijn ouders hebben me gestimuleerd en in staat gesteld om een universitaire opleiding te volgen. Bedankt voor de ondersteuning die jullie me hebben gegeven. Daarnaast dank ik jullie, Edward Scholten en Wim van der Ploeg voor de hulp bij het ontwerpen van de voorkant. Martine (Stimu-)Lans, bedankt voor het zorgen dat ik me naast mijn werk ook met andere zaken heb bezig gehouden.

Han de Wit

Contents

Chapter 1

Introduction

Introduction

For plant nutrition the role of the organic matter in the cycle of major elements like C, N, S and P is of great importance and as a consequence, the relation between the organic matter content and soil fertility has been an important research topic from the early ages of soil and agronomic sciences on (eg. 1-16). The acid buffering capacity and the cation exchange capacity are other important functions of the soil organic matter (eg. 10-17). Binding of micro-nutrients, trace metals, pesticides and other toxic compounds to organic matter, together with binding to clay minerals and hydrous oxides, highly controls the chemo-stat of soil systems and the bio-availability and mobility of these compounds (13-18).

In many areas in the world deficiencies of micro nutrients limit plant growth which results in low crop yields (14,19). In the industrial world the use of fertilizers has solved the problems of a deficiency. Unfortunately in this *civilized* world the problems of deficiency are often replaced by problems of overabundance of micro nutrients and by soil pollution due to excessive use of fertilizers and pesticides, industrial activities and dumping of waste materials (20-30). To analyze the fate of micro-nutrients and the risks of hazardous and toxic compounds their binding properties to the solid phase and to colloidal particles in the soil solution should be well understood (31-32). The aim of this thesis is to contribute to this understanding, with specific reference to the role of the soil organic matter.

In this study the binding of protons and metal ions to humic substances is investigated. Humic substances are mixtures of complex organic substances which are dissimilar to the biopolymers of microorganisms and higher plants. Despite a major research effort (eg. 12-13, 15-18, 32-41) the properties of humic substances and their ion binding behaviour are not yet well resolved. In this first chapter the geochemistry of humic substances, their properties and the state of the art of the description metal ion binding to humic substances are addressed.

In the next chapters models are developed for competitive ion binding over a large range of conditions such as pH, ionic strength and composition of the solution.

Table 1. Definitions after Stevenson (16).

Term	Definition
Organic Residues	Undecayed plant and animal tissues and their partial decomposition products.
Soil Biomass	Organic matter present as live microbial tissue.
Humus	Total of the organic compounds in soil exclusive of undecayed plant and animal tissues, their "partial decomposition" products, and the soil biomass.
Soil Organic Matter	Same as humus.
Humic Substances	A series of relatively high-molecular-weight, brown to black coloured substances formed by secondary synthesis reactions. The term is used as a generic name to describe the cellaret material or its fractions obtained on the basis of solubility characteristics. These materials are distinctive to the soil (or sediment) environment in that they are dissimilar to the biopolymers of microorganisms and higher plants (including lignin).
Nonhumic Substances	Compounds belonging to known classes of biochemistry such as amino acids, carbohydrates, fats, waxes, resins, organic acids, etc. Humus probably contains most, if not all, of the biochemical compounds synthesized by living organisms.
Humin	The alkali insoluble fraction of soil organic matter or humus.
Humic Acid	The dark-cellaret organic material which can be extracted from soil by various reagents and which is insoluble in dilute acid.
Fulvic Acid	The cellaret material which remains in solution in after removal of humic acid by acidification.
Hymatomelanic Acid	Alcohol soluble portion of humic acid.

Humic Substances

In the soil ecosystem a large variety of different organic substances is present (eg. 12-13, 15-16, 18, 33) and these substances can be divided into several fractions. The diagram in Table 1 gives an overview of a classification of the organic matter by Stevenson (16). Part of the organic matter is present as microbial tissues. Depending on the definitions chosen, the soil biomass consists also of the sub soil part of higher plants and of the soil fauna. The remainder of the organic matter is "dead" organic matter, which can be subdivided into the organic residues and the soil organic matter or humus.

4

The organic residues are undecayed plant and animal tissue and their partial decomposition products. The humus or soil organic matter is defined as the total of the organic compounds minus the biomass and the organic residues.

The humus fraction consists of the non-humic substances and the humic substances. The non-humic substances are compounds which belong to known classes of biochemistry, such as amino acids, proteins and enzymes, lignin, carbohydrates, fats, waxes, resins and simple organic acids like citrate and malonic acid. The non-humic substances are formed as decay products and by active excretion by micro-organisms and plant roots. The excreted acids play a role in the weathering of minerals (eg. 14-16,42) and amino acids and enzymes are of importance both for the formation of the organic matter and for its degradation and mineralization.

The humic fraction is a group of complex, brown to black cellaret and relatively high molecular weight organic compounds which are dissimilar to the biopolymers of microorganisms and higher plants. Humic substances is a general term used for the dark material which is extracted from the soil by using extraction techniques. In practice a distinction between non-humic and humic substances cannot always be made. The extraction techniques are in general non-specific and, at least to some extent, the humic fraction will contain some non-humic substances.

The humic substances can be further fractionated on the basis of their solubility characteristics. The fraction which is not soluble in base is the humin fraction, whereas the humic fraction and the fulvic fraction are soluble in base. After treating the extract with acid the humic acids precipitate and the fulvic acids remain in solution.

In contrast to the mineral soil constituents such as hydrous oxides and clay minerals, the definitions of the fractions of the organic matter do not refer to specific chemical structures. The definitions are operational and each fraction is a complex and polydisperse mixture of different organic compounds.

Because the mineral constituents disturb measurements and influence the behaviour of the organic matter it is essential to study "purified" organic matter extracted from the soil systems in order to obtain a first insight in the

5

characteristics and properties of the organic matter itself. Since the humin fraction is defined as the fraction that stays behind, in most cases the "purified" organic matter studied are the fulvic acid and the humic acid fractions. However, due to the use of material from different sources, obtained by different fractionation procedures, the obtained, sometimes conflicting results, can not be easily compared. The last decade the International Humic Substance Society (IHSS) has stimulated the standardization of extraction procedures and standard and reference materials has been made available to researchers worldwide (38,43-50). In this way the IHSS hopes to advance the knowledge, research and applications of humic substances (38,51).

Humic Substances in The Environment

Although historically most of the research on humus and on humic substances has been performed by soil scientists (e.g. 43), these substances are not typical for soils, but are found in all type of ecosystems (13,18,34-35,36-37,52). The diagram in Figure 1 gives the different flowpaths of humic substances in the environment. The amount of humic material in a system is determined by the net balance of formation, degradation or transformation, addition, removal and transfer (16,18,34,37,53). In soil systems the addition of organic matter from other systems is negligible and organic matter content is mainly determined by the net balance of formation and degradation. The contribution of the transfer to other systems to the balance is relatively small, but cannot be neglected since it forms an important source for aquatic systems like streams and rivers and for ground water (34,37,54-56).

The organic matter and the humic substance content of soils depend on various soil formation factors such as climate, time, topography, vegetation, parent material and land use (16). The major sources for the humic material are plants and mosses. The "fresh" organic residues can be decomposed rather easily, whereas the resistance of humic material for decomposition is large. The synthesis of humic substances is very complex and not yet well resolved (12,16,18,41,57). In general one can say that humic substances are formed by polymerization and condensation of decomposition
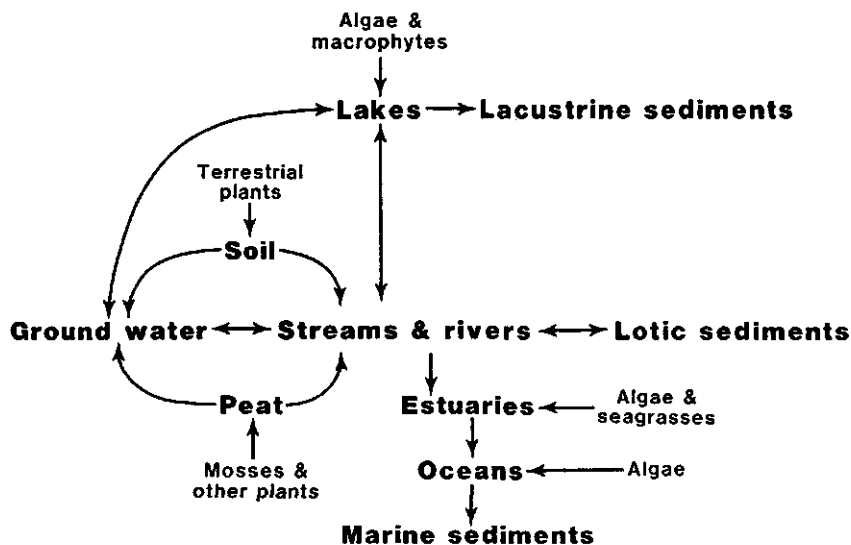
6

Figure 1. Diagram of the many possible environmental flowpaths of humic substances (18).

products or of resynthesis of humic substances. The decomposition products may originate both from fresh organic material and from degradation of existing humic substances. Micro-organisms are assumed to play an important role in the formation of humic material. The micro-organisms form the decomposition products actively. Inactively they may catalyze the condensation processes, for instance by the excretion of extracelluar enzymes.

In soil systems and in sediments the humic substances are predominantly insoluble and associated to the mineral phases (12-16,53). Although our prime interest in the proton and metal ion interactions originates from the field of soil pollution, ion binding is also of great importance for the soil formation. The stability of the organic matter/mineral complexes and the solubility of the humic substances depend strongly on the pH and on the type and amount of ions present (16,37,58-62).

The association of organic matter with minerals influences both the properties of the mineral surfaces and of the organic matter, which makes that the properties studied for the individual soil constituents cannot be simple added to obtain the properties of the system as a whole. Nevertheless

7

following the well accepted deterministic scientific approach, knowledge of the individual constituents is essential in order to understand the more complex system. This is the excuse for this thesis in which we only study purified humic substances.

The humic material can migrate to deeper parts of the soil by bioturbification by soil organisms and by leaching of soluble organic matter (16,54,63). This migration facilitates the transport of hazardous compounds bound to the humics and should be taken into account in a risk assessment. A large migration of organic matter is observed in podzols, which have distinct B horizons in which sesquioxides and organic matter are the major accumulation products (16,53).

The dissolved organic carbon (DOC) content of soil water changes with depth. The median concentration of the dissolved organic carbon decreases from 20 mg C/l in the A horizon to 2 mg C/l in the C horizon (54). In general the solubility of fulvic acids is larger than that of humic acids and as a consequence the humic acid/fulvic acid ratio decreases with depth.

The organic carbon in ground water depends on the type aquifer. In most aquifers the DOC concentration is less than 1 mg C/l (64). Higher DOC concentrations originates form aquifers receiving their recharge from organically rich waters, for instance from peatlands and swamps. The humic fraction of the DOC is highly determined by the origin of the recharge water and varies from 10-90 % (63,54).

In soil the humic substance are predominantly autochthon; they are formed locally. In all other systems allochthonous humic substances; originating from different systems form a major fraction of the total amount of humic substances. In most aquifers the humic substances in ground water originate from the overlying soils. In some sediments organic matter is deposited with the sediment. This kerogen rich sediments may result to very high DOC values (54).

In aquatic systems the allochthonous humic substances originate from soil or from connecting lakes and streams (37,55-56,65). The soil humic material is added via surface runoff or via ground water. In running water like rives and bogs the allochthonous humic material predominates. In lakes

and in lake sediments a considerable fraction of humic substances is autochthonous and is formed from algae detritus. The dissolved organic carbon in aquatic systems range from 0 to 50 mg C/l. The DOC and its humic fraction is not constant but varies in time and in space. Tipping and Woof (66) found that humic carbon comprised 60-70% of the DOC in winter and early spring, but only 30-40% in summer. During the season of thermal stratification the concentration of DOC in the lower stratas is more constant but somewhat lower than in the upper stratas (65).

The aquatic humic substance are rather small, have a low molecular weight, and the fulvic acids strongly dominate over humic acids. In sediments humic substances undergo diagenetic changes. These changes include a gradual decrease with depth of burial of humic and fulvic acids and a concomitant increase of humin.

Like in soil systems, in aquatic systems humic substances play an important role in the geochemical cycling of macro and micro nutrients and in controlling the free concentration toxic compounds. The significance of the organic matter fraction can be illustrated from the work of Verweij (67) on the copper speciation in lake Tjeukemeer. In this alkaline, humic-substance rich, polder lake in the northern Netherlands the binding of copper to the humic substances has reduced the free copper concentration so much that it became a limiting factor for the growth of algae. This while on the basis of the total copper concentration, copper toxicity was expected.

In estuaria the concentration of humic substance ranges from undetectable to 2 mg/l and the bulk of the humic substance is allochthonous and derives from input of rivers (68). In open seawater the concentration rarely exceeds 0.25 mg/l and part of the humic substances are formed from the free radical auto-oxidative cross-linking of unsaturated lipids released into the water by plankton (69). Due to the higher ionic strength in marine systems the humic substance will contract, and form condensed structure. The high salt level also promotes aggregation of humic molecules.

Humic substances in marine sediments originate both from marine and terrestrial sources (70). The formation and evolution of humic substance in sediments is believed to be the key in understanding the mechanisms by

9

which kerogen forms. Because knowledge on the formation of kerogen is important in order to estimate the petroleum potential of sediments, further research in this area is both of economic and scientific interest (70,71).

Properties of Humic Substances

A comprehensive review of the different techniques that can be used to characterize the humic material can be found in Humic Substance II, In search of Structure (39). Unfortunately a unified structure for humic substances does not exist. Humic substances are complex mixtures of (macro)molecules, with a composition that changes in time and space. Techniques to study the structural properties of molecules are often developed for mono disperse systems. The interpretation of the obtained data on humic substances is highly restricted (39,72). On top of that the techniques often influence the structure of the humic substances.

A first and rather simple procedure to characterize humic material is the elemental analysis. Table 2 gives the results of a statistical evaluation of the elemental composition of a large number of humic acids and fulvic acids isolated from environments all over the world. On a weight basis C and O are the most important elements. For humics the contribution of C, S and N elements is larger than that of fulvic acids. The content of H is about equal and the content of O is smaller.

For most fulvic acids the molecular weight ranges from 500-5000 g.mol^{-1}. The molecular weight of humic acids is larger than that of fulvic acids and range from 1500 up to $>10^5$ g.mol^{-1} (13,16,37,39,74). The low molecular weight humic molecules are more or less flexible cylinders or more compact globular particles or ellipsoids. The high molecular weight molecules are large enough to form random coils or gels, structures that may easily change their conformation as a function of the environment conditions. However when the cross linking between the chains and the hydrophobicity of the molecules is large the high molecular weight molecules may be fairly condensed and rigid (39).

Table 2. Mean elemental composition of humic and fulvic acids from different sources expressed as weight percent (73).

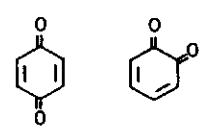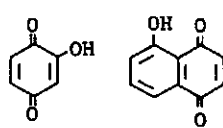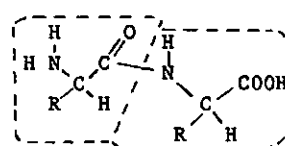| Element	Humic Acid				Fulvic Acids			
	Soil	Fresh-water	Marine	Peat	Soil	Fresh-water	Marine	Peat
C	55.4	51.2	56.3	57.1	45.3	46.7	45.0	54.2
H	4.8	4.7	5.8	5.0	5.0	4.2	5.9	5.3
N	3.6	2.6	3.8	2.8	2.6	2.3	4.1	2.0
S	0.8	1.9	3.1	0.4	1.3	1.2	2.1	0.8
O	36.0	40.4	31.7	35.2	46.2	45.9	45.1	37.8

Another important characteristic of humic substances is type and content of the functional groups (13,16,37,39,75-77). The functional groups are of great importance since ion binding occurs at the functional groups of the humic substances. In Table 3 an overview is given of the some of the different functional groups encountered in humic acids. The functional group content of humic substances ranges from 1 to 10 eq.kg^{-1}. Per unit mass the functional group content of the fulvic acids is larger than that of humic acids.

Metal Ion binding to Humic Substances

A general accepted picture is that metal ions form complexes with the functional groups of humic substances (16,37,75,78). A first characteristic of metal ion binding is the *stoichiometry* of the binding to the sites. The metal ions can be bound in various ways, for instance by forming mono dentate complexes to a single site or multi dentate complexes to structure in which several functional groups are coordinated.

The reactivity of a functional group depend on its type and its environment. For the bulk of the metal binding the -COOH and the -COH groups are of importance. At very low concentrations binding mainly occurs at sites which have a high and specific affinity. Among these high affinity

11

Table 3. Some important Structural Groups of Humic Substances (16).

Amino	$-NH_2$	Anhydride	$R-\overset{\overset{O}{\|}}{C}-O-\overset{\overset{O}{\|}}{C}-R'$
Amine	$R-\overset{\overset{H}{\|}}{\underset{\underset{H}{\|}}{C}}-NH_2$	Imine	$R-\overset{\overset{H}{\|}}{C}=NH$, $R-CHNH$
Amide	$R-\overset{O}{C}-NH_2$	Imino	$=NH$
Alcohol	$R-CH_2OH$	Ether	$R-CH_2-O-CH_2-R'$
Aldehyde	$R-\overset{\overset{H}{\|}}{C}=O$, $R-CHO$	Ester	$R-\overset{\overset{O}{\|}}{C}-O-R'$, $R-COOR'$
Carboxyl	$R-\overset{O}{C}-OH$, $R-COOH$	Quinone	
Carboxylate ion	$R-C\overset{O}{\underset{O}{}}{}^{\ominus}$, $R-COO^-$		
Enol	$R-CH=CH-OH$	Hydroxyquinone	
Ketone	$R-\overset{O}{C}-R'$, $R-CO-R'$		
Keto acid	$R-\overset{O}{C}-COOH$	Peptide	
Unsaturated carbonyl	$\overset{H}{-C}=\overset{H}{C}-\overset{H}{C}=O$		

sites there are nitrogen or sulphur containing functional groups and coordinated sites such as phthalic acid or salicylic acid type of groups (16,37,41). Owing to the different types of functional groups in humic substances (16,37,75-76,79), humic substances are heterogeneous ligands. This *chemical heterogeneity* is the second characteristic which determines the metal ion binding.

A third factor to be considered is the *competition* between different ions (e.g. 31,37,79). In aqueous systems protons (or hydroxyl ions) are by definition present. Because protons largely determine the state of the functional groups and the charge of the humic substances, at least a proton effect on the metal ion binding is to be expected. Additionally in soil

12

solutions a cocktail of different ions are present which bind to the humic substances. Think for instance of cations such as Ca^{2+}, Mg^{2+}, and Al^{3+} ions and of heavy metal ions such as Cu^{2+}, Cd^{2+} and Zn^{2+}.

The fourth factor that influences metal ion binding is *electrostatics* (37,79-82). Humic substances have a pH dependent negative charge, due to the dissociation of the functional groups. The negative charge promotes the adsorption of cations in two ways. First of all the concentration of the cations in the double layer around the humic colloids is larger than in the bulk, due to coulombic interactions. The binding by coulombic interaction is non-specific and depends only on the valency of the ion. The second effect is that a higher concentration of metal ions near the functional groups will result in a larger specific binding than expected on the basis of the concentration in the bulk solution.

The electrostatics or variable charge effects do also influence the secondary properties of the humic molecules like their conformation and the aggregation of molecules in larger complexes (37,39,59). Both conformational changes and aggregation will in turn affect the metal ion binding (and vice versa).

Modelling Ion Binding to Humic Substances

A model for metal ion binding should in principle be able to describe and to predict binding for a wide range of conditions with respect to pH, solution composition and ionic strength. The complexity of the systems is such that a strictly thermodynamic model is not feasible (36,37,41) and a quasi particle approach should be used. In a quasi particle approach a mathematical description is chosen in which the complex mixture of humic molecules is replaced by a set of hypothetical particles, whose behaviour mimics closely that of the actual mixture (83). The quasi particle models range from simple empirical models, consisting of fitted binding and exchange relations to more mechanistic models in which several of the factors mentioned above are explicitly taken into account. In every quasi particle model several arbitrary assumptions have been made which depend on the purpose of the model and on the good taste and scientific background of the

scientist. As a consequence all models are on the edge of science and fiction. Nevertheless the value of a model increases when the number of adjustable parameters is small and it still allows for the prediction of the outcome of experiments it was not calibrated on.

The major advantage of binding models is that they provide a basis for the calculation of the speciation of ions in the environment. Although the results should be examined carefully, the calculations are essential for a sound risk assessment. Models can also be used to design new experiments, which in turn help to make a further selection between different models.

In literature a large number of different quasi particle models have been proposed (eg. 16,36-37,40-41). On the basis of the way the binding models treat heterogeneity and electrostatics a simple subdivision into four classes of models can be made:

1. discrete heterogeneous, non electrostatic models

2. continuous heterogeneous, non electrostatic models

3. discrete heterogeneous, electrostatic models

4. continuous heterogeneous, electrostatic models

In the first and largest class a discrete number of different site types is assumed to be present (eg. 86-133). The different sites types in the model can be part of a larger molecule or can be present as a mixture of simple ligands in the solution. The stoichiometry of the binding equation depends on the type of the sites and often both mono and multi dentate binding equations are used. In some of these models both the constants of the binding equations and the fraction of the different site types are fitted. In others the constants are chosen equal to constants for corresponding simple organic ligands, and only the contribution of the different site types are fitted. As long as the number of ligands is large enough a "good" (mathematical) description is obtained. For the discrete heterogeneous mixture models the extension to multi component binding is straightforward and every site may have a different stoichiometry.

An alternative for the use of complex mixture of different ligands is to limit the binding to only one or a few ligands with a given stoichiometry and to analyze the binding coefficients (86-114). The value of the binding coefficients depend on factors like electrostatics, chemical heterogeneity, competition and true stoichiometry of the binding. As a consequence the value of the coefficients (or conditional "constants") is in general a function of the environmental conditions. When conditions exist over which the coefficients are constant over a large part of the binding curve, a simple model can be used to describe the data. In general, however, the distribution of the conditional constants is continuous and a description on the basis of a continuous (apparent) heterogeneity seems logical (134-138).

For continuous affinity distributions the overall binding equation is in general a complicated expression which can only be solved numerically. However for a few, fairly realistic distribution functions analytical solutions are known (139-141). The advantage of the models for continuous heterogeneity is the small number of parameters involved. In many cases only two parameters, suffices to describe the binding; a parameter that determines the width of the distribution and a median affinity constant. Disadvantages are that the extension to multi component binding is complicated and in most cases for all sites the same type of binding equation should be used (142).

In the electrostatic binding models the coulombic interactions are explicitly taken into account (79-82,143-157). In these models it is assumed that the electrostatic effect predominates the observed non ideality of the binding. The magnitude of the electrostatic interactions depend on the shape, size, nature and conformation of the humic particles. Consequently the poly dispersity of humic substances and the structure of the humic molecules are important. In order to simplify this situation the humics are treated as averaged sized particles which have a simple poly dispersity or are mono disperse.

The electrostatic binding models combine a description of the electrostatic effects with a description of the site binding. Like for the non electrostatic binding models most research groups use a discrete heterogen-

eous site binding model (80-82,143-155), while only a few use a continuous heterogeneous model (79,156-157).

The mechanistic nature of the electrostatic models makes that they allow for prediction of the binding behaviour for different environmental conditions. If the model for the electrostatic interactions is correct, the affinity constants in the site binding model are intrinsic and can be related to the chemical structure of the groups. Nevertheless since quasi particle models are by definition over simplifications, one should interpret the results with care.

Present Approach

In this thesis models for competitive binding have been developed using advanced data analysis techniques (79,156-159) to select appropriate models and to determine model constants. In order to avoid a priori assumptions as much as possible we start with the analysis of proton binding. Proton binding has the advantage of a simple stoichiometry and is a mono component binding process when it is measured in an indifferent electrolyte. In chapter 2 a procedure for the analysis of proton binding data is presented that allows for the assessment of a model for the electrostatic effects followed by the determination of the proton affinity distribution. In the chapters 3 and 4 the procedure is applied to proton binding data for 11 different humic substances. The obtained distributions for this samples indicate that a continuous heterogeneous binding model is the most appropriate choice.

In the chapters 2, 5-6 we work out 2 models for competitive metal ion binding to humic substances and apply them to experimental data for cadmium and calcium binding. In both models analytical binding expressions for continuous heterogeneous ligands are used, and the electrostatic effects are incorporated on the basis of the double layer model which was assessed on the basis of the proton binding data.

The two models differ with respect to competition between metal ions and protons and with respect to the correlation between the proton and the metal affinity distribution. In the so called *uncoupled* binding model it is

assumed that the affinity distributions for the metal ions and the protons are fully independent and that the sites for metal ions differ from the proton sites. Metal ion and proton do only interact via the electrostatics. In the *fully coupled* adsorption model both the metal ion and the proton compete for the same surface sites and the shape of the metal and proton distributions are assumed to be identical. Only their position on the log K axis differs.

In the chapters 7 and 8 a set of analytical equations for multi component binding are derived, in which the affinity distribution may differ from one component to another. The intriguing features of these equations are illustrated on the basis of model calculations. We did not yet apply these equations to experimental data, but consider this an interesting future challenge.

References

1.   Wallerius, *Agriculturae Fundamenta Chemica.* Upsala, 1761.

2.   *Verhandelingen uitgegeven door de maatschappij ter bevoordering van den landbouw te Amsterdam,* Cesar Noël Guerin, Amsterdam, 1778, part 1.

3.   Komov, I.I. *Agriculture (O zemledelii),* Moscow, 1789.

4.   Sprengel, C. *Die Bodenkunde oder die Lehre vom Boden,* Müller: Leipzig, 1837

5.   Berzelius, J.J., *Lehrbuch der Chemie,* Wöhler, Dresden, 1839.

6.   Liebig, J. von *Organic Chemistry in its Applications to Agriculture and Physiology,* Tr.J.W. Webster, J.Owen: Cambridge, 1841.

7.   Boussingault, J. B., *Economie Rurale considérée dans ses Rapports avec La Chimie, La Physique et La Météorologie,* Béchet Jeune: Paris, 1844, part 1 and 2.

8.   J.A. Stöckhardt, *Algemeene Landbouw-Scheikunde,* J.H. Siddré: Utrecht, 1854.

9.   Mulder, G.J., *De Scheikunde der Bouwbare Aarde,* H.A. Kramer, 1860.

10.   S. Odén *Die Huminsäure,* Kolloidchemische Beihefte 11, Verlag von Theodor Steinkopff: Dresden, 1919.

11.   Waksman, S.A. *Humus, Origin, Chemical Composition and Importance in Nature,* The Williams and Wilkins Company: Baltimore 1936

12.   Konova, M.M., *Soil Organic Matter, Its Nature, Its Role in Soil Formation and in Soil Fertility.* Pergamon Press: Oxford, 1961.

13.   Schnitzer, M. and S.U. Khan, *Humic Substance in the Environment*, Marcel Dekker Inc.: New York, 1972

14.   Allison, F.E., *Soil Organic Matter and Its Role in Crop Production*, Elsevier: Amsterdam, 1973.

15.   Schnitzer, M. and S.U. Khan, *Soil Organic Matter*, Elsevier: Amsterdam, 1978.

16.   Stevenson, F.J., *Humus Chemistry. Genesis, Composition, Reactions*; Wiley Interscience: New York, 1982.

17.   Mortensen, J.L. *Soil Sci. Soc. Amer. Proc.*, **27**, 179-186.

18.   Aiken, G.R., D.M. McKnight, R.L.Wershaw and P. MacCarthy (Eds.) *Humic Substances in Soil, Sediment, and Water*; Wiley Interscience: New York, 1985

19.   Aubert, H.; Pinta, M. *Trace Elements in Soils*, Elsevier: Amsterdam, 1977.

20.   Edwards, C.A. *Environmental Pollution by Pesticides*, Plenum Press: New York, 1973.

21.   Nriagu, J.O. (Ed.), *Copper in the Environment*. Wiley-Interscience: New York, 1979, part 1 and 2.

22.   Nriagu, J.O. (Ed.), *Cadmium in the Environment*. Wiley-Interscience: New York, 1980, part 1 and 2.

23   Nriagu, J.O.(Ed.), *Zinc in the Environment*. Wiley-Interscience: New York, 1980, part 1 and 2.

24.   Canter, L.W. *Environmental Impact of Agricultural Production*, Lewis Publishers Inc.: Chelsea, Michigan, 1986.

25.   Assink, J.W.; Van den Brink, W.J. (Eds.) *Contaminated Soil*, Martinus Nijhoff Publishers: Dordrecht, 1986.

26.   Wolf, K.; Van den Brink, W.J.; Colon, F.J. (Eds.) *Contaminated Soil '88*, Kluwer Academic Publishers: Dordrecht, 1988. Vol. I and II.

27.   Arendt, F.; Hinsenveld, M.H.; Van den Brink, W.J. (Eds.) *Contaminated Soil '90*, Kluwer Academic Publishers: Dordrecht, 1990. Vol I and II.

28.   Vernet, J.P. (Ed.) *Heavy Metals in the Environment*, CEP Consultants: Edinburgh, 1989.

29.   Bareló, J. (Ed.) *Environmental Contamination*, CEP Consultants: Edinburgh, 1990.

30.   De Haan, F.A.M.; Henkens, C.H.; Zeilmaker, D.A. *Handboek voor Milieubeheer. Deel IV. Bodembescherming*, Samson H.D. Tjeenk Willink: Alphen aan den Rijn, 1984.

31. Van Riemsdijk, W.H.; De Wit J.C.M.; Nederlof, M.M.; Koopal, L.K. In *Contaminated Soil'90*, Arendt, F.; Hinsenveld, M.; Van Den Brink, W.J. (eds.), Kluwer Academic Publishers: Dordrecht, 1990 359-366.

32. Bolt, G.H.; De Boodt, M.F.; Hayes, M.H.B.; McBride M.B. (Eds.), *Interactions at the Soil Colloid - Soil Solution Interface*, NATO ASI Series Series E: Applied Sciences-Vol. 190, Kluwer Academic Publishers, Dordrecht, 1991.

33. Eglington, G.; Murphy, M.T.J. (Eds.) *Organic Geochemistry*, Longman Springer-Verlag: Berlin, 1969.

34. Buffle, J. In *Metal Ions in Biological Systems*. Vol 18. Dekker: New York, 1984, Ch. 6.

35. Christman, R.F.; Gjessing, E.T. (Eds.) *Aquatic and Terrestrial Humic Materials*, Ann Arbor Science: Ann Arbor, Michigan, 1983.

36. Sposito, G., *CRC Crit. Rev. Environ. Control* 1986, *16*, 193-229.

37. Buffle, J. *Complexation Reactions in Aquatic Systems: An Analytical Approach*; Ellis Horwood Limited: Chichester, 1988.

38. Suffet, I.H.; MacCarthy, P. (Eds.) *Aquatic Humic Substances*, American Chemical Society: Washington, 1989.

39. Hayes, M.H.B.; MacCarthy, P.; Malcolm, R.L.; Swift, R.S. (Eds.), *Humic Substances II: In Search of Structure*; Wiley Interscience: New York, 1989.

40. Lund, W. In *Metal Speciation in the Environment*; Broekaert, J.A.C.; Güçer, Ş.; Adams, F. (Eds.); NATO ASI Series Vol. G 23, Springer-Verlag: Berlin, 1990,43-56.

41. Livens, F.R., *Environ. Pollution* 1991, *70*, 183-208.

42. Hoffland, *Mobilization of Rock Phosphate by Raper (Brassica Napus L.)*, Wageningen Agricultural University, Wageningen, 1991, PhD Thesis.

43. Aiken, G.R, McKnight, D.M.; Wershaw, R.L.; MacCarthy, P. In *Humic Substances in Soil, Sediment, and Water*; Aiken, G.R., D.M. McKnight, R.L.Wershaw and P. MacCarthy (Eds.) Wiley Interscience: New York, 1985. Ch 1.

44. Hayes, M.H.B. In *Humic Substances in Soil, Sediment, and Water*; Aiken, G.R., D.M. McKnight, R.L.Wershaw and P. MacCarthy (Eds.) Wiley Interscience: New York, 1985. Ch 13.

45. Aiken, G.R. In *Humic Substances in Soil, Sediment, and Water*; Aiken, G.R., D.M. McKnight, R.L.Wershaw and P. MacCarthy (Eds.) Wiley Interscience: New York, 1985. Ch 14.

46. Swift, R.S. In *Humic Substances in Soil, Sediment, and Water*; Aiken, G.R., D.M. McKnight, R.L.Wershaw and P. MacCarthy (Eds.) Wiley Interscience: New York, 1985. Ch 15.

47. Leenheer, J.A. In *Humic Substances in Soil, Sediment, and Water*; Aiken, G.R., D.M. McKnight, R.L.Wershaw and P. MacCarthy (Eds.) Wiley Interscience: New York, 1985. Ch 16.

48. MacCarthy, P.; Malcolm, R.L.; Hayes, M.H.B.; Swift, R.S.; Campbell, W.L. *Establishment of a Collection of Standard Humic Substance*, IHSS, Commun. to Members, 1985.

49. International Humic Substances Society, *List of Characterization*, IHSS, Commun. to Purchasers of Standard and Reference Humic and Fulvic Acids, 1985.

50. International Humic Substances Society, *Sample of Analytical Data for IHSS Standard and Reference Humic and Fulvic Acids*, IHSS, Commun. to Purchasers of Standard and Reference Humic and Fulvic Acids, 1987.

51. International Humic Substances Society, *Bylaws*, Art II, Section 3, 1982, 1985.

52. Horne, R.A. *Marine Chemistry*. Wiley-Interscience: New York, 1969.

53. Stevenson, F.J. in Aiken et al Ch. 2.

54. Thurman, E.M. In *Humic Substances in Soil, Sediment, and Water*; Aiken, G.R., D.M. McKnight, R.L.Wershaw and P. MacCarthy (Eds.) Wiley Interscience: New York, 1985. Ch. 4.

55. Steinberg, C.; Muenster, U. In *Humic Substances in Soil, Sediment, and Water*; Aiken, G.R., D.M. McKnight, R.L.Wershaw and P. MacCarthy (Eds.) Wiley Interscience: New York, 1985. Ch. 5.

56. Malcolm, R.L. In *Humic Substances in Soil, Sediment, and Water*; Aiken, G.R., D.M. McKnight, R.L.Wershaw and P. MacCarthy (Eds.) Wiley Interscience: New York, 1985. Ch 7.

57. Haider, K.; Martin, J.P.; Filip, Z. In *Soil Biochemistry, Vol 4.*, Paul, E.A.; McLaren, A.D. (Eds.), Marcel Dekker: New York, 1975, pp. 195-244.

58. Tipping, E. *Geochim. Cosmochim. Acta* 1981, *45*, 191-199.

59. Tipping, E.; Cooke, D. *Geochim. Cosmochim. Acta* 1982, *46*, 75-80.

60. Tipping, E.; Higgins, D. C. *Colloids Surf.* 1982, *5*, 85-92.

61. Tipping, E.; Griffith, J.R.; Hilton, J. *Croat. Chem. Acta* 1983, *56*, 613-621.

62. Tipping, E. *Mar. Chem.* 1986, *18*, 161-169.

63.   Thurman, E.M. *Isolation, characterization, and geochemical signifincace of humic substances from groundwater*, University of Colorado: Boulder, 1979, PhD thesis.

64.   Leenheer, J.A.; Malcolm, R.L.; McKinley, P.W.; Eccles, L.A. *U.S. Geol. Surv. J. Res.* **1974** 2, 361-369.

65.   Ishiwatari, In *Humic Substances in Soil, Sediment, and Water*; Aiken, G.R., D.M. McKnight, R.L.Wershaw and P. MacCarthy (Eds.) Wiley Interscience: New York, 1985. Ch 6.

66.   Tipping, E.; Woof, C. *Limnol. Oceanogr.*, **1983** *28*, 168-72.

67.   Verweij W, *Speciation and Bioavailability of Copper in Lake Tjeukemeer*, Wageningen Agricultural University, Wageningen, 1991, PhD thesis.

68.   Mayer, L.M. In *Humic Substances in Soil, Sediment, and Water*; Aiken, G.R., D.M. McKnight, R.L.Wershaw and P. MacCarthy (Eds.) Wiley Interscience: New York, 1985. Ch 8.

69.   Harvey, G.R.; Boran, D.A. In *Humic Substances in Soil, Sediment, and Water*; Aiken, G.R., D.M. McKnight, R.L.Wershaw and P. MacCarthy (Eds.) Wiley Interscience: New York, 1985. Ch. 9.

70.   Vandenbroucke, M.; Pelet, R.; Debyser, Y. In *Humic Substances in Soil, Sediment, and Water*; Aiken, G.R., D.M. McKnight, R.L.Wershaw and P. MacCarthy (Eds.) Wiley Interscience: New York, 1985. Ch 10.

71.   Hatcher, P.G.; Breger, I.A.; Maciel, G.E.; Szeverenyi, N.M. In *Humic Substances in Soil, Sediment, and Water*; Aiken, G.R., D.M. McKnight, R.L.Wershaw and P. MacCarthy (Eds.) Wiley Interscience: New York, 1985. Ch 11.

72.   Hayes, M.H.B.; MacCarthy, P.; Malcolm, R.L.; Swift, R.S. In Hayes, M.H.B.; MacCarthy, P.; Malcolm, R.L.; Swift, R.S. (Eds.), *Humic Substances II: In Search of Structure*; Wiley Interscience: New York, 1989. Ch. 24.

73.   Rice, J.A.; MacCarthy, P.; *Org. Geochem.* **1991**, *17*,   635-648.

74.   Wershaw, R.L.; Aiken, G.R. In *Humic Substances in Soil, Sediment, and Water*; Aiken, G.R., D.M. McKnight, R.L.Wershaw and P. MacCarthy (Eds.) Wiley Interscience: New York, 1985. Ch. 19.

75.   Perdue, E.M. In *Humic Substances in Soil, Sediment, and Water*; Aiken, G.R., D.M. McKnight, R.L.Wershaw and P. MacCarthy (Eds.) Wiley Interscience: New York, 1985. Ch. 20.

76.   MacCarthy, P.; Rice, J.A. In *Humic Substances in Soil, Sediment, and Water*; Aiken, G.R., D.M. McKnight, R.L.Wershaw and P. MacCarthy (Eds.) Wiley Interscience:

21

New York, 1985. Ch 21.

77.   Wershaw, R.L. In *Humic Substances in Soil, Sediment, and Water*; Aiken, G.R., D.M. McKnight, R.L.Wershaw and P. MacCarthy (Eds.) Wiley Interscience: New York, 1985. Ch 22.

78.   MacCarthy, P.; Perdue, E.M., 1991, In *Interactions at the Soil Colloid - Soil Solution Interface*; Bolt, G.H.; De Boodt, M.F.; Hayes, M.H.B.; McBride M.B. (Eds.); NATO ASI Series Series E: Applied Sciences-Vol. 190, Kluwer Academic Publishers, Dordrecht, 469-489.

79.   De Wit, J.C.M.; Van Riemsdijk, W.H.; Nederlof, M.M.; Kinniburgh, D.G.; Koopal, L.K. *Analytica Chim. Acta* 1990, 232, 189-207.

80.   Marinsky, J.A. In *Aquatic Surface Chemistry*; Stumm, W. (Ed.); Wiley Interscience: New York, 1987, Ch. 3.

81.   Tipping, E.; Backes C.A.; Hurley, M.A. *Water Res.* 1988, 22, 597-611.

82.   Bartschat, B.M.; Cabaniss, S.E.; Morel, F.M.M. *Environ. Sci. Technol.* 1992, 26, 284-294.

83.   Sposito G. *Environ. Sci. Technol.* 1981, 15, 396.

84.   Cabaniss, S.E.; Shuman, M.S.; Collins, B.J. in Kramer, C.J.M.; Duinker, J.C. (Eds.) *Complexation of Trace Metals in Natural Waters*, 1984. Martinus Nijhoff/Dr W. Junk Publishers: Den Haag 165-179.

85.   Turner, D.R.; Varney, M.S.; Whitfield, M.; Mantoura, R.F.C.; Riley, J.P. *Geochim. Cosmochim. Acta*, 1986, 50, 289-297.

86.   Schnitzer, M.; Hansen, E.H. *Soil Sci.* 1970, 6, 333-340.

87.   Gamble, D.S. *Can. J. Chem.* 1970, 48, 2663-2669.

88.   Gamble, D.S. *Can. J. Chem.* 1972, 50, 2680-2690.

89.   Gamble, D.S. *Can. J. Chem.* 1973, 51, 3217-3222.

90.   Gamble, D.S.; Langford, C.H. *Anal. Chem.* 1980, 52, 1901-1908.

91.   Gamble, D.S.; Langford, C.H.; *Environ. Sci. Technol.* 1988, 22, 1325-1336.

92.   Ardakani, M.S.; F.J. Stevenson, *Soil Sci. Soc. Amer. Proc.* 1972 36, 884-890.

93.   Stevenson, F.J. *Soil Sci. Am. J.* 1976, 40, 665-672.

94.   Stevenson, F.J. *Soil Sci.* 1977, 123, 10-17.

95.   Fitch, A.; Stevenson, F.J. *Soil Sci. Am. J.* 1984, 48,1044-1050.

96.   Fitch, A; Stevenson, F.J.; Chen, Y. *Org. Geochem.* 1986, 9, 109-116.

97   Sikora, F.J.; Stevenson, F.J. *Geoderma*, **1988**, *42*, 353-363.

98.   Reuter, J.H.; Perdue, E.M. *Geochim. Cosmochim. Acta* **1977**, *41*, 325-334.

99.   Buffle, J.; Greter, F. L.; Haerdi, W. *Anal. Chem.* **1977**, *49*, 216-222.

100.   Buffle, J.; Deladoey, P.; Greter, F. L.; Haerdi, W. *Anal. Chim. Acta* **1980**, *116*, 255-274.

101.   Buffle, J. *Anal. Chim. Acta* **1980**, *118*, 29-44.

102.   Bresnahan, W.T.; Grant, C. L.; Weber, J. H. *Anal. Chem.* **1978**, *50*, 1675-1679.

103.   Shuman, M.S.; Cromer, J.L. *Environ. Sci. Technol.* **1979**, *13*, 543-545.

104.   Saar, R.A.; Weber, J.H. *Environ. Sci. Technol.* **1980**, *17*, 877-880.

105.   Saar, R.A.; J.H. Weber, *Environ. Sci. Technol.* **1982**, *16*, 510A-517A.

106.   Davis, H.; Mott, C.J.B. *J. Soil Sci.* **1981**, *32*, 379-391.

107.   Young, S.D.; Bache, B.W.; Linehan, D.J. *J. Soil Sci.* **1982**, *33*, 467-475.

108.   Young, S.D.; Bache, B.W. *J. Soil Sci.* **1985**, *36*, 261-269.

109.   Alberts, J.J.; Giesy, J.P. In *Aquatic and Terrestrial Humic Materials*; Christman, R.F.; Gjessing E.T.(Eds.), Ann Arbor Science: Michigan, 1983. Ch 16.

110.   Cressey, P.J.; Monk, G.R.; Powell, H.K.J.; Tennent, D.J. *J. Soil Sci.* **1983**, *34*, 783-799.

111.   Bizri, Y.; Cromer, M.; Scharff, J.P.; Guillet, B.; Rouiller J. *Geochim. Cosmochim. Acta* **1984**, *48*, 227-234.

112.   Torres, R.A.; Choppin, G.R.L *Radiochimica Acta* **1984**, *35*, 143-148.

113.   Baham, J.; Sposito, G. *J. Environ. Qual.* **1986**, *15*, 239-244.

114.   Kim, J.I.; Rhee, D.S.; Buckau G. *Radiochimica Acta* **1991**, *52/53*, 49-55.

115.   Zunino, H.; Martin, J.P., *Soil Sci.* **1977**, *123*, 5-76.

116.   Takamutsu, T.; Yoshida, T. *Soil Sci.* **1978**, *125*, 377-386.

117.   Van den Berg, C.M.G.; Kramer, J.R. *Analytica Chim. Acta* **1979** *106*, 113-120.

118.   Ryan, D.K.; Weber, J.H. *Environ, Sci. Technol.* **1982**, *16*,866-872.

119.   Dempsey, B.A., O'Melia C.R., In *Aquatic and Terrestrial Humic Materials*; Christman, R.F.; Gjessing E.T.(Eds.), Ann Arbor Science: Michigan, 1983; Chapter 12.

120.   Byrne, R,H. *Marine Chem.* **1983**, *12*, 15-24.

121.   Murray, K.; Linder, P.W. *J. Soil Sci.* **1983**, *34*, 511-523.

23

122. Murray, K.; Linder, P.W.; *J. Soil Sci.* **1984**, *35*, 217-222.

123. Paxéus, N.; Wedborg, M. *Anal. Chimica Acta* **1985**, *169*, 87-98.

124. Dzombak, D.A.; Fish, W.; Morel, F.M.M. *Environ Sci Technol.* **1986** *20*, 669-675.

125. Leuenberger, B.; Schindler, P.W. *Anal. Chem.* **1986**, *58*, 1471-1474.

126. Fish, W.; Dzombak, D.A.; Morel, F.M.M. *Environ. Sci. Technol.* **1986** *20*, 676-683.

127. Gregor, J.E.; Powell, H.K.J. *J. Soil Sci.* **1988**, *39*, 243-252.

128. Pommery, J.; Ebenga, J.P.; Imbenotte, M.; Palavit, G.; Erb, F. *Wat. Res.* **1988**, *22*, 185-189.

129. Lamy, I.; Cromer, M.; Scharff, J.P. *Anal. Chimica Acta* **1988**, *212*, 105-122.

130. Hering, J.G.; Morel, F.M.M. *Environ. Sci. Technol.* **1988**, *22*, 1234-1237.

131. Hansen, A.M.; Leckie, J.O.; Mandelli; E.F.; Altmann, R.S. *Environ. Sci. Technol.* **1990**, *24*, 683-688.

132. Seki, H.; Suzuki, A.; Kashiki, I. *J. Colloid Interface Sci.* **1990**, *134*, 59-65.

133. Gomez, M.J.; Martí, I.; Donoso, L. *Fresenius J. Anal. Chem.* **1991**, *339*, 664-668.

134. Perdue, E.M.; Lytle, C.R. In *Aquatic and Terrestrial Humic Materials*; Christman, R.F.; Gjessing E.T.(Eds.), Ann Arbor Science: Michigan, 1983. Ch 14.

135. Perdue, E.M. In *Metal Speciation: Theory, Analysis and Application*, J.R. Kramer, H.E. Allen Lewis Publishers, Inc.: Chelsea MI, 1988. Ch 7.

136. Dobbs, J.C.; Susetyo, W.; Knight, F.E.; Castles, M.A.; Carreira, L.A.; Zarraga, L.V. *Anal. Chem.* **1989**, *61*, 483-488.

137. Dobbs, J.C.; Susetyo, W.; Knight, F.E.; Castles, M.A.; Carreira,L.A.; Zarraga, L.V. *Intern. J. Environ. Anal. Chem.* **1989** *37*, 1-17.

138. Perdue, E.M.; Lytle, C.R. *Environ. Sci. Technol.* **1983**, *17*, 654-660.

139. Sips, R. *J. Chem. Phys.* **1948**, *16*, 490.

140. Sips, R. *J. Chem. Phys.* **1950**, *18*, 1024.

141. Tóth, J.; Rudzińsky, W.; Waksmundsku, A.; Jaroniec, M.; Sokolowsky, S. *Acta Chim. Hungar.* **1974**, *82*,11.

142. Van Riemsdijk, W.H.; Koopal, L.K. In *Environmental Particles*; Buffle, J.; Van Leeuwen, H.P. Lewis Publishers: Chelsea, Michigan, 1992, Chapter 12.

143. Wilson, D.E.; Kinney, P. *Limnol. Oceanogragr.* **1977**, *22*, 281-289.

144. Marinsky, J.A.; Wolf, A.; Bunzl, K. *Talanta* **1980**, *27*, 461-468.

145.   Marinsky, J.A.; Gupta, S; Schindler, P. *J. Colloid Interface Sci.* **1982**, *89*, 401-411.

146.   Marinsky, J.A.; Reddy, M.M. *Org. Geochem.* **1984**, *7*, 215-221.

147.   Marinsky, J.A.; Ephraim, J. *Environ. Sci. Technol.* **1986**, *20*, 349-354.

148.   Varney, M.S.; Mantoura, R.F.C.; Whitfield, M.; Turner, D.R.; Riley, J.P. *Potentiometric and Conformational Studies of the Acid-Base Properties of Fulvic Acid from Natural Waters* NATO Conf. Ser., [Ser.] 4, 9(Trace Met. Sea Water), 751-772, 1983

149.   Arp, P.A. *Can J. Chem.* **1983**, *61*, 1671-1682.

150.   Ephraim. J.; Marinsky, J.A. *Environ. Sci. Technol.* **1986**, *20*, 367-354.

151.   Ephraim, J; Alegret, S.; Mathuthu, A.; Bicking, M.; Malcolm, R.L.; Marinsky, J.A. *Environ. Sci. Technol.* **1986**, *20*, 354-366.

152.   Ephraim, J.H.; Borén, H.; Pettersson, C.; Arsenie, I.; Allard, B. *Environ. Sci. Technol.* **1989**, *23*, 356-362.

153.   Dudley, L.M.; McNeal, B.L. *Soil Sci.* **1987**, *143*,329-340.

154.   Tipping, E.; Reddy, M.M.; Hurley, M.A. *Environ. Sci. Technol.* **1990**, *24*, 1700-1705.

155.   Tipping, E., Woof, C.; Hurley, M.A. *Water. Res.*, **1991**, *25*, 425-435.

156.   De Wit, J.C.M.; Nederlof, M.M.; Van Riemsdijk, W.H.; Koopal, L.K. *Water, Air and Soil Pollution* **1991**, *57-58*, 339-349.

157.   De Wit, J.C.M.; Van Riemsdijk, W.H.; and Koopal, L.K.; *Finnish Humus News* **1991**, *3*, 139-144.

158.   Nederlof, M.M.; Van Riemsdijk, W.H.; Koopal, L.K.; *J. Colloid Interface Sci.* **1990**, *135*, 410-426.

159.   Nederlof, M.M. *Analysis of Binding Heterogeneity*, Wageningen Agricultural University: Wageningen, 1992, PhD thesis.

Chapter 2

Analysis of Ion Binding on Humic Substances and the Determination of Intrinsic Affinity Distributions

Abstract

Humic substances are characterized by a variable electric potential and by a variety of binding sites leading to chemical heterogeneity. Binding of ions to these substances is influenced by both factors. A methodology based on acid-base titrations at several salt levels is presented that allows for the assessment of an appropriate electrostatic double layer model and the intrinsic proton affinity distribution. The double layer model is used for the conversion of pH to pH_S for each data point, where H_S is the proton concentration in the diffuse layer near the binding site. It is shown that with an appropriate double layer model the proton binding curves at different salt levels converge into one 'master curve' when plotted as a function of pH_S. The intrinsic proton affinity distribution can then be derived from the 'master curve' using the LOGA method.

A rigorous analysis of metal binding to humic substances is complex and in practice is not feasible. Under two different (simplifying) assumptions, namely fully coupled and uncoupled binding, it is shown how intrinsic metal ion affinity distributions can be obtained. Model calculations show that apparent metal ion affinity distributions do not resemble the intrinsic metal ion affinity distribution.

J.C.M. de Wit, W.H. van Riemsdijk, M.M. Nederlof, D.G. Kinniburgh, L.K. Koopal. Analysis of Ion Binding on Humic Substances and the Determination of Intrinsic Affinity Distributions. *Analytica Chimica Acta*, 232, 1990, 189-207.

Introduction

Interactions between metal ions and organic materials such as humic substances determine to a large extent the bio-availability and mobility of heavy metal ions. For example, the binding of metal ions onto insoluble soil organic matter will strongly reduce the availability of heavy metal ions, whereas complexation with dissolved organic matter will enhance the metal ion mobility (1-4).

Research on the chemical structure and genesis of humic material has shown that both the structure and origin of humic material are very diverse (5-7). Humic acids and fulvic acids are mixtures of complex heterogeneous organic polyelectrolytes. Their acid-base properties are determined by a variety of functional groups (2-8). In principle, each specific type of group in a given local molecular structure has its own intrinsic affinity for the binding of a proton or metal ion. Ion binding to humic and fulvic acids is therefore characterized by a distribution of intrinsic affinity constants.

In general, natural organic matter has an overall negative charge caused by the dissociation of the functional groups or the desorption of protons (7,9-11). This charge leads to an electric field, which depends on the magnitude of the charge, the geometry of the organic colloid and the ionic strength. The electric field in turn affects the adsorption of protons and metal ions. For the description of the overall adsorption of ions on organic matter both the chemical heterogeneity, characterized by a distribution of intrinsic affinities, and the electrostatic effects are of prime importance.

In environmental and soil sciences, the main interest is focused on the adsorption behaviour of trace metal ions (3-4). Because protons (or hydroxyl ions) are always present in aqueous solutions, they determine the state of the surface sites. Knowledge of proton adsorption is therefore of critical importance for understanding the adsorption of other charged components.

The addition of metal ions to humic material in solution will not only lead to metal ion adsorption, but also to a change in the protonation of the surface, due to electrostatic interactions and/or competition (10,12,13). A rigorous analysis of metal adsorption data is extremely complex, if not impossible. In order to be able to describe metal ion adsorption it is therefore

necessary to make some assumptions about the nature of the adsorption process.

In this paper, a general description of proton adsorption and a new method for the analysis of proton adsorption data are first presented. In general, proton adsorption isotherms depend on the ionic strength due to electrostatic effects. In our analysis, the electrostatic effects are eliminated from the isotherm using a model for the electric double layer. Ideally, if an appropriate electrostatic model is used, the dependency of the isotherms on ionic strength should vanish and the corrected isotherms will merge into a 'master curve' (14).

The 'master curve' then only reflects the effects of chemical heterogeneity on adsorption. The intrinsic proton affinity distribution can be obtained from the 'master curve' using an approximate method as suggested for example by Nederlof et al. (15) and Koopal et al. (16).

In the second part of the paper, metal ion adsorption is discussed. In order to describe metal ion adsorption, assumptions about the nature of the adsorption process have to be made. Two limiting cases are considered, namely the case in which the proton and metal ion affinity distributions are fully correlated and the case in which the affinity distributions are fully independent. On the basis of model calculations both situations are compared. It is demonstrated that it can be checked whether or not it is justified to use the limiting situations for the description of metal ion adsorption.

Charging of a Heterogeneous Polyelectrolyte

Complexation Model

Consider an ensemble of identical acid organic polyelectrolytes, with n different types of functional groups, each type i with a proton association reaction given by:

30

$$S_iO^- + H^+ \rightleftharpoons S_iOH \tag{1}$$

Equation 1 can be characterized by an intrinsic equilibrium constant $K_{i,H}^{int}$ (17):

$$K_{i,H}^{int} = \frac{\{S_iOH\}}{\{S_iO^-\}[H^+]\exp\left(-\dfrac{F\psi_s}{RT}\right)} \tag{2}$$

Or by an apparent or conditional affinity coefficient $K_{i,H}^{app}$:

$$K_{i,H}^{app} = \frac{\{S_iOH\}}{\{S_iO^-\}[H^+]} \tag{3a}$$

which equals:

$$K_{i,H}^{app} = K_{i,H}^{int} \cdot \exp\left(-\frac{F\psi_s}{RT}\right) \tag{3b}$$

The Boltzmann factor $\exp(-F\psi_s/RT)$ accounts for the electric field around the charged groups; ψ_s is the potential at the location of the functional groups of the polyelectrolyte relative to the potential in bulk solution. Equation 2 applies to the situation where all surface groups experience the same average ψ_s. In the case of a (partially) penetrable polyelectrolyte this implies a constant potential throughout the penetrable domain of the polyelectrolyte, whereas for an impenetrable particle it implies a smeared out surface potential.

The braces {} in Eqns. 2 and 3 refer to site densities, the brackets [] to concentrations. This implies that apart from the coulombic interactions, ideal behaviour of both the polyelectrolyte and solution is assumed. In the case of non-ideal solution behaviour, the solution concentrations can be replaced by their activities. For the calculation of the activity coefficients, use can be made of, for example the Davies Equation (18). In contrast with $K_{i,H}^{app}$, $K_{i,H}^{int}$ is not

experimentally accessible as it is a function of ψ_s.

The degree of protonation or degree of association, $\theta_{i,H}$, for a group of type i can be expressed as:

$$\theta_{i,H} = \frac{\{S_iOH\}}{\{S_iOH\}+\{S_iO^-\}} \tag{4}$$

Combination of Eqns. 2 and 4 leads to:

$$\theta_{i,H} = \frac{K_{i,H}^{int}[H^+]\exp\left(-\dfrac{F\psi_s}{RT}\right)}{1+K_{i,H}^{int}[H^+]\exp\left(-\dfrac{F\psi_s}{RT}\right)} \tag{5}$$

In order to simplify Eqn. 5 we define H_S as:

$$H_S = [H^+]\exp\left(-\frac{F\psi_s}{RT}\right) \tag{6}$$

H_S is the proton concentration at the location of the binding sites. Substitution of Eqn. 6 in Eqn. 5 leads to an adsorption equation for the protons which is mathematically equivalent to the Langmuir adsorption isotherm:

$$\theta_{i,H} = \frac{K_{i,H}^{int}H_S}{1+K_{i,H}^{int}H_S} \tag{7}$$

Eqn. 7 (or Eqn. 5) essentially describes the adsorption on a homogeneous surface. For a heterogeneous surface it represents the adsorption on a specific type of surface group and is therefore called the local isotherm.

For a heterogeneous particle with a discrete affinity distribution, the overall degree of protonation, $\theta_{t,H}$, is given by the weighted summation of the degree of protonation of the different types of sites:

32

$$\theta_{t,H} = \sum_{i=1}^{n} f_i \theta_{i,H} \qquad (8)$$

where f_i is the fraction of proton sites of type i with respect to the total number of proton sites.

For a continuous distribution of affinities, $\theta_{t,H}$ is given by:

$$\theta_{t,H} = \int_0^\infty \theta\left(K_{i,H}^{int}, H_s\right) f\left(\log K_{i,H}^{int}\right) d\left(\log K_{i,H}^{int}\right) \qquad (9)$$

where $f(\log K_{i,H}^{int})$ is the normalized distribution function of the intrinsic proton affinity constants and $\theta(\log K_{i,H}^{int}, H_s)$ is the *local* adsorption isotherm, for which Eqn. 7 will be used. The proton adsorption in absolute quantities is found by multiplying $\theta_{t,H}$ by the maximum adsorption, $\Gamma_{H,max}$.

Again it is stressed that Eqns. 2-9 are derived with the assumption that near each functional group, the same average ψ_s holds. If ψ_s is not the same near all functional groups, $K_{i,H}^{int}$ (Eqn. 2) has to be redefined. When the particles are identical, but there is a potential profile over the surface or in the penetrable domain of the polyelectrolyte, $K_{i,H}^{int}$ is defined as:

$$K_{i,H}^{int} = \frac{\{S_iOH\}_x}{\{S_iO^-\}_x [H^+] \exp\left(-\dfrac{F\psi_x}{RT}\right)} \qquad (10)$$

where the subscript x indicates a certain position inside the polyelectrolyte or at its surface. As a consequence $\theta_{i,H}$ (Eqn. 7) has to be replaced by $\theta_{i,H,x}$. To obtain $\theta_{t,H}$ one has to integrate twice, once over the intrinsic affinity and once over the position variable x.

In the case of considerable polydispersity (in particle size) at least a double integral results. The overall relative adsorption for the mixture, $\theta_{T,H}$, is obtained by integration of $\theta_{t,H}$ over the particle distribution.

For the moment these complications will be neglected and humic substances will be treated as an ensemble of identical heterogeneous polyelectrolytes for which an average potential holds near all groups. Under

33

these assumptions $\theta_{T,H}=\theta_{t,H}$.

Note that these assumptions do not necessarily imply rigidity. Changes of the conformation, e.g. swelling, can be treated with Eqns. 2-9 as long as an average ψ_S holds for all functional groups.

Electrostatic Interactions

The negative charge of the particle depends on the degree of protonation. The overall charge, Q (C.kg^{-1}), of an acid surface characterized by Eqns. 1, 7 and 8 or 9 is given by:

$$Q = Q_{max}\left(1-\theta_{T,H}\right) \tag{11a}$$

or

$$Q = Q_{max}\alpha_T \tag{11b}$$

where α_T is the degree of dissociation, and, Q_{max} is the maximum charge (including sign) of the polyelectrolyte (C.kg^{-1}). For an acid colloid Q_{max} is a simple function of $\Gamma_{H,max}$:

$$Q_{max} = -F\Gamma_{H,max} \tag{12}$$

In order to use Eqn. 8 or 9 to describe proton adsorption, some knowledge of ψ_S is required. As ψ_S cannot be determined directly, we have to rely on electrostatic models relating ψ_S to the charge of the polyelectrolyte.

In theoretical expressions ψ_S is often related to the charge number Z (C.mol^{-1}) of the polyelectrolyte (4,11,19,20):

$$\psi_S = 2wZ\left(\frac{RT}{F}\right) \tag{13}$$

where w is an electrostatic interaction function. Z is related to Q by:

$$Z = MQ \qquad (14)$$

where M (kg.mol^{-1}) is the molecular weight of the polyelectrolyte.

The function w is determined by the structure and composition of the double layer and by the nature and geometry of the colloidal particles. When humic colloids are treated as rigid impermeable particles the surface charge density, σ_s (C.m^{-2}) can be used instead of Z, where σ_s is defined as:

$$\sigma_s = \frac{Q}{S} = \frac{Z}{MS} \qquad (15a)$$

where S (m^2.kg^{-1}) is the specific surface area of the particles.
σ_s follows also from $\theta_{t,H}$ and the total proton site density N_s (mol.m^{-2}):

$$\sigma_s = -N_s F\left(1 - \theta_{T,H}\right) \qquad (15b)$$

N_s is related to Q_{max} by:

$$N_s = -\frac{Q_{max}}{SF} \qquad (15c)$$

Formally the electrical double layer around a particle can be seen as a condenser which is characterized by the capacitance K. K provides the relation between ψ_s and σ_s:

$$\psi_s = \frac{\sigma_s}{K} \qquad (16)$$

and determines the ease of charging the surface. According to Eqns. 13, 15 and 16 K is related to w by:

$$K = \frac{1}{2w} \frac{1}{MS} \frac{F}{RT} \qquad (17)$$

Expressions for w or K can be derived by solving the Poisson-Boltzmann equation, which gives the variation of the potential with distance

from a charged boundary of arbitrary shape (19,21). For low ψ_s (Debye-Hückel approximation) where ψ_s and Z or σ_s are directly proportional, and for rigid impermeable colloidal particles with a simple geometry, the Poisson-Boltzmann equation can be solved analytically. The derived relations for w or K depend on the radius, r, of the particle, the ionic strength and the type of electrolyte.

For higher surface potentials ψ_s and Z or σ_s are no longer directly proportional and only for a flat plate the Poisson-Boltzmann equation results in an analytical expression. In this case w or K is given by the Gouy-Chapman theory (21-23). For both spherical and cylindrical particles the Poisson-Boltzmann equation has to be solved numerically (24) or approximate analytical expressions (24-31) can be used. Expressions for w or K for permeable particles (19) and for flexible polyelectrolytes (32,33) are also known. In the following the humic colloids will be treated as rigid impermeable spheres.

As an illustration of the relationship between K and σ_s, some results obtained with the double layer model for rigid spheres are presented in Fig. 1. The radius of the particles is varied from 0.5 nm to ∞ and three values of the ionic strengths are considered. For r=∞ the Gouy-Chapman theory for flat plates results.

For extremely small particles (r<0.5 nm) and not too high ionic strength, K is almost constant, which indicates a linear relationship between ψ_s and σ_s, also for high values of ψ_s. For such colloids the differences between the Debye-Hückel approach and the numeric calculations are negligible.

For larger particles and high potentials the relation is clearly non-linear. For large particles, r»10 nm, the curvature of the surface is negligible, so that hardly any difference can be observed between the behaviour of spheres and plates.

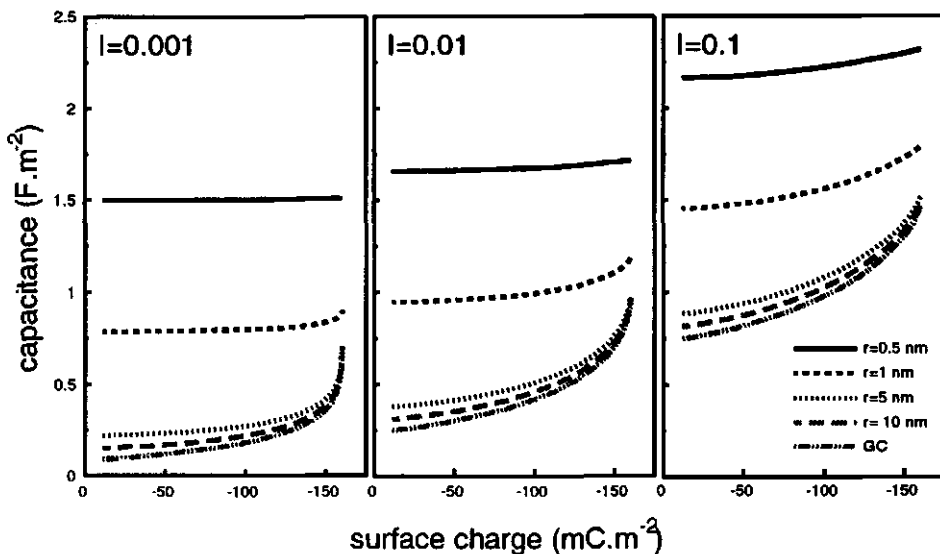**Figure 1.** The capacitance (F.m^{-2}) as a function of the surface charge σ_s (mC.m^{-2}) for a flat plate and a series of spheres at three ionic strengths.

Model Calculations

By combining the complexation model (Eqns. 1-11) plus a double layer model (Eqn. 13 or 16) with a certain surface heterogeneity, proton adsorption isotherms at several ionic strengths can be calculated.

In the model calculations in this paper it will be assumes that the heterogeneity of the surface is given by the following "Sips"-distribution (34) for the affinities:

$$f\left(\log K_{i,H}^{int}\right) = \frac{\ln(10) \sin(m\pi)}{\pi\left[\left(\dfrac{K_{i,H}^{int}}{\tilde{K}_H}\right)^{-m} + 2\cos(m\pi) + \left(\dfrac{K_{i,H}^{int}}{\tilde{K}_H}\right)^{m}\right]} \qquad (18)$$
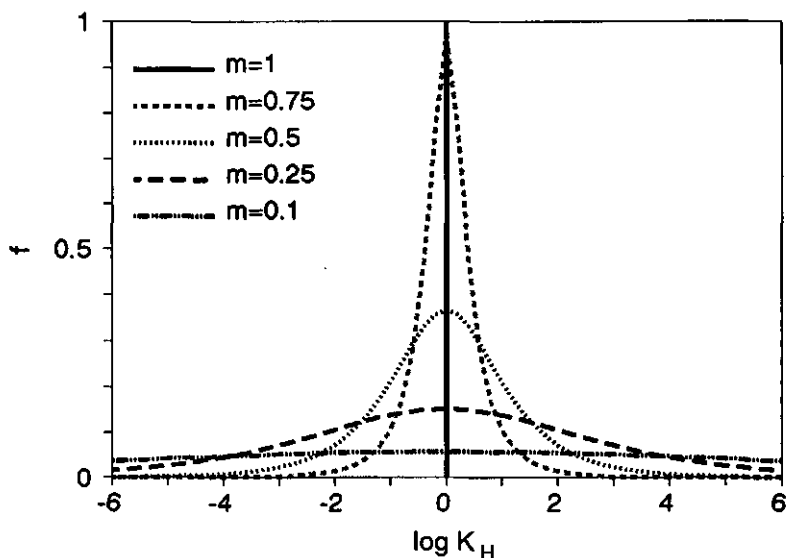
37

Figure 2. Sips distribution (f) for m=0.1, 0.25, 0.50, 0.75 and 1.0 and log $\check{K}_H$=0. Log K_H is the affinity.

The parameter $\check{K}_H$ determines the position of the affinity distribution on the log K_H^{int} axis and m determines the width of the distribution. For m=1 a Dirac delta function is obtained, which corresponds with the homogeneous case. In Fig. 2 Eqn. 18 is plotted for some values of m and for log $\check{K}$=0. For low values of m the distribution is very wide, whereas already at m=.75 the distribution becomes narrow.

Substitution of Eqn. 18 for $f(\log K_H^{int})$ and Eqn. 7 for $\theta(K_{i,H}^{int}, H_s)$ in the overall adsorption equation, Eqn. 9, results in the following analytical expression for the adsorption (35):

$$\theta_{T,H} = \frac{\left(\check{K}_H H_s\right)^m}{1+\left(\check{K}_H H_s\right)^m} \tag{19}$$

In Fig. 3 proton adsorption isotherms $\theta_{T,H}(pH)$ at three ionic strengths are presented. The calculations are based on Eqn. 19 with log $\check{K}_H$=5 and m=0.25 for two different double layer models, that of a flat plate (Fig. 3a) and

38

of a spherical particle with a radius of 1 nm (Fig. 3b).

For both geometries the proton adsorption curves plotted as $\theta_{T,H}(pH)$ show an ionic strength dependence. The ionic strength dependence for the small particles is significantly smaller than that of the large (flat) particles because of the radial distribution of the electrostatic field. This is in agreement with the results shown in Fig. 1.

The ionic strength dependence disappears if the data are replotted as a function of pH_S and the curves merge into one 'master curve' (Fig 3). The 'master curves' are identical in both cases, because in the calculations for the flat plate and for spherical particle the same heterogeneity is assumed. By plotting $\theta_{T,H}$ versus pH_S, the electrostatic interactions are eliminated and the site binding part, reflecting the intrinsic heterogeneity, remains.
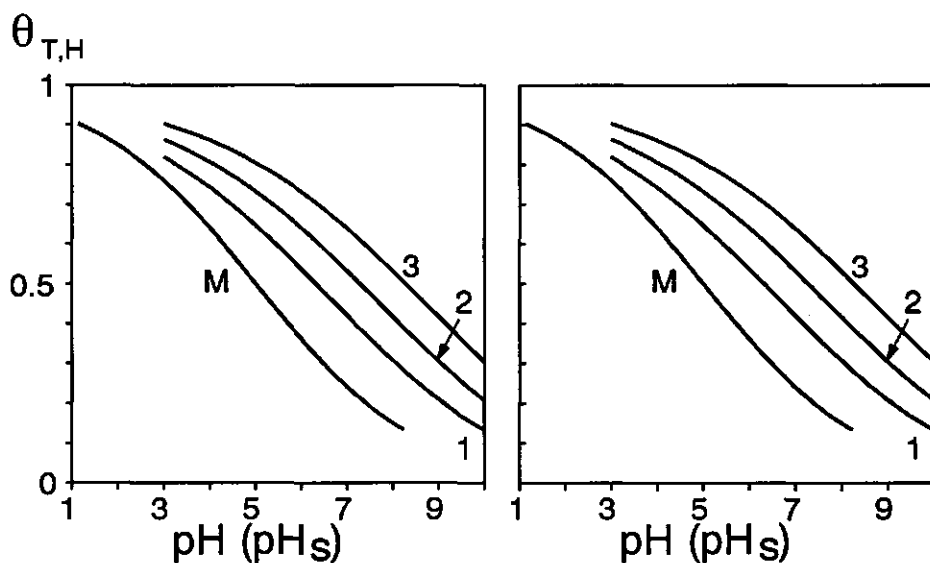
Figure 3. Proton adsorption isotherms and their corresponding 'master curve', M, for (a) a flat plate and (b) a sphere of radius of 1 nm with log K_H^{Int}=5.0, m=0.25 and N_S=1 (sites.nm^{-2}) (1.66x10^{-6} mol.m^{-2}). The numbers along the curves represent the ionic strength: 1, I=0.1; 2, I=0.01; 3, I=0.001.

39

In the case of model calculations it is easy to calculate the correct pH_s because the correct double layer model is known. In practice, however, a double layer model has to be assumed. In this case the extent to which the calculated $\theta_{T,H}(pH_s)$ curves merge is an indication of the adequacy of the chosen double layer model (14).

Affinity Distribution Analysis Using Adsorption Data

Above it has been assumed that the heterogeneity can be described with a "Sips" distribution. However, in general the intrinsic affinity distribution is not known and has to be established. For this objective the overall adsorption isotherm can be used. To eliminate the electrostatic effects, the overall adsorption isotherm should be expressed as $\theta_{T,H}(pH_s)$. As explained above, this procedure applied to adsorption isotherms measured at different ionic strengths, should result in a 'master curve'. For the calculation of the intrinsic affinity distribution from the $\theta_{T,H}(pH_s)$ 'master curve' several methods are known (8,15,35-39). An elegant approach based on approximations of the local isotherm is developed by Nederlof et al. (15). Briefly this group of methods is called the Local Isotherm Approximation or LIA family.

In the LIA family the local isotherm relation as given by Eqn. 7 is approximated by a functionality which allows Eqn. 9 to be solved analytically for the distribution function. Well known methods such as the condensation approximation (40,41), the asymptotically correct condensation approximation (42), the Rudzinski Jagiello method (43-45) and the affinity spectrum method (46-48) can be considered as members of the LIA-family (15). In this paper the so called LOGA-1 method (15,16) will be used. In the LOGA-1 method the local isotherm (Eqn. 7) is approximated by an isotherm which can be written as:

$$\theta_{i,H} = 0.5 \left(K_{i,H}^{int}H_s\right)^{0.7} \quad \text{for} \quad \theta_{i,H} \leq 0.5 \tag{20}$$

$$\theta_{i,H} = 1 - \frac{0.5}{\left(K_{i,H}^{int}H_s\right)^{0.7}} \quad \text{for} \quad \theta_{i,H} > 0.5 \tag{21}$$

When $\theta_{i,H}$ is plotted as function of log H_s, the second part of the isotherm (Eqn. 21) is the image of the first (Eqn. 20) when mirrored at $\theta = 0.5$. Because of the logarithmic concentration scale the approximation is called LOGA. The LOGA-1 approximation results in the following expression for the distribution function:

$$f_{LOGA-1}\left(\log K_{i,H}^{int}\right) = \frac{\partial \theta_T(H_s)}{\partial \log H_s} - 0.386 \cdot \frac{\partial^3 \theta_T(H_s)}{\partial (\log H_s)^3} \tag{22a}$$

with

$$\log K_{i,H}^{int} = -\log H_s \tag{22b}$$

The distribution function as calculated by the LOGA-1 method is thus obtained by taking the first and the third derivative of the 'master curve'.

For highly accurate data the LOGA-1 method results in an excellent representation of the distribution function for wide distributions. For nearly homogeneous distributions the LOGA-1 distribution is too wide (15).

Most data are subject to considerable experimental error, however, and this may disturb the calculated affinity distributions strongly (16,49). In order to obtain a suitable distribution function the overall isotherm has to be smoothed (16,49,50). A smoothing spline (SP) algorithm in combination with an error estimate can be used (51,52). This procedure is combined with the LOGA-1 method (16). Within the experimental error, the smoothed isotherm can be considered as the best representation of the experimental data.

Instead of using the LOGA-1 method to obtain the intrinsic affinity distribution, the method can also be used to obtain apparent affinity distributions. In that case the $\theta_{T,H}(pH)$ isotherms are analyzed and $(K_{i,H}^{int}H_s)$ in Eqns. 20 and 21 is replaced by $(K_{i,H}^{app},H)$. The expression for the distribution function is then based on the first and third derivative of the normal

41

isotherms. In this case electrostatic interactions contribute to the apparent heterogeneity.

Model Calculations

The application of the LOGA-1 method to the $\theta_{T,H}(pH)$ isotherms in Figs 3a and b will result in 6 different apparent heterogeneity distributions as is shown in Figs. 4a and b. Included is also the true intrinsic affinity distribution (dotted curve). The differences between the apparent heterogeneity distributions and the intrinsic affinity distribution are caused by electrostatic effects. From Fig. 4 it is clear that the apparent affinity distributions are rather poor representations of the intrinsic affinity distribution. They allow hardly any conclusions with respect to the presence of certain functional groups.
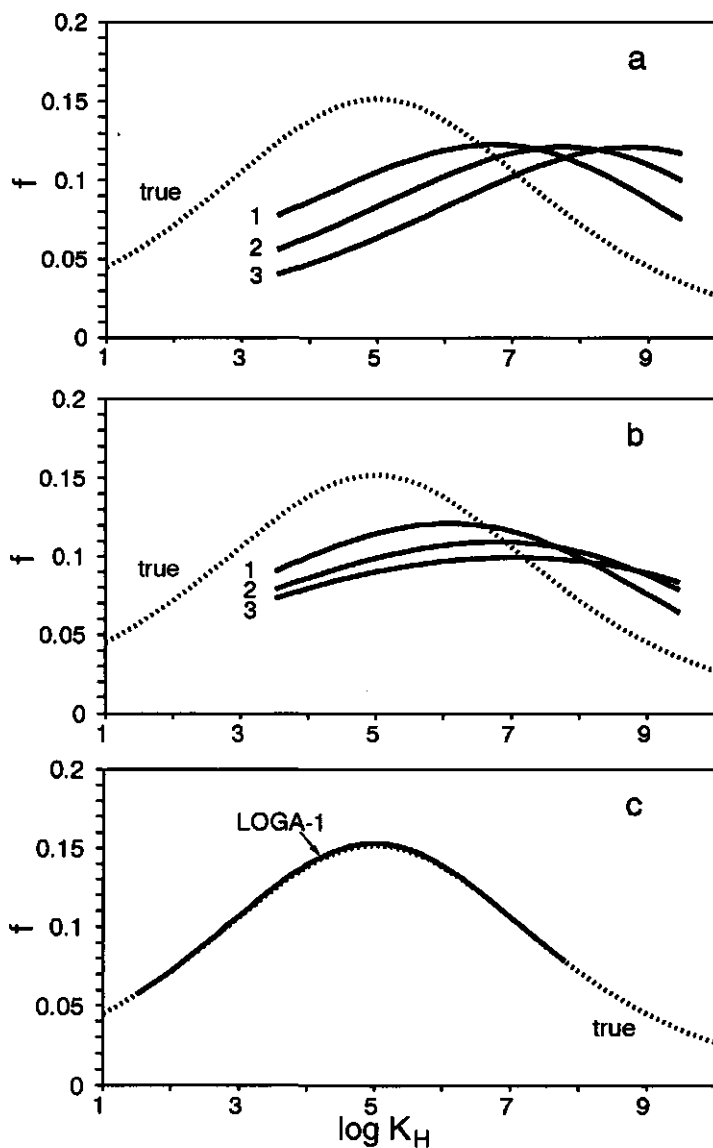
The intrinsic affinity distribution of the polyelectrolytes shown in Figs. 3a and b was obtained by applying the LOGA-1 method to the $\theta_{T,H}(pH_s)$ 'master curve', and the results are given in Figure 4c. As the chosen distribution is wide the LOGA-1 affinity distribution corresponds very well with the true affinity distribution. In this case the obtained log K_H^{int} values can be compared with literature values for simple organic acids.

The Analysis of Experimental Data

Procedure for Analysis of Experimental Data

In this section the procedure is described for the calculation of the 'master curve' from experimental proton titration data, followed by the heterogeneity analysis. The starting point of the analysis is a set of potentiometric titration curves over (preferably) a wide pH range and several ionic strengths. An arbitrary chosen set of curves is shown in Fig. 5a.

In a potentiometric titration the pH is measured as function of the amount of acid or base added to a sample at an approximately constant ionic strength. The proton consumption, ΔQ, of the sample is obtained by the subtraction of the blank titration curve from the sample curve. In a proper

Figure 4. Apparent affinity distributions (a and b) obtained from the application of the LOGA-1 method to the $\theta_{T,H}$(pH) data presented in Fig. 3 and (c) the intrinsic affinity distribution obtained from the $\theta_{T,H}$(pH$_s$) data. Distributions (a) for a sphere with r=1 nm and (b) for a flat plate. The intrinsic distributions (c) holds for both geometries. As a reference the true intrinsic distribution is plotted in all figures. The numbers on the curves represent the ionic strength: 1, I=0.1; 2, I=0.01; 3, I=0.001.

a. Experimental Data

pH

base or acid added

subtraction of blank $\longrightarrow$

b. "Relative" Charge

delta Q

pH

reference point $\longrightarrow$

c. "Absolute" Charge
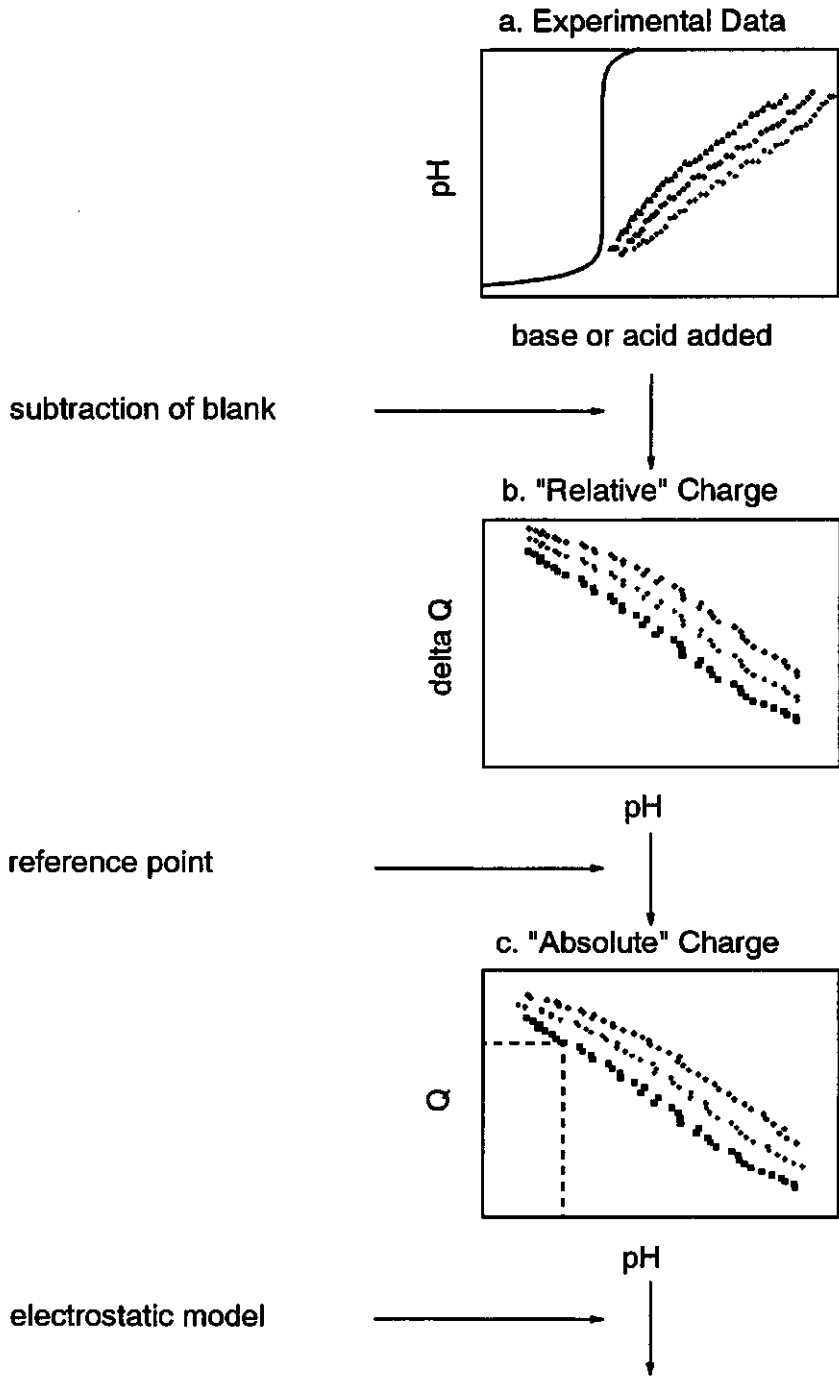
Q

pH

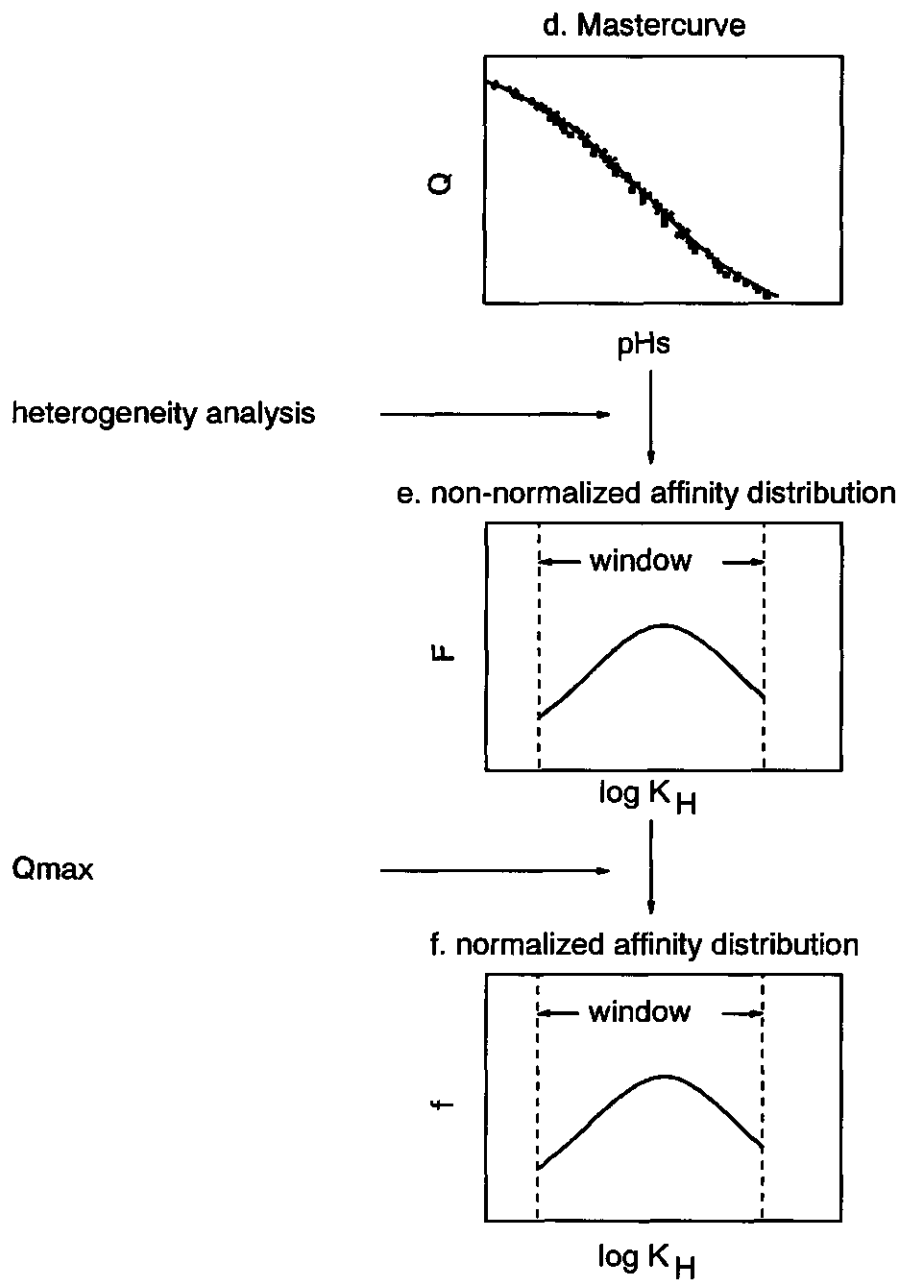electrostatic model $\longrightarrow$

Figure 5.

Figure 5 (continued). Schematical flow chart for the analysis of proton titration data.

titration set-up the experimental blank and the theoretical blank have to be in good agreement. At pH values below 3.0 and above 11.0 both the blank titration and the sample curves are nearly flat and parallel, so a small error in the curves leads to a relatively large error in the calculated proton consumption.

The proton consumption, ΔQ, is plotted in Fig. 5b as a function of the pH. ΔQ is a measure of the change of the surface charge. If the surface charge is known for one datapoint the ΔQ (Fig. 5b) curves can be converted into $Q(pH)$ curves (Fig. 5c), where Q is the absolute surface charge per kg of sample.

For amphoteric surfaces such as oxides the point of zero charge (pzc) can be used as a reference point for the $Q(pH)$ curves. Acid surfaces, like most natural organic colloids, have no measurable pzc, and the charge approaches zero asymptotically. In these cases the absolute value of the surface charge can be determined from the pH shift which occurs when a sample, which should initially be in its fully protonated form, is dissolved in an electrolyte of given pH (7,20). Under these conditions the proton release by the sample corresponds with the absolute surface charge.

The $Q(pH)$ curves (Fig. 5c) can be converted to $Q(pH_s)$ curves (Fig. 5d) using a double layer model. If the appropriate double layer model is used for the calculation of pH_s, the $Q(pH_s)$ curves for different ionic strengths should merge into one 'master curve'.

In the double layer equations ψ_s is expressed as a function of Z or σ_s (Eqns. 13 and 16). Therefore a transformation of Q to Z or σ_s is necessary. The transformation into σ_s is only justified in the case of rigid particles. For the specific surface area S, which is necessary in the transformation (Eqn. 15a), the BET surface area can be used. For natural organic colloids the BET surface area determined on the dried sample may not reflect the correct S. S is then treated as an adjustable parameter in the double layer model. For the transformation of Q into Z the molecular weight M has to be specified (Eqn. 14). In principle the magnitude of an average value for M can be established by several techniques (6,7). However, it should be realized that owing to electrostatic interactions the determination of an average $\overline{M}$ is conditional as

46

the estimated $\overline{M}$ will depend on the ionic strength and pH. Moreover the type of average found will depend on the method used.

In order to select the appropriate double layer equations, assumptions have to be made about the size, geometry, rigidity and permeability of the humic particles. For the time being we shall consider the particles as rigid impermeable spheres, and use the average radius, $\overline{r}$, as an adjustable parameter in the double layer model. Note that for a rigid impermeable colloid S, r (or $\overline{r}$) and M (or $\overline{M}$) are interrelated. The estimated average radius can then be compared with experimentally determined values of $\overline{r}$. For the determination of $\overline{r}$ hydrodynamic techniques such as viscosimetry and gel permeation may be used (7,53). Again it should be realized that such a determination of $\overline{r}$ is conditional.

By applying the SP-LOGA-1 method to the $\sigma_S(pH_S)$ data, a smoothed 'master curve' (Fig. 5d) is first obtained and this curve is then used to calculate the intrinsic affinity distribution function expressed as F_{LOGA-1}. F_{LOGA-1} is a non-normalized affinity distribution, because the integration of the distribution over the whole log K range does not equal one, as is the case with a normalized distribution, but equals the maximum surface charge.

In practice often only a part of the adsorption isotherm can be obtained experimentally and also only a part or window of the affinity distribution can be calculated. The distribution can be normalized if the maximum surface charge, Q_{max}, is known. The non-normalized F_{LOGA-1} and the normalized f_{LOGA-1} are related by:

$$F_{LOGA-1}(\log K) = Q_{max}\left[f_{LOGA-1}(\log K)\right] \qquad (23)$$

It is best to normalize the adsorption data as the last step in the analysis procedure. A complication is that it is very difficult to determine the true adsorption maximum for humic substances (54). In practice the adsorption maximum is almost always operationally defined. A consequence of not using the true adsorption maximum is that the estimated distribution function is not normalized in the correct way. Different operational definitions for the maximum adsorption lead to different $\theta_{T,H}(pH)$ curves for the same experimental Q(pH) curve, apparently implying different adsorption

behaviour. This illustrates that one has to be very careful in comparing data sets presented as $\theta_{T,H}(pH)$ curves.

The derived intrinsic affinity distribution can be used as such or to select a simplified adsorption model for the description of the data. When several narrow peaks are obtained, the adoption of a discrete heterogeneity model seems logical. The intrinsic affinity constants can be estimated from the peak positions in the affinity spectrum, and their relative abundance follows from the area under the peaks. In the case of a smooth distribution with one peak, a treatment on the basis of an adsorption model such as Eqns. 18 and 19 or similar equations (35) can be considered.

Analysis of Proton Titration Data for Humic Substances

Unfortunately only a few reports are available in the literature where the proton adsorption behaviour of humic materials is measured in the absence of metal ions at several ionic strengths. In Fig. 6, three such data sets are given. The open symbols represent the data as taken from literature (20,55,56) and are plotted as a function of pH; the solid symbols show the results replotted as a function of pH_S.

The replotted data converge within experimental error reasonably well into one 'master curve'. For comparison the curve that belongs to a homogeneous Langmuir isotherm is plotted as a solid line. The Langmuir isotherm has been chosen to intersect the 'master curve' at $\theta_{T,H}=0.5$. The 'master curves' of the fulvic acid (Fig. 6a) and the aquatic humic substances (Fig. 6b) have a slope that is lower than that of the Langmuir curve indicating intrinsic heterogeneity of the proton binding sites.

Surprisingly the 'master curve' of the peat sample (Fig. 6c) closely follows the Langmuir curve, suggesting the presence of a homogeneous polyelectrolyte with a $\log K_{i,H}^{int} \approx 3.1$. The proton titration curves for the peat can thus be modelled by using Eqn. 7 in combination with a flat plate double layer model.

The 'master curves' of the fulvic acid (Fig. 6a) and the aquatic humic substances (Fig. 6b) were obtained using the same parameters for the
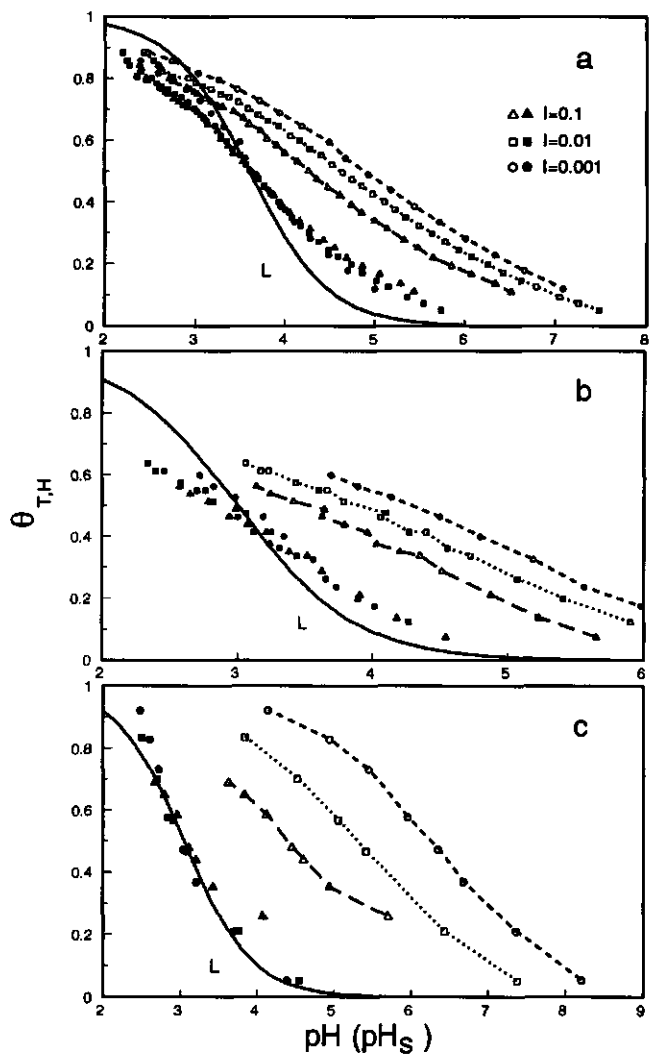
Figure 6. Experimental $\theta_{T,H}(pH)$ data (open symbols) and the best fitting $\theta_{T,H}(pH_S)$ data (solid symbols) for various humic substances. (a) $\theta_{T,H}(pH_S)$ data for Armadale Horizons Bh fulvic acids (55). $\theta_{T,H}(pH_S)$ data calculated for a sphere with a radius of 1 nm. $N_S=0.7$ (sites.nm^{-2}) (1.16×10^{-6} mol.m^{-2}). (b) $\theta_{T,H}(pH_S)$ data for aquatic humic substances from a stream at Lochard Forest (Central Region of Scotland) (20). $\theta_{T,H}(pH_S)$ data calculated with a sphere with a radius of 1 nm, $N_S=0.7$ (sites.nm^{-2}) (1.16×10^{-6} mol.m^{-2}). (c) $\theta_{T,H}(pH_S)$ data for Sphagnum peat (56). $\theta_{T,H}(pH_S)$ data calculated with a flat plate, $N_S=1$ (sites.nm^{-2}) (1.66×10^{-6} mol.m^{-2}). For reference, a monocomponent Langmuir isotherm is included. It has been chosen to coincide with the 'master curve' at $\theta_{T,H}(pH_S)=0.5$.

49

spherical double layer model, namely r=1 nm and N_S=0.7 sites.nm^{-2} (1.16x10^{-6} mol.m^{-2}). A radius of 1 nm for these materials is in agreement with literature (57).

The fulvic acid and the aquatic humic substances also show a very similar intrinsic proton affinity distribution characterized by a large peak in the region log $K_{i,H}{}^{int}$=3-4 (Fig. 7). A smaller number of higher affinity sites shows up in the region of log $K_{i,H}{}^{int}$=4-5.

Sites with even higher intrinsic affinities will be present but cannot be determined from these titration data. Note that the increasingly negative electric potential that develops with increasing pH suppresses the dissociation of the higher affinity sites considerably. This effect and the low accuracy of the titration data at very high pH values prevent the assessment of very high proton affinity sites from this type of data.
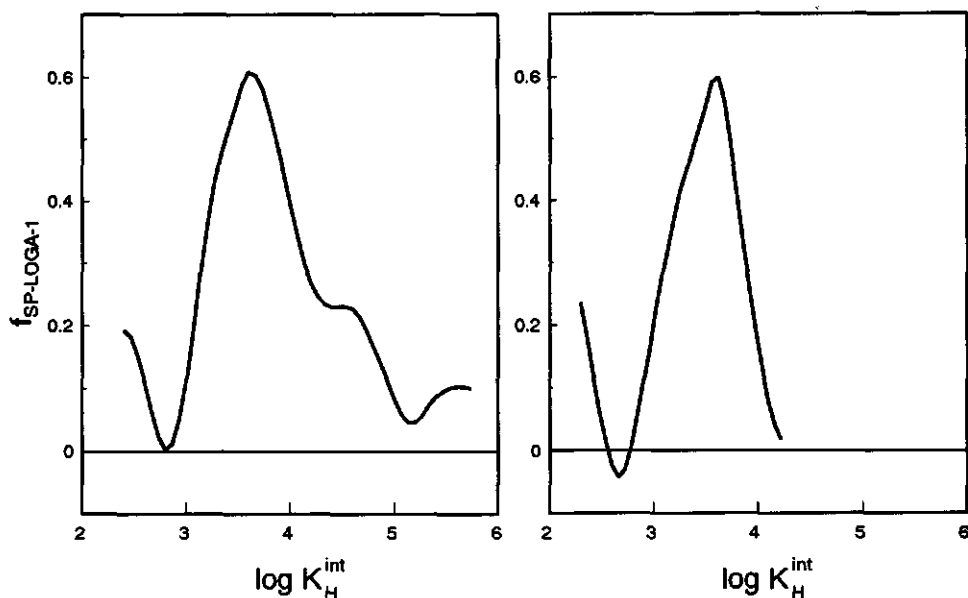

Figure 7. The SP-LOGA-1 intrinsic proton affinity distribution obtained from (a) the fulvic acid $\theta_{T,H}(pH_s)$ data and (b) the aquatic humic substances $\theta_{T,H}(pH_s)$ data (b) presented in Fig 6a and b.

Metal Ion Adsorption

In studying metal ion adsorption a perturbation of the system due to the introduction of metal ions will not only lead to metal ion adsorption but, owing electrostatic interactions, also to a change in the protonation of the surface (10,12,13). An analysis of proton adsorption as given in the previous section is therefore of help in understanding metal ion adsorption.

Apart from electrostatic effects, metal ions and protons may compete for the same surface sites. In that case both metal ion and proton adsorption are multi-component processes. For a heterogeneous surface, site competition not only affects the expression for the local adsorption, it also turns the expression for the overall adsorption into a multiple integral equation. The equation for the overall metal adsorption for a two component (M,H) adsorbate system is in general:

$$\theta_{t,M} = \int_{\Delta M} \int_{\Delta H} \theta_M \left(H_S, M_S, K_H^{int}, K_M^{int} \right) f \left(\log K_H^{int}, \log K_M^{int} \right) d\log K_H^{int} \, d\log K_M^{int} \quad (24)$$

where H_S and M_S are respectively the H and M concentrations near the binding sites and $\theta_M(H_S, M_S, K_H^{int}, K_M^{int})$ is the local isotherm for multi-component adsorption. Equation 24 holds under the assumption that the same average potential applies near each functional group. The intrinsic affinity distribution $f(\log K_H^{int}, \log K_M^{int})$ is a two-dimensional function which can in principle be obtained if the local isotherm is well established. Even then it requires a very large amount of high-quality experimental data and a complex mathematical analysis (58).

At present we see little prospect of using Eqn. 24 for the analysis of metal ion adsorption data on natural colloids. A simpler treatment, however, requires a number of simplifying assumptions about the nature of the adsorption process. Below two extreme situations are discussed which are related to the degree of correlation between the proton and metal ion affinities: namely that (1) the proton and metal ion affinity distributions are fully correlated or fully coupled, or that (2) these distributions are entirely independent or uncoupled.

The term fully coupled or correlated adsorption will be used if: (1)

51

proton ions and metal ions are in competition for the same surface sites, and (2) the shape of the distribution of the metal ions is identical with that of the protons, the only difference being the position of the affinity distributions on the log K axis. For a fully coupled system for which the proton affinity distribution has been determined, metal ion adsorption can be described with only one additional parameter for each metal ion species present. This parameter determines the position of the affinity distribution on the log K_M^{int} axis.

The term uncoupled adsorption will be used if protons and metal ions do not compete for the same surface sites. Therefore, the site density and intrinsic affinity distribution for the metal ion are entirely independent of those of the proton. Consequently, in the uncoupled case both protonation and metal ion complexation can be described as one-component adsorption processes. If there is more than one metal ion species present, all the species are assumed to adsorb as separate components. The adsorption of the various components is, however, interrelated through electrostatic interactions.

Fully Coupled Adsorption

Consider an ensemble of identical acid organic polyelectrolytes with n different types of functional groups, each type i with a proton association reaction given by Eqn. 1 with a $K_{i,H}^{int}$ and $K_{i,H}^{app}$ defined by Eqns. 2 and 3 respectively. In the case of formation of a monodentate surface complex with a divalent metal ion M^{2+}, the binding can be represented by:

$$S_iO^- + M^{2+} \rightleftharpoons S_iOM^+ \qquad (25)$$

Bidentate complexes are considered under Discussion. Equation 25 can be characterized by an intrinsic equilibrium constant $K_{i,M}^{int}$:

$$K_{i,M}^{int} = \frac{\{S_iOM^+\}}{\{S_iO^-\}[M^{2+}]\exp\left(-2\dfrac{F\psi_s}{RT}\right)} \tag{26}$$

or by the apparent affinity coefficient $K_{i,M}^{app}$:

$$K_{i,M}^{app} = \frac{\{S_iOM^+\}}{\{S_iO^-\}[M^{2+}]} \tag{27}$$

The degree of metal complexation $\theta_{i,M}$ by the groups of type i can be expressed as:

$$\theta_{i,M} = \frac{\{S_iOM^+\}}{\{S_iO^-\}+\{S_iOH\}+\{S_iOM^+\}} \tag{28}$$

The combination of Eqn. 28 with Eqns. 2 and 26 leads to:

$$\theta_{i,M} = \frac{K_{i,M}^{int}[M^{2+}]\exp\left(-2\dfrac{F\psi_s}{RT}\right)}{1+K_{i,H}^{int}[H^+]\exp\left(-\dfrac{F\psi_s}{RT}\right)+K_{i,M}^{int}[M^{2+}]\exp\left(-2\dfrac{F\psi_s}{RT}\right)} \tag{29}$$

Equation 29 is the multi-component local adsorption isotherm for metal ion adsorption. For a simpler notation M_s, the metal ion concentration in the diffuse layer near the functional groups is defined as:

$$M_s \equiv [M^{2+}]\exp\left(-2\dfrac{F\psi_s}{RT}\right) \tag{30}$$

The substitution of H_s (Eqn. 6) and M_s into Eqn. 29 leads to an expression which is mathematically identical with the multi-component Langmuir isotherm equation:

$$\theta_{i,M} = \frac{K_{i,M}^{int}M_S}{1 + K_{i,H}^{int}H_S + K_{i,M}^{int}M_S} \tag{31}$$

Note that for fully coupled adsorption $\theta_{i,H}$ has to be redefined:

$$\theta_{i,H} = \frac{\{S_iOH^+\}}{\{S_iO^-\} + \{S_iOH\} + \{S_iOM^+\}} \tag{32}$$

Along the same line of reasoning as for the metal ion, the following multi-component local proton adsorption isotherm equation results:

$$\theta_{i,H} = \frac{K_{i,H}^{int}H_S}{1 + K_{i,H}^{int}H_S + K_{i,M}^{int}M_S} \tag{33}$$

For a discrete affinity distribution, the overall metal ion adsorption is given by a weighted summation of $\theta_{i,M}$ (Eqn. 31) similar to Eqn. 8. For a continuous distribution and fully coupled adsorption, Eqn. 24 can be simplified to a single integral equation because $\log K_{i,M}^{int}$ can be expressed as $\log \beta K_{i,H}^{int}$, where β is a constant (59).

For a few specific distribution functions and with Eqn. 31 as the local isotherm, the multi-component overall isotherm can be expressed in a relatively simple form. For the Sips distribution (34) the following result is obtained (59):

$$\theta_{T,M} = \frac{\tilde{K}_M M_S}{\tilde{K}_H H_S + \tilde{K}_M M_S} \cdot \frac{\left(\tilde{K}_H H_S + \tilde{K}_M M_S\right)^m}{1 + \left(\tilde{K}_H H_S + \tilde{K}_M M_S\right)^m} \tag{34}$$

where $\tilde{K}_M$ is an average K_M^{int} value fixing the position of the metal ion distribution function.

The association reactions (Eqns. 25 and 1) show that both metal ion and proton adsorption affect the charge of the polyelectrolyte. For coupled adsorption the charge is given by:

$$Q = Q_{max}(1 - \theta_{T,H} - \theta_{T,M}) - Q_{max}(\theta_{T,M}) \qquad (35a)$$

or

$$Q = Q_{max}\left(1 - \theta_{T,H} - 2\theta_{T,M}\right) \qquad (35b)$$

The first term in the RHS of Eqn. 35a is related to the charge contribution of the negatively charged SO^- species, the second term to the charge contribution of the positive SOM^+ species. Note that the minus sign in front of the contribution of the positive SOM^+ species ($\theta_{T,M}$) is due to the definition of Q_{max} (Eqn. 12).

The surface potential and hence pH_S and pM_S can be calculated from the surface charge with an electrostatic model in the manner described in the first section of this paper. Preferably the double layer model is determined from the proton adsorption curves. The experimental determination of the surface charge in the presence of metal ions can be made at each equilibrium pH and pM value by the combination of (1) the charge of the colloid in the absence of metal ions Q_H, (2) the metal ion adsorption Γ_M and (3) the metal ion/proton exchange ratio r_{ex}:

$$Q = Q_H + (2 - r_{ex})F\Gamma_M \qquad (36)$$

where

$$r_{ex} = \frac{\Delta\Gamma_H}{\Gamma_M} \qquad (37)$$

and $\Delta\Gamma_H$ is the difference between Γ_H at the equilibrium pH in the absence of metal ions and Γ_H in the presence of metal ions.

Metal ion affinity distribution

In the case of fully coupled adsorption the determination of the metal ion affinity distribution from metal ion adsorption data is complicated

because the local isotherm for metal ion adsorption has a multi-component character. However, the shape of the metal ion affinity distribution follows directly from the proton affinity distribution and only the value of $\bar{K}_M$, fixing the position of the metal affinity distribution, has to be determined from the metal adsorption data.

Uncoupled Adsorption

Consider an ensemble of identical acid organic polyelectrolytes with n different types of functional groups for the protons and m different types of functional groups for the metal ions. In that case the protonation reactions are given by Eqns. 1-10 and the complexation reaction of a M^{2+} ion with a metal ion site j is given by:

$$S_j + M^{2+} \rightleftharpoons S_j M^{2+} \tag{38}$$

In Eqn. 38 only the charge contribution of the metal ion is taken into account. The overall surface charge is the sum of the charges due to proton adsorption and metal ion complexation. Note further that with uncoupled adsorption the formation of multidentate complexes is treated simply as the complexation of M^{2+} on a certain S_j site given by Eqn. 38. This illustrates that the site S_j can have a complex structure and does not correspond with the proton sites.

Eqn. 38 can be characterized by a $K_{j,M}^{int}$ defined as:

$$K_{j,M}^{int} = \frac{\{S_j M^{2+}\}}{\{S_j\}[M^{2+}]\exp\left(-2\dfrac{F\psi_s}{RT}\right)} \tag{39}$$

For uncoupled adsorption the degree of metal complexation for a group of type j is expressed relative to the total number of metal ion sites of type j:

56

$$\theta_{j,M} = \frac{\{S_j M^{2+}\}}{\{S_j M^{2+}\}+\{S_j\}} \qquad (40)$$

The substitution of the definition of $K_{j,M}^{int}$ in Eqn. 40 followed by introduction of M_S (Eqn. 30) results in the following mono-component Langmuir type adsorption equation:

$$\theta_{j,M} = \frac{K_{j,M}^{int}M_S}{1+K_{j,M}^{int}M_S} \qquad (41)$$

The overall metal ion adsorption for various types of heterogeneity is given by Eqn. 8 or Eqn. 9 with H replaced by M and i by j and by using Eqn. 41 as the local isotherm.

For the Sips distribution with $\tilde{K}_M$ as the peak value and μ as the heterogeneity parameter, the following isotherm equation results (59):

$$\theta_{T,M} = \frac{\left(\tilde{K}_M M_S\right)^\mu}{1+\left(\tilde{K}_M M_S\right)^\mu} \qquad (42)$$

Remember that in the uncoupled case $\tilde{K}_M$ and μ are not related to the $\tilde{K}_H$ and m of Eqn. 19.

The overall smeared out surface charge is given by:

$$Q = Q_{H,max}(1-\theta_{T,H})+Q_{M,max}\theta_{T,M} \qquad (43)$$

with

$$Q_{M,max} = 2\Gamma_{M,max}F \qquad (43a)$$

At first sight Eqn. 43 and Eqn. 36 (the surface charge for the fully coupled case) look very similar. Note however the different definitions of $\theta_{j,M}$ and $\theta_{T,M}$ between the fully coupled case (Eqns. 31-34) and the uncoupled case (Eqns. 39-42). As before Q can be converted into σ_S or Z and can be used to

calculate the surface potential ψ_s using the double layer model which was assessed on the basis of the proton adsorption data.

Metal ion affinity distribution

Because in the uncoupled situation the overall metal adsorption is only a function of M_s and not of H_s, experimental adsorption data replotted as a function of pM_s have to merge into one master curve. The extent to which the $\theta_{T,M}(pM_s)$ data merge determines whether or not we are dealing with uncoupled adsorption. With the SP-LOGA-1 method the intrinsic affinity distribution can be obtained from the $\theta_{T,M}(pM_s)$ data.

Comparison of Coupled Adsorption and Uncoupled Adsorption on the Basis of Model Calculations

In this section the differences between coupled adsorption and uncoupled adsorption will be illustrated on the basis of model calculations. In order to show the effect of the competition most clearly, the same Sips distribution functions are chosen for both cases. For the coupled case the distributions are given by log $\tilde{K}_H$=5 and log $\tilde{K}_M$=5 and m=0.25. For the uncoupled case the proton distribution is given by log $\tilde{K}_H$=5, m=0.25 and the metal ion distribution by log $\tilde{K}_M$=5, μ=0.25. The electrostatics have been calculated with the Gouy-Chapman model.

In Fig. 8 the adsorption (a,b), and the exchange ratio (c,d) are calculated for the uncoupled case (b,d) and the fully coupled case (a,c) for several pH values. In the uncoupled case the metal ion adsorption isotherms show a considerable pH dependence because the overall surface charge depends on the protonation of the surface. In the fully coupled case, owing to the site competition, the M adsorption is even more strongly pH dependent. In both cases, however, the pH dependence becomes smaller, the higher the pH. Eventually the pH dependence disappears at very high pH values, as the overall surface is almost fully deprotonated in both cases. Therefore, the contribution of $\theta_{T,H}$ to the overall surface charge is negligible and the surface charge becomes independent of pH. Further, for the fully coupled

case the local multi-component adsorption equation, Eqn. 33, simplifies at these high pH values to a one-component adsorption isotherm because the $K_{i,H}{}^{int}H_S$ term is negligibly small in this case. For the example chosen this implies that the adsorption becomes identical in both cases.

In the uncoupled case, there is already considerable amount of metal ion adsorption at high pM because of the absence of site competition. In the coupled case at high pM the protons are competitors and the metal ion complexation will be smaller than for comparable uncoupled adsorption. Another important parameter is r_{ex}, which is quite different in both cases (see fig 8c,d). In the uncoupled case r_{ex} results only from the indirect influence of the surface charge and is relatively low. In the fully coupled case, at pH values where the surface is initially considerably protonated, extra protons have to be released from the surface in order to make sites available for metal ion adsorption. In this case r_{ex} is close to 1. Hence the r_{ex} in the coupled case is larger than that in the uncoupled case. The lower the value of r_{ex}, the larger is the decrease in overall negative surface charge on metal ion adsorption. The value of r_{ex} and the slope of the metal ion isotherm are related. The lower r_{ex} is, the larger is the electrostatic effect, and the lower the slope of the isotherm.

An analysis of the adsorption data given as $\theta_{T,M}(pH)$ with LOGA-1 will result in apparent affinity distributions. Each apparent affinity distribution is determined by both electrostatic and surface heterogeneity effects (60). Owing to the complex effect of electrostatics, the relationship between the apparent heterogeneity and the intrinsic heterogeneity is not obvious. Even in the very simple case of uncoupled metal ion adsorption it is difficult to obtain an insight into the intrinsic affinity distribution from the apparent affinity distribution. This is illustrated in Fig. 9a where the apparent metal ion affinity distributions obtained for the uncoupled adsorption isotherms of Fig. 8b are plotted. As could be expected from the shape of the isotherm, these distributions are rather wide and flat. The intrinsic metal ion affinity distribution is plotted as a reference. None of the apparent affinity distributions shows a correspondence with the intrinsic affinity distribution. The apparent affinity distributions exaggerate the degree of surface heterogeneity and are pH dependent.
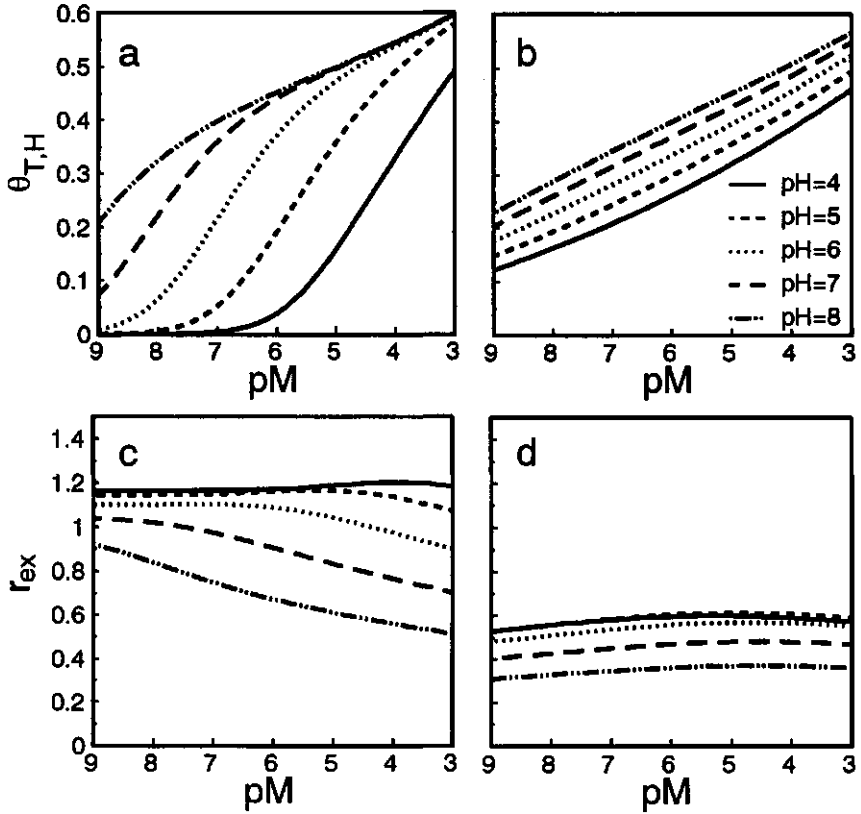
Figure 8. Calculated adsorption isotherms (a,b), and metal proton exchange ratio (c,d) for the formation of SOM surface complexes at pH 4,5,6,7 and 8. In figs. a and c, fully coupled adsorption is assumed with log $\tilde{K}_H$=5.0; log $\tilde{K}_M$=5.0 and m=0.25. In figs b and d, uncoupled adsorption is assumed with log $\tilde{K}_H$=5.0; m=0.25 and log $\tilde{K}_M$=5.0 and μ=0.25. The ionic strength has been set to 0.1. The proton and the metal site densities have been fixed at 1.0 sites.nm^{-2} (1.66x10-6 mol.m^{-2}) in both cases.

The intrinsic affinity distribution reflects only the heterogeneity of the surface and is to be preferred over an apparent distribution. In the uncoupled case, the intrinsic metal ion affinity distribution can be obtained by analysing the adsorption data replotted as function of pM_s. The result is shown in Fig. 9b and c. For the well defined case used in this example, all of the data points merge exactly into a single 'master curve', see Fig. 9b. The f_{LOGA-1} (log K_M^{int}) distribution (Fig. 9c) obtained from the $\theta_{T,M}(pM_s)$ 'master curve' (Fig. 9b) corresponds very well with the true affinity distribution.
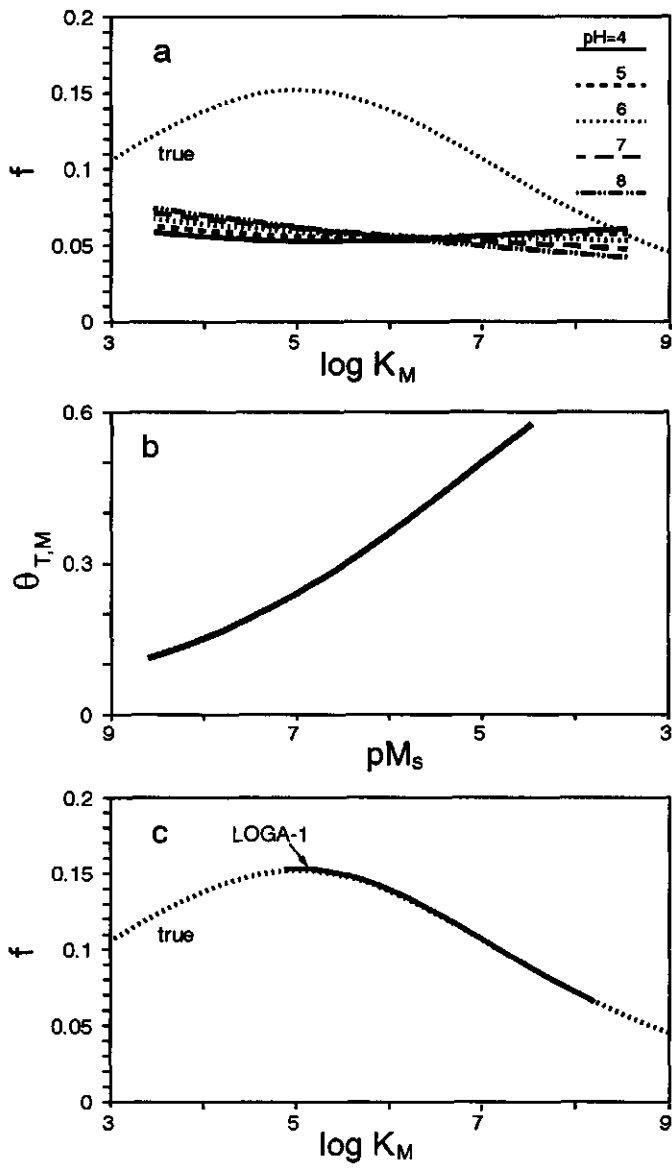
Figure 9. (a) Apparent affinity distributions; (b) the $\theta_{T,M}(pM_s)$ 'master curve'; (c) the intrinsic affinity distribution (c) obtained from this 'master curve' for the uncoupled metal ion adsorption data presented in Fig. 8b. The distributions are obtained from the application of the LOGA-1 method. As a reference the true intrinsic distribution is plotted in figures (a) and (c).

61

Discussion

As indicated above, owing to the complexity of metal ion adsorption, assumptions have to be made about the nature of the metal ion adsorption process in order to describe the adsorption data. In our opinion, a first step in the analysis of metal ion adsorption data is to test whether or not one of the limiting cases (uncoupled adsorption or fully coupled adsorption) suffices for a description.

For uncoupled adsorption $\Gamma_{T,M}(pM_S)$ curves can be calculated relatively easily. When a series of adsorption isotherms measured under different conditions, merges into one 'master curve' when plotted as $\Gamma_{T,M}(pM_S)$ then the uncoupled description suffices and the intrinsic heterogeneity can be determined. This procedure was illustrated for the formation of S_jM species (Eqn. 38) but it can be easily adapted for the formation of different surface species, such as S_jMOH. In this case the metal species in solution is MOH and the $\Gamma_{T,M}(pMOH_S)$ curves should merge into one 'master curve'.

When the above procedure is unsuccessful the fully coupled case can be tested. For the fully coupled case the shape of the intrinsic distribution function is obtained from the analysis of the proton adsorption isotherms, its position from fitting $\tilde{K}_M$ on the basis of the metal adsorption data. The assumption that we are dealing with fully coupled adsorption is justified if the adsorption data can be described well with one value of $\tilde{K}_M$ independent of pH and ionic strength. For every different monodentate surface species formed one $\tilde{K}$ has to be specified.

A special case of fully coupled adsorption may occur with the formation of a bidentate surface complex. It is known from coordination chemistry that metal ions often form multidentate complexes or chelates with functional groups which are in close proximity. In the literature (4,6-8,10,20), particular attention is given to the formation of bidentate metal complexes with phthalic acid- and salicylic acid-like structures in humic and fulvic acids. Salicylic and phthalic acid groups can be treated as $S_iO_2^{2-}$ groups, which can be protonated in two consecutive steps. A rigorous analysis of bidentate metal ion binding in the coupled case is rather complicated because the affinity distribution of the bidentate sites can in general not be derived

directly from the total proton affinity distribution.

However, at pH values below 6.5 the fraction of the fully deprotonated $S_iO_2^{2-}$ species is negligible with respect to the fraction of the $S_iO_2H_2$ and $S_iO_2H^-$ species (14). On the basis of model calculations it has been demonstrated that as long as the fraction of the $S_iO_2^{2-}$ species is small, the description of the bidentate adsorption is equivalent to that of the formation of an S_iOMOH complex (14). Hence, at low pH values fully coupled bidentate adsorption can be described as fully coupled S_iOMOH adsorption.

If neither fully coupled nor uncoupled adsorption suffices for the description of metal ion adsorption, other simplifications have to be made in order to describe the metal ion adsorption. One may also be satisfied by a less rigorous description and obtain "conditional" metal ion affinity distributions. Such a "conditional" metal ion affinity distribution can be obtained by considering the metal ion adsorption as fully uncoupled. The adsorption isotherms measured, say, at different pH values and at specific ionic strengths are replotted as $\Gamma_{M,T}(pM_S)$ curves, so that the electrostatic effect is eliminated. The conditional affinity distributions can be obtained by applying the SP-LOGA-1 method to the $\theta_{M,T}(pM_S)$ curves at the different pH values. The derived distributions are not only related to the type of surface groups but also to their state of protonation at the particular pH and salt concentration. In other words, with the conditional affinity distribution the metal ion affinity for, say a R-COOH group and the corresponding R-COO⁻ group can be discriminated. The information obtained in this way can be compared with information obtained from other sources such as spectroscopic techniques.

Conclusions

- Two prime factors influencing ion binding to natural polyelectrolytes are the variable potential of the particles and chemical heterogeneity.

- With an appropriate double layer model, it is possible to eliminate the electrostatic effects from the proton binding-pH curves, leading to a proton adsorption 'master curve' which is independent of the salt level.

- The intrinsic proton affinity distribution can be derived from the

63

proton 'master curve'.

- For metal ion adsorption assumptions have to be made in order to determine the intrinsic affinity distribution .

- In the case of fully coupled adsorption, it is assumed that the shape of the intrinsic metal ion affinity distribution is the same as that of the proton affinity distribution, the only difference being the position on the affinity axis.

- In the case of uncoupled adsorption the metal ion adsorption is assumed to be fully independent of the proton adsorption. In this case the metal ion affinity distribution can be assessed in a manner comparable with that for the proton distribution.

- Model calculations show that apparent metal ion affinity distributions do not resemble the intrinsic metal ion affinity.

Acknowledgement

References

1   C.J.M. Kramer and J.C. Duinker (Eds.), Complexation of Trace Metals in Natural Waters. Martinus Nijhoff, The Hague, 1984.

2   J. Buffle, in Sigel (Ed.), Metal Ions in Biological Systems, Vol 18, Circulation of Metal in the Environment, Marcel Dekker, New York, 1984, Ch. 6.

3   G. Sposito, CRC Critical Rev. Environ. Control, 16(1986)193.

4   J. Buffle, Complexation Reactions in Aquatic Systems: An Analytical Approach,

Ellis Horwood Limited, Chichester, 1988.

5   M. Schnitzer and S.U. Khan, Humic Substances in the Environment, M. Dekker, New York, 1972.

6   M. Schnitzer, in M. Schnitzer and S.U. Khan (Eds.), Soil Organic Matter, Developments In Soil Science 8, Elsevier, Amsterdam, 1978, Ch.1.

7   F.J. Stevenson, Humus Chemistry. Genesis, Composition, Reactions. Wiley-Interscience, New York, 1982.

8   D.S. Gamble, A.W. Underdown and C.H. Langford, Anal. Chem. 52(1980)1901-1908.

9   A.M. Posner Trans. Int. Congr. Soil Sci., 8th, Meeting Date 1964, 3(1967)161.

10   H. van Dijk, Geoderma, 5(1971)53.

11   D.E. Wilson and P. Kinney, Limnol. Oceanogr. 22(1977)281.

12   F.J. Stevenson, Soil Sci. Soc. Am. J. 40(1976)665.

13   I. Lamy, M. Cromer, and J.P. Scharff Anal. Chim. Acta, 212(1988)105.

14   J.C.M. de Wit, W.H. van Riemsdijk and L.K. Koopal, Proceedings "Second International Symposium on Metal Speciation, Separation and Recovery", Rome, May 14-19 1989, Lewis Publishers, Chelsea, USA, in Press

15   M.M. Nederlof, W.H. van Riemsdijk and L.K. Koopal, Determination of adsorption distributions: a general framework for methods related to local isotherm approximations, J.Colloid and Interface Sci., in press.

16   L.K. Koopal, M.M. Nederlof and W.H. van Riemsdijk, Progress in Colloid and Polymer Sci. 81(1989), in press.

17   T.W. Healy and L.R. White, Adv. Colloid Interface Sci. 9(1978)303.

18   C.W. Davies, Ion Association, Butterworth, London, 1962.

19   C. Tanford, Physical Chemistry of Macromolecules, Wiley, New York, 1961.

20   Tipping, E., C.A. Backes and M.A. Hurley. Wat. Res. 22(1988)597.

21   J. Th. G. Overbeek, in Kruyt, H.R., Colloid Science, Vol. 1, Elsevier, 1952, pp. 115-193.

22   G. Gouy, J. Phys., 9(1910)457.

23   D.L. Chapman, Philos. Mag., 6(1913),475.

24   A.L. Loeb, J. Th. G. Overbeek and P.H. Wiersema. M.I.T. Press,Cambridge, USA, 1961.

25   D. Stigter, J. Electroanal. Chem. 37(1972)61.

26   P.A. Arp, Can. J. Chem. 61(1983)1671.

27   A. Katchalsky, Pure Appl. Chem. 26(1971)327.

28   G.S. Manning, Q. Rev. Biophy. 11(1978)179.

29   D. Stigter, J. Colloid Interface Sci. 53(1975)296.

30   D. Stigter, Cell Biophysics 11(1987)139.

31   W.P.J.T. Van der Drift, A. de Keizer and J. Th. G. Overbeek, J. Colloid Interface Sci. 71(1979)67.

32   Th. Odijk, J. Polym. Sci. Polym. Phys. Ed. 15(1977)477.

33   Th. Odijk and A.C. Houwaart, J. Polym. Sci. Polym. Phys. Ed. 16(1978)627.

34   R. Sips, J. Chem. Phys. 16(1948)490.

35   W.H. van Riemsdijk, G.H. Bolt, L.K. Koopal and J. Blaakmeer, J. Colloid Interface Sci. 109(1986)219.

36   W.A. House J. Colloid Interface Sci. 67(1978)166.

37   S. Ross and I.D. Morrison, Surface Sci. 52(1975)103.

38   C.H.W. Vos and L.K. Koopal, J. Colloid Interface Sci. 105(1985)183.

39   R.S. Altman and J. Buffle, Geochim. Cosmochim. Acta 52(1988)1505.

40   S.S. Roginsky, Adsorption and Catalysis on Heterogeneous Surface, Academy of Sciences of U.S.S.R., Moscow 1948 (in Russian).

41   L.B. Harris, Surface Sci. 10, 129 (1968).

42   G.F. Cerofolini, Surface Sci. 10(1971)391.

43   C.C. Hsu, B.W. Wojciechowski, W. Rudzinski and J. Narkiewicz, J. Colloid Interface Sci. 67(1978)292.

44   W. Rudzinski and J. Jagiello, J. Low. Temp. Phys. 45(1981)1.

45   W. Rudzinski, J. Jagiello and Y. Grillet, J. Colloid Interface Sci. 87(1982)478.

46   K. Ninomiya and J.D. Ferry, J. Colloid Interface Sci. 14(1959)36.

47   D.L. Hunston, Anal. Biochem. 63(1975)99.

48   A.K. Thakur, P.J. Munson, D.L. Hunston and D. Rodbard, Anal. Biochem. 103(1980)240.

49   M.M. Nederlof, W.H. van Riemsdijk and L.K. Koopal, Proceedings "Heavy Metals in the Environment, Vol II ", 7th Int. Conf. Geneve, September 12-15 1989,

CEP consultants Ltd. Edinburgh, UK, p.400.

50   M.M. Nederlof, W.H. Van Riemsdijk and L.K. Koopal, in M. Astruc and J.N. Lester (Eds.) Heavy Metals in the Hydrological Cycle, Selper Ltd., London, 1988, p.361.

51   I. J. Schoenberg Proc. N.A.S. 52(1964)947.

52   C.M. Reinsch, Numer. Math. 16(1971)451.

53   K. Ghosh and M. Schnitzer, Soil Sci. 129(1980)266.

54   D.R. Turner, M.S. Varney, M. Whitfield, R.F.C. Mantoura and J.P. Riley, Geochim. Cosmochim. Acta 50(1986)289.

55   J. Ephraim, S. Alegnet, A. Mathuthu, M. Bicking, R.L. Malcolm and J.A. Marinsky, Envir. Sci. Technol. 20(1986)354.

56   J.A. Marinsky, A. Wolf and K. Bunzl, Talanta 27(1980)461.

57   G.G. Leppard, J. Buffle and R. Baudat, Wat. Res. 20(1986)185.

58   S. Ljung, Fast Algorithms for Integral Equations and Least Squares Identification Problems. Linköping Studies in Science and Technology. Dissertations. no 93, Linköping, 1983.

59   W.H. van Riemsdijk, J.C.M. de Wit, L.K. Koopal and G.H. Bolt, J. Colloid Interface Sci. 109(1986)219.

60   W.H. Van Riemsdijk, L.K. Koopal and J.C.M. De Wit. Netherlands J. Agricultural Sci. 35(1987)241.

Chapter 3

Proton Binding to Humic Substances.

A. Electrostatic Effects.

Abstract

Ion binding to humic substances is influenced by the chemical heterogeneity and by the variable charge behaviour of the humics. In this paper we concentrate on the variable charge effects. To study these effects acid/base titration data of 11 humic substances, measured at a series of salt levels are analyzed. In a first order approach the organic matter molecules are treated as an ensemble of small rigid and impermeable cylindrical or spherical particles of a certain size and a variable surface charge density depending on pH and salt concentration. With double layer models for such particles the electrostatic effects on the proton binding can be described reasonably well. When the density of the humic material is used as a constraint the radius of the spheres or the cylinders is the only adjustable parameter in the model. The particle radii of the humic studied range from 0.6 to 4.4 nm, with 0.85 nm as median for the spherical double layer model. For the cylindrical double layer model the assessed radii are smaller and range from 0.19 to 2.5 nm, with 0.32 nm as median. The obtained molecular dimensions correspond reasonably well to data reported in literature. Apparently in the samples under consideration the polydispersity effects and conformational changes due to electrostatic are of second order.

.

70

Introduction

Knowledge of the speciation of trace metal ions in the environment is essential for understanding the (bio-)availability of these ions and for a correct risk assessment. Complexation of trace metals with small inorganic ligands in the solution phase is relatively well known (1-3) and several models for the calculation of the chemical equilibrium exist (4-5). The binding of metal ions to the solid and suspended phase is not yet resolved satisfactory and no consensus of opinion exists about the modelling. This holds especially for the metal ion binding to humic substances, like fulvic acids and humic acids (6-8).

Humic substances are complex and ill defined polydisperse mixtures of heterogeneous organic polyelectrolytes (9-13). The metal binding capacity of humic substances finds its origin in the presence of functional groups, for instance carboxylic and phenolic groups: metal ions form complexes with the functional groups. Due to the large variety of different functional groups, even within a given humic substance, these materials should be considered as heterogeneous ligands. The chemical heterogeneity, or the distribution of the affinity constants for the different functional groups is in general unknown. In this paper a procedure for the characterization of the chemical heterogeneity of humic substances, based on the analysis of proton binding curves (14-18) is further elaborated.

Protons determine the state of the functional groups. At low pH the functional groups are protonated and uncharged, at higher pH the functional groups dissociate and become negatively charged. Around charged particles a diffuse double layer develops (e.g. 19-20). The double layer screens the charge so that the overall system remains uncharged. In the case of a negatively charged particle the concentration of the positively charged metal ions and protons is larger in the double layer than in the bulk of the solution. This charge induced accumulation results to an increase of the specific binding of the positively charged ions. The background electrolyte ions, which dominate the composition of the bulk solution, determine the efficiency of the screening of the surface charge. At low ionic strength the electric field around the particle extends relatively

far in the solution and the double layer is thick. At high ionic strength a strong screening results in a thin double layer. The influence of the ionic strength on the electrostatics makes ion binding ionic strength dependent.

The dependency of the proton binding on the ionic strength can be used to assess an adequate model for the description of the diffuse double layer (e.g. 15-18, 21-23). The double layer model allows for the calculation of the electric potential at the surface of the humic particles and of the pH_s, the pH near the binding sites. When the proton binding curves measured at different salt levels are replotted as a function of pH_s, the salt dependency should vanish and all curves should merge into one master curve (16). The extent to which the curves merge is a measure for the adequacy of the double layer model used to calculate pH_s; if the curves do not merge the model description should be adapted or even rejected.

Since the electric effects are filtered out when transforming pH to pH_s, the master curve reflects the underlying chemical heterogeneity of the humic colloid (16,24). With the help of an affinity distribution analysis (e.g. 11,25-27), the intrinsic proton affinity distribution can be obtained from the master curve. The intrinsic affinity distribution can be used to select an appropriate proton binding equation.

Previous studies on some humic acid or fulvic acid samples (16-18) have shown that the electrostatic effects can be described rather well with the existing diffuse double layer models for rigid and impermeable spheres or cylinders (e.g. 19-20,28-29). In this paper the potential of such simple diffuse double layer models for the description of the electrostatics will be further evaluated by analysing the protonation of 11 different humic substances. In a subsequent paper the intrinsic affinity distribution for the samples and a model description for proton binding will be presented.

In the double layer models used we assume that all functional groups of the humic samples experience the same smeared-out electric potential. Both for the spherical and the cylindrical geometry this implies that all particles are characterized by the same average radius. When the density of the particles can be estimated independently, the radius is the

single adjustable parameter in the double layer models.

Especially when a spherical geometry is assumed various properties of the averaged particles can be calculated on the basis of the assessed radius. These properties are the size, the molecular weight, the specific surface area, as well as an indication of the number of reactive groups per particle, the reactive site density and the chemical heterogeneity. Because in this paper a large number of humic substances are analyzed an impression can be obtained of the range of these properties.

In this first order approach using double layer models assuming average sized rigid particles the polydisperse nature of the humics, their permeability and changes of conformation are not explicitly taken into account. When these phenomena are important the application of the simple double layer models should not result in curves which merge into one master curve. However, when a reasonably good master curve is obtained the effects mentioned are of second order and the use of simple double layer models is appropriate.

Double layer models for rigid and impermeable cylinders and spheres

According to the Boltzmann distribution law the concentration of ion i, at a certain position, x, in the electric field is given by (e.g. $19,20,29$):

$$c_i(x) = c_{i,0} \cdot \exp\left(-\frac{z_i F \psi(x)}{RT}\right) \tag{1}$$

where $c_{i,0}$ is the bulk concentration of i, z_i the charge number (including sign), $\psi(x)$ the electric potential at position x, T the temperature, F is Faraday's constant and R the gas constant.

Following Eq. (1) H_s, the concentration of the protons near the charged particle at the location of the binding sites can be defined as:

$$H_s = [H^+] \cdot \exp\left(-\frac{F\psi_s}{RT}\right) \qquad (2)$$

where ψ_s is the electric potential of the humic particle.

By treating the humic particles as hypothetical impermeable particles, with the different site types randomly distributed over the surface, one electrostatic potential ψ_s suffices to describe the electrostatic interactions. The effects of polydispersity, conformational changes and the permeability of the molecules are neglected for the moment.

For a known surface charge density, σ_s, the surface potential ψ_s can be calculated by solving the Poisson Boltzmann equation for a certain geometry of the electric field around the charged particles (e.g. *19,20,28-31*). For a spherical and a cylindrical geometry the radius is the single adjustable parameter for the calculation of ψ_s. The radius determines the curvature of the surface and the shape of the electric field. For spheres this may be clear, for cylinders this applies as long as the length of the cylinder is much larger than the radius so that the end effects can be neglected and the actual length of the cylinder is irrelevant.

A characteristic parameter in the diffuse double layer models is the reciprocal Debye Length κ:

$$\kappa^2 = \frac{F^2 \sum_i z_i^2 c_{i,0}}{\varepsilon_0 \varepsilon_r RT} \qquad (3)$$

where z_i is the valency of the ions, ε_0 is the permittivity of vacuum and ε_r is the dielectric constant.

The Debye length $1/\kappa$ can be seen as a measure of the thickness of the diffuse double layer. When the concentration of the electrolyte ion is high, κ is high and the Debye length is small which implies a strong screening of the electrostatic effects. The screening of the radial electric field around a sphere is more effective than the screening for the curvilinear field around a cylinder. In other words, for equal radii the salt

effect will be more pronounced in the case of a cylinder than in the case of a sphere. For both geometries the curvature of the surface becomes irrelevant for radii large with respect to the Debye Length and the electric field resembles that of the planar geometry.

The solution of the Poisson Boltzmann equation gives ψ_s as a function of the radius and the surface charge density, σ_s. The surface charge density σ_s is related to the measurable charge per unit mass, Q, by the specific surface area, S:

$$\sigma = \frac{Q}{S} \qquad (4)$$

The value of S is unknown. For some systems like oxides the specific surface area can be determined reasonably well with the BET method (eg. 32). For the humic colloids, however, it is known that the BET surface area, which is measured on the dried samples may only be a small part of the surface area which is exposed in solution (eg. 11). The BET surface area can therefore not be used for humics so that S is an adjustable parameter.

If both S and r are treated as adjustable parameters a whole series of combinations of S and r will lead to merging of the individual charge-pH curves in a master curve (15-18). In that case the obtained values of S and r are rather meaningless. However, when the density, ρ, is known it is not necessary to treat S as an adjustable parameter since both for rigid spheres and for cylinders S is a simple function of ρ and r:

$$S = \frac{a}{\rho r} \qquad (5)$$

where the constant a=3 for a sphere and a=2 for a cylinder.

Both Q and S are normally expressed per unit mass of the dry humic material. In solution the humic particles are hydrated and part of their volume will consist of water. The particle density in equation (9) is the mass of the dry humic material divided by its hydrated volume. Only when the density of the humic material is known the radius is the single

75

adjustable parameter for the calculation of ψ_S. The range in ρ is rather well established. The density of humic material determined with partial volume measurements ranges from 1400 to 1700 kg.m^{-3} (11,33-34). Humic and fulvic acids can easily absorb up to 100 (weight) % water (11). The humic acid density based on the hydrated volume may thus easily be half the density based on the partial volume. A sound combination of r and S should thus correspond to a value of ρ ranging from about 700 kg.m^{-3} to 1700 kg.m^{-3}.

For spheres the obtained combination of r and S leads to the molecular weight M_{sph}:

$$M_{sph} = \frac{4}{3}\pi r^3 N_{Av}\rho \qquad (6a)$$

or alternatively:

$$M_{sph} = \frac{4\pi r^2 N_{Av}}{S} \qquad (6b)$$

with N_{Av} is Avogadro's number.

The molecular weight M_{sph} that results from the master curve procedure is an electrostatic average molecular weight and its value can be compared to the molecular weights determined with other methods.

The expression for the molecular weight of the cylinder is not only related to r and ρ, but also to the (average) length l of the cylinder:

$$M_{cyl} = \pi r^2 l \rho N_{Av} \qquad (7)$$

The magnitude of l can not be determined experimentally. However, from some basic considerations the minimum value for l can be determined. For the cylindrical geometry we have assumed that the two end surfaces can be neglected compared to the cylinder surface. In other words, when the site density is everywhere the same, the surface area of the ends, A_{end} should be much smaller than the surface area of the cylinder, A_{sur}. This implicates that at least $A_{end}/A_{sur} << 0.1$ or $l/r >> 10$.

Table I. Origin and Characteristics of the humic substances studied.

name	reference	presentation	approximate molecular weight g.mol^{-1}	estimated Tmax meq.g^{-1} humus
FA#3	35-36	meq.g^{-1} TOC (pH)	1500-2500[a]; 5000-10000[b]	8.5[c]
FA#1	35-36	meq.g^{-1} TOC (pH)	1500-2500[a]; 5000-10000[b]	8.5[c]
Suwannee River Fulvic Acid	37	α(pH)	829[d]	5.6
Sweden	37	α(pH)	1000[e]	5.6
Armadale Horizons Bh Fulvic Acid	37	α(pH)	951[f]	5.6
Bersbo FA	38	pK^{app}(α)	1750[g]	4.65
LFHS	22	pH(Total Base)	15000	5.46
MBHA	22	pH(Total Base)		4.8
PRHS-A	22	pH(Total Base)	30000	2.98
Humic Acid	39	α(pH)		3.5
Peat	40	pK$^{app}_{(HA)v}$(α)		1.46

a determined with small-angle x-ray scattering (35-36)
b determined with gel-permeation (35-36)
c A factor of 2 was used to convert g TOC to g humic substances
d Aiken and Malcolm (41)
e Paxeus and Wedborg (42)
f Hansen and Schnitzer (43).
g Xu et al 1989 (44)

Application to Experimental Data

In contrast to the large array of metal ion binding data the number of proton titration data sets, measured at different constant salt levels is somewhat limited. In this paper 11 data sets are analyzed. The characteristics of the different sets are tabulated in table I. The names in table I correspond to the names used in the original papers.

All data sets are analyzed as Q(pH) curves. Most of the data sets were not presented as *raw* experimental data, but were already processed by the authors. The processing consists of the subtraction of the blank, the positioning of the curves relative to one another and the conversion of the relative charge ΔQ into the absolute charge Q. Although processing of titration data is often complicated and somewhat arbitrary, the Q(pH) curves are taken as published.

Data sets originally published as degree of dissociation, α, as a function of the pH were converted to Q with the help of the total functional group content, T_M, as given by the authors (eq.kg^{-1}):

$$Q = -T_M F\alpha \qquad (8)$$

Note that the normalization factor T_M is an operationally defined quantity, which not necessarily reflects all titratable sites. The published α values therefore not necessarily corresponds to the true degree of dissociation of the humic material (16,45).

For all data sets we have tried to obtain master curves for the cylindrical and the spherical double layer model. The results will be discussed below.

The Optimum Values of the Adjustable Parameters

The cylindrical and the spherical model result in equally well merging curves. In figure 1a the theoretical relationship between r and S for a spherical particle is given for three densities. The lower dashed curve corresponds to ρ=1700 (kg.m^{-3}), the middle curve to ρ=1000 (kg.m^{-3}) and the dashed curve to ρ=700 (kg.m^{-3}). The solid lines result for three of the humic samples when both r and S are treated as adjustable parameters. The bold parts of the curve correspond to physically realistic combinations of r and S. In figure 1b the same is done for the cylindrical geometry.
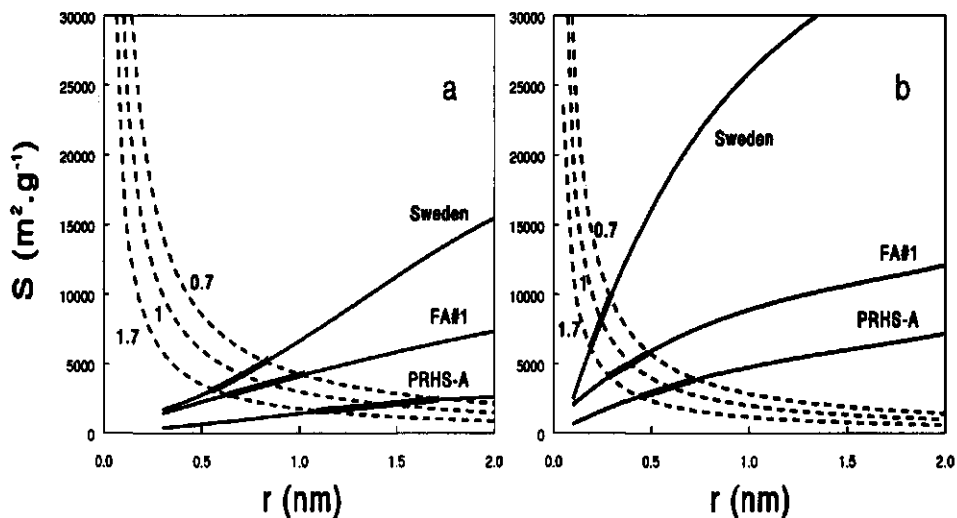
Figure 1. Combinations of S and r which result in good merging curves for the spherical double layer model (1a) and the cylindrical double layer model (1b) for three of the experimental data sets. The bold parts of the curves give the optimal combinations of S and r. The dashed curves show the theoretical relation of S and r for ρ is respectively 0.7, 1 and 1.7 g.cm^{-3}.

The assessed S(r) lines for the humic samples have a positive slope This can be easily understood; for a constant specific surface area an increase of the radius leads to an increase of the calculated salt effect in the charging curves. Since the salt effect is fixed by the experiment, the surface area has to increase in order to give rise to a lower calculated surface charge density. The lower charge density counter balances the effect of the increase of r.

The estimated range in density from ρ=700 to ρ=1700 (kg.m^{-3}) results in a narrow range of possible particle sizes (bold parts of fig 1a,b). Because the Q(pH$_s$) data obtained for this range of particle sizes are very similar, we will only present the results for ρ=1000 (kg.m^{-3}). This ρ value is a convenient value within the density range.

79

Individual Data and Master Curves

In the figs. 2 and 3 the experimental data sets are plotted together with the master curve obtained for the spherical and the cylindrical double layer model. Figure 2 contains the data sets which are titrated up to pH=11 (FA#3 and FA#1), fig. 3 the data sets titrated up to pH=8. In both figures the order of the datasets correspond to an increasing ionic strength effect. Figure 3 shows that an increasing ionic strength effect seems inversely proportional to the number of groups that is titrated. Especially the peat sample has a small acidity; even at pH=8, the negative charge is no more than 1.5 (eq.kg^{-1}).

In both figures a general point to notice is that the pH$_s$ values are smaller than the corresponding pH values. Due to the electric effects the proton concentration near the functional groups is larger than the concentration in the bulk of the solution. The difference between pH and pH$_s$ is not constant, but increases the more negatively charged the humic material is. This results in a pH$_s$ range that is smaller than the pH range. The transformation from pH into pH$_s$ does also influence the shape of the curve. The Q(pH$_s$) curve is steeper than the Q(pH) curves. The slope of the master curve is a measure of the degree of heterogeneity (14-18,24-25,46). Therefore the apparent heterogeneity underlying the Q(pH) curves is larger than the (intrinsic) heterogeneity underlying the Q(pH$_s$) curves.

In general the spherical and the cylindrical model result in equally well merging curves. The pH shift from pH to pH$_s$ is larger for the spherical double layer than for the cylindrical double layer model. The master curves of the spheres are shifted up to an extra 0.5 pH unit towards a lower pH. This is due to the fact that the calculated electrostatic interactions for the spherical double layer model are larger than those for the cylinders.

Figure 3. The experimental Q(pH) curves and the calculated $Q(pH_s)$ curves for the spherical and the cylindrical double layer model for the datasets which were titrated over a small. The optimal r for $\rho = 1$ g·cm^{-1} are used to construct the $Q(pH_s)$ curves. $\Diamond = 0.001$ M, $\nabla = 0.005$ M, $\triangle = 0.01$ M, $\blacktriangle = 0.02$ M, $O = 0.1$ M, $\bullet = 0.2$ M, $\square = 1$ M and $\blacksquare = 2$ M.

81
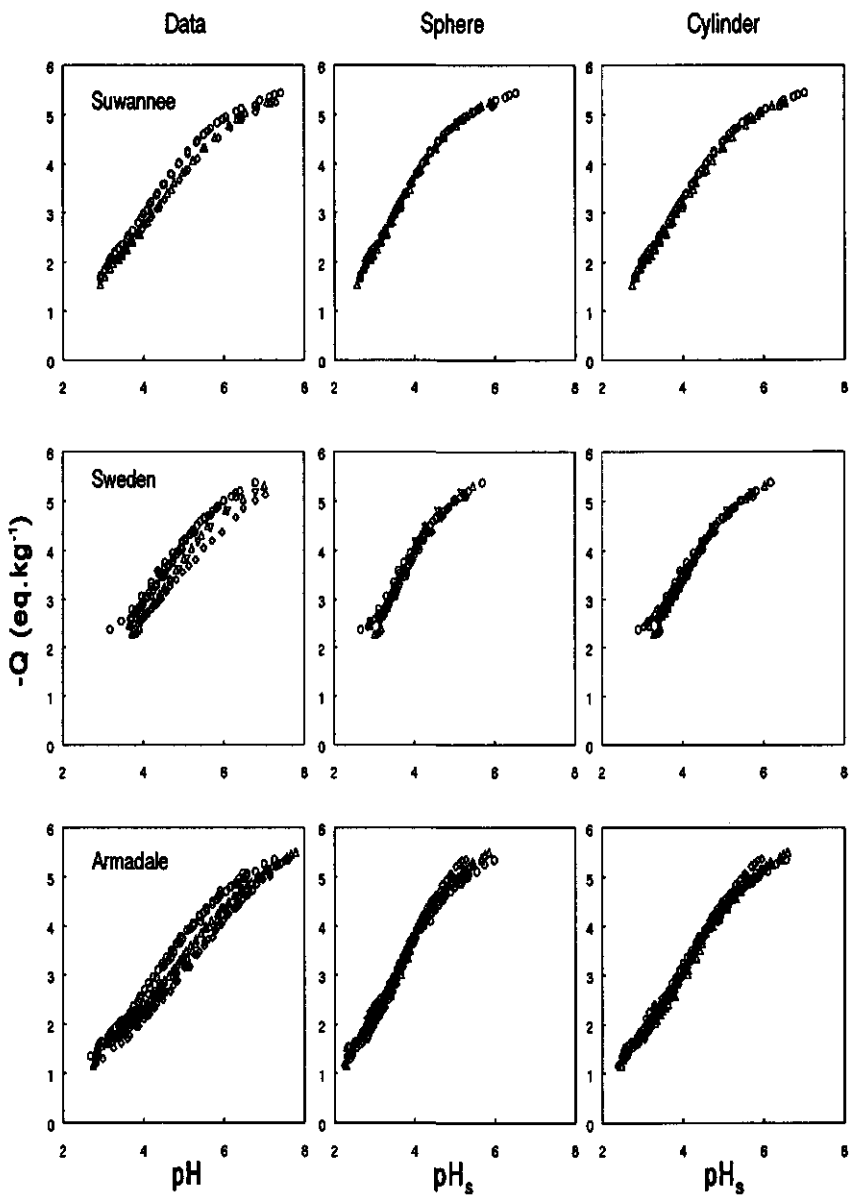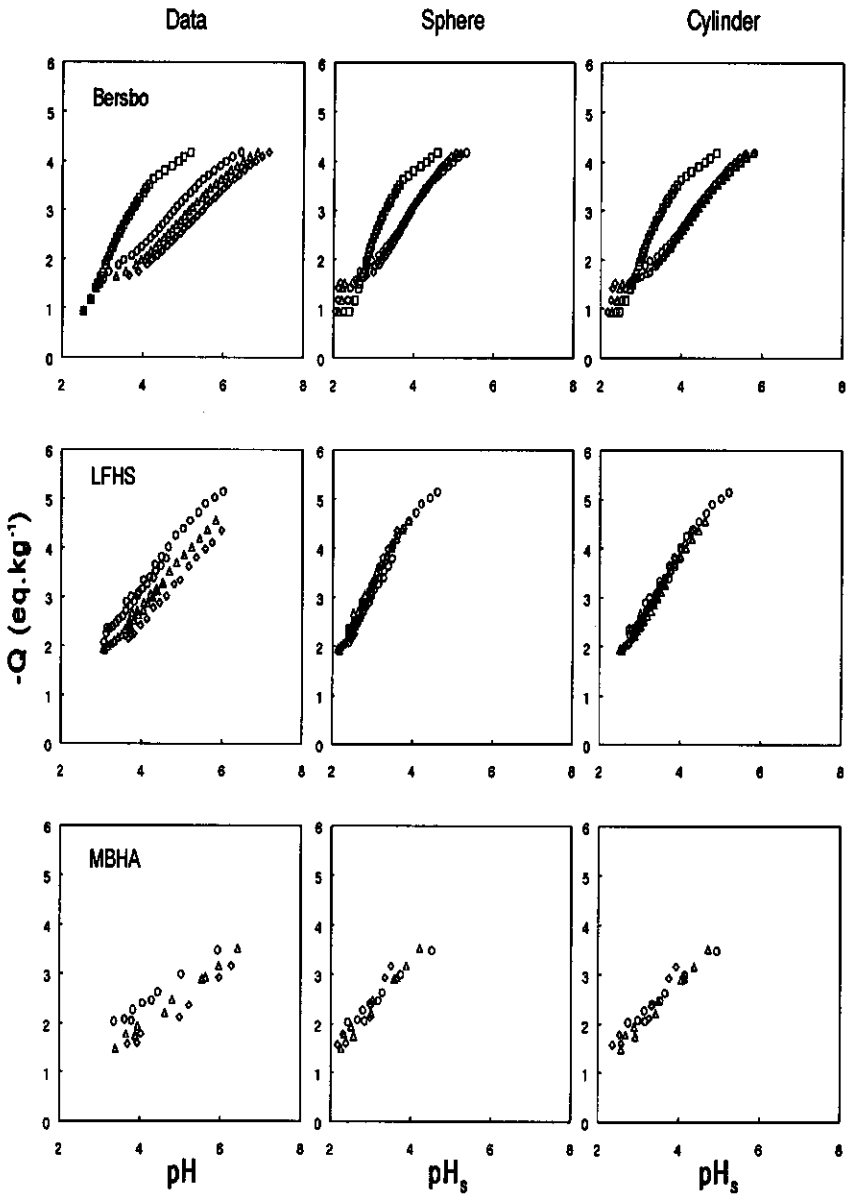
Figure 3.

Figure 3. (continued).
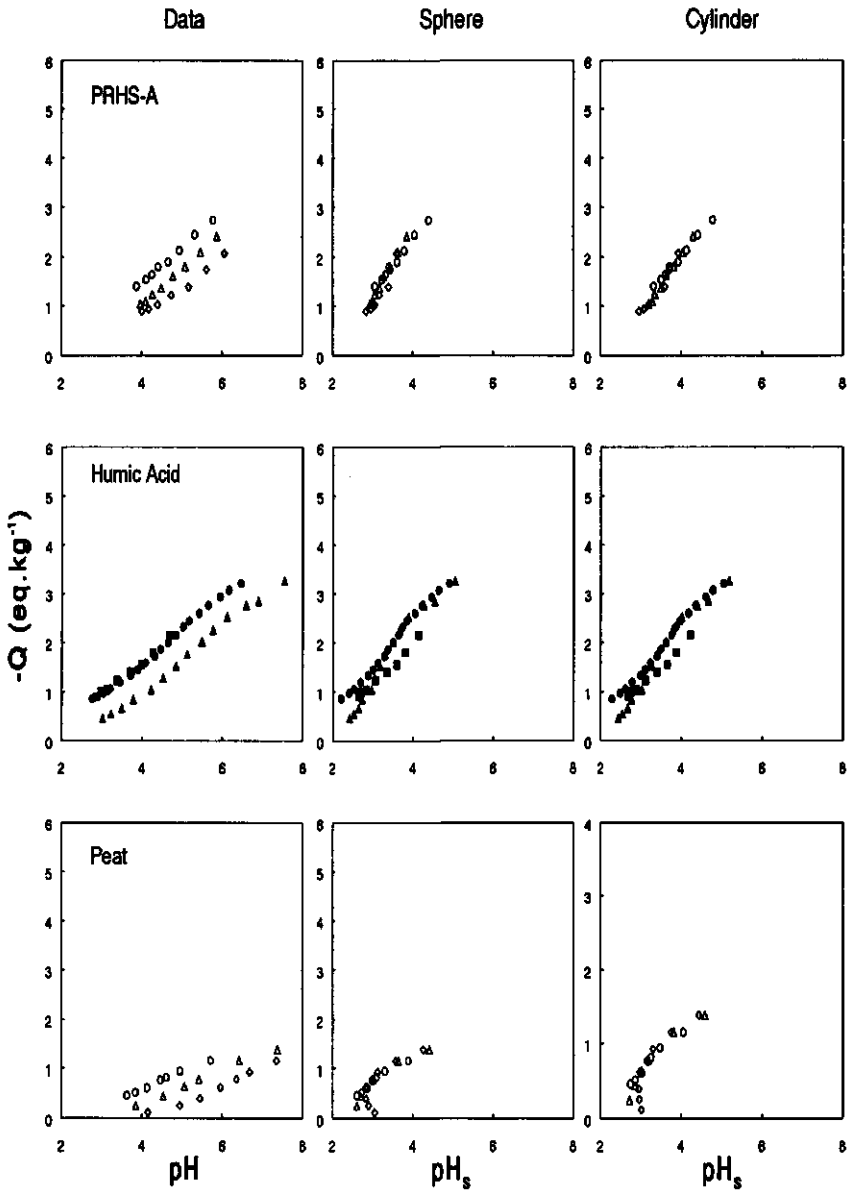
83

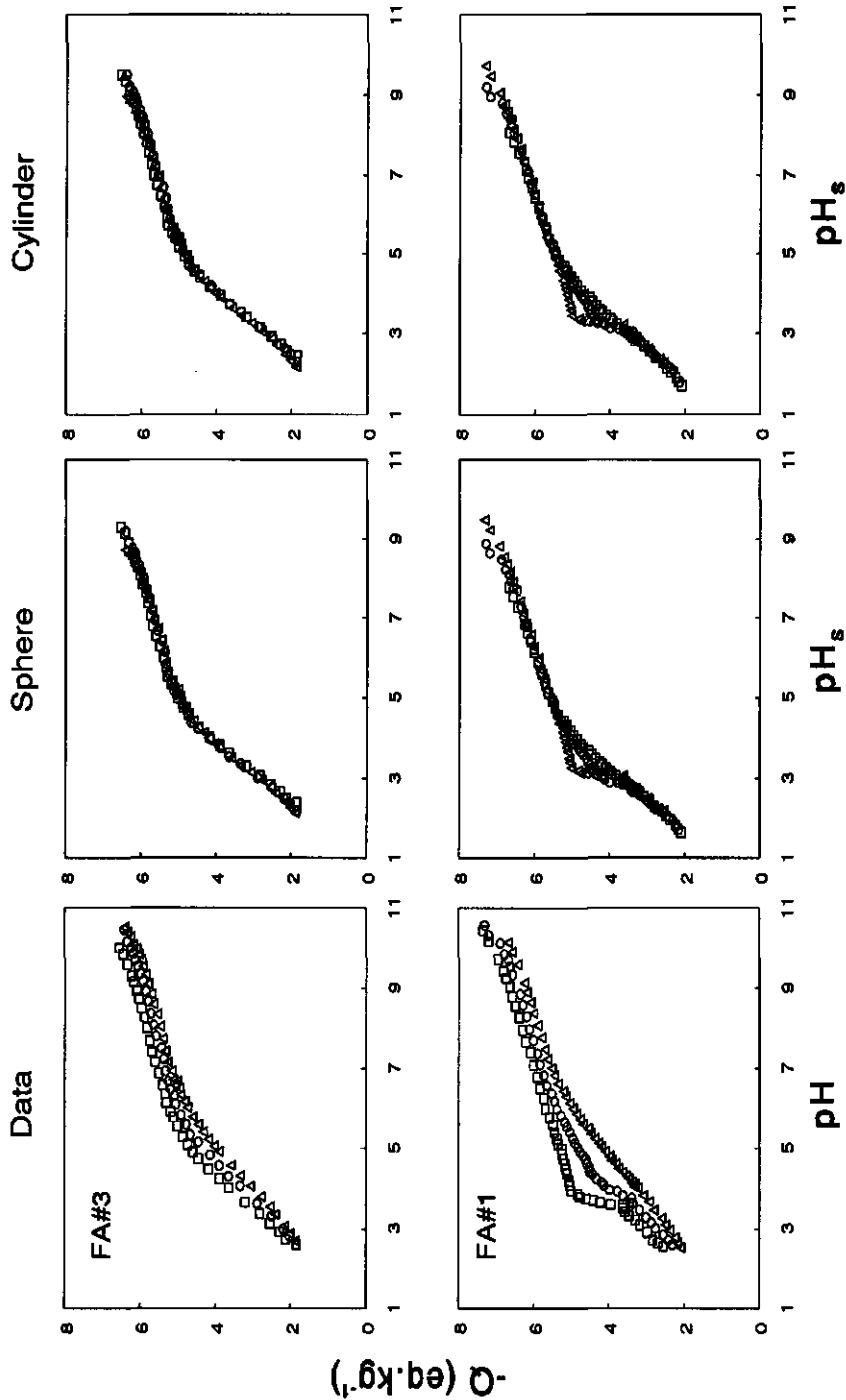**Figure 3.** The experimental Q(pH) curves and the calculated Q(pH$_s$) curves for the spherical and the cylindrical double layer model for the datasets which were titrated over a small. The optimal r for $\rho=1$ g.cm^{-1} are used to construct the Q(pH$_s$) curves. $\lozenge$=0.001 M, ∇=0.005 M, $\triangle$= 0.01 M, $\blacktriangle$=0.02 M, O=0.1 M, $\bullet$=0.2 M, $\square$= 1 M and $\blacksquare$=2 M.

Up to an ionic strength of 0.2 M the $Q(pH_S)$ curves merge rather well to a master curve. For ionic strength $\geq$ 1 M some of the $Q(pH_S)$ curves deviate strongly (fig 3; Bersbo and Humic Acid). We have no clear explanation for this, only two notes. (1) At high ionic strength the processing of the data is very delicate, especially with respect to the activity coefficients, and may easily lead to significant deviations. (2) At high ionic strength the electrolyte may not be considered as indifferent.

At low ionic strength the actual ionic strength may deviate significantly from the concentration of background electrolyte that is added. For instance when the titration starts at pH=3 and the concentration of the background electrolyte added is 0.001 M the actual ionic strength is 0.002 M, i.e. twice the value based on the concentration of the background electrolyte. The uncertainty at the lower ionic strength affects the optimal parameters obtained in the master curve procedure. For instance, if we leave out the lowest ionic strength value of the Suwannee River Fulvic Acid (fig.3) and use a cylindrical double layer model we find r=0.25 nm instead of 0.19 nm. When a too low value of the lowest ionic strength is reported the master curve will underestimate the electrostatic interactions. This results to smaller molecular dimensions. Despite this uncertainty in the lower salt levels we have used the values as published in the original papers.

The $Q(pH_S)$ curves of FA#1 (fig, 2) do not merge around pH_S 3 to 4. This strange behaviour may indicate a large and rapid change of the conformation (35-36).

Radius and Specific Surface Area

In table II (spheres) and table III (cylinders) the radii obtained for $\rho=1000$ (kg.m^{-3}) are listed. The value of the median of all samples is also listed in tables II and III. The median value is used instead of the average because extreme values have a smaller influence on the median than on the average.

Table II. Optimum values for the spherical double layer model and $\rho=1000$ kg.m^{-3}

Name	r (nm)	S (m^2.g^{-1})	N$_s$ (sites.nm^{-2})	sites per molecule	M (g.mol^{-1})
FA#3	0.7	4300	1.2	7	865
FA#1	0.85	3500	1.5	13	1550
Suwannee River Fulvic Acid	0.6	5000	0.7	3	545
Sweden	0.7	4300	0.8	4	865
Armadale Horizons Bh Fulvic Acid	0.8	3800	0.9	7	1290
Bersbo FA	0.85	3500	0.9	8	1540
LFHS	0.9	3300	1.0	10	1840
MBHA	1.2	2500	1.2	21	4360
PRHS-A	1.4	2100	0.8	21	6920
Humic Acid	1.8	1700	1.3	51	14700
Peat	4.4	700	1.3	310	215000
median	0.85	3500	1.0	10	1550

Table III. Optimum values for the cylindrical double layer model and $\rho=1000$ kg.m^{-3}

Name	r (nm)	S (m^2.g^{-1})	N$_s$ (sites.nm^{-2})	length per site (nm.site^{-1})
FA#3	0.3	6600	0.8	0.7
FA#1	0.4	5100	1.0	0.4
Suwannee River Fulvic Acid	0.19	10500	0.3	2.6
Sweden	0.25	8000	0.4	1.5
Armadale Horizons Bh Fulvic Acid	0.28	7100	0.5	1.2
Bersbo FA	0.31	6500	0.4	1.2
LFHS	0.32	6300	0.5	0.9
MBHA	0.5	4000	0.7	0.4
PRHS-A	0.6	3300	0.5	0.5
Humic Acid	1.0	2000	1.1	0.15
Peat	2.5	800	1.1	0.06
median	0.32	6300	0.5	0.54

The median radius for the spherical model is around 0.8 nm, whereas for the cylindrical model a value of 0.3 nm is obtained. The radii of the last four humics of table II and III are clearly above the median value.

The value of the radius reflects the magnitude of the ionic strength effect of the proton binding. The larger the radius, the larger is the experimentally determined salt effect. Because a sphere is more curved than a cylinder, the radii obtained for the spheres are about a factor 2.5 larger than those obtained for the cylinders.

Due to the small size of the particles the obtained specific surface area of the humic substances is very large. Experimentally much smaller values are determined (11,47). Specific surface areas determined from a BET analysis of nitrogen adsorption to a dried sample will result in too small values of S (e.g. 11,48).

The specific surface area for the spheres is about a factor 0.6 smaller than that of the corresponding cylinders, consequently the calculated surface charge density on the spheres is larger than that on the cylinders.

Molecular Weight and Cylinder Length

For the spherical geometry the molecular weight can be calculated from the r and S, the results are presented in table II. The molecular weights are somewhat smaller than the directly determined molecular weights (see table I). For polydisperse mixtures the molecular weight is an averaged property (e.g. 49). In most experimental techniques the molecular weight is averaged on a weight basis. The low values of the electrostatic molecular weight indicate that this average is more close to a number averaged molecular weight than to a weight averaged molecular weight.

For cylinders the actual length determines the molecular weight. This length does not follow from our analysis and, hence, the molecular weight can not be estimated. However, we may check our assumption that the end-effects can be neglected. For $l/r=10$ the surface area of the edges is 10% of the area of the cylinder.

For all samples a $l/r=10$ results in M values, which are considerably

lower than those shown in table I. This indicates that indeed $l/r>10$ for the samples, so that the assumption that the edges can be neglected is met. For the samples with r around 0.3 the l/r, for which an agreement with M from table I is obtained, ranges from 20-50. This range corresponds reasonably well to the range of 9-32 found by Chen and Schnitzer (50).

Site Density

Despite its experimental uncertainty the total acidity can be used to calculate the site density, N_s, once S is known:

$$N_s = \frac{T_M}{S} \tag{9}$$

The calculated values of N_S are presented in tables II and III.

For the cylindrical model N_S ranges from 0.3-1.1, For the spherical model the values are higher and range from 0.7-1.3. Although N_S seems to be somewhat correlated to the particle radius, the variation in N_S is much smaller than the variation in the radius.

For the spheres not only the site density can be calculated but also the number of sites per molecule (table II). The number of sites ranges from 3-314 sites/molecule, with a median value of 10 sites/molecule. The sites per molecule for a cylinder can only be calculated when a certain length is assumed. Using $20<l/r<50$ for the samples with r around 0.3 leads to numbers of sites per molecule in the same order of magnitude as for spheres.

For both geometries the number of sites per molecule for the smaller molecules is low. Calling this type of molecules *poly*-electrolytes or *macro*-molecules is an exaggeration. The term multi-site ligand or oligo-electrolyte is more appropriate (41,23).

In the electrostatic model it is assumed that the separate sites do not build up their own electric field but contribute to an average and smeared-out field. The assumption of a smeared out electric field is justified when the distance between the sites (table II and III) is smaller than twice the

88

Debye Length, κ^{-1}. Up to an ionic strength of 0.1 M, this assumption is met for the data sets under consideration. At high ionic strength values the Debye length becomes too small, and overlap of the electric fields around the individual sites is not very likely. However, at high ionic strength values the screening of the charge is very good and ψ_s is rather small. Because of the small ψ_s pH and pH_s hardly differ and the error made by considering the potential as smeared-out potential will be small.

Discussion

Although humic substances are mixtures of very different molecules, our first order approach for the electrostatics in which humic substances are treated as identical rigid and impermeable particles with a certain radius, describes the ionic strength effects surprisingly well. When either the polydispersity of a sample is very large, the changes of the conformation are considerable, or the permeability of the humic molecules is significant, a first order approach as used above should not be successful in describing the electrostatic interactions. Below we briefly investigate why polydispersity, conformational changes and permeability are, most probably, second order effects for the samples under consideration.

First polydispersity. Experimentally polydispersity is often determined as a variation in the molecular weight. The variation in molecular weight is far more pronounced than the variation in radius. For the spherical geometry the molecular weight is proportional to r^3. For instance when the molecular weight of a molecule is a factor 8 larger, its radius increases only by a factor 2. For the cylindrical geometry one may even visualize that the different molecules only differ with respect to their length. In such a (hypothetical) case the electric field around the cylinders is the same and the polydispersity is not affecting the result. So despite polydispersity, the variation in the dimensions which determine the electric field around the particles may be limited.

In the discussion on the conformational changes and the permeability we will make a distinction between the low molecular weight samples and the high molecular weight samples.

Let's first discuss the low molecular weight humic substances and consider them as cylinders. The small radii obtained from the master curve procedure suggest simple linear oligo-electrolytes. The obtained radii are in agreement with the range of 0.3-0.45 nm obtained by Chen and Schnitzer (50). A randomly coiled structure is not very likely for the low molecular weight humic substances. The statistics for a random coil structure do only apply for linear poly-electrolytes with at least 100 statistical segments (e.g. 20). Because a statistical segment can be composed of several ordinary segments, the low molecular weight samples will consist of a very limited number of statistical segment. The overall flexibility will be limited and the overall shape will be more or less cylindrical. These considerations are in favour of assuming average sized rigid cylinders as a first order approach.

Another visualization of low molecular weight humic substances is that they are rigid particles with an irregular structure. The molecule will be rather small and the hydrophillic functional groups will be located in the outer shell of the particle. When the x, y and z axes that characterize the shape of such a particle are of the same order of magnitude a treatment on the basis of a rigid sphere is justified. When one of the axes is much larger than the others the shape will approximate a cylinder.

With respect to the high molecular weight humic substances, these can be considered as linear polyelectrolytes with sufficient statistical segments to form a random coil structure. In that case significant conformational changes are to be expected when the particles become charged. However, in our opinion, a fully flexible linear polyelectrolyte is probably not the most likely structure for a high molecular weight humic molecule. High molecular weight humics are formed by polymerisation of different smaller molecules (9,12-13). This polymerisation will not occur along only one axis. Instead of a flexible linear polyelectrolyte a fibre of cross linked chains, a spheroid or a sheet like structure will be formed (e.g. 50-51). Due to cross linking the flexibility of the molecule will be far more restricted than that of a random coil. In the case of a significant cross linking the molecules will be fairly rigid with a rather hydrophobic core and the functional groups predominantly at the outside. The ion permea-

bility of the humic molecule will then be limited to the outer shell, which contains the bulk of the functional groups.

Within this picture also high molecular weight humics can be approximated as rigid and impermeable particles. More accurately the particles should be modelled as a rigid impenetrable core with a permeable outer shell. Stigter and Dill (52) have evaluated the electrostatic interactions for such a particle for the case of a spherical geometry. An alternative procedure could be the application of the polyelectrolyte adsorption theory (53-54) to describe the particles as a solid core onto which flexible polyelectrolytes are grafted. It will be clear that such models are complex and need significantly more parameters than the present approach.

A final possibility is to consider the high molecular weight humics as permeable micro gels. The most simple way to model such a gel phase is to assume that the potential ψ_s is the same throughout the gel phase. In that case the potential profile outside the gel is similar to that for an impermeable colloid. Outside the gel the potential decreases from ψ_s in the gel to 0 in the bulk of the solution. As a consequence the screening of the electric charge around a permeable colloid with a constant ψ_s is identical to that of an impermeable colloid, and can be described by the double layer models used. In a permeable particle only a part of the sites are located at the interface, the surface charge σ_S is now given by:

$$\sigma_S = \frac{fQ}{S} \qquad (10)$$

with f is the fraction of the total sites which contributes to σ_S. By defining an apparent specific are $S_{app} \equiv S/f$ the fitting procedure for this gel model is identical to that described above.

An alternative and conceptual simple model to calculate ψ_s is the "micro-Donnan" model (eg. 55). In the micro-Donnan model the charge Q, which is distributed throughout the gel volume, is fully screened by electrolyte ions inside the gel. The existence of a double layer around the gel phase is neglected. The concentration of the electrolyte ions in the gel

91

phase is simply given by the product of the concentration in solution and the Boltzmann factor for the potential in the gel phase, which again is assumed to be everywhere the same in the gel phase. The electric potential is found by solving the charge balance relation for the gel. The gel volume is now the single adjustable parameter in the charge balance equation. Marinsky and co-workers have suggested an experimental determination of the gel volume (e.g. 37-40,56).

A more accurate treatment of permeability will result in a potential profile throughout the permeable region of the gel phase (e.g. 20) and to osmotic effects (eg. 19,55-56). A rigorous and self consistent description of the screening of the charge is however very complex and not well feasible without making assumptions about the proton affinity for the functional groups. The same holds for a rigorous and self-consistent description of the screening in the case of conformational changes of the humic molecules.

Instead of the theoretical models for the electrostatic screening (semi-)empirical relations can be used to calculate ψ_s as done by for instance Tipping et al (22). In contrast to semi-empirical models, theoretical models, even the simple ones, are not only descriptive, but also predictive, therefore we prefer to use the simple diffuse double layer models above the empirical models.

Conclusions

- The ionic strength dependency of Q(pH) curves for humic material can be described well with double layer models derived for rigid and impermeable spheres or cylinders with a given radius, r. Although this approach is clearly a first order approximation, the obtained molecular dimensions of the average particles are realistic.

- For the datasets analyzed the cylindrical and spherical double layer model describe the ionic strength dependency equally well. The assessed r for the spherical double layer model is larger than that for the cylindrical model. For the specific surface area the opposite holds. The electrostatic

interactions for the spherical model turn out to be stronger than those for the cylindrical model. As a consequence the $Q(pH_s)$ curves for the spherical model are shifted towards a lower pH_s value, than those for the cylindrical model

A preference for the cylindrical or the spherical double layer model is a matter of taste. The spherical geometry has the advantage that an average molecular weight value follows directly from the analysis, and that the number of sites/molecule can be calculated. For the low molecular weight samples this number is around 10 sites/molecule. The number of sites for the high molecular weight humic acids can be far beyond this value, and their size can be very large.

Low molecular weight humics are relatively small molecules which can be easily seen as very small rigid particles. Due to cross linking, and association by for instance inorganic bridging ions like Fe^{3+} and Al^{3+} the high molecular weight humics can be fairly rigid too, with the bulk of the functional groups in the outer shell. This may explain why a description assuming rigid impermeable spheres and cylinder gives such satisfactory results.

Acknowledgement

References

1. Stumm, W.; Morgan, J.J. *Aquatic Chemistry*; Wiley Interscience: New York, 1970.

2. Lindsay, W.L. *Chemical Equilibria in Soil Solutions*; Wiley Interscience: New York, 1979.

3. Sposito, G. *The Thermodynamics of Soil Solutions*, Oxford University Press: Oxford, 1981.

4. Westall, J.C.; Zachary J.L.; Morel, F.M.M., *MINEQL*, Technical Note 18, Ralph

M. Parsons Laboratory, Department of Civil Engineering, M.I.T.: Cambridge, Massachusetts, 1976.

5. Sposito, G.; Mattigod, S.V. *GEOCHEM*; Kearney Foundation of Soils Sciences, University of Califronia: Riverside, 1980.

6. Sposito, G., *CRC Crit. Rev. Environ. Control* **1986**, *16*, 193-229.

7. Van Riemsdijk, W.H.; De Wit J.C.M.; Nederlof, M.M.; Koopal, L.K. In *Contaminated Soil'90*, Arendt, F.; Hinsenveld, M.; Van Den Brink, W.J. (eds.), Kluwer Academic Publishers: Dordrecht, 1990 359-366.

8. MacCarthy, P.; Perdue, E.M., 1991, In *Interactions at the Soil Colloid - Soil Solution Interface*; Bolt, G.H.; De Boodt, M.F.; Hayes, M.H.B.; McBride M.B. (Eds.); NATO ASI Series Series E: Applied Sciences-Vol. 190, Kluwer Academic Publishers, Dordrecht, 469-489.

9. Stevenson, F.J., *Humus Chemistry. Genesis, Composition, Reactions*; Wiley Interscience: New York, 1982.

10. Buffle, J. *Complexation Reactions in Aquatic Systems: An Analytical Approach*; Ellis Horwood Limited: Chichester, 1988.

11. Buffle, J. In *Metal Ions in Biological Systems, Vol 18, Circulation of Metal in the Environment*, Sigel, H. (Ed.); Marcel Dekker: New York, 1984, Chapter 6.

12. Aiken, G.R.; Malcolm, R.L. *Geochim. Cosmochim. Acta* **1987**, *51*, 2177-2184.

13. Hayes, M.H.B.; MacCarthy, P.; Malcolm, R.L.; Swift, R.S. (Eds.), *Humic Substances II: In Search of Structure*; Wiley Interscience: New York, 1989.

14. De Wit, J.C.M.; Van Riemsdijk, W.H.; Koopal, L.K. In *Heavy Metal in the Hydrological Cycle*, Astruc, M.; Lester, J.N. (Eds.); Selper: London, 1988, 369-376.

15. De Wit, J.C.M.; Van Riemsdijk, W.H. and Koopal, L.K., In *Metal Speciation, Separation and Recovery, Vol II*, J.W. Patterson; R. Passino (Eds); Lewis Publishers: Chelsea USA, 1989, 329-353.

16. De Wit, J.C.M.; Van Riemsdijk, W.H.; Nederlof, M.M.; Kinniburgh, D.G.; Koopal, L.K. *Analytica Chim. Acta* **1990**, *232*, 189-207.

17. De Wit, J.C.M.; Nederlof, M.M.; Van Riemsdijk, W.H.; Koopal, L.K. *Water, Air and Soil Pollution* **1991**, *57-58*, 339-349.

18. De Wit, J.C.M.; Van Riemsdijk, W.H.; and Koopal, L.K.; *Finnish Humus News* **1991**, *3*, 139-144.

19. Overbeek, J.Th.G., In *Colloid Science, Vol. 1*; Kruyt, H.R. (Ed.); Elsevier:

Amsterdam, 1952, 115-193.

20.   Tanford, C. *Physical Chemistry of Macromolecules*; Wiley Interscience: New York, 1961.

21.   Tipping, E.; Backes C.A.; Hurley, M.A. *Water Res.* **1988**, 22, 597-611.

22.   Tipping, E., Reddy, M.M., Hurley, M.A. *Environ. Sci. Technol.* **1990**, 24, 1700-1705.

23.   Bartschat, B.M.; Cabaniss, S.E.; Morel, F.M.M. *Environ. Sci. Technol.* **1992**, 26, 284-294.

24.   Van Riemsdijk, W.H., Bolt, G.H.; Koopal, L.K. In *Interactions at the Soil Colloid - Soil Solution Interface*; Bolt, G.H.; De Boodt, M.F.; Hayes, M.H.B.; McBride M.B. (Eds.); NATO ASI Series Series E: Applied Sciences-Vol. 190, Kluwer Academic Publishers: Dordrecht, 1991, 81-113.

25.   Nederlof, M.M.; Van Riemsdijk, W.H.; Koopal, L.K.; *J. Colloid Interface Sci.* **1990**, 135, 410-426.

26.   Nederlof, M.M., Van Riemsdijk, W.H.; Koopal, L.K.; *Environ. Sci. Technol.* **1992**, 26, 763-771.

27.   Van Riemsdijk, W.H.; Koopal, L.K. In *Environmental Particles*; Buffle, J.; Van Leeuwen, H.P. Lewis Publishers: Chelsea, Michigan, 1992, Chapter 12.

28.   Loeb, A.L.; Overbeek, J.Th.G.; Wiersema, P.H. *The Electrical Double Layer around a Spherical Colloid Paricle*; M.I.T. Press: Cambridge, USA, 1961.

29.   Lyklema, J. *Fundamentals of Interface and Colloid Science. Vol I: Fundamentals*; Academic Press: London, 1991.

30.   Stigter, D. *J. Colloid Interface Sci.* **1975**, 53, 296-306.

31.   Van der Drift, W.P.J.T.; De Keizer, A.; Overbeek J.Th.G.; *J. Colloid Interface Sci.* **1979**, 71, 67-78.

32.   Gregg, S.J.; Sing, K.S.W. *Adsorption, Surface Area and Porosity*, Academic Press: London, 1982.

33.   Cameron, R.S.; Thornton, B.K.; Swift, R.S.; Posner, A.M. *J. Soil Sci.* **1972**, 23, 394-408.

34.   Brown, P.A.; Leenheer, J.A. In *Humic Substances in the Suwannee River Georgia: Interactions, Properties and Porposed Structures*; Averett, R.C.; Leenheer, J.A.; McKnight, D.M.; Thorn K.A. (Eds.); U.S. Geologicval Survey, Open-File Report 87-557, 1989, p. 315.

95

35.   Dempsey, B.A., O'Melia C.R., In *Aquatic and Terrestrial Humic Materials*; Christman, R.F.; Gjessing E.T.(Eds.), Ann Arbor Science: Michigan, 1983; Chapter 12.

36.   Dempsey, B.A. *The Protonation, Calcium Complexation, and Adsorption of a Fractionated Aquatic Fulvic Acid*, Ph.D. Thesis, The Johns Hopkins University: Chapel Hill, 1981, pp 201.

37.   Ephraim, J.; Alegret, S.; Mathuthu, A.; Bicking, M.; Malcolm, R.L.; Marinsky, J.A.; *Envir. Sci. Technol.* **1986**, *20*, 354-366.

38.   Ephraim, J.H.; Borén, H.; Pettersson, C.; Arsenie, I.; Allard, B. *Environ. Sci. Technol.* **1989**, *23*, 356-362.

39   Marinsky, J.A.; Gupta, S; Schindler, P. *J. Colloid Interface Sci.* **1982**, *89*, 401-411.

40.   Marinsky, J.A.; Wolf, A.; Bunzl, K. *Talanta* **1980**, *27*, 461-468.

41.   Aiken, G.R., D.M. McKnight, R.L.Wershaw and P. MacCarthy (Eds.) *Humic Substances in Soil, Sediment, and Water*; Wiley Interscience: New York, 1985

42.   Paxeus, N.; Wedborg M. In *Volunteered Papers 2nd International Conference International Humic Substances Society*, Hayes, M.H.B.; Swift, R.S. (Eds), The Printing Section, University of Birminghan: Birmingham, United Kingdom, 1984, 120-122.

43.   Hansen, E.H.; Schnitzer, M. *Anal. Chem. Acta* **1969**, *46*,247-254

44.   Xu, H.; Ephraim, J.; Ledin, A; Allard B. *Sci. Total Environ.* **1989**, *81/82*:653-660.

45.   Turner, D.R.; Varney, M.S.; Whitfield, M.; Mantoura R.F.C.; Riley J.P. *Geochim. Cosmochim. Acta* **1986**, *50*, 289-297.

46.   Van Riemsdijk, W.H.; Koopal; L.K.; De Wit, J.C.M. *Neth. J. Agricult. Sci.* **1987**, *35*, 241-257.

47.   Chiou, C.T.; Lee, J.F.; Boyd S.A. *Environ. Sci. Technol.* **1990**, *24*, 1164-1166.

48.   Herrington, T.M.; Midmore B.R. *J. Chem. Soc. Faraday Trans. I.* **1984**, *80*, 1539-1552.

49.   Swift, R.S. In *Humic Substances II: In Search of Structure*; Hayes, M.H.B., MacCarthy, P.; Malcolm, R.L.; Swift, R.S. (Eds.); Wiley Interscience: New York, 1989. Chapter 16.

50.   Chen, Y.; Schnitzer, M. *Soil Sci. Soc. Am. J.* **1976**, *40*, 866-872.

51.   Chen Y.; Schnitzer, M In *Humic Substances II: In Search of Structure*; Hayes, M.H.B., MacCarthy, P.; Malcolm, R.L.; Swift, R.S. (Eds.); Wiley Interscience:

New York, 1989, Chapter 22.

52. Stigter, D.; Dill, K.A. *Biochemistry* 1990, *29*, 1262-1273.

53. Böhmer, M.R.; Evers, O.A.; Scheutjens, J.M.H.M. *Macromolecules*, 1990, *23*, 2288

54. Evers, O.A.; Fleer, G.J.; Scheutjens, J.M.H.M.; Lyklema, J. *J. Colloid Interface Science* 1986, *111*, 446-454.

55. Bolt, G.H. In *Soil Chemistry B. Physico-Chemical Models*; G.H. Bolt (Ed.); Elsevier: Amsterdam, 1982, Chapter 3.

56. Marinsky, J.A. In *Aquatic Surface Chemistry*; Stumm, W. (Ed.); Wiley Interscience: New York, 1987, Ch. 3.

C h a p t e r 4

Proton Binding to Humic Substances. B. Chemical Heterogeneity and Adsorption Models.

Abstract

Ion binding to humic substances is influenced by chemical heterogeneity and by the variable charge behaviour of the humics. In this paper we focus on chemical heterogeneity. To study the chemical heterogeneity the affinity distribution is calculated from the $Q(pH_s)$ master curves which were obtained from the acid/base titration data measured at a series of salt levels for 11 humic substances. The proton concentration in the diffuse double layer near the binding site, H_s, is calculated with the help of a double layer model in which the humic particles are considered rigid impermeable spheres or cylinders.

For all samples the calculated affinity distributions are characterized by a large peak with a peak position in the log K range 3-4. In samples which were titrated over a large pH range there is a smaller second peak with a peak position around log K=8-9.

On the basis of the calculated affinity distributions a site binding model to describe the data can be selected. Because the peaks in the affinity distributions are broad and smooth a description on the basis of adsorption equations for continuous heterogeneous ligands is to be preferred over equations for discrete heterogeneity. The $Q(pH_s)$ master curves can be described very well with normalized Freundlich type of binding equations. In general the Langmuir Freundlich equation and the Tóth equation give slightly better results than the Generalised Freundlich equation. From the combination of the site binding model with the double layer model the $Q(pH)$ curves can be calculated for various values of the ionic strength. This leads to a good description of the experimental data.

Introduction

The fact that proton and metal ion binding to humics and fulvics is affected by both electrostatics and chemical heterogeneity is well known (e.g. 1-6). However, until very recently electrostatic effects and heterogeneity were not considered explicitly in most models to describe ion binding to humic substances. As a consequence such models could not describe competitive binding as a function of a wide range of pH and salt levels. However, very recently several research groups have realized that explicit incorporation of electrostatics and chemical heterogeneity has the advantage that the binding can be described over a wide range of conditions (e.g. 2,7-11).

The electrostatic effects and the chemical heterogeneity can be modelled in various way. Often a model description is chosen a priori and the model parameters are obtained by fitting the data to the model (e.g. 9-11). Although this is a step forward, in our opinion, it is to be preferred to avoid pure fitting as much as possible.

We advocate (1) to analyze the proton binding data with the master curve procedure in order to obtain a double layer model which describes the electrostatic effects (2) to determine the affinity distribution on the basis of the master curve and (3) to select an appropriate site binding model on the basis of the calculated affinity distribution (2-4,12) . The combination of the site binding model with the double layer model allows for a description over a wide range of environmental conditions.

In a previous paper (12) the electrostatic effects of humics were analyzed with the help of the master curve procedure. In the master curve procedure the proton binding curves, expressed as charge Q as a function of the pH, are replotted as a function of pH_s. This pH_s, the pH near the functional groups at location of binding, is a function of the pH in the bulk and the electric potential near the functional groups, ψ_s:

$$pH_s = pH - 0.434\frac{F\psi_s}{RT} \qquad (1)$$

The potential ψ_s is a function of the charge of the humics and of the ionic

strength; ψ_s can be calculated from the electric double layer model. When the adopted double layer model describes the electric effects adequately, the ionic strength dependence of the binding curves scaled as a function of pH_s, vanishes and the curves merge to a master curve. The extent to which the curves merge is a criterion for the adequacy of the model.

Based on the analysis of proton binding curves for 11 different samples, it was concluded that the electrostatics of humics could be described reasonably well either with a spherical or a cylindrical double layer model (12). In both double layer models the humic substances were treated as rigid impermeable particles with an adjustable size. For the samples studied the effects of polydispersity, changes of the conformation and permeability on the electrostatics are of second order, as they were not required to obtain an adequate description of the electrostatics involved in the proton binding.

Because in the $Q(pH_s)$ master curve the electrostatic effects are filtered out, the shape of the master curve is directly related to the chemical heterogeneity of the sample (e.g. 2,13-14). From a master curve the affinity distribution can be obtained by using the methods described by Nederlof et al (15) and Van Riemsdijk et al (13-14). In this paper the affinity distributions obtained for the 11 different samples considered in the previous paper (12) will be presented and discussed.

On the basis of the calculated affinity distributions an appropriate site binding model can be selected. When the affinity distribution shows nicely separated narrow peaks, the surface is characterized by a few discrete sites and a description of the binding on the basis of a multi-site Langmuir can be used (1, 13, 16). The number of site classes is then equal to the number of peaks and the affinity constants follows from the peak positions.

When the distribution is wide and rather smooth a description based on the binding equation for continuous heterogeneous ligands (1, 4, 13, 16, 17) is the most logical choice. The binding equation for a continuous heterogeneous surface follows from integrating the distribution function multiplied by the local binding equation, which holds for the individ-

ual site types (i.e. the Langmuir equation), over the relevant log K range. In general this integration should be done numerically, only in some special cases analytical binding equations result. Three well known analytical binding equations for continuous heterogeneous surfaces are the Langmuir Freundlich equation (LF) (18), the Generalised Freundlich equation (GF) (19) and the Tóth equation (20). The binding equations differ with respect to the underlying affinity distribution. In this paper these analytical binding equations will be used to describe the proton binding. All three analytical, Freundlich type of equations are derived for affinity distributions characterized by a single broad peak. For a heterogeneous ligand with an affinity distribution which is characterized by several broad peaks, we use a series of Freundlich type of equations.

Finally it will be shown that the assessed binding equations for the $Q(pH_s)$ curves, in combination with the electrostatic model provide a description of the measured $Q(pH)$ curves.

Determination of the affinity distribution

In this article the previously obtained the $Q(pH_s)$ master curves (12) are used as a starting point for the chemical heterogeneity analysis. Several methods are known that determine the affinity distribution on the basis of a binding curve (1, 15, 21) underlying the master curve. In our previous work (2-4) we have used the LOGA method in combination with a smoothing spline technique. In the LOGA method the affinity distribution is related to the first and third derivative of the master curve. Recently Nederlof et al (17) have shown that the error in the calculated third derivative may be quite significant. This error leads to a large uncertainty in the LOGA approximation of the affinity distribution. Nederlof et al (17) concluded that the LOGA method should only be used for high quality data, in other cases the CA method is advised. In principle the resolution of the CA affinity distribution is lower than the resolution of the LOGA distribution, however, because the CA distribution is only related to the first derivative the uncertainty in the distribution is much smaller (15,17, 21). By applying the CA method the distribution function F is obtained as

the first derivative of the master curve:

$$F_{CA}(\log K_H) = \frac{dQ}{dpH_s} \qquad (2a)$$

with

$$\log K_H = pH_s \qquad (2b)$$

where $\log K_H$ is the affinity constant of the protonation reaction for a certain group.

The distribution function F_{CA} is a non-normalized distribution, which can be normalized if Q_{max} is known. The true Q_{max} is, however, very difficult to determine experimentally (22). The normalization does not change the location of the distribution on the log K axis, nor does it affect the shape of the distribution function.

Description of the $Q(pH_s)$ Curves with Isotherm Equations

The affinity distribution gives information about the chemical heterogeneity of the humic acid sample. In order to describe the proton binding, a binding equation for heterogeneous ligands is required. When the affinity distribution is characterized by a series of peaks, Q can be represented by a weighted summation of the charge contribution of the different site classes:

$$Q = Q_{max} \sum_{i=1}^{n} f_i (1 - \theta_{i,H}) \qquad (3)$$

where f_i is the fraction of the sites of class i. The $1-\theta_{i,H}$ term is due to the fact that the charge is not proportional to the degree of protonation, $\theta_{i,H}$, but to the degree of dissociation.

When the degree of protonation is given by the Langmuir equation Eq. 3 is the multi-site Langmuir equation. This equation can be used when

the distribution is characterized by a set of nicely separated narrow peaks.

When the distribution is characterized by one rather wide peak, the overall degree of protonation is given by the integral binding equation for heterogeneous ligands. Three well known specific forms of the binding equation for heterogeneous ligands are (1) the Langmuir Freundlich (LF) equation (*18*):

$$\theta_{i,H} = \frac{\left(\tilde{K}_{i,H}H_s\right)^{m_i}}{1+\left(\tilde{K}_{i,H}H_s\right)^{m_i}} \tag{4}$$

(2) the Generalised Freundlich (GF) equation (*19*):

$$\theta_{i,H} = \left(\frac{\tilde{K}_{i,H}H_s}{1+\tilde{K}_{i,H}H_s}\right)^{m_i} \tag{5}$$

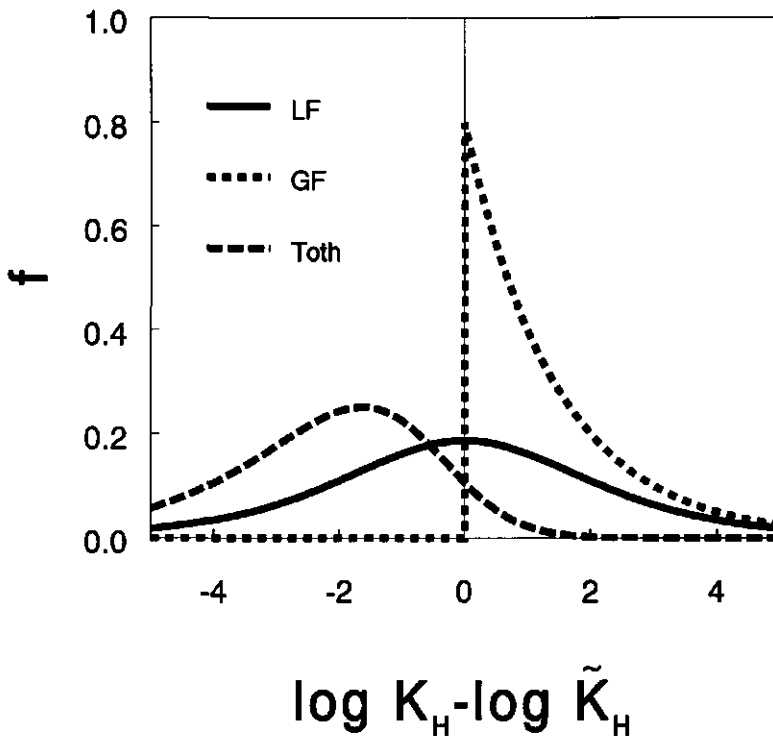and (3) the Tóth equation (*20*):

$$\theta_{i,H} = \frac{\tilde{K}_{i,H}H_s}{\left[1+\left(\tilde{K}_{i,H}H_s\right)^{m_i}\right]^{1/m_i}} \tag{6}$$

where m_i determines the width of the distribution function of the sites of class i and $\tilde{K}_{i,H}$ the location on the log K axis. For $m_i=1$ all three isotherms are identical to the Langmuir equation, and the distribution is a Dirac delta function. In figure 1 the distributions underlying the Eqs. 4-6 are plotted for $m_i=0.25$. The distribution function underlying the LF equation is symmetrical and pseudo-Gaussian. The distribution for the GF is exponential with a high affinity tail. The distribution for the Tóth is asymmetrical with a low affinity tail.

For strongly heterogeneous samples with an affinity distribution with several broad peaks, the overall binding equation can be considered as a weighted summation over a series of Freundlich (or Tóth) type of equations analogous to Eq. 3.

105

Figure 5. The normalised affinity distribution f(log K) for the Langmuir Freundlich equation (LF), the Generalised Freundlich equation (GF) and the Tóth equation as a function of log K_H-log $\tilde{K}_H$ for m=0.25.

In principle a combination of different type of binding equations can be used, for instance a Langmuir Freundlich isotherm combined with a Tóth isotherm. In this paper, however, only combinations of isotherms of the same type are considered.

Description of the Q(pH) Curves

In order to describe the experimentally determined Q(pH) data the electric double layer model used to obtain the Q(pH$_s$) curves can be used to calculate the electric potential at each pH$_s$ value for a series of ionic strength values (2-4, 12).

106

Table I Characteristics of the data sets

| name | reference | assessed radius (nm) | |
		sphere	cylinder
FA#3	23,24	0.7	0.3
FA#1	23,24	0.85	0.4
Suwannee River Fulvic Acid	7	0.6	0.19
Sweden	7	0.7	0.25
Armadale Horizons Bh Fulvic Acid	7	0.8	0.28
Bersbo FA	25	0.85	0.31
LFHS	9	0.9	0.32
MBHA	9	1.2	0.5
PRHS-A	9	1.4	0.6
Humic Acid	26	4.4	2.5
Peat	27	1.8	1
median		0.85	0.32

In this way the pH_s can be rescaled to the pH (eg. Eq. 1), and the $Q(pH_s)$ master curve can be rescaled into a series of $Q(pH)$ curves. For the pH_s-pH transformation the spherical and the cylindrical double layer models presented in the preceding paper (12) should be used. In both models the humic colloids are treated as rigid impermeable particles with a certain size, characterized by their radius.

Experimental Data

All datasets are taken from literature. The relevant characteristics of the different sets are tabulated in table I. This table includes the optimal parameters for the spherical and the cylindrical double layer model assessed in the previous paper on the basis of the master curve procedure (12). For most samples the $Q(pH_s)$ curves merged reasonably to a master

107

curve. The high ionic strength $Q(pH_s)$ curve for the Bersbo samples did not merge with the curves for the lower salt levels and is therefore not taken into consideration in this paper. For the other data sets all experimental points were included. In the FA#1 sample the curves did not merge around $pH_s=3$, probably due to a change of the conformation. The $Q(pH_s)$ curves of the HA sample still showed some salt dependence. A consequence of the spreading in the $Q(pH_s)$ curves for the FA#1 and the HA sample is that there is a larger uncertainty in the obtained affinity distributions for these samples.

Calculations

The affinity distributions were calculated with the AFFINITY program developed by Nederlof (28). For the fits of the binding equations Kinniburgh's ISOTHERM program was used (29). The $Q(pH)$ curves were calculated with the ECOSAT program (30).

Results and Discussion

Affinity Distributions

The proton affinity distributions obtained from the $Q(pH_s)$ master curves by using the CA method are given in figure 2. In general, the distributions obtained under the assumption that the particles are spheres are shifted towards lower log K_H values and the peaks are somewhat sharper than for the distributions obtained under the assumption that the particles are cylinders.

The differences between the two models were already observed in the preceding paper (12). The electrostatic interactions for the assessed spherical double layer model are stronger than for the cylindrical model, therefore the corresponding $Q(pH_s)$ curves are shifted to lower pH values and are steeper, indicating a smaller heterogeneity.

In general, the characteristics of the distributions obtained for the different samples are similar. For most samples the distribution is wide

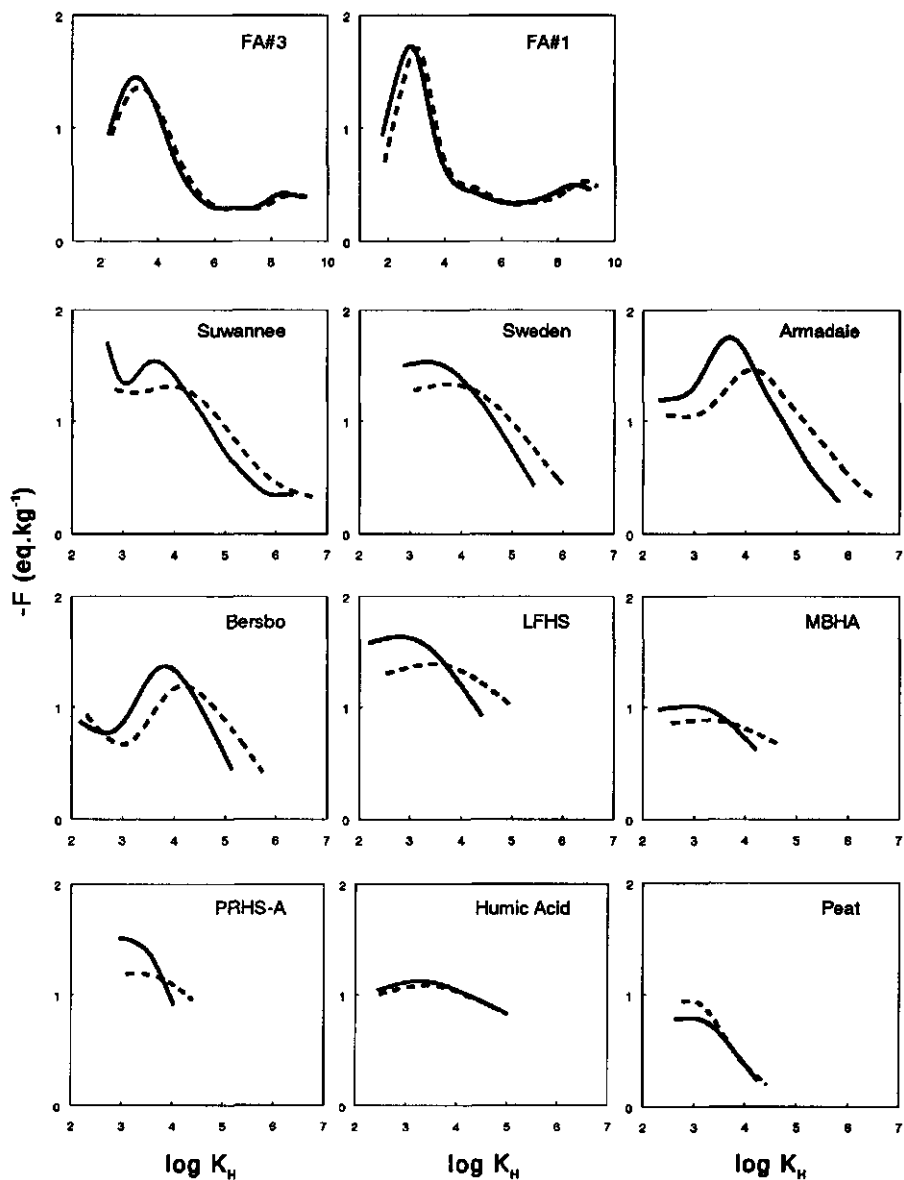**Figure 2.** The CA proton affinity distribution obtained from the $Q(pH_s)$ mastercurves for the humic substances obtained with the spherical double layer model (———————) and the cylindrical double layer model (- - - - - - - - - - - - -). Note: because Q has the dimensions eq charge.kg^{-1}, the non normalised distribution has the dimension eq charge.kg^{-1}. Since the humics are negatively charged F is also negative.

and rather smooth and there are no distinct, nicely separated peaks. All affinity distributions are dominated by a large, somewhat asymmetric and rather broad peak with a peak position in the log K range 3-4. These log K values correspond with log K values for carboxylic groups. The obtained distributions show that on the basis of available proton data there is no reason for proposing a description of the protonation on the basis of a limited number of certain functional groups.

At the low log K end the distributions differ strongly from one sample to another. For some samples it seems that there is a smaller peak of very acidic sites. The $Q(pH_s)$ curves at the lower end of the pH_s range are often determined by only one ionic strength, and by only a few data points, for which the experimental uncertainty is rather large. This makes the error in the distribution the largest at the low log K_H end (17). Because of this error we do not want to over interpret the low log K_H part of the affinity distributions.

The FA#1 and the FA#3 samples have been titrated over a much larger pH range than the other data. As a result a much larger part of the affinity distribution is obtained. Up to log K_H=6, the general characteristics of the affinity distribution for FA#1 and FA#3 correspond to the other distributions. The peak of the FA#3 sample is wider than the peak for the FA#1 sample. For the FA#1 sample the $Q(pH_s)$ data do not merge very well around pH_s=3 due to a change of the conformation. As a consequence, the uncertainty in the shape of the first peak of the distribution is large. The first peak is probably too narrow and reflects not only the chemical heterogeneity of the sample, but also the change of conformation.

The additional part of the affinity distributions for the FA#1 and FA#3 samples show that there is a significant amount of groups present with a log K_H>6. These groups form a broad peak with a peak position near log K_H=9. Note that the error in the distribution at the upper end of the log K_H range is also rather large (17), which implicates considerable uncertainty in the shape and the peak position of the second peak.

In potentiometric titrations a pH range from 3 to 11 is about the

110

largest pH range for which a set of high quality proton adsorption iso-therms for several ionic strength can be determined. Outside this range the correction for the blank titration gives large errors and at high pH carbon dioxide becomes a serious problem, even when the experiments are per-formed under a nitrogen atmosphere. The limited pH range implies that the existence of sites with a log K_H>10, cannot be identified with the titration technique. On the other hand such groups do not affect the observed proton binding behaviour.

Description of the $Q(pH_s)$ Curves

The obtained affinity distributions can be used to select an appropri-ate binding equation. Because in most cases the distribution is rather wide and smooth we prefer a description based on binding equations for con-tinuous heterogeneous ligands (Eqs 3-6). In the case the distribution is characterized by one major peak, a description based on one single hetero-geneous equation is used. If the distribution indicates the presence of two (wide) peaks, like the FA#1 and FA#3 sample, a weighted summation of two heterogeneous binding equations of the same type is used. Because only a window of the complete distribution can be obtained from the experimental data, it is not possible to select one of the three analytical distribution functions as the preferred choice, therefore we will use all three analytical binding equations to describe the master curves.

There is no doubt that the master curve can be described perfectly well by using a series of discrete Langmuir equations. One of the problems in such a model is to select the type and number of discrete site types that is used to describe the data. This problem is solved easily when the obtained affinity distributions would show a series of rather small and nicely separated peaks. The number of peaks and their affinity follows then directly from the heterogeneity analysis. However, if the system is characterized by a large number of discrete site types, with only a slightly different affinity constant, the heterogeneity analysis can not recover the individual peaks and will result in a smooth and wide distribution. In that case it is much better to use a continuous distribution function because

less parameters are involved. Since the obtained affinity distributions give no clear indication for a series of narrow peaks, the discrete Langmuir option is not taken into consideration.

Table II gives the parameters for a description of the $Q(pH_S)$ data for the spherical double layer model with the LF equation. Table III gives the parameters for the LF equation in combination with the cylindrical double layer model. The assessed parameters for the GF are tabulated in appendix 1 and the parameters for the Tóth equation in appendix 2. For all but the peat sample a good description of the $Q(pH_S)$ data is obtained. The poor description for the peat sample ($r^2 < 0.9$) is due to three datapoints which do not merge to the master curve. When those three datapoints are ignored r^2 becomes 0.97 for the cylindrical double layer model and 0.96 for the spherical model. In some cases the obtained parameters are not realistic although they result in a reasonable description. This is for instance the case for the GF description for the Bersbo sample; the obtained m value is extremely small and the maximum extremely large.

The calculated affinity distributions (fig. 2) already showed that the distribution for the cylindrical particles was wider than that for the spherical particles and that the peak positions were shifted to higher log K_H values. The values of log $\tilde{K}_H$ and m reflect this observation. Especially when the LF and the Tóth models are used the log $\tilde{K}_H$(cylinder)>log $\tilde{K}_H$(sphere) and m(cylinder)<m(sphere), the latter implicates a larger heterogeneity when the particles are assumed to be cylinders instead of spheres.

Despite some differences in r^2, the goodness of fit for the spheres and cylinders and for the different equations is very similar. The model parameters, however, differ significantly. In general, log $\tilde{K}_H$(Tóth)>log $\tilde{K}_H$(LF)>log $\tilde{K}_H$(GF) and the differences between the log $\tilde{K}_H$ for two consecutive model can be up to two log units.

The obtained sequence is caused by the different characteristics of the affinity distributions underlying the binding equation. For instance, in the LF model the log $\tilde{K}_H$ corresponds with the peak position and equals the average log K_H of the log K_H distribution, whereas for the GF model

Table II The assessed parameters for the Langmuir Freundlich equation describing the $Q(pH_s)$ data obtained with the spherical double layer model

Name		log K_H	m	$-Q_{max}$ (eq.kg^{-1})	r^2 *	RMSE **
FA#3	site 1	2.95	0.44	5.61	0.998	0.058
	site 2	8.47	0.59	1.18		
FA#3	pH$_s$<5.5	2.97	0.43	5.66	0.997	0.065
FA#1	site 1	2.79	(1.00)	2.65	0.983	0.176
	site 2	(13.16)	(0.07)	(12.86)		
Suwannee River Fulvic Acid		3.38	0.47	5.59	0.999	0.045
Sweden		3.33	0.47	5.86	0.982	0.115
Armadale Horizons Bh Fulvic Acid		3.48	0.48	5.88	0.991	0.119
Bersbo FA		3.80	0.36	5.63	0.986	0.108
LFHS		2.88	0.49	5.97	0.981	0.114
MBHA		2.76	0.42	4.24	0.948	0.142
PRHS-A		3.27	0.87	3.01	0.953	0.117
Humic Acid		3.46	0.57	3.65	0.936	0.205
Peat		3.10	1.00	1.45	0.776	0.178
median		3.10	0.48	4.24		

Table III The assessed parameters for the Langmuir Freundlich equation describing the $Q(pH_s)$ data obtained with the cylindrical double layer model

name		log K_H	m	$-Q_{max}$ (eq.kg^{-1})	r^2 *	RMSE **
FA#3	site 1	3.08	0.41	5.64	0.998	0.061
	site 2	8.71	0.61	1.12		
FA#1	site 1	2.49	0.46	5.77	0.981	0.187
	site 2	8.82	0.35	2.36		
Suwannee River Fulvic Acid		3.68	0.41	5.66	0.997	0.061
Sweden		3.66	0.40	5.98	0.984	0.109
Armadale Horizons Bh Fulvic Acid		3.92	0.40	5.99	0.994	0.099
Bersbo FA		4.20	0.32	5.66	0.989	0.094
LFHS		3.48	0.39	6.33	0.988	0.099
MBHA		3.19	0.35	4.42	0.951	0.138
PRHS-A		3.64	0.66	3.22	0.978	0.081
Humic Acid		3.57	0.55	3.67	0.949	0.183
Peat		3.23	1.00	1.45	0.861	0.141
median		3.57	0.41	5.66		

with values between braces () are not realistic and:

$$* \quad r^2 = 1 - \frac{\sum_{i=1}^{np}(n_i - \hat{n}_i)^2}{\sum_{i=1}^{np}(n_i - \bar{n}_i)^2}$$

$$** \quad RMSE = \left(\frac{\sum_{i=1}^{np}(n_i - \hat{n})^2}{m - np}\right)^{0.5}$$

n_i measured value for datapoint i
$\hat{n}_i$ fitted value for datapoint i
np   number of datapoints
p   number of parameters
$\bar{n}$ average value of measured datapoints

113

the log $\bar{K}_H$ corresponds with the lowest log K_H value of the distribution (see fig. 1).

The parameter m, which determines the width of the distribution varies in the order m(GF)«m(Tóth)≤m(LF). For most samples the order in the calculated Q_{max} is Q_{max}(GF)>Q_{max}(Tóth)>Q_{max}(LF).

When m is treated as an adjustable parameter a m>1 is obtained for the peat sample for all three models. The Q(pH$_S$) master curve is thus somewhat steeper than the Langmuir equation. From a point of view of physics this is impossible. The deviation from the Langmuir equation is however minor and a description based on a homogeneous Langmuir equation is still satisfactory. In principle m>1 is an indication that the double layer model used to obtain the Q(pH$_S$) curves is not fully adequate. Another illustration of m>1 is obtained with the LF and the Tóth models for the first peak of the FA#1 sample. At the location of the first peak the Q(pH$_S$) curves do not merge well and there seems to be a change of the conformation. As is noted before the first peak results not only from the chemical heterogeneity, but also from the change of conformation. As a consequence the assessed m for the first peak indicates to a too narrow peak and the assessed m for the second class of sites to a too wide peak.

The major reason that all three models describe the data almost equally well is the fact that only a rather small window of the total Q(pH$_S$) is obtained experimentally, and that the variation in the Q(pH$_S$) data is still rather large. In fig. 3a the model description of the Q(pH$_S$) curves for the Armadale sample (spherical double layer model) is shown for three models (LF, GF and Tóth). It follows that within the limited data range all three model descriptions merge. However, outside the data range the curves may deviate significantly. In fig. 3b the distributions which correspond to various model descriptions obtained with the CA method are plotted together with the distribution obtained from the experimental data. Note that the CA method is not able to reproduce the sharp end of the exponential GF distribution at log K=log $\bar{K}_H$ (compare fig 3 with fig 1) and it results in an asymmetrical peak with a peak position somewhat larger than log $\bar{K}_H$.
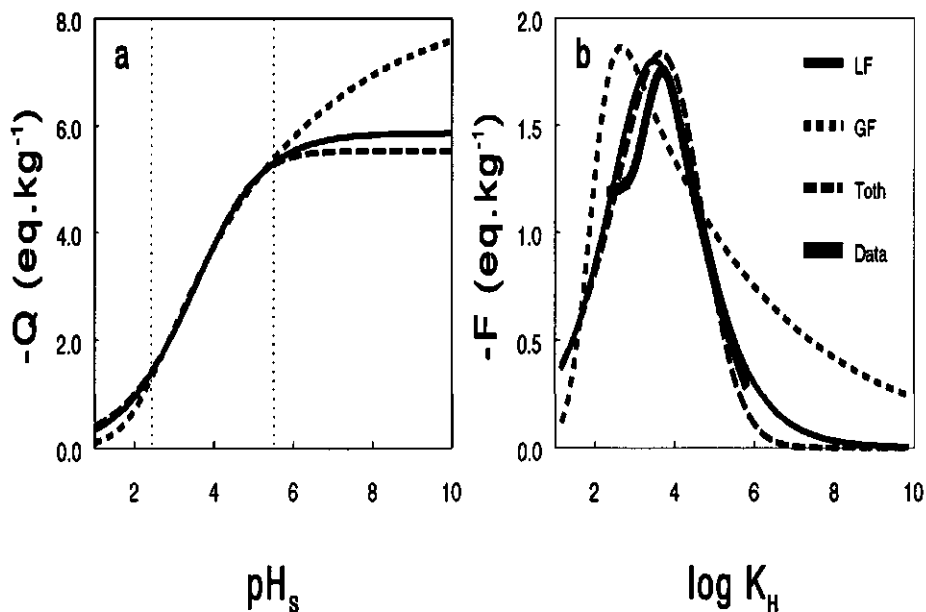
Figure 3. (a). the calculated $Q(pH_s)$ curves for the Langmuir Freundlich (LF), the Generalised Freundlich (GF) and the Tóth equation for the $Q(pH_s)$ data obtained for the Armadale sample with the spherical double layer model. The vertical dotted lines indicate the pH_s range of the experimental data. LF equation: log $\tilde{K}_H$=3.48, m=0.48, Q_{max}=5.86; GF equation: log $\tilde{K}_H$=1.98, m=0.13, Q_{max}=8.43; Tóth equation: log $\tilde{K}_H$=4.51, m=0.42, Q_{max}=5.53. (b). The CA affinity distribution obtained from the calculated $Q(pH_s)$ curves shown in fig. 3a. together with the CA affinity distribution calculated from the $Q(pH_s)$ data obtained for the Armadale sample with the spherical double layer model.The normalised affinity distribution f(log K) for the Langmuir Freundlich equation (LF), the Generalised Freundlich equation (GF) and the Tóth equation as a function of log K_H-log $\tilde{K}_H$ for m=0.25.

With most of the samples the LF and the Tóth equation correspond better to the experimentally determined distribution than the GF equation. Because of this trend we have a slight preference for the LF or the Tóth equation above the GF equation.

The FA#1 and FA#3 sample show that there is a considerable num-

115

ber of high affinity sites. The bimodal character of the distribution makes that despite the large window the degrees of freedom are such that all three models are able to describe the data equally well. Another consequence of the introduction of a second wide peak is that it may affect the parameters for the first peak. For the FA#2 sample we have analyzed this effect by fitting a single Freundlich type of equation, while taking only the data obtained for the spherical double layer model with $pH_s < 5.5$ into account. Comparison of the resulting parameters, tabulated in table II and appendices I and II with those obtained for the bimodal distribution show that for this case the effects are minor. For the T6th and the LF model the fitted log $\tilde{K}_H$, m and Q_{max} correspond very well with those for the first peak. For the GF model the deviation is somewhat larger.

The existence of high affinity sites outside the experimentally determined window does not seem to influence the description of the protonation much. They may, however, strongly influence the multicomponent binding of metal ions at trace level.

Description of the Q(pH) Curves

By combining the electrostatic model with the binding equation, the experimental Q(pH) curves can be calculated and compared with the experimental datapoints. Because the goodness of fit is in the same order for all three binding equations and for both double layer models the quality of the description of the Q(pH) data is very similar. We have chosen to work out only one combination. In fig 4 the model description based on the spherical double layer model and the LF binding equation are plotted together with the experimental data. The curves represent the calculated results and the points are the experimental data. In general, the description of the experimental data is very satisfactory.

It has been pointed out before that the high ionic strength for the Bersbo sample and the HA sample did not merge well to a master curve. As a consequence the description of data for the high ionic strength level is poor for these samples. The same holds for the FA#1 sample around pH=4, where at high salt concentration a change of conformation mani-
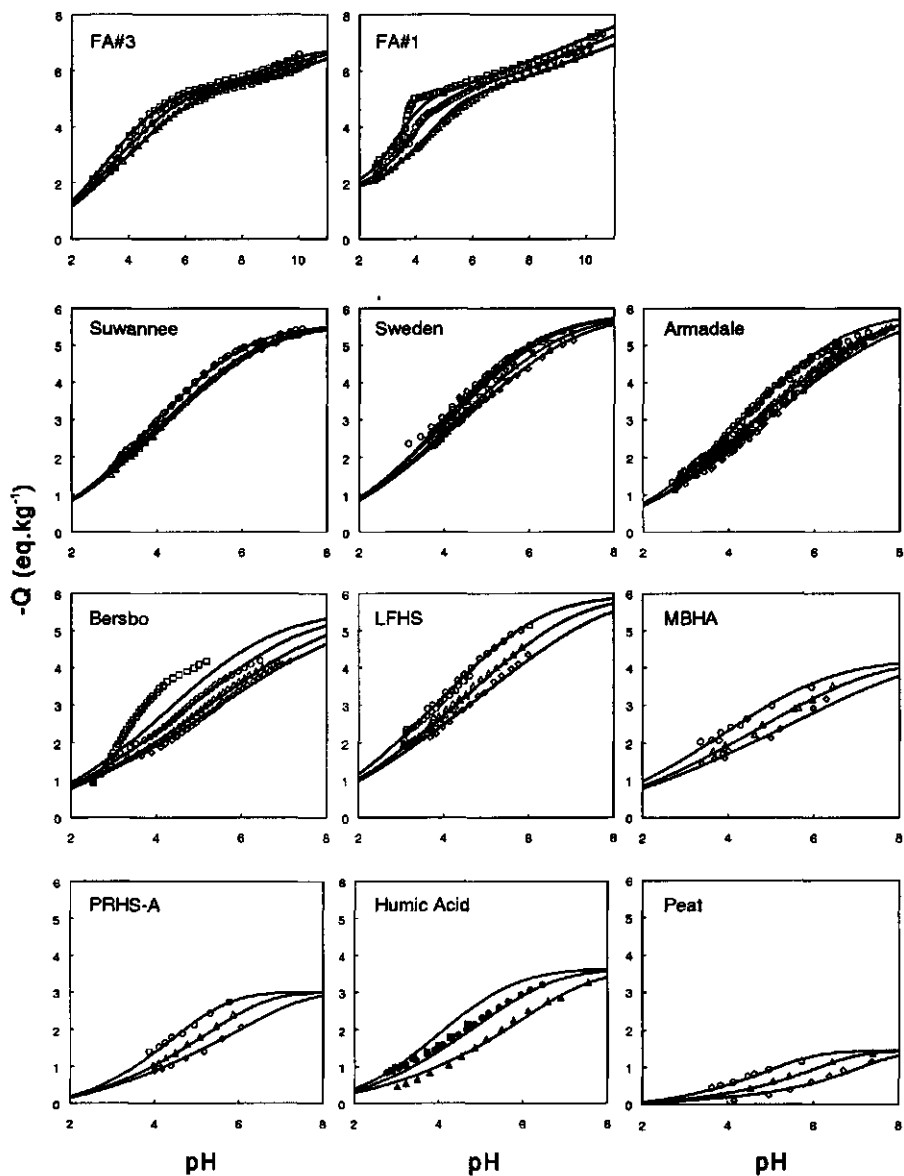
Figure 4. The calculated Q(pH) curves based on the assessed Langmuir Freundlich equation in combination with the spherical double layer model compared with the experimental Q(pH) data. $\Diamond$=0.001 M, ∇=0.005 M, $\blacktriangle$= 0.01 M, $\blacktriangle$=0.02 M, O=0.1 M, $\bullet$=0.2 M, $\Box$= 1 M and $\blacksquare$=2 M.

fests. Despite the low r^2 for the $Q(pH_S)$ fit of the peat sample, the description of the data is still satisfactory.

The Surface Charge Density and Surface Potential as a Function of the pH

The assessed model description allows for the calculation of the surface charge σ_S and the surface potential, ψ_S, of the humic particles as a function of ionic strength and pH. In fig. 5 an example is given for a hypothetical humic acid, panel a shows $\sigma_S(pH)$, panel b $\psi_S(pH)$. The proton binding of this "humic acid" is described by a double LF equation, for the electrostatic effects a spherical double layer is used. The parameters for the low affinity peak and for the radius of the sphere are the median values for the data sets analyzed. The values for the high affinity peak correspond to the values for the FA#3 sample.

Because σ and Q are directly proportional, the calculated surface charge density versus pH graphs (fig. 5a) are very similar to the experimental $Q(pH)$ curves. The maximum negative charge of the humic particle is around -160 $mC.m^{-2}$, which corresponds to a site density of approximately 1 $sites.nm^{-2}$. Compared to iron(hydr-)oxide particles, which are also important particles in natural systems, the salt dependence and the overall change of the charge density of humics in a given pH range is smaller. The integral capacitance, $\Delta\sigma/\Delta pH$, of the humics is about 5 to 50 % of that of oxides.

The course of ψ_S as a function of the pH (fig. 5b) is clearly not linear and non-Nernstian. Again this behaviour differs from the behaviour of amphoteric oxides, like iron oxides, for which ψ_S is by approximation Nernstian over a fairly wide pH range around the point of zero charge.
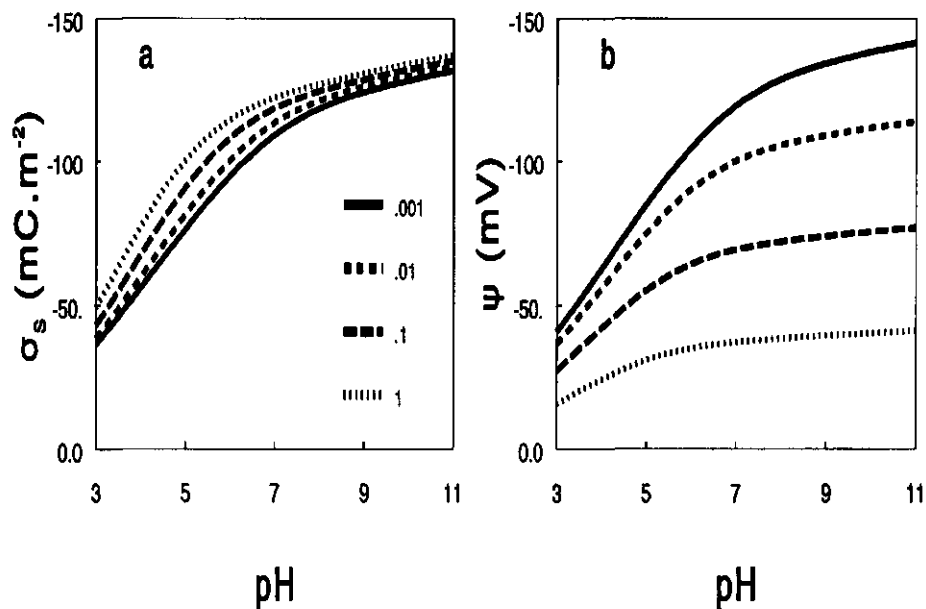
a

σ_s (mC.m^{-2})

-150

-100

-50.

0.0

.001
.01
.1
1

b

ψ (mV)

-150

-100

-50.

0.0

3 5 7 9 11

pH

3 5 7 9 11

pH

Figure 5. The surface charge density σ_s (mC.m^{-2}) and the surface potential ψ_s (mV) of a hypothetical humic acid as a function of the pH. The proton binding to the humic acid is given by a double LF equation with Q_{1max}=4.24 (eq.kg^{-1}), log $\tilde{K}_{1,H}$=3.10, m_1=0.48, Q_{2max}=1.18 (eq.kg^{-1}), log $\tilde{K}_{2,H}$=8.47, m_2=0.59 and a spherical double layer model with r=0.85 nm.

Figure 5b clearly shows the effect of the ionic strength. For high ionic strength the screening of the charge is more efficient which results in small electrostatic interactions and to a small ψ_s. The lower electrostatic interactions make the surface more easily to charge, hence the higher the ionic strength the lower the pH for which the humic particle has a certain σ_s (fig 5a). Apparently in figure 5a the salt effect becomes smaller around pH=7. The fact that in fig 5b, ψ_s at pH≥7 is rather different for the different salt concentrations clearly indicates that the impression of a smaller effect is an optical illusion caused by the decrease of the slope of the titration curves around pH=7.

119

Conclusions

- In potentiometric titrations high quality data for different ionic strength can be determined for a pH range from 3-11. A pH range 3-11 corresponds to a maximum pH_s and log K_H range from 2.5 to 9.5.

- The obtained distribution functions are all characterized by a large peak with a peak position in the log K range 3-4. This large peak corresponds to carboxylic groups. In samples which were titrated over a large pH range a smaller second peak is found. The peak position for this peak is around log K=8-9. This peak probably corresponds to phenolic type of groups.

- Based on the calculated distribution functions the selection of a site binding model is straightforward. Hence, the heterogeneity analysis is a powerful tool in the analysis of ion binding .

- The $Q(pH_s)$ masters curve can be described well with a single Freundlich type of equation or a combination of Freundlich type of equations for continuous heterogeneous surfaces. In general, a description based on the LF and the Tóth equation give slightly better results than the GF equation. The reason that it is not possible to discriminate between the three models analyzed is that only a window of experimental data is available, so that also only a part of the distribution can be derived.

- The combination of the electrical double layer model (spherical or cylindrical) derived from the master curve analysis with the site binding model that describes the master curve, allows for the description of the Q(pH) curves for various values of the ionic strength. With the parameters resulting from the analysis an excellent description of the experimental data is found.

- On the basis of the overall binding model the surface charge and the surface potential of the humics can be calculated. It is shown that humic substances exhibit a strong non Nernstian behaviour.

Acknowledgement

References

1. Buffle, J. *Complexation Reactions in Aquatic Systems: An Analytical Approach*; Ellis Horwood Limited: Chichester, 1988.

2. De Wit, J.C.M.; Van Riemsdijk, W.H.; Nederlof, M.M.; Kinniburgh, D.G.; Koopal, L.K. *Analytica Chim. Acta* 1990, 232, 189-207.

3. De Wit, J.C.M.; Nederlof, M.M.; Van Riemsdijk, W.H.; Koopal, L.K. *Water, Air and Soil Pollution* 1991, 57-58, 339-349.

4. De Wit, J.C.M.; Van Riemsdijk, W.H.; and Koopal, L.K.; *Finnish Humus News* 1991, 3, 139-144.

5. MacCarthy, P.; Perdue, E.M., 1991, In *Interactions at the Soil Colloid - Soil Solution Interface*; Bolt, G.H.; De Boodt, M.F.; Hayes, M.H.B.; McBride M.B. (Eds.); NATO ASI Series Series E: Applied Sciences-Vol. 190, Kluwer Academic Publishers, Dordrecht, 469-489.

6. Livens, F.R., *Environ. Pollution* 1991, 70, 183-208.

7. Ephraim, J.; Alegret, S.; Mathuthu, A.; Bicking, M.; Malcolm, R.L.; Marinsky, J.A.; *Envir. Sci. Technol.* 1986, 20, 354-366.

8. Marinsky, J.A. In *Aquatic Surface Chemistry*; Stumm, W. (Ed.); Wiley Interscience: New York, 1987, Ch. 3.

9. Tipping, E.; Backes C.A.; Hurley, M.A. *Water Res.* 1988, 22, 597-611.

10 Tipping, E., Woof, C.; Hurley, M.A. *Water. Res.*, 1991, 25, 425-435.

11. Bartschat, B.M.; Cabaniss, S.E.; Morel, F.M.M. *Environ. Sci. Technol.* 1992, 26, 284-294.

12. De Wit, J.C.M.; Van Riemsdijk, W.H.; Koopal, L.K., Proton Binding to Humic Substances. A. Electrostatic Effects. Submitted to *Environ. Sci. Technol.* 1992

13. Van Riemsdijk, W.H., Bolt, G.H.; Koopal, L.K. In *Interactions at the Soil Colloid - Soil Solution Interface*; Bolt, G.H.; De Boodt, M.F.; Hayes, M.H.B.; McBride M.B. (Eds.); NATO ASI Series Series E: Applied Sciences-Vol. 190, Kluwer Academic Publishers: Dordrecht, 1991, 81-113.

14. Van Riemsdijk, W.H.; Koopal, L.K. In *Environmental Particles*; Buffle, J.; Van Leeuwen, H.P. Lewis Publishers: Chelsea, Michigan, 1992, Chapter 12.

15. Nederlof, M.M.; Van Riemsdijk, W.H.; Koopal, L.K.; *J. Colloid Interface Sci.* **1990**, *135*, 410-426.

16. Kinniburgh, D.G.; Barker, J. A.; Whitfield, M. *J. Colloid Interface Sci.* **1983**, *95*, 370-384.

17. Nederlof, M.M. *Analysis of Binding Heterogeneity*, Wageningen Agricultural University: Wageningen, 1992, PhD thesis, chapter 5.

18   Sips, R. *J. Chem. Phys.* **1948**, *16*, 490.

19. Sips, R. *J. Chem. Phys.* **1950**, *18*, 1024.

20. Tóth, J.; Rudziński, W.; Waksmundsku, A.; Jaroniec, M.; Sokolowsky, S. *Acta Chim. Hungar.* **1974**, *82*,11.

21   Nederlof, M.M., Van Riemsdijk, W.H.; Koopal, L.K.; *Environ. Sci. Technol.* **1992**, *26*, 763-771.

22. Turner, D.R.; Varney, M.S.; Whitfield, M.; Mantoura R.F.C.; Riley J.P. *Geochim. Cosmochim. Acta* **1986**, *50*, 289-297.

23   Dempsey, B.A., O'Melia C.R., In *Aquatic and Terrestrial Humic Materials*; Christman, R.F.; Gjessing E.T.(Eds.), Ann Arbor Science: Michigan, 1983; Chapter 12.

24.. Dempsey, B.A. *The Protonation, Calcium Complexation, and Adsorption of a Fractionated Aquatic Fulvic Acid*, Ph.D. Thesis, The Johns Hopkins University: Chapel Hill, 1981, pp 201.

25. Ephraim, J.H.; Borén, H.; Pettersson, C.; Arsenie, I.; Allard, B. *Environ. Sci. Technol.* **1989**, *23*, 356-362.

26   Marinsky, J.A.; Gupta, S; Schindler, P. *J. Colloid Interface Sci.* **1982**, *89*, 401-411.

27. Marinsky, J.A.; Wolf, A.; Bunzl, K. *Talanta* **1980**, *27*, 461-468.

28. Nederlof, M.M., *AFFINITY. A Computer Program for the Calculation of Affinity Distributions from Binding Data*, Technical Note of the Department of Soil Science and Plant Nutrition, Wageningen Agricultural University, Wageningen, 1992.

29. Kinniburgh, D.G., *Isotherm. A Computer Program for Analyzing Adsorption Data*; Report, WD/ST/8502; British Geological Survey. Wallingford, 1985.

30. Keizer, M.G.; De Wit; J.C.M.; Meeussen, J.C.L.; Bosma, J.P., Nederlof, M.M.; Van Riemsdijk; W.H.; Van der Zee, S.E.A.T.M. *ECOSAT*; Technical Note of the Department of Soil Science and Plant Nutrition, Wageningen Agricultural University, Wageningen, 1992.

Appendix 1. The assessed parameters for the description of the $Q(pH_s)$ data with the Generalised Freundlich equation

Table 1.I The assessed parameters for the Generalised Freundlich equation describing the $Q(pH_s)$ data obtained with the spherical double layer model

name		log K_H	m	$-Q_{max}$ (eq.kg^{-1})	r^{2*}	RMSE**
FA#3	site 1	1.66	0.21	6.16	0.996	0.088
	site 2	8.65	1.00	0.61		
FA#3	pH$_s$<5.5	1.47	0.15	7.08	0.993	0.096
FA#1	site 1	1.25	0.23	6.47	0.978	0.203
	site 2	7.19	0.02	12.62		
Suwannee River Fulvic Acid		2.11	0.20	6.43	0.996	0.074
Sweden		2.02	0.17	7.28	0.977	0.130
Armadale Horizons Bh Fulvic Acid		1.98	0.13	8.43	0.985	0.149
Bersbo FA		1.20	(5.85E-15)	(8.04E+13)	0.981	0.126
LFHS		1.45	0.12	9.21	0.978	0.124
MBHA		1.11	0.11	6.44	0.945	0.146
PRHS-A		2.97	0.58	3.20	0.953	0.117
Humic Acid		2.21	0.13	5.85	0.934	0.208
Peat		3.10	1.00	1.45	0.776	0.178
median		1.98	0.15	6.44		

Table 1.II The assessed parameters for the Generalised Freundlich equation describing the $Q(pH_s)$ data obtained with the cylindrical double layer model

name		log K_H	m	$-Q_{max}$ (eq.kg^{-1})	r^{2*}	RMSE**
FA#3	site 1	1.68	0.19	6.22	0.995	0.091
	site 2	8.95	1.00	0.58		
FA#1	site 1	1.27	0.21	6.58	0.978	0.201
	site 2	7.73	0.04	5.25		
Suwannee River Fulvic Acid		2.11	0.15	6.80	0.995	0.086
Sweden		2.00	0.12	8.06	0.979	0.125
Armadale Horizons Bh Fulvic Acid		1.93	0.08	10.24	0.989	0.132
Bersbo FA		1.21	(2.25E-13)	(1.84E+12)	0.985	0.112
LFHS		1.42	0.05	15.47	0.985	0.100
MBHA		1.00	0.05	9.20	0.948	0.142
PRHS-A		2.75	0.21	4.39	0.977	0.082
Humic Acid		2.20	0.11	6.38	0.947	0.187
Peat		3.23	1.00	1.45	0.861	0.141
median		1.93	0.12	6.58		

with values between braces () are not realistic and:

$$* \ r^2 = 1 - \frac{\sum_{i=1}^{np} (n_i - \hat{n}_i)^2}{\sum_{i=1}^{np} (n_i - \bar{n}_i)^2}$$

$$** \ RMSE = \left(\frac{\sum_{i=1}^{np} (n_i - \hat{n}_i)^2}{m - np} \right)^{0.5}$$

n_i measured value for datapoint i
$\hat{n}_i$ fitted value for datapoint i
np number of datapoints
p number of parameters
$\bar{n}$ average value of measured datapoints

123

Appendix 2. The assessed parameters for the description of the $Q(pH_s)$ data with the Tóth equation

Table 2.I The assessed parameters for the Tóth equation describing the $Q(pH_s)$ data obtained with the spherical double layer model.

name		log K_H	m	-Q_{max} (eq.kg^{-1})	r^{2*}	RMSE**
FA#3	site1	4.25	0.37	5.10	0.998	0.055
	site 2	11.02	0.26	2.07		
FA#3	pH$_s$<5.5	4.38	0.36	5.36	0.997	0.059
FA#1	site 1	2.79	(1.00)	2.66	0.983	0.176
	site 2	(30.49)	(0.06)	(8.95)		
Suwannee River Fulvic Acid		4.61	0.39	5.37	0.998	0.049
Sweden		4.49	0.39	5.53	0.983	0.111
Armadale Horizons Bh Fulvic Acid		4.51	0.42	5.53	0.991	0.114
Bersbo FA		5.25	0.33	4.91	0.987	0.104
LFHS		3.81	0.43	5.56	0.981	0.113
MBHA		4.06	0.37	3.90	0.949	0.141
PRHS-A		3.38	0.84	2.97	0.953	0.117
Humic Acid		4.06	0.53	3.44	0.936	0.206
Peat		3.10	1.00	1.45	0.776	0.178
median		4.06	0.42	3.90		

Table 2.II The assessed parameters for the Tóth equation describing the $Q(pH_s)$ data obtained with the cylindrical double layer model

Name		log K_H	m	-Q_{max} (eq.kg^{-1})	r^{2*}	RMSE**
FA#3	site 1	4.56	0.35	5.13	0.998	0.058
	site 2	11.06	0.27	1.96		
FA#1	site 1	2.98	(1.00)	2.52	0.984	0.170
	site 2	(30.94)	(0.06)	(8.93)		
Suwannee River Fulvic Acid		5.32	0.34	5.39	0.997	0.064
Sweden		5.26	0.33	5.57	0.985	0.105
Armadale Horizons Bh Fulvic Acid		5.44	0.34	5.55	0.994	0.095
Bersbo FA		6.07	0.29	4.89	0.990	0.091
LFHS		4.90	0.35	5.71	0.988	0.091
MBHA		4.94	0.31	3.97	0.952	0.137
PRHS-A		4.02	0.62	3.06	0.978	0.081
Humic Acid		4.23	0.50	3.44	0.949	0.184
Peat		3.23	1.00	1.45	0.861	0.141
median		4.56	0.35	3.97		

$$* \ r^2 = 1 - \frac{\sum_{i=1}^{np} (n_i - \bar{n}_i)^2}{\sum_{i=1}^{np} (n_i - \bar{n}_i)^2}$$

$$** \ RMSE = \left(\frac{\sum_{i=1}^{np} (n_i - \hat{n})^2}{m - np} \right)^{0.5}$$

n_i measured value for datapoint i
$\hat{n}_i$ fitted value for datapoint i
np   number of datapoints
p   number of parameters
ñ   average value of measured datapoints

Chapter **5**

The Description of Cadmium Binding to a Purified Peat Humic Acid

Abstract

In this paper experimental cadmium binding data to a purified peat humic acid measured at three constant pH values for 7 decades of cadmium concentration are described with two different models: a fully coupled model and an uncoupled binding model.

The description of the proton binding, in absence of metal ions forms the basis for both models. The proton binding is described with analytical expressions for continuous heterogeneous ligands in combination with a spherical double layer model to account for the electrostatic effects. In order to describe metal ion binding an approximate binding stoichiometry is assumed, in which upon the binding of one metal ion, x protons are released in the solution.

For the uncoupled model a scaling procedure was presented that allows to obtain the parameter x and that can be used to test the validity of the assumption of uncoupled binding. It is shown that the uncoupled model can describe the pH dependent binding over the whole cadmium concentration range.

In order to describe the cadmium binding over the whole cadmium concentration range with the fully coupled model, the presence of a small number of sites (around 1 %) has to be assumed which have a higher affinity for cadmium than the bulk of the sites.

125

This paper is submitted for publication in *Environmental Science and Technology*:
J.C.M. de Wit, W.H. van Riemsdijk, L.K. Koopal, C.J. Milne, D.G. Kinniburgh, The
Description of Cadmium Binding to a Purified Peat Humic Acid.

126

Introduction

The evaluation of the speciation of trace metal ions in the environment is essential for the determination of their (bio-)availability and for a sound risk assessment. The complexation of trace metals with other inorganic ions in the solution phase is relatively well known (1-4) and several models for the calculation of the chemical equilibrium do exist (5-6). The binding onto the solid phase and the colloidal particles is not yet resolved satisfactory, and no consensus of opinion exists about the modelling. This holds especially for the binding of trace metals to natural organic matter, like fulvic acids and humic acids (7).

A general accepted picture is that metal ions do form complexes with the functional groups of the humic materials (8-13). A first characteristic of metal ion binding is the stoichiometry of the binding to the sites. The metal ions can be bound to the sites in various ways. Secondly, natural organic matter is a complex and polydisperse mixture of organic polyelectrolytes (8-15), containing a large number of different types of functional groups. This chemical heterogeneity is the second characteristic which determines the metal ion adsorption.

A third factor to be considered is the competition between different ions (eg. 7,11,16). In natural systems we are dealing with multi-component systems. In addition to metal ions, protons (and/or hydroxyl ions) and other electrolyte ions are present in the most simple aqueous humic acid system one may think of. Even if the electrolyte ions are indifferent, that is to say they interact with the humics by coulombic forces only, there is still competition between the metal ions and the protons for the binding sites. This results in a rather strong pH dependency of the metal ion adsorption. This type of competition also occurs when other specifically adsorbing electrolyte ions are present.

The fourth factor that influences adsorption is electrostatics (eg. 16-19). Humic materials have, due to the dissociation of the functional groups, a pH dependent negative charge. The negative charge promotes the adsorption of positive ions in two ways. First of all the concentration of the positive ions in the double layer around the humic colloid is larger

than in the bulk. This binding by coulombic interactions is non-specific and depends only on the valency of the ion. The second effect is that a higher concentration of metal ions near the functional groups will result in a larger specific binding than expected on the basis of the concentration in the bulk solution.

The electrostatics or variable charge effects do also influence secondary properties of the humic molecules like their conformation and the aggregation of molecules in large complexes. Both conformational changes and aggregation will in turn affect the metal ion binding (and vice versa).

A model for metal ion binding should in principle be able to describe and to predict binding for a wide range of conditions with respect to pH, solution composition and ionic strength. In order to achieve this the four factors mentioned: stoichiometry of the binding equation, chemical heterogeneity, competition and electrostatics should be incorporated explicitly. Yet the complexity of the system is such that simplifying assumptions about the nature of the binding have to be made (10-12,16). Undoubtedly these assumptions are to some extent arbitrary and do highly depend on the "good-taste" and the scientific roots of the modellers. From point of view of those who use the models in practice, a preferred option would be to reach a set of generally accepted conventions.

Important modelling efforts made in literature are, in our opinion, those in which at least several of the above mentioned factors are taken into account explicitly. Many authors (eg. 10-12, 20-22) treat humics as a mixture of different site functional groups each with its own stoichiometry and binding constant for a specific ion. The different functional groups can be part of a larger molecule or can be present as a mixture of simple ligands in solution. In some cases this approach is combined with explicit incorporation of the electrostatic interactions or of the polydispersity (eg. 17-19, 23-33). The models for the electric interactions ranges from (semi-)empirical relations to (semi-)theoretical double layer models.

A major disadvantage of the models in which a discrete distribution is used is that the choice of the set of site types is highly arbitrary.

Although the opposite is sometimes suggested, there is no sound scientific basis for selecting certain typical discrete site types a priori. If a priori different site types are chosen in combination with binding constants derived from the corresponding simple organic ligands, the degree of freedom in adjusting the site densities is still such that a reasonable description of the data can be obtained, for many combinations of different site types. This is especially the case if the model description is only used to describe binding under limited conditions.

As an alternative for the discrete distributions, continuous affinity distributions can be used (34-44). For continuous affinity distributions the overall binding equation is, in general, a complicated expression which can only be solved numerically. However for a few, fairly realistic distribution functions analytical solutions are known (45-46). The advantage of the models for continuous heterogeneity is the small number of parameters involved. In many cases only two parameters, suffices to describe the binding; a parameter that determines the width of the distribution and a median affinity constant. Disadvantages are that the extension to multi component binding is complicated.

In this paper we will work out two approaches which allow for the description of metal ion binding for a wide range of conditions. This is achieved by using an alternative relation for the binding stoichiometry in combination with a continuous heterogeneity and a model for the electrostatic interactions derived from proton adsorption studies. The two approaches used, differ with respect to the formulation of the site competition between metal ions and protons. In the coupled binding model metal ions and protons compete for the same surface sites, and multi component binding equations for heterogeneous ligands should be used to describe the binding (16). In the uncoupled binding model protons and metal ions each have their own type of surface sites, and for each component the binding can be described with a monocomponent binding equation for heterogeneous ligands (16).

For both approaches important information is derived from proton binding: the choice of the double layer model and the description of the

chemical affinity distribution for the proton binding. Since these characteristics are determined independently from the analysis of the metal ion binding data we will summarize the proton adsorption model briefly.

In order to be able to check the model efforts a detailed study has been made of the binding of cadmium on a humic acid isolated from peat. The binding is measured over a large cadmium concentration range and at three pH values.

Proton and Metal Ion Binding

Proton Binding

The proton binding to a site S^- can be described with the following binding stoichiometry:

$$S^- + H^+ \rightleftharpoons SH \tag{1}$$

Proton binding in the presence of an indifferent electrolyte is essentially a mono component binding process (eg. 16). For a given pH the degree of protonation is mainly influenced by the chemical heterogeneity of the humic material and by the electrostatic effects, which are a function of the ionic strength. A set of proton binding curves measured at different constant ionic strength, allows for the assessment of a double layer model that accounts for the salt dependency of the proton binding (16, 40-44). After the assessment of the double layer model it is possible to derive the frequency distribution of intrinsic proton binding constants using heterogeneity analysis (16, 41-44). Based on the heterogeneity analysis a model can be chosen that allows for description of proton binding for chemical heterogeneous ligands.

The analysis of a large number of different humic acid samples showed that the electric effects could be described fairly well by assuming rather simple diffuse double layer models for rigid impermeable spherical or cylindrical particles with average dimensions (43-44). For the quality of the description the choice of the geometry turned out to be irrelevant. The

polydispersity of the humic material and the changes of their conformation did not strongly influence the proton binding, and can be considered as second order processes.

The determined proton affinity distributions were characterized by a broad peak with a peak position in the log K range 3-4. The affinity distribution for samples which were titrated over a wide pH range up to 11 did show a second broad peak with a peak position in the log K range around log K=9. In general the proton affinity distributions were not characterized by sharp peaks, which would indicate a discrete heterogeneity. Because of the relatively simple continuous distributions, analytical equations could be used to describe the proton binding. Use was made of the Generalised Freundlich (GF) equation (45), the Langmuir Freundlich (LF) equation (46) and the Tóth equation (46). Although the goodness of fit for all three models was satisfactory the LF and the Tóth type equations did give a somewhat better description, than the GF equations. For that reason we do not consider the GF equation in this paper.

Metal Ion Binding

The characterization of the proton behaviour forms a good starting point for the description of the metal ion binding. However in order to extend the proton adsorption model to include metal ion adsorption some further assumptions have to be made about the nature of the metal ion binding.

The first assumption is that for metal ion binding the assessed double layer model remains applicable. In other words, metal ion binding does not significantly influence the radius of the particles.

The second assumption is on the stoichiometry of the metal binding equation. A very simple and often used description of monodentate binding of a divalent metal ion to a site S^- is:

$$S^- + M^{2+} \rightleftharpoons SM^+ \qquad (2)$$

An alternative monodentate binding equation is:

$$S^- + M^{2+} + H_2O \rightleftharpoons SMOH + H^+ \qquad (3)$$
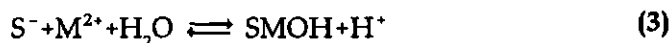
Equation (3) can be interpreted as (a) adsorption of a metal-OH complex or (b) as the formation of a hydrolysed surface group. Next to the formation of monodentate species, also bidentate or multi-dentate surface complexes can be formed. According to several authors (eg. 11, 18, 48) bidentate binding of metal species to phthalic acid and salicylic acid type of groups in humic and fulvic acids plays an important role. These groups will protonate in two consecutive steps. Because the two acidic groups in such structures are in close proximity one can treat these structures as one surface group with two reactive dents (40). The corresponding formation of a bidentate metal species can be given by:

$$S_2^{2-} + M^{2+} \rightleftharpoons S_2M \qquad (4)$$

The equations (2-4) are only examples of relevant binding equations. For humic substances, which contain many different chemical structures forming different functional groups, a whole series of stoichiometries, may be proposed. The selection of one specific equation to describe the binding is therefore rather arbitrary. On the other hand a binding model in which a series of different stoichiometries is taken into account is also not very satisfactory as it requires a whole series of adjustable parameters. In order to limit the number of adjustable model parameters we propose to use an average stoichiometry:

$$S^- + M^{2+} + xH_2O \rightleftharpoons SM(OH)_x^{1-x} + xH^+ \qquad (5)$$
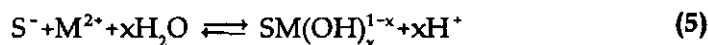
In Eq. (5) x is an adjustable parameter with can have a non-integer value. This value depends on the type of cation and may range from 0 to 2. The definition of equation (5) suggests that the factor x accounts for the (partial) hydrolysation of the surface complex and that only the formation

of monodentate species are taken into account. This is not necessarily the case. For instance for a fully dissociated salicylic acid type of group the first proton affinity constant is very high (log $K_H > 13$). As a consequence the fraction of the fully dissociated S_2^{2-} surface species is negligible even under extreme conditions with respect to the pH, and only the S_2H^- and the S_2H_2 species are relevant. Because the S_2^{2-} to S_2H^- protonation step is apparently not present, the observed bidentate binding can be described by (40):

$$S_2H^- + M^{2+} \rightleftharpoons S_2M + H^+ \tag{6}$$
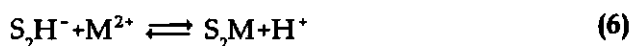
The net effect of this equation with respect to the metal proton exchange is identical to that of Eq. (3): adsorption of a metal ion is followed by the release of a proton. It should however be realized that in Eq. (3) the proton release originates from the dissociation of water whereas in Eq. (6) it originates from the dissociation of a proton that binds very strongly to the humics.

In equation (5) the factor x determines the number of protons which are released per bound metal ion. Apart from the number x of protons released directly through the binding of a metal ion, protons may also be released from the surface because of an increase in the surface charge due to metal ion adsorption. When $x < 2$ the divalent metal ion adds positive charge to the humic particle. This causes a non-specific coulombic proton release. The release of such protons is not accounted for in Eq. (5). Consequently in general the value of x does not correspond to the experimentally determined proton/metal exchange ratio r_{ex}, which is determined by the total proton release.

The third assumption in the models concerns the relation between the affinity distributions for the protons and the metal ions. We will consider two limiting cases: the case of coupled adsorption and the case of uncoupled adsorption (16). In the case of coupled adsorption we assume that metal ions and protons are in competition for the same surface sites S and that the shapes of the metal ion affinity distribution and the proton affinity distribution are identical, only the location of the

133

distributions on the log K axis is different. The proton binding stoichiometry is given by Eq. (1), that for the metal ion binding by Eq. (5). In order to describe the metal binding, a multi-component binding equation for heterogeneous ligand should be used.

In the case of uncoupled adsorption, the intrinsic metal affinity distribution is not related to the proton affinity distribution. Metal ions are assumed to have their own sites, T, which are different from the proton sites, S. Because of this, there is no direct site competition between metal ions and protons and the metal binding can be described with monocomponent binding equations for heterogeneous ligands.

For the uncoupled case the proton binding stoichiometry is given by Eq. (1) and the metal binding by:

$$T + M^{2+} + xH_2O \rightleftharpoons TM(OH)_x^{2-x} + xH^+ \qquad (7)$$
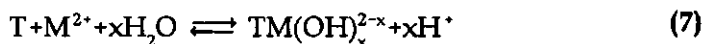
The proton binding to the S^- sites and the metal binding to the T sites are only interrelated through the electrostatic interactions. In absence of metal ions the charge of the humic particles is fully determined by the degree of dissociation of the proton sites S^-. The metal sites, T, are therefore assumed to be uncharged. The binding of metal ions adds 2-x positive charges to the surface charge. This affects the charge of the humic particles, and thus also the electrostatic interactions.

The overall release of protons upon metal binding in the uncoupled model results from the assumed stoichiometry of Eq. (7) plus a release of protons from the SH sites due to the net increase of particle charge through electrostatic interactions. In the coupled binding model, also the direct competition between protons and metal ions for the same sites affects the metal ion/proton exchange.

Analytical Monocomponent Binding Equations for Continuous Heterogeneous Ligands

The binding to a continuous heterogeneous ligand follows from the integration of the product of the affinity distribution and the local binding

function for a certain type of site over the relevant log K range. In general this integration should be solved numerically, only for a few types of distributions an analytical solution can be obtained. Two well known solutions based on a Langmuir type of local isotherm are the Langmuir Freundlich (LF) equation (46) and the Tóth equation (47).

The LF equation is derived for a symmetrical pseudo-Gaussian distribution. For binding of a component C the LF equation is given by:

$$\theta_C = \frac{\left(\tilde{K}_C c\right)^m}{1 + \left(\tilde{K}_C c\right)^m} \tag{8}$$

where m is a measure for the width of the distribution ($0 < m \leq 1$) and $\tilde{K}_C$ determines the location of the distribution on the log K axis. In its most simple form c is the concentration of the component C sorbed. However, c can also be a more complex quantity as will be discussed below. θ_C is the binding of component C expressed as fraction of the total number of sites available. θ_C is dimensionless. The adsorption in practical units, Γ_C is obtained by multiplying θ_C with the adsorption maximum, $\Gamma_{C,max}$.

The Tóth equation is derived for an asymmetric distribution with a low affinity tail and is defined as:

$$\theta_C = \frac{\tilde{K}_C c}{\left[1 + \left(\tilde{K}_C c\right)^m\right]^{1/m}} \tag{9}$$

The parameters have the same meaning as in the LF equation (Eq. 8).

For both equations the value of m determines the degree of heterogeneity. For m=1 the surface is homogeneous and the resulting binding equations become identical to the Langmuir equation. The smaller m, the wider the distribution and the larger the heterogeneity of the ligand.

At low coverage (small θ_C) the $(\tilde{K}_C c)^m$ term in the denominator of both equations is much smaller than 1, and only the numerator determines the binding. At low coverage the LF equation becomes identical to the

135

classical non linear, non normalized Freundlich equation. For the Tóth equation a linear binding equation results, which is a principle advantage.

The LF and the Tóth equation describe binding to a ligand for which the affinity distribution is characterized by one more or less broad peak. For ligands with an affinity distribution which shows several peaks a weighted summation of LF and/or Tóth equations can be used:

$$\theta_{T,C} = \sum_j f_j \theta_{j,C} \qquad (10)$$

with $\theta_{T,C}$ is the overall binding for component C, $\theta_{j,C}$ is the binding corresponding with one peak of the distribution, and f_j is the fraction this peak contributes to the total number of sites.

Uncoupled Binding

In the limiting case of uncoupled binding the adsorption sites for protons and metal ions are independent. The affinity distributions for the proton and the metal ion are not related, and protons and metal ions do only interact electrostatically. For a heterogeneous surface the binding equations as given by Eqs. (8-10) apply. In order to incorporate the electrostatic interactions the "concentration" c to be used in the proton binding equation equals H_S:

$$c = H_s \qquad (11)$$

H_S can be seen as the proton concentration in solution at the location of the binding sites, it is defined as:

$$H_S \equiv [H^+] \exp\left(-\frac{F\psi_s}{RT}\right) \qquad (12)$$

with $[H^+]$ the proton concentration in the bulk of the solution and ψ_s the electric potential near the functional groups. F is Faraday's constant, R the gas constant and T the temperature.

For metal binding according to Eqs [5] and [8-10] the "concentration" c is somewhat more complex:

$$c = \frac{M_S}{\left(H_S\right)^x}$$ (13)

with M_S for divalent cations defined as:

$$M_S = [M^{2+}] \exp\left(-2\frac{F\psi_S}{RT}\right)$$ (14)

It is assumed that both protons and metal ions experience the same smeared out surface potential, which is independent of the location at the surface.

$\Gamma(H_S)$ and $\Gamma(M_S/H_S^x)$ Master Curves

For the monocomponent binding equations the binding plotted as a function of c is only one single curve. This observation is the basis of the master curve procedure for the assessment of the double layer model on the basis of proton binding data (16). The proton binding data, measured as a function of pH show an ionic strength dependency. This ionic strength dependency should vanish when the curves are replotted as a function of pH_S. pH_S can be calculated from the pH and ψ_S, and ψ_S follows from the chosen double layer model once the surface charge density is established.

Metal ion binding to humic type materials is rather pH dependent. When binding curves are measured for a series of pH values, a series of different curves result. If the uncoupled binding adsorption in combination with the assumed binding Eq. (5) is appropriate, the metal ion binding curves, measured for different pH, should merge to a single metal binding "master curve" when the metal binding is plotted as a function of M_S/H_S^x. By constructing a master curve the parameter x is assessed and it is tested if the assumption of uncoupled adsorption is appropriate; if no good

137

merging of the curves is obtained it should be concluded that the assumption of uncoupled adsorption is inadequate.

For the calculation of the M_S/H_S^x ratio a double layer model and the charge of the humic sample are prerequisites. As is stressed in the introduction our model is essentially an extension of a proton binding model. In that perspective we assume that the proton binding is analyzed before metal ion binding is studied. This implicates that the double layer model has been assessed independently, and that the initial charge of the humic particles in absence of other specifically adsorbing ions can be calculated.

By determining the metal proton exchange ratio experimentally, the change of the charge due to the metal ion binding is established. In combination with the initial charge this allows for the calculation of the final charge and for the calculation of ψ_S using the double layer model.

In the case the exchange ratio is not known, the ψ_S based on the initial charge can be used to construct the master curve. At trace metal levels the degree of metal adsorption is small and the change of ψ_S is negligible. Hence, at the low end of the metal ion binding curves good merging curves should be obtained, if the assumption of uncoupled adsorption is appropriate. When the metal adsorption increases, the initial ψ_S will change and the curves start to deviate.

The construction of the M_S/H_S^x curves is straightforward provided that the non-specific binding of the metal ion in the diffuse layer is small. In general this is the case if the ionic strength is dominated by another electrolyte. When the non-specific binding is considerable an iterative procedure should be used to calculate the part of the measured binding which is due to specific binding, Γ_M^{spec}, the part due to non-specific binding Γ_M^{non}, and the M_S/H_S^x ratio.

On the basis of the $\Gamma(M_S/H_S^x)$ master curves the metal ion affinity distribution can be obtained by applying heterogeneity analysis methods like the CA or the LOGA method (49-50). In this paper this will not be done, we will use the master curve data for obtaining the model parameters of the LF and the Tóth binding equation. In order to describe

the binding with the uncoupled binding equations 4 parameters have to be determined; x, m, $\Gamma_{M,max}$ and $\bar{K}_M$.

Coupled Binding and Multicomponent Binding Equations

Multicomponent Binding Equations

The multicomponent LF and Tóth equations are derived by assuming that the affinity constant of every component consists of two parts (51-53). One part is typical for the type of component, the other is a characteristic of the heterogeneous ligand. The component dependent part is a constant, while the ligand dependent part is distributed. This distribution is the same for all components. With these assumptions the integral equation, which describes metal ion binding to heterogeneous ligands, can again be solved analytically for the earlier mentioned LF and Tóth distribution functions (51-53).

For the distribution underlying the LF equation the following equation is obtained:

$$\theta_i = \frac{\bar{K}_i c_i}{\sum \bar{K}_i c_i} \cdot \frac{\left(\sum \bar{K}_i c_i\right)^m}{1 + \left(\sum \bar{K}_i c_i\right)^m} \tag{15}$$

with i referring to the different components. $\Sigma \bar{K}_i c_i$ is the summation over i of the $\bar{K}_i c_i$ product for the different components. Like for the uncoupled case the $\bar{K}_i c_i$ can be rather complex functionalities, instead of simple products of a constant and a component concentration.

The multicomponent expression for the Tóth equation reads:

$$\theta_i = \frac{\bar{K}_i c_i}{\sum \bar{K}_i c_i} \cdot \frac{\sum \bar{K}_i c_i}{\left[1 + \left(\sum \bar{K}_i c_i\right)^m\right]^{1/m}} \tag{16}$$

Both the LF and the Tóth multi component equations have some characteristic features. The first factor at the RHS in Eqs. (15-16) is the

expression for the selectivity of i with respect to all other components. The first factor is the same for both models and is not influenced by the chemical heterogeneity of the ligand. The second term of the RHS is in both equations equal to $1-\theta_{ref}$, with θ_{ref} is the fraction of the sites in their reference state (unoccupied sites). The difference $1-\theta_{ref}$ equals the summation of the adsorption of all components minus that of the reference, henceforth we will call this summation θ_T.

At low surface fractions for a certain component i, the change in $\Sigma\tilde{K}_i c_i$ upon sorption of i is negligible. Hence, $\Sigma\tilde{K}_i c_i$ is approximately constant and the adsorption is only determined by the $\tilde{K}_i c_i$ term of the numerator of the first fraction of the RHS of the Eqs (15) and (16), this implies linear adsorption for both equations.

When one of the components binds far more strongly than the others its $\tilde{K}_i c_i$ dominates the $\Sigma\tilde{K}_i c_i$. Consequently for this component the first fraction of the RHS approaches one. Its binding is then given by the second fraction, which for the given condition approximates to the monocomponent relation.

A third limiting case occurs when θ_T approaches one. This is for instance the case at low pH, were the surface is nearly fully protonated. In this case the first ratio of the RHS determines the binding, i.e. the binding selectivity of i rather than the heterogeneity determines the binding.

In similarity to the monocomponent binding equations (Eqs. (8-9)) the multicomponent equations (15) and (16) hold for affinity distributions which are characterized by only one peak. When the distribution shows several wide peaks the binding is obtained by a weighted summation as formulated in equation (10).

Coupled Adsorption

The expression for the terms c_i which are to be used in the multi-component binding equations in the case of M-H competition are given by Eq (11) for the proton and by Eq. (13) for the divalent metal ion.

Due to the multicomponent character of the binding equations the

metal ion binding curves, replotted as a function of M_S/H_S^x do not merge into a mastercurve. For the two component case the binding plotted as a function of $(H_s, M_S/H_S^x)$ merges to a three dimensional master plane. In principle this plane can be analyzed for the affinity distribution. However in practice the number of datapoints and the H_S and the M_S/H_S^x ranges are limited and make that only a small window of the master plane can be constructed.

Although a mastercurve type of analysis is in normal practice not feasible, fully coupled binding is still a tractable approach. From the analysis of the proton binding the parameters m, $\tilde{K}_H$ and the electric double layer parameters are obtained. For every type of metal ion that binds only two extra parameters have to be assessed, $\tilde{K}_M$ and x. When there are different site classes present (eg. Eq. (10)) a $\tilde{K}_M$ and x for every site class should be specified.

Experimental

The HA used was a suspension of Purified Peat Humic Acid (PPHA) derived from a commercial Irish horticultural peat and containing 5.28 mg HA g^{-1} suspension. The preparation of the PPHA and the proton binding is detailed in an earlier paper (54). The proton binding could be described with a combination of two LF equations or two Tóth equations with a spherical double layer model or a cylindrical double layer model. The parameters for the model descriptions for the spherical double layer model are given in table 1. For brevity the cylindrical model is not addressed in this paper.

We elected to measure cadmium concentrations potentiometrically using an ion-selective electrode (ISE). This approach has a number of potential advantages:

(i)   It is a non-invasive technique and does not require phase separation. There is no need to disturb the sample equilibrium or environment in order to extract an aliquot for analysis. The electrode can remain in position from the beginning of the titration.

Table 1. The parameters obtained for the description of the proton binding to the PPHA humic acid with the spherical double layer model (54).

parameter		Langmuir Freundlich	Tóth
radius (nm)		0.80	0.80
class 1	log $\acute{K}_{1,H}$	4.51	4.58
	m_1	0.94	0.89
	$\Gamma_{1,max}$ (mmol/g)	1.45	1.48
class 2	log $\acute{K}_{2,H}$	9.87	13.89
	m_2	0.18	0.17
	$\Gamma_{2,max}$ (mmol/g)	5.64	4.23

(ii)   The cadmium activity can therefore be monitored continuously, giving a higher density of data points than discrete sampling and hence improving the resolution of the titration curves.

(iii)   The logarithmic nature of the ISE response function enables several orders of magnitude of concentration to be measured directly. Such a range can be difficult to achieve by other analytical techniques.

There were, of course, also disadvantages which had to be overcome. Firstly ISEs for divalent cations are intrinsically insensitive (29 mV decade^{-1}). We had also heard several reports that the response of Cd ISEs could be erratic and unreproducible. Secondly, the concentration limit below which the electrodes tend to deviate from Nernstian behaviour was higher than some of the concentrations which we hoped to measure.

All the experiments reported here were accomplished at Wallingford using the programmable titrator which has been fully described previously (55). An IBM PC interfaced to a Microlink frame and modules (Biodata Ltd) is used to control three motorized burettes (Metrohm) and to read up to four electrodes. The pH electrodes used were standard glass half-cells (Russell pH Ltd) measured against a saturated calomel reference (Russell or Schott) with a flowing electrolyte bridge and calibrated using NBS primary standard pH buffer solutions; the Cd ISE was a sulphide based

solid state electrode (Orion 9448).

Calibration of Cadmium ISE

The nominal measurable concentration range of the Cd ISE was 10^{-1} to 10^{-7} M but a simple calibration titration revealed that Nernstian response deteriorated below pCd $\approx$ 5.5. The position of the threshold is in rough agreement with the manufacturers quoted limitations for an unbuffered direct calibration. However, buffered solutions with high Cd_T but low (Cd^{2+}) offered considerable promise as a alternative method of calibration which would extend the range of Nernstian performance.

Using ethylenediaminetetraacetic acid (EDTA) derivatives as complexing ligands (56-57) a Nernstian response has been demonstrated for a cadmium electrode down close to the theoretical concentration limit imposed by the solubility product of the cadmium sulphide membrane material (log K_{sp} = -25.8 at ionic strength of 1.0 M (58), therefore limiting pCd = 12.9). Simulation of a cadmium/EDTA titration using chemical speciation models indicated that the system is too weakly buffered over the activity range of interest (pCd 2-8) to be a useful calibration titration for our purposes; the complexation end-point is very sharp and a small increase in the concentration of EDTA reduces the free Cd activity by several orders of magnitude.

An alternative ligand is ethylenediamine (en) which has been used to demonstrate Nernstian behaviour for the similarly sulphide-based solid-state cupric ion-selective electrode for activities as low as pCu = 19 (59). Simulation of a cadmium/en titration showed a smoothly graded transition from pCd 2 to pCd 10 as the mole fraction of en was increased, suggesting that it would be a good choice for calibration.

The electrode performance was determined by titrating aqueous en (0.254 M) into 10^{-2} M $Cd(NO_3)_2$. Experimental data from regular intervals throughout the titration was fed into a speciation model to calculate the free Cd activity. The calculated activities were plotted against the observed ISE emf readings to give an electrode calibration curve which was linear

from pCd > 2 to pCd 10. At activities below pCd 10 the performance curved away towards a limiting emf of ~ -440 mV, corresponding to a theoretical activity of pCd ~12.5, which is in good agreement with the limit predicted from the solubility of the membrane. Data below pCd 10 was therefore discarded, while data for pCd 2 - 10 was fitted to a straight line, yielding the electrode calibration parameters.

Four such titrations, bracketing a ten week period, showed good reproducibility. All fitted a linear function with a correlation coefficient of 0.9998 or better. Comparing the electrode parameters from each of the four calibrations gave an average slope of 28.69 ±0.08 mV/decade (97% of theoretical Nernstian) and an average intercept, E_0, of -82.5 ±1.7 mV (95% confidence limits).

Small dose increments were used during the titrations and up to twenty minutes were allowed for each dose to equilibrate (electrode drift criteria <0.002 pH min^{-1}, <0.004 pCd min^{-1} (0.1 mV min^{-1})) before a reading was taken. The full titrations therefore took approximately 16 hours to complete. This was too long to be effective as a routine calibration procedure when the experiments themselves were of similar duration. A shorter procedure, based on a discrete number of calibration points rather than a continuous titration curve, was required. Moving between these 'discrete' points by dosing (effectively a titration with very large dose increments) was also ineffective; the chemical equilibration was slow for large changes in activity, particularly at the highly complexed, low activity end of the range.

The most effective approach was to have a selection of prepared, equilibrated metal-ion buffer solutions of known Cd activity into which the ISE could be placed directly. Even so, using highly complexed buffers at low activity the electrode response time was still sometimes extremely long (>30 min) while the time taken for the electrode to stabilise (to a drift of <0.05 mV min^{-1}, <0.002 pCd min^{-1}) in buffers at the higher uncomplexed activities (pCd 2-5) was usually only 5-10 min. The slow titrations had demonstrated that the electrode response could be considered to be linear throughout the experimental range, the measured slope was consistent

within a small uncertainty range, but the uncertainty in the intercept was larger. For a routine calibration it was therefore more important to fix the intercept than the slope. Our final procedure was to calibrate routinely before (and if possible after) each experiment using four buffer solutions of pCd 2, 3, 4 and 5, hence determining the intercept and providing a check on the slope. A full titrated calibration was repeated periodically to ensure that the electrode continued to demonstrate a consistent response for the full activity range from pCd 2 - 10.

pH Stat Experiments

Stat experiments were carried out at pH 4, 6 and 8.1. It was impossible to cover the full desired range of Cd concentrations in one experiment because the variation in dose sizes which would be required using a single Cd stock solution was too large (eg. 0.1 ml to 1000 ml if 10^{-3} M Cd solution was used). Therefore, two subsets of stat experiments were performed, one covering high concentrations of Cd (pCd 7-3), the other covering the lower end of the range (pCd 10-5). In both cases the pH of a sample of PPHA was maintained at the specified pH by titrating with 0.1 M KOH or HNO_3 whilst the total concentration of Cd in the system was increased by successive doses of Cd solution. For the low Cd range 10^{-3} M $Cd(NO_3)_2$ in 0.1 M KNO_3 solution was used, replaced by 0.1 M $Cd(NO_3)_2$ for the high range.

All experiments began with 20 ml of PPHA diluted to give 25 ml in a 0.1 M KNO_3 background electrolyte. This was titrated to the stat pH and then maintained for up to 12 hr to stabilize the HA at the new pH (it is stored in a refrigerator as a suspension at pH 3.2). Cadmium was then added in doses, causing the pH to drop, and the mixture was titrated back to the stat pH with base. The stat pH must be held for five minutes within a tolerance of 0.004 pH (0.2 mV) *and* the electrode readings must be stable to within drifts of <0.004 pH min^{-1} and <0.007 pCd min^{-1} (0.2 mV min^{-1}) before a reading was recorded and the next dose of Cd was added. The size of the Cd doses was increased progressively from the initial 0.1 ml to a final 10.0 ml after which a total of 30 ml of Cd solution had been added.

Individual data points took between 7 and 30 min to meet the read criteria. Complete experiments typically contained 20 data points and lasted between 4 hr (pH 4, low Cd) and 10 hr (pH 8, high Cd).

In the experiments the cadmium sorption is calculated by the difference of the total cadmium added minus the total amount of cadmium in solution. The total amount in solution is calculated from the monitored free cadmium concentration by the electrode, the constants in this chemical equilibrium calculation were taken from Smith and Martell (58).

The proton/metal ion exchange ratio r_{ex} is difficult to measure precisely since it is a function of a large number of experimentally determined variables. When sorption is measured by difference and when the free metal ion concentration is estimated by electrode, accurate metal ion electrode readings are essential. The measured emf varies with the log of free concentration. This combination of measurement by differences and the log response of the electrode results in a highly non-linear error response.

The largest errors occur when the percent sorption (concentration change) is small. This can occur at both low and high sorption densities and depends on the solid/solution ratio as well as the sorption affinity. It tends to be the dominant source of error at high concentrations when the isotherm is approaching the sorption maximum.

The precision of the pH statting system (and stability of the suspension pH) is also critical especially where the proton release is small (eg. high % sorption but low metal ion concentration, or low change in % sorption and high metal ion concentration). This tends to be the major source of error at low metal ion concentrations.

We have followed how the errors in the individual parameters pass through the final estimate of r_{ex} by a Monte Carlo approach. This consisted of calculating the stoichiometry using random values for each of the 'adjustable' parameters. The spread of random values was defined by a normal distribution having a specified mean and standard deviation. The chosen mean is equal to the analytical value of the parameter measured

assuming no error. The standard deviation values chosen are extracted from analysis of the electrode calibration data and from estimates of the likely burette errors. Typically we would use 1000 cycles of the simulation. The standard deviation of the simulated distribution of r_{ex} values is then calculated. We think r_{ex} with standard deviations less than 0.1 are worth keeping, the rest have too large errors.

Calculations

For all calculations in this paper the ECOSAT program is used (60). The ECOSAT program combines chemical speciation calculations following the MINEQL scheme, with state of the art binding equations, electrostatic double layer models and transport models.

In the calculations of the electrostatics the presence of a mixed electrolyte, composed of K^+, NO_3^-, Cd^{2+}, H^+, OH^- and their complexes, is explicitly taken into account. The ECOSAT model also allows for the calculation of the composition of the double layer and for the calculation of the non-specific adsorption. Interaction between the humic particles are not taken into account in the calculations.

Results

Figure 1 shows the cadmium binding as a function of log Cd ($\blacksquare$ log $[Cd^{2+}]$) for three pH values in two ways: a lin/log plot (1a) and a log/log plot (1b). The binding shows a pronounced pH effect and as to be expected the higher the pH the higher the metal binding. The low adsorption parts of the log-log curves have a slope of 0.65 to 0.95 indicating that even in this region we are not in the Henry region. The small deviations between duplicate experiments show that the experimental set-up gives reproducible results.

In figure 2 the measured proton metal exchange ratio is plotted. The constraint that only r_{ex} for which the standard deviation is less than 0.1 are included in the figure, results in a strong reduction of the data points. Nevertheless figure 2 shows that even for these data points the variation
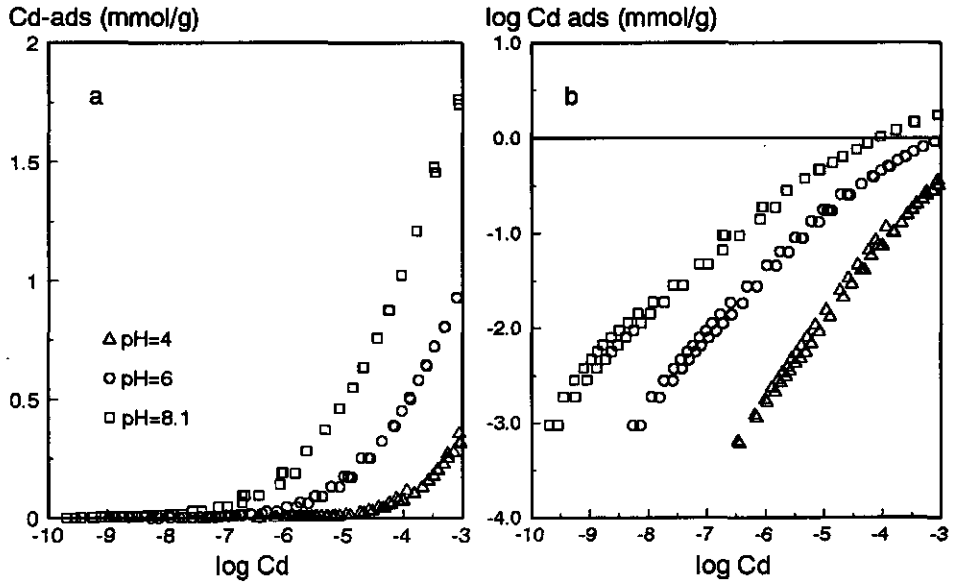
147

Figure 1. The cadmium binding to the PPHA as a function of log Cd for three pH values in a lin/log format (fig 1a) and a log/log format (fig 1b).
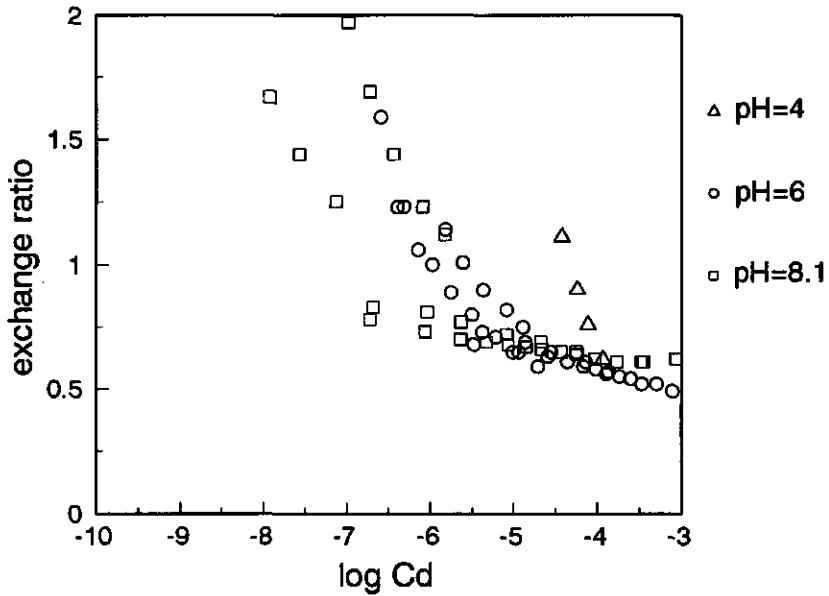

Figure 2. The measured proton metal exchange ratio r_{ex} as a function of log Cd for three pH values.

in r_{ex} is very large, while the spreading in the binding curves is small (eg. Fig .1).

At a low log Cd the number of protons which is released is larger than at high log Cd and r_{ex} decreases from 2 to a minimum value of ca. 0.5. The pH dependence of r_{ex} is somewhat surprising. At pH=8, where a large part of the surface groups are deprotonated, the r_{ex} at low log Cd is still almost 2, which seems rather high. Moreover, because of the smaller degree of protonation, one would expect that the higher the pH is, the lower is the exchange ratio. For pH=6 and pH=8 at high metal concentration this seems not to be the case; $r_{ex}(pH=8)>r_{ex}(pH=6)$. We have no clear explanation for this. However, since (1) the differences are small, (2) r_{ex} is difficult to measure precisely and (3) the r_{ex} show quite significant deviations, we should not over interpret the measured r_{ex} values.

Modelling and Discussion

Uncoupled Adsorption

In figure 3 the cadmium binding as a function of log (Cd_S/H_S^x) curves are plotted. Although the curves do not fully merge to a master curve, it is the best result that can be obtained. In our opinion the result is satisfactory since most of the pH dependency is accounted for. For all data non-specifically bound cadmium in the double layer was negligible compared to specifically bound cadmium.

The curves in figure 3 are constructed for x=0.5. This implies that, irrespective of the degree of protonation of the humic particles, at least 0.5 protons are released when one metal ion is bound. The obtained value for x corresponds well with the experimentally determined minimum value of r_{ex}.

The solid lines in fig. 3 correspond to the LF and Töth relation which were fitted to the $\Gamma_{Cd}(\log(Cd_S/H_S^x))$ data. The obtained parameters are given the table 3. Both equations give an equally good description of the binding data. In principle however, when the curves merge very well, the limiting slope of the $\Gamma_{Cd}(\log(Cd_S/H_S^x))$ curves, which is obtained at

149

Table 2. The parameters obtained for the description of the pH dependent cadmium binding to the PPHA humic acid in a 0.1 M KNO$_3$ electrolyte with the uncoupled binding model. For the parameters for the electrostatic model and the proton binding reference is made to table 1.

parameter	Langmuir Freundlich	Tóth
x	0.50	0.50
log $\tilde{K}_{Cd}$	-0.03	0.65
m	0.73	0.23
$\Gamma_{Cd,Max}$ (mmol/g)	1.56	6.88
r^2	0.98	0.98
RMSE	0.13	0.13

$$* \quad r^2 = 1 - \frac{\sum_{i=1}^{np}(n_i - \bar{n}_i)^2}{\sum_{i=1}^{np}(n_i - \bar{n}_i)^2}$$

$$** \quad RMSE = \left(\frac{\sum_{i=1}^{np}(n_i - \hat{n})^2}{m - np} \right)^{0.5}$$

n_i measured value for datapoint i
$\hat{n}_i$ fitted value for datapoint i
np   number of datapoints
p   number of parameters
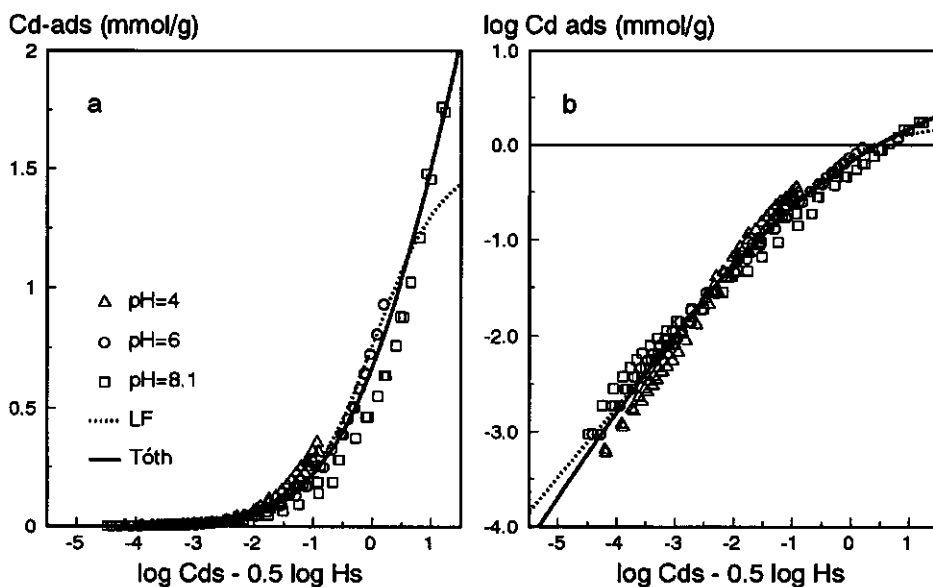$\bar{n}$ average value of measured datapoints

Figure 3. The cadmium binding to the PPHA replotted as a function of log Cd$_s$-0.5 log H$_s$ for three pH values in a lin/log format (fig. 3a) and a log/log format (fig. 3b) together with the fitted LF and Tóth relations.

very low cadmium binding, can be used to discriminate between the two equations. At a low binding the limiting slope of the Tóth in the log-log plot equals 1, which corresponds to linear binding, while the limiting slope for the LF equation is equal to m, which corresponds to a Freundlich type of binding.

In figure 4 the descriptions for the metal binding, the proton binding and for the electrostatics are combined to calculate the cadmium binding curves as a function of log Cd for the three different pH values. For the proton binding model the LF description is used, for the cadmium binding the Tóth description. The description of the data is fairly good for the entire experimental data range, which comprises a concentration range of about 7 log Cd units, and a pH range of 4 units. The use of the Tóth description for the proton binding or the LF description for metal binding results in an equally good description.

From the model description one can also calculate the exchange ratio (fig. 5). The correspondence between the calculated and the experimental r_{ex} is much less good than the description of the cadmium binding. The observed increase in the experimental r_{ex} at low log Cd is not reproduced by the calculations. The calculated exchange ratios are almost constant over the whole log Cd range and r_{ex} is around 0.7 for all three pH values. For pH=4 r_{ex} is some what larger, for pH=8 r_{ex} is somewhat smaller. For pH=6 the variation in r_{ex} is the largest, but still very small compared to the measured range. At low log Cd the r_{ex} for pH=6 is identical to r_{ex} for pH=4. At high log Cd it approaches the r_{ex} for pH=8.

With uncoupled adsorption there is no site competition between protons and metal ions. This implicates that exchange ratios beyond 0.5 are caused by the electrostatic interactions which are influenced by the metal ion binding.

Fully coupled adsorption

In the fully coupled model we assume that the value of x is the same for both site classes. The fitted log $\tilde{K}_{Cd}$ and x seem to be somewhat
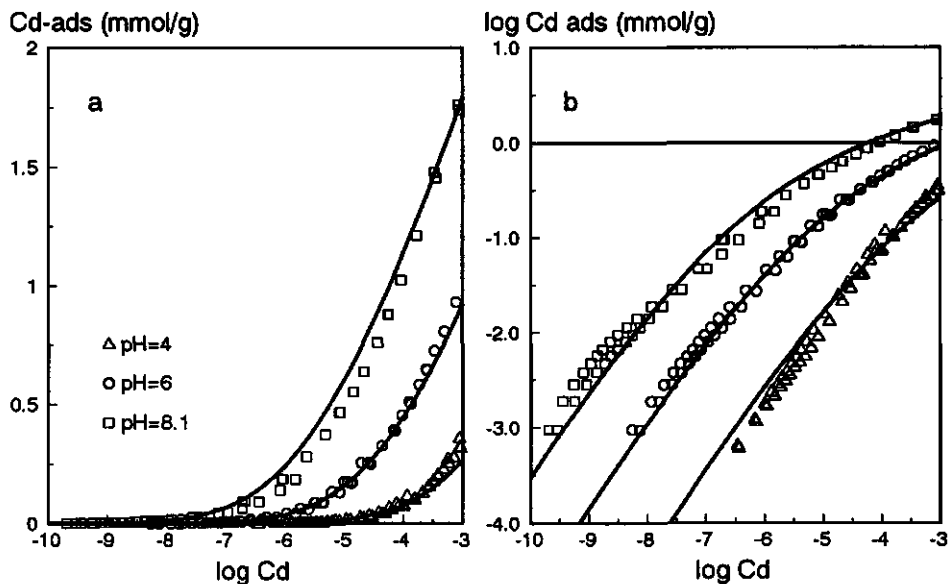
Figure 4. The calculated cadmium binding for the uncoupled model based on the Tóth equation, compared with the experimental data in a lin/log format (fig 4a) and a log/log format (fig 4b). For the parameter values reference is made to tables 1 and 2.
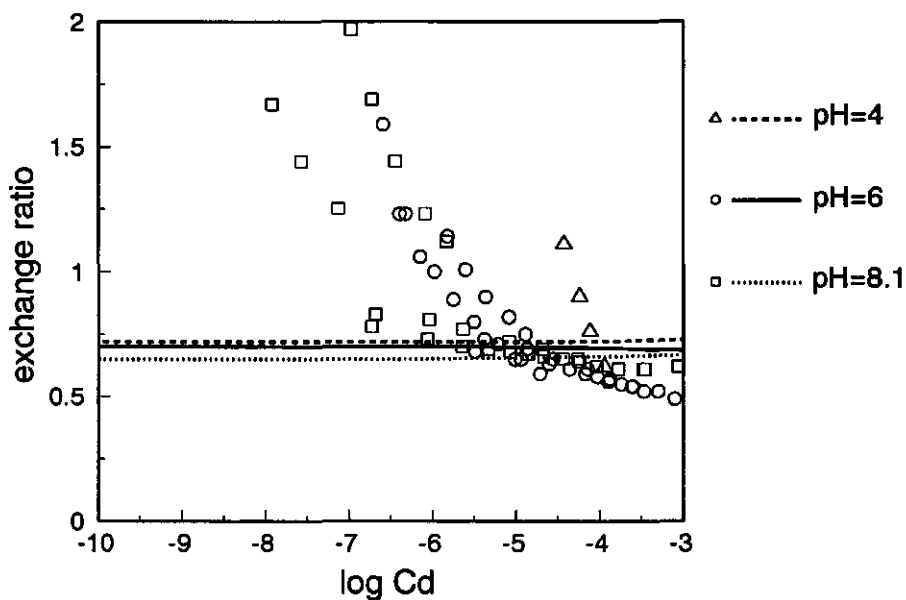

Figure 5. The calculated r_{ex} for the uncoupled model based on the Tóth equation, compared with the experimental data. For the parameter values reference is made to tables 1 and 2.

152

interrelated. For both the LF and the Tóth equation x=0.1 gave the best description although the description for x=0.2 was also reasonable. For x>0.2 the calculated pH dependency is too pronounced, while for x<0.1 the pH dependency is too small. In both cases the description of the data becomes less good. In table 3 the parameters for the competitive binding equations are given that were obtained for the fully coupled model.

The value of log $\tilde{K}_{1,Cd}$ for the first class of sites is almost equal for the LF and the Tóth equation, the value for log $\tilde{K}_{2,Cd}$ differs however strongly. For the LF equation the log $\tilde{K}_{2,Cd}$ is of the same order as log $\tilde{K}_{1,Cd}$, for the Tóth equation log $\tilde{K}_{2,Cd}$ is about 4 log units higher than log $\tilde{K}_{1,Cd}$. Because for the Tóth equation the log $\tilde{K}_{H,2}$ is also 4 log units higher than log $\tilde{K}_{2,H}$ for the LF equation, it seems that the log $\tilde{K}_{i,Cd}$ value for a certain class is mainly correlated to the log $\tilde{K}_{i,H}$ of the sites class, and does not so much depend on the type of equation.

In figure 6 the calculated adsorption for the fully coupled case and the LF equation is plotted in a lin-log format (6a) and a log-log format (6b), together with the experimental results. The results for the Tóth equation are very similar and will not be shown nor further discussed.

The dotted lines in fig. 6 give the binding when binding to the second peak is not taken into consideration. It follows that metal binding at the sites of the second proton peak does only play a significant role for pH=8.

In general, the coupled adsorption model results in a reasonable description of the adsorption in the high concentration range, but a poor description at low coverage. The description in that region can be improved by assuming that an extra class of sites is present with a high affinity for the metal ions. The existence of a small number of high affinity sites is a well accepted phenomenon for humic materials (8-12). Because the number of high affinity sites is small compared to the total number of sites, their existence cannot be picked up from the analysis of the proton binding.

153

Table 3. The parameters obtained for the description of the pH dependent cadmium binding to the PPHA humic acid in a 0.1 M KNO_3 electrolyte with the fully coupled binding model. For the parameters for the electrostatic model and the proton binding reference is made to table 1.

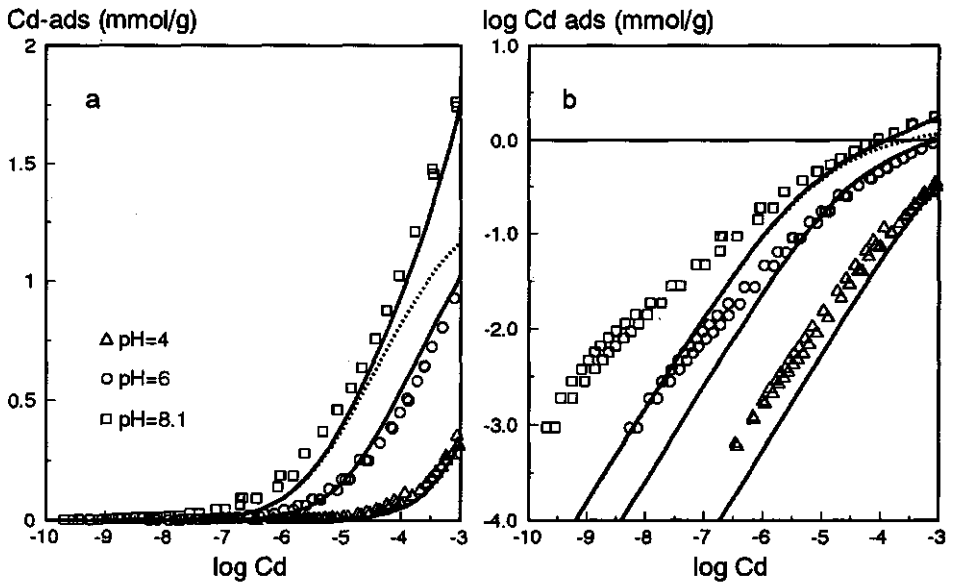| parameter		Langmuir Freundlich	Tóth
class 1	x_1	0.10	0.10
	$\log \tilde{K}_{1,Cd}$	2.50	0.65
class 2	x_2	0.10	0.10
	$\log \tilde{K}_{2,Cd}$	3.10	7.40

Figure 6. The calculated cadmium binding for the coupled model based on the LF equation, compared with the experimental data in a lin/log format (fig 4a) and a log/log format (fig 4b). For the parameter values reference is made to tables 1 and 2. The dotted lines give the binding when binding to the second class of sites is not taken into consideration.

In figure 7 the calculated adsorption isotherms for the LF equation are given for the case that an extra 1% of high affinity sites are present in addition to the major sites. Comparison of the results in this figure with those in fig. 6 illustrates that the adoption of a class of high affinity sites strongly improves the description of the binding at low metal concentrations. In the calculations for fig. 7 m_3 and $\tilde{K}_{3,H}$ of the LF equation for the extra 1% of high affinity sites were assumed to be identical to those for the first proton peak. This choice, and the value of 1% are arbitrary, but have the advantage that only x and log $\tilde{K}_{3,Cd}$ had to be optimized. The obtained values for these parameters are $x_3=0.5$ and the log $\tilde{K}_{3,Cd}=2.3$. This log K value for the high affinity sites is somewhat surprising since it is smaller than the value for lower affinity sites. It can however be explained by comparing the apparent metal binding constants for the low and the high affinity sites. The apparent metal binding constant is determined by the ratio $\tilde{K}_M/H_S^x$. Due to higher value of x, the apparent constant for the high affinity sites is larger than that for the low affinity sites as long as $pH_S>0.5$. Under natural conditions this is the case.

A more rigorous adjustment of the parameters may further improve the description of the experimental data, nevertheless it is demonstrated clearly that the assumption of the presence of a small number of extra sites has a large influence in the low concentration range.

Like for the uncoupled case the calculated proton metal exchange ratio, given in figure 8, does not describe the measured ratio well. Again the increase of the r_{ex} at low log Cd is not reproduced. The calculated exchange ratio is however considerably more pH dependent than r_{ex} for the uncoupled adsorption, and r_{ex} is clearly not constant as a function of log Cd. For the higher log Cd values the calculated r_{ex} reproduces the trend in the r_{ex}, at least to some extent. Like for the experimental data the model calculates at higher log Cd a larger r_{ex} for pH=8 than for pH=6. The increase of the r_{ex} at pH=8 is caused by the metal binding to the second class of sites, which have a relatively high affinity for the protons. At pH=6 cadmium binding to these sites is negligible.

In the case of coupled adsorption the release of protons is caused by

155
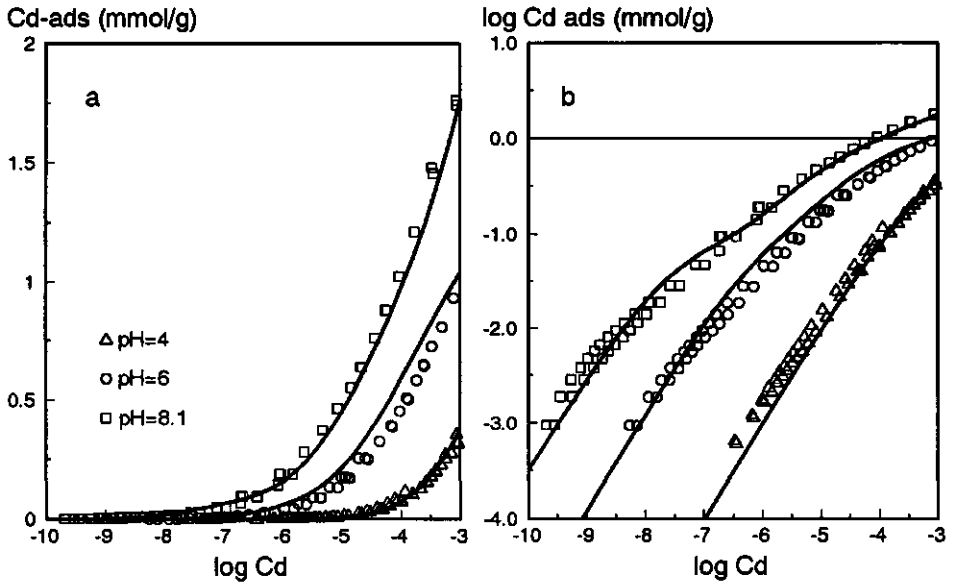
Figure 7. The calculated cadmium binding for the coupled model based on the LF equation with an extra class of high affinity sites, compared with the experimental data in a lin/log format (fig 4a) and a log/log format (fig 4b). For the parameter values of the first two site classes reference is made to tables 1 and 2. For the third class $\Gamma_{3,max}$=0.07 meq/g, log $\tilde{K}_{3,H}$=4.51, m_3=0.94, x_3=0.5 and log $\tilde{K}_{3,Cd}$=2.3.
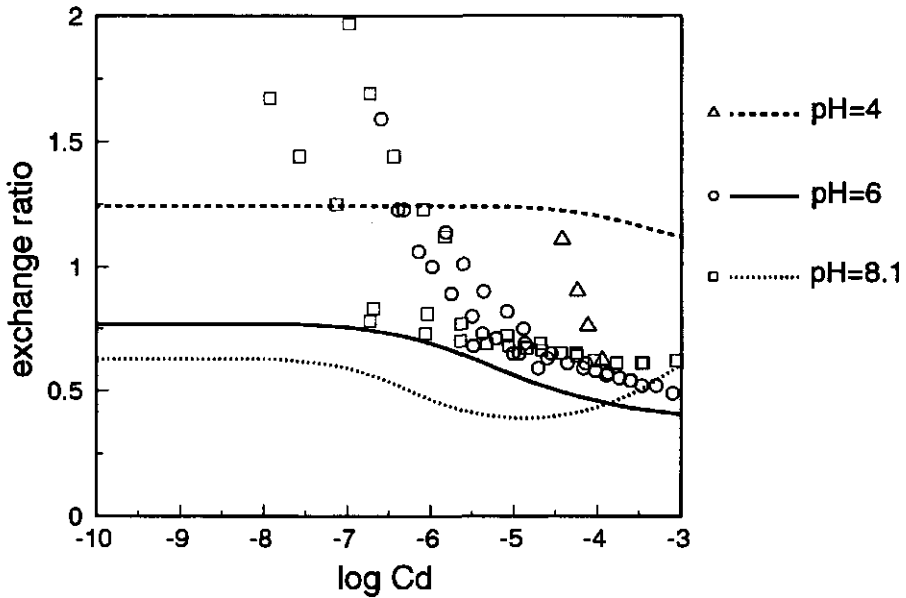
Figure 8. The calculated r_{ex} for the coupled model based on the LF equation with an extra class of high affinity sites, compared with the experimental data. For the parameter values reference is made to tables 1 and 2 and to the figure caption of fig. 7.

the stoichiometric factor x, by site competition between protons and metal ions and by electrostatic effects. Since x=0.1 for the two major peaks a large part of the r_{ex} is due to the competition and the electrostatic effects. The competition effects are especially important at pH=4. At this pH the surface is strongly protonated. In order to bind cadmium the protonated sites have to dissociate, which causes a large r_{ex}.

Concluding Remarks

For the dataset under consideration the uncoupled adsorption allows for a good description of the experimental data over a concentration range of 7 log units and a pH range of 4 units. In this description only 4 adjustable parameters are required for metal ion binding. A convenient feature of the uncoupled adsorption is that the adjustable parameter x can be obtained graphically by constructing a $\Gamma_M(M_S/H_S^x)$ mastercurve.

The coupled proton-metal binding model could only describe the pH dependent metal binding over a concentration range of about 4 units in the high concentration region. In order to be able to describe the binding over the entire concentration and pH range the adoption of a minor class of sites with a high affinity for metal ions was necessary. The number of these high affinity sites is in the order of 1 % of the total number of sites. The characteristics of the extra peak of high affinity sites cannot be determined on the basis of the proton binding. As a consequence the number of adjustable parameters required for the coupled model becomes relatively large.

A preference for one of the two models is a matter of taste. The elegancy of the uncoupled model is the fact that a mastercurve can be constructed and the values of x, $\bar{K}_M$, m and Γ_{max} can be derived from fitting the chosen heterogeneous equation to the mastercurve. A good description results over a very wide range of conditions with only a few parameters that characterize the metal ion binding.

However, to our opinion the assumption of site competition is physically more realistic than the assumption of independent sites.

157

Nevertheless, the fully coupled option is less attractive due to the large number of adjustable parameters that have to be determined, and the simplifying assumption of affinity distribution with identical shapes which are only shifted on the log K axis is most probably too crude. As a suggestion for improvement of this situation in a forthcoming paper we will present some analytical multi-component binding equations in which the distributions are not only shifted but also transformed.

Acknowledgement

References

1.   Stumm, W.; Morgan, J.J. *Aquatic Chemistry*, Wiley Interscience: New York, 1970, 1st Ed.

2.   Lindsay, W.L. *Chemical Equilibria in Soils*, Wiley Interscience: New York, 1979.

3.   Sposito, G., 1981, The Thermodynamics of Soil Solutions, Oxford University Press, Oxford.

4.   Morel, F.M.M., *Principles of Aquatic Chemistry*, Wiley Interscience: New York, 1983.

5.   Westall, J.C. , J.L. Zachary, F.M.M. Morel, 1976, MINEQL, Technical Note 18, Ralph M. Parsons Laboratory, Department of Civil Engineering, M.I.T., Cambridge, Massachusetts.

6.   Sposito, G. and S.V. Mattigod, 1980, GEOCHEM, Kearney Foundation of Soils Sciences, University of Califronia, Riverside.

7.   Van Riemsdijk, W.H.; De Wit J.C.M.; Nederlof, M.M.; Koopal, L.K. In *Contaminated Soil'90*, Arendt, F.; Hinsenveld, M.; Van Den Brink, W.J. (eds.), Kluwer Academic Publishers: Dordrecht, 1990 359-366.

8.   Stevenson, F.J., *Humus Chemistry. Genesis, Composition, Reactions*; Wiley Interscience: New York, 1982.

9.   Buffle, J. In *Metal Ions in Biological Systems*. Vol 18. Dekker: New York, 1984,

Ch. 6.

10.   Sposito, G., *CRC Crit. Rev. Environ. Control* **1986**, *16*, 193-229.

11.   Buffle, J. *Complexation Reactions in Aquatic Systems: An Analytical Approach*; Ellis Horwood Limited: Chichester, 1988.

12.   Livens, F.R., *Environ. Pollution* **1991**, *70*, 183-208.

13.   MacCarthy, P.; Perdue, E.M., 1991, In *Interactions at the Soil Colloid - Soil Solution Interface*; Bolt, G.H.; De Boodt, M.F.; Hayes, M.H.B.; McBride M.B. (Eds.); NATO ASI Series Series E: Applied Sciences-Vol. 190, Kluwer Academic Publishers, Dordrecht, 469-489.

14.   Aiken, G.R., D.M. McKnight, R.L.Wershaw and P. MacCarthy (Eds.) *Humic Substances in Soil, Sediment, and Water*; Wiley Interscience: New York, 1985

15.   Hayes, M.H.B.; MacCarthy, P.; Malcolm, R.L.; Swift, R.S. (Eds.), *Humic Substances II: In Search of Structure*; Wiley Interscience: New York, 1989.

16.   De Wit, J.C.M.; Van Riemsdijk, W.H.; Nederlof, M.M.; Kinniburgh, D.G.; Koopal, L.K. *Analytica Chim. Acta* **1990**, *232*, 189-207.

17.   Marinsky, J.A. In *Aquatic Surface Chemistry*; Stumm, W. (Ed.);   Wiley Interscience: New York, 1987, Ch. 3.

18.   Tipping, E.; Backes C.A.; Hurley, M.A. *Water Res.* **1988**, *22*, 597-611.

19.   Bartschat, B.M.; Cabaniss, S.E.; Morel, F.M.M. *Environ. Sci. Technol.* **1992**, *26*, 284-294.

20.   Murray, K.; Linder, P.W. *J. Soil Sci.* **1983**, *34*, 511-523.

21.   Murray, K.; Linder, P.W.; *J. Soil Sci.* **1984**, *35*, 217-222.

22.   Murray, K.; Linder, P.W.; *Sci. Total Environ.* **1987**, *64*, 149-161.

23.   Marinsky, J.A.; Reddy, M.M. *Org. Geochem.* **1984**, *7*, 215-221.

24.   Marinsky, J.A.; Ephraim, J. *Environ. Sci. Technol.* **1986**, *20*, 349-354.

25.   Varney, M.S.; Mantoura, R.F.C.; Whitfield, M.; Turner, D.R.; Riley, J.P. *Potentiometric and Conformational Studies of the Acid-Base Properties of Fulvic Acid from Natural Waters* NATO Conf. Ser., [Ser.] 4, 9(Trace Met. Sea Water), 751-772, 1983

26.   Arp, P.A. *Can J. Chem.* **1983**, *61*, 1671-1682.

27.   Ephraim. J.; Marinsky, J.A. *Environ. Sci. Technol.* **1986**, *20*, 367-354.

28.   Ephraim, J; Alegret, S.; Mathuthu, A.; Bicking, M.; Malcolm, R.L.; Marinsky,

J.A. *Environ. Sci. Technol.* **1986**, *20*, 354-366.

29.   Ephraim, J.H.; Borén, H.; Pettersson, C.; Arsenie, I.; Allard, B. *Environ. Sci. Technol.* **1989**, *23*, 356-362.

30.   Dudley, L.M.; McNeal, B.L. *Soil Sci.* **1987**, *143*, 329-340.

31.   Tipping, E.; Hurley, M.A. *J. Soil Sci.,* **1988**, *39*, 505-519.

32.   Tipping, E.; Reddy, M.M.; Hurley, M.A. *Environ. Sci. Technol.* **1990**, *24*, 1700-1705.

33.   Tipping, E., Woof, C.; Hurley, M.A. *Water. Res.,* **1991**, *25*, 425-435.

34.   Perdue, E.M.; Lytle, C.R. In *Aquatic and Terrestrial Humic Materials*; Christman, R.F.; Gjessing E.T.(Eds.), Ann Arbor Science: Michigan, 1983. Ch 14.

35.   Perdue, E.M. In *Metal Speciation: Theory, Analysis and Application*, J.R. Kramer, H.E. Allen Lewis Publishers, Inc.: Chelsea MI, 1988. Ch 7.

36.   Perdue, E.M.; Lytle, C.R. *Environ. Sci. Technol.* **1983**, *17*, 654-660.

37.   Dobbs, J.C.; Susetyo, W.; Knight, F.E.; Castles, M.A.; Carreira, L.A.; Zarraga, L.V. *Anal. Chem.* **1989**, *61*, 483-488.

38.   Dobbs, J.C.; Susetyo, W.; Knight, F.E.; Castles, M.A.; Carreira,L.A.; Zarraga, L.V. *Intern. J. Environ. Anal. Chem.* **1989** *37*, 1-17.

39.   Susetyo, W.; Dobbs, J.C.; Carreira, L.A.; Azarraga, L.V.; Grimm, D.M., *Anal. Chem.* **1990**, *62*, 1215-1221.

40.   De Wit, J.C.M., W.H. van Riemsdijk and L.K. Koopal, 1989, Metal Speciation, Separation and Recovery, Vol II, Lewis Publishers, Chelsea, USA, 329-353.

41.   De Wit, J.C.M., M.M. Nederlof, W.H. Van Riemsdijk and L.K. Koopal, 1991a, Water, Air and Soil Pollution 57-58:339-349.

42.   De Wit, J.C.M., W.H. Van Riemsdijk and L.K. Koopal, 1991b, Finnish Humus News 3:139-144.

43.   De Wit, J.C.M., W.H. Van Riemsdijk and L.K. Koopal, *Proton Binding to Humic Substances. A. Electrostatic Effects.* Submitted to *Environ Sci. Technol.*

44.   De Wit, J.C.M., W.H. Van Riemsdijk and L.K. Koopal, *Proton Binding to Humic Substances. B. Chemical Heterogeneity and Adsorption Models.* Submitted to *Environ Sci. Technol.*

45.   Sips, R. *J. Chem. Phys.* **1950**, *18*, 1024.

46.   Sips, R. *J. Chem. Phys.* **1948**, *16*, 490.

47. Tóth, J.; Rudzińsky, W.; Waksmundsku, A.; Jaroniec, M.; Sokolowsky, S. *Acta Chim. Hungar.* **1974**, *82*,11.

48. Gamble, D.S.; Langford, C.H. *Anal. Chem.* **1980**, *52*, 1901-1908.

49. Nederlof, M.M.; Van Riemsdijk, W.H.; Koopal, L.K.; *J. Colloid Interface Sci.* **1990**, *135*, 410-426.

50. Nederlof, M.M.; Van Riemsdijk, W.H.; Koopal, L.K.; *Environ. Sci Technol.* **1992**, *26*, 763-771.

51. Jaroniec, M. *Adv. Colloid Interface Sci.* **1983**, *18*, 149-225.

52. Jaroniec, M.; Madey, R. *Physical Adsorption on Heterogeneous Solids*, Elsevier: Amsterdam, 1988.

53. Van Riemsdijk, W.H., L.K. Koopal and J.C.M. De Wit, 1987, Netherlands J. Agricultural Sci. 35:241-257.

54. De Wit, J.C.M.; Koopal, L.K; Van Riemsdijk, W.H.; Kinniburgh, D.G.; Milne, C.J. *Analysis of Proton Binding by a Peat Humic Acid*, in preparation, (to be submitted to Analytica Chimica Acta).

55. Kinniburgh, D.G.; Milne, C.J. Guide to the Wallingford Titrator. *British Geological Survey Technical Report* WD/92/14, 1992, 160pp.

56. Růžička, J.; Hansen, E.H. *Analytica Chimica Acta,* **1973**, *63*, 115.

57. Yuchi, A.; Wada, H.; Nagakawa, G. *Analytica Chimica Acta,* **1983**,. *149*, 209.

58. Smith, R.M.; Martell, A.E. *Critical Stability Constants Vol.4: Inorganic Complexes.* Plenum Press, New York, 1976.

59. Avdeef, A.; Zabronsky, J.; Stuting, H.H. *Analytical Chemistry,* **1983**, *55*, 298.

60. Keizer, M.G.; De Wit; J.C.M.; Meeussen, J.C.L.; Bosma, W.J.P., Nederlof, M.M.; Van Riemsdijk; W.H.; Van der Zee, S.E.A.T.M. *ECOSAT*; Technical Note of the Department of Soil Science and Plant Nutrition, Wageningen Agricultural University, Wageningen, 1992.

Chapter 6

The Speciation of Calcium and Cadmium in the Presence of Humic Substances

Abstract

In addition to protons in natural systems there are other ions, like calcium, present that bind specifically to humic substances and therefore will influence the binding of hazardous heavy metal ions like cadmium. In this paper experimental calcium binding data are presented for a humic acid extracted from a peaty soil. The proton binding and the cadmium binding to this humic acid have been studied previously.

The calcium binding is described using the proton binding behaviour as a starting point for the electrostatic interactions and a continuous affinity distribution for the calcium binding. A non competitive overall binding stoichiometry is assumed, in which upon the binding of one cation x (non-integer value) protons are released in the solution.

The competition between calcium and cadmium for binding to the humic acid can be calculated using a model for competitive binding of calcium and cadmium. The calculated results illustrate the effect of calcium on the cadmium binding. As long as cadmium is at trace level, the cadmium binding at constant pH, both in the absence and in the presence of calcium, can be described by a simple (mono-component) Freundlich or even linear binding equation. The parameters of these relations are however conditional, and depend in a complicated way on the environmental conditions. On the basis of the results we discuss the cadmium extraction from soil samples with 0.01 M $CaCl_2$.

Introduction

For a sound assessment of the fate of micro-nutrients and the risks of hazardous and toxic compounds knowledge of sorption and exchange processes in the soil is essential (eg.1). Together with precipitation reactions these processes determine the buffering capacity and the chemostat of soil systems and control the bioavailability and the mobility of micro-nutrients and toxic compounds. The binding capacity of a soil depends on the properties and the amount of clay minerals, hydrous oxides and soil organic matter (1-3). In this paper we examine the effects of binding to the humic fraction of the soil organic matter on the speciation of metal ions like calcium and cadmium in soil systems.

Humic substances are complex mixtures or organic (poly)electrolytes which are found in soils and in aquatic systems (4-11). Because of their ability to bind metal ions they control, at least to some extent, the concentration of metal ions in solution. In soils a large part of the humic substances belong to the solid phase. These humic substances can be present as macromolecular organic material but are also often associated with clay minerals or hydrous oxides. A smaller fraction of the humic substances are dissolved in solution. In most soil systems the total dissolved organic carbon (DOC) of the soil solution varies from 0 to 20 mg C/l, in peaty and other organic rich soils the DOC can be somewhat higher (12).

The humic fraction of the DOC ranges from 10-90 % (12). The remaining part of the DOC is non humic which implies that these compounds belong to known classes of organic or biochemical compounds. The non humic substances present in soils vary from simple acids like acetic acid and citric acid to complex molecules like enzymes and lignin.

Because it is experimentally impossible to resolve ion binding in soil systems into binding to soil constituents, the intrinsic properties of humic substances are often studied on purified humic substances extracted from soils or collected from aquatic sources. In this paper we will present experimental calcium binding data to a Purified Peat Humic Acid (PPHA).

The calcium binding data will be analyzed with the uncoupled binding model (13,14). In the uncoupled binding model it is assumed that metal ion

165

binding sites are independent from the proton sites. Based on previous experience the binding of protons is described with a combination of two Langmuir Freundlich (LF) binding equations and a double layer model that accounts for the electrostatic effects (13-19). For the description of the metal ion binding a single LF equation is combined with the double layer model as established for the protons. The pH dependency of the binding is accounted for in two ways. Firstly an approximate, pH dependent metal ion binding reaction is used. Secondly the metal ions and protons interact electrostatically since they are both cations and influence the charge of the humic substances. The same type of modelling has been used before to describe the pH dependent cadmium binding to the PPHA over seven decades of cadmium concentration (14).

In the second part of the paper we combine the assessed model for calcium with the description of the cadmium binding and use a competitive binding model to predict the cadmium binding in the presence of calcium chloride. The predictions will illustrate the use of 0.01 M $CaCl_2$ electrolyte, as extractant for cadmium. The 0.01 M $CaCl_2$ electrolyte is believed to extract the easily exchangeable and bioavailable fraction of the heavy metal cations from soil samples (20-24)

In soil systems the binding of metal ions is often determined on the basis of batch experiments. The metal ion binding is then calculated as the difference between the amount added and the total amount in solution (which includes dissolved metal ion complexes). The concentration of the "free" metal ions is sometimes calculated from the total metal ion in solution by means of chemical equilibrium calculations. In general only inorganic species are taken into account in the chemical equilibrium calculations. The binding to the dissolved organic carbon is unknown and therefore neglected. The negligence of binding to the dissolved organic matter makes that the chemical equilibrium calculations result in too high free metal ion concentrations. The same problems exist if one wants to know the cadmium activity of natural waters. The order of magnitude of the error can be evaluated with the help of a model for metal ion binding to the DOC. We will also use the derived model to illustrate this and to estimate the magnitude of the Cd binding to the DOC as a function of pH in absence and in presence of

166

calcium.

Theory and model description

Proton Binding

In the case of uncoupled binding, protons and metal ions bind to their own type of sites. In this paper we use a combination of two Langmuir Freundlich (LF) equations to describe the proton binding:

$$\Gamma_H = \Gamma_{1,H,max} \frac{(\tilde{K}_{1,H} H_s)^{m_1}}{1 + (\tilde{K}_{1,H} H_s)^{m_1}} + \Gamma_{2,H,max} \frac{(\tilde{K}_{2,H} H_s)^{m_2}}{1 + (\tilde{K}_{2,H} H_s)^{m_2}} \tag{1}$$

The LF equation describes the binding to a continuous heterogeneous ligand with a symmetrical pseudo Gaussian affinity distribution (25). The parameter m_i determines the width of the distribution and $\log \tilde{K}_{i,H}$ is the median $\log K$ value of the affinity distribution. The maximum proton binding for a LF equation is given by $\Gamma_{i,H,max}$. The value of $\Gamma_{i,H,max}$ may be expressed in any convenient unit.

In equation (1) the proton binding is not expressed as a function of the proton activity, (H^+), in the bulk solution but as a function of H_S. The parameter H_S can be seen as the proton activity near the functional groups at the location of binding and is defined by:

$$H_S \equiv (H^+) \exp\left(\frac{-F\psi_S}{RT}\right) \tag{2a}$$

where ψ_S is the potential near the functional groups and F and R,T have their usual meaning. In shortened notation Eq. (2a) can be written as:

$$H_S \equiv (H^+) \, Y \tag{2b}$$

where Y is the Boltzmann factor expressing the coulombic interactions.

Because the electric potential ψ_S can not be determined experimentally,

167

we have to calculate ψ_S using a double layer model taking the charge of the humic particles as a starting point. In this paper we will use a double layer model in which we treat the humic particles as an ensemble of rigid and impermeable spheres characterized by a certain radius (13-19).

The parameters for the proton binding equation and the electrostatic model can be obtained on the basis of potentiometric titration experiments measured at several constant ionic strength, in absence of other specifically interacting (metal) ions (13). Although the assumed double layer model seems a severe simplification, on the basis of proton titration data for different types of humic substances it has been established that this first order approach results in a fairly good description of the electrostatic interactions (15-19).

Metal Ion Binding

For the description of the divalent metal ions we propose the following average binding stoichiometry:

$$S+M^{2+}+xH_2O \rightleftharpoons SM(OH)_x^{2-x}+xH^+ \tag{3}$$
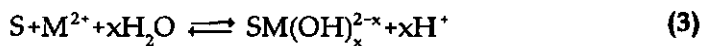
where x may have a non integer value.

In humic substances there are many different types of functional groups, each of which may bind metal ions according to a specific stoichiometry (4-11). Nevertheless the incorporation of a large number of different binding equations in a model is to our opinion not very attractive. First of all it results in a large number of adjustable parameters, and secondly the selection of the different binding equations remains very arbitrary indeed. Equation (3) is a convenient choice since it is characterized by a small number of parameters and accounts for the pH dependency of metal ion binding in a simple way (14).

Note that the experimentally determined proton/metal ion exchange ratio, r_{ex}, is not equal to x. Apart from the protons exchanged directly the binding of the metal ions leads to a decrease of the negative charge and, due to the electrostatic interactions, to a concomitant release of bound protons.

When metal ion binding and proton binding is assumed to be

uncoupled, metal ion binding according to equation (3) results in the following LF equation:

$$\Gamma_M = \Gamma_{M,max} \frac{\left(\bar{K}_M \dfrac{M_S}{H_S^x}\right)^m}{1 + \left(\bar{K}_M \dfrac{M_S}{H_S^x}\right)^m} \tag{4}$$

where M_S is the metal ion concentration near the functional groups at the location of binding, which for a divalent ions is defined by:

$$M_S \equiv (M^{2+}) \exp\left(\frac{-2F\psi_S}{RT}\right) \tag{5a}$$

or

$$M_S = (M^{2+})\, Y^2 \tag{5b}$$

The magnitude of ψ_S depends on the charge of the humic particles, which is determined by both the proton binding and the metal ion binding.

In absence of metal ions the charge of the humics is fully determined by the degree of protonation of the humic sample. The charge for a certain degree of metal ion binding is given by the combination of the initial charge (in absence of metal ions), the measured metal ion binding and r_{ex}. With this charge and by using the electrostatic model determined on the basis of the proton titration behaviour in absence of other specifically binding ions, ψ_S, H_S and M_S can be calculated (13-14).

The possibility to calculate H_S and M_S provides a basis to test whether uncoupled binding is an appropriate model to describe the metal ion binding and it can be used to obtain the optimal value of x. This is done by replotting the experimental data as a function of M_S/H_S^x. When Eq. (4) is an appropriate model and when the optimal value for x is used the binding data measured at different pH should merge into a single "master" curve. We will use this

169

master curve procedure to analyze the experimental calcium binding data.

Competition Between Cadmium and Calcium

In so far we did assume that the proton sites are independent from metal ion sites, but did not discuss whether or not the sites for different metal ions, like calcium and cadmium are identical. Because cadmium and calcium have similar properties we assume in this paper that the sites for cadmium and calcium are identical. A consequence of this assumption is that a multicomponent binding equation is needed to describe the competition between cadmium and calcium. When the pH dependent binding of both cadmium and that of calcium can be described by Eq. (5) and when the assessed m is the same, the cadmium binding in the presence of calcium is given by:

$$
\Gamma_{Cd} = \Gamma_{max} \frac{\tilde{K}_{Cd}\dfrac{Cd_S}{H_S^{x_{Cd}}}}{\left[1+\left(\tilde{K}_{Cd}\dfrac{Cd_S}{H_S^{x_{Cd}}}+\tilde{K}_{Ca}\dfrac{Ca_S}{H_S^{x_{Ca}}}\right)^m\right]\cdot\left(\tilde{K}_{Cd}\dfrac{Cd_S}{H_S^{x_{Cd}}}+\tilde{K}_{Ca}\dfrac{Ca_S}{H_S^{x_{Ca}}}\right)^{1-m}}
\tag{6a}
$$

which can also be written as:

$$
\Gamma_{Cd} = \Gamma_{max} \frac{\tilde{K}_{Cd}\dfrac{Cd_S}{H_S^{x_{Cd}}}}{\tilde{K}_{Cd}\dfrac{Cd_S}{H_S^{x_{Cd}}}+\tilde{K}_{Ca}\dfrac{Ca_S}{H_S^{x_{Ca}}}} \cdot \frac{\left(\tilde{K}_{Cd}\dfrac{Cd_S}{H_S^{x_{Cd}}}+\tilde{K}_{Ca}\dfrac{Ca_S}{H_S^{x_{Ca}}}\right)^m}{1+\left(\tilde{K}_{Cd}\dfrac{Cd_S}{H_S^{x_{Cd}}}+\tilde{K}_{Ca}\dfrac{Ca_S}{H_S^{x_{Ca}}}\right)^m}
\tag{6b}
$$

In Eq. (6) Ca_S and Cd_S are defined by Eq. (5), and x_{Ca} and x_{Cd} can be different for the different ions. Γ_{max} is the adsorption maximum which is in this case the same for both calcium and cadmium (but will differ from the adsorption maximum for the protons).

170

An equal m for both ions implies that the affinity distributions are congruent (they have an identical shape), which is an essential condition for the derivation of Eq. (6) (26-28). When this condition is not met, we have to rely on more complex analytical functions (29-30).

Experimental

A set of pH stat experiments were recorded at pH 6, 8 and 10 for a Purified Peat Humic Acid (PPHA) in the presence of a range of Ca concentrations (pCa 5-2). The HA suspension (5.28 mg HA g^{-1} suspension) was prepared from a commercial Irish horticultural peat (19) by the standard IHSS method (31). The preparation of the PPHA, the proton binding and the cadmium binding are detailed in earlier papers (14,19). The parameters for the description of the proton and cadmium binding and the electrostatics are given in table 1.

The experiments were carried out potentiometrically using a programmable titrator which has been described previously (32). An IBM PC interfaced to a Microlink frame and modules (Biodata Ltd) is used to control three motorized burettes (Metrohm) and to read up to four electrodes. The pH electrodes used were standard glass half-cells (Russell pH Ltd) measured against a saturated calomel reference (Russell or Schott) with a flowing electrolyte bridge and calibrated using NBS primary standard pH buffer solutions. Calcium was measured by a liquid membrane calcium ion-selective electrode (ISE) (Orion 9320).

The ISE was calibrated by placing it successively in 10^{-5}, 10^{-4}, 10^{-3} and 10^{-2} M solutions of $Ca(NO_3)_2$. The electrode response was observed to be linear over this range but curved away below pCa 5 as anticipated in the manufacturer's specification. Liquid membrane ISEs are not as stable or wide-ranging as the available solid state ISEs (eg Cu, Cd) so better performance could not really be expected. Fortunately, environmental concentrations of Ca are often within the range pCa 2-4 so the more limited capabilities of the Ca ISE did not seriously restrict the experiments that we were able to do. The electrode was also less efficient than the Nernstian ideal, often calibrating at -26 mV decade^{-1} (89% response) rather than the theoretical 29 mV decade^{-1}.

Table 1. Parameters for the description of the proton binding and the cadmium binding to the PPHA with the uncoupled binding model based on the LF equation and the spherical double layer model (14,19).

parameter	value
radius (nm)	0.80
Proton Binding	
class 1 $\log \tilde{K}_{1,H}$	4.51
m_1	0.94
$\Gamma_{1,max}$ (mmol/g)	1.45
class 2 $\log \tilde{K}_{2,H}$	9.87
m_2	0.18
$\Gamma_{2,max}$ (mmol/g)	5.64
Cadmium Binding	
x	0.50
$\log \tilde{K}_{Cd}$ (I=0.1 M)	-0.03
m_{Cd}	0.73
$\Gamma_{Cd,max}$ (mmol/g)	1.56

A sample of 20 ml PPHA suspension, diluted to give 25 ml in 0.1 M KNO_3 background, was titrated to the required pH and statted there for 12 hr. It was found that if this long preliminary stat was not used then the sample would tend to drift during the course of the experiment towards the more acid pH at which the PPHA was stored, giving falsely high measurements of the apparent proton release by Ca adsorption onto the HA. Next 0.1 M $Ca(NO_3)_2$ was added in steps, beginning with 0.1 ml and then progressively increasing the dose up to 3 ml until a total volume of 10 ml had been added. Between each dose the sample was titrated back to the stat pH and held there within a tolerance of 0.004 pH (0.2 mV) for 15 min or until the drifts of the electrode readings were <0.004 pH min^{-1} and <0.008 pCa min^{-1} (0.2 mV min^{-1}), whichever was the longer.

The 15 min stat time was used in preference to the 5 min of some of our earlier experiments (14). We had observed that in some instances when

very small doses of metal were added the stat and drift criteria of the experiment were met without the addition of any further base, even though the ISE measurements suggested that some cation had been adsorbed and some proton release was therefore to be expected. We suspected that this situation was caused by the drift criteria being met before true equilibrium was achieved. Forcing the experiment to stat for longer before taking a reading reduced the likelihood of this problem occurring. Undoubtedly allowing an even longer stat time would reduce the risk still further but the increased benefit must be balanced against the problems of electrode drift away from the calibration, which increase with time. A stat time of 15 min represents a compromise; experiments then took a total of ~24 hr to complete, including the 12 hr preliminary stat.

Calculations

For all calculations in this paper the ECOSAT program is used (33). The ECOSAT program combines chemical speciation calculations following the MINEQL scheme, with state of the art binding equations, electrostatic double layer models and transport models.

In the calculations of the electrostatics the presence of a mixed electrolyte, composed of K^+, NO_3^-, Cd^{2+}, H^+, OH^- and their complexes, is explicitly taken into account. The ECOSAT model also allows for the calculation of the composition of the double layer and for the calculation of the non-specific adsorption. Interaction between the humic particles are not taken into account in the calculations.

Experimental Results.

In figure 1 the calcium binding at pH's 6, 8 and 10 is shown as a function of the calcium concentration in a lin-log and a log-log format. The curves show a pH effect, and as to be expected the higher the pH the higher the calcium binding. Comparing the calcium binding with the cadmium binding, measured previously (14), indicates that cadmium is more strongly bound than calcium and that the pH effect is larger for the cadmium binding
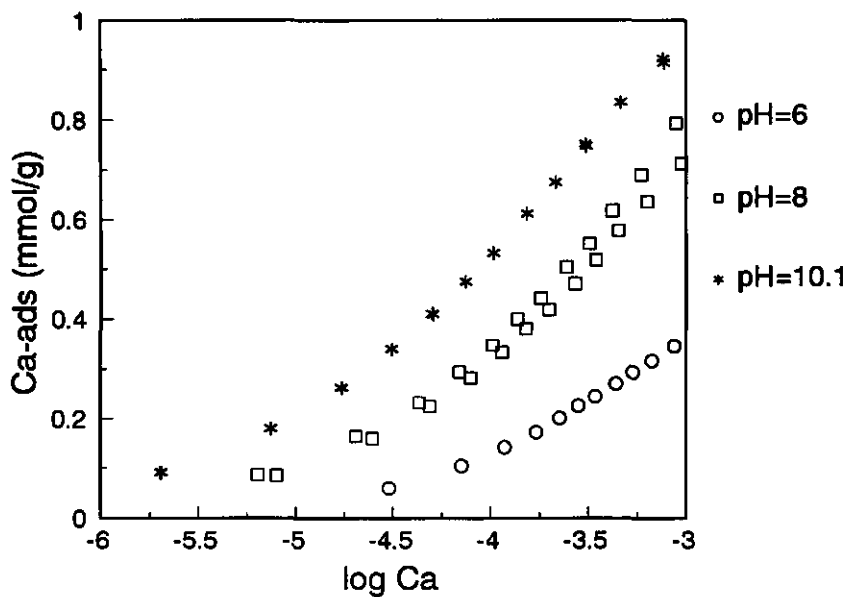
Figure 1. The calcium binding to the PPHA as a function of log Ca for three pH values.
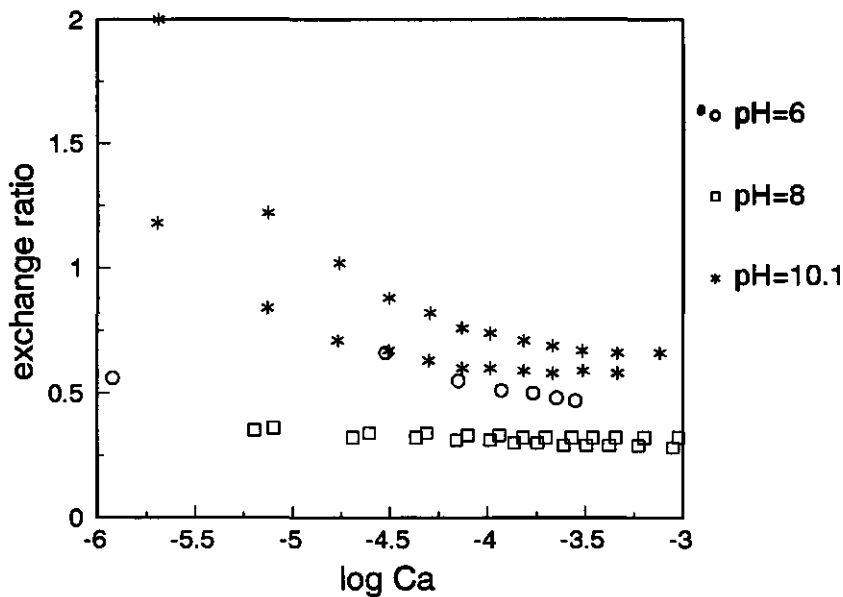

Figure 2. The measured proton metal exchange ratio r_{ex} as a function of log Ca for three pH values.

than for calcium.

In figure 2 the experimental proton metal ion exchange ratio is given. As is discussed in an earlier paper (14), the proton/metal ion exchange ratio r_{ex} is difficult to measure precisely since it is a function of a large number of experimentally determined variables. We have followed how the errors in the individual parameters pass through the final estimate of r_{ex} by a Monte Carlo approach. This consisted of calculating the stoichiometry using random values for each of the 'adjustable' parameters. The spread of random values was defined by a normal distribution having a specified mean and standard deviation. The chosen mean is equal to the analytical value of the parameter measured assuming no error. The standard deviation values chosen are extracted from analysis of the electrode calibration data and from estimates of the likely burette errors. Typically we would use 1000 cycles of the simulation. The standard deviation of the simulated distribution of r_{ex} values is then calculated. We think r_{ex} with standard deviations less than 0.1 are worth keeping, the rest have too large errors. This constraint results in a strong reduction of the data points. Nevertheless figure 2 shows that even for these data points the variation in r_{ex} is very large, while the spreading in the binding curves is small (eg. Fig .1).

The observed pH dependency of r_{ex} is somewhat surprising. Because at low pH the surface is highly protonated one would expect that the lower the pH, the larger r_{ex}. The r_{ex} for pH 6 and 8 correspond with this intuition. However, the r_{ex} for pH=10 do not, since their value is even larger than r_{ex} for pH=6. We have no clear explanation for this.

Modelling the Calcium Binding

To model the calcium binding the results are plotted as a function of $\log Ca_S/H_S^x$. In figure 3 the best merging curves that could be obtained for the calcium binding data are shown. These curves are obtained for x=0.1. Although the curves do merge poorly, most of the pH dependence of the calcium binding is accounted for. The curves do merge best at a low calcium binding. A low degree of calcium binding, the binding hardly influences the charge and potential of the humics. The actual value of r_{ex} is then not very

175

relevant since the potential is still identical to the initial value predicted by the proton binding model. At a higher calcium binding the surface charge is influenced by the binding and the r_{ex} ratio becomes crucial for the calculation of the surface charge and potential. The uncertainty in r_{ex} may be the major reason that the curves deviate at higher log Ca_s/H_s^x.

On the basis of the master curve we have fitted the parameters of the monocomponent LF equation (Eq. 4) for the description of the calcium binding. The optimal values are given in table 2. When all three parameters ($Q_{Ca,max}$, m_{Ca} and log $\tilde{K}_{Ca}$) are treated as adjustable parameters the obtained values for $Q_{Ca,max}$ and m_{Ca} are very similar to the values obtained for cadmium. Choosing $Q_{Ca,max}=Q_{Cd,max}$ and $m_{Ca}=m_{Cd}$ and fitting log $\tilde{K}_{Ca}$ only, gives an almost equally good description of the data. The fitted parameters support the idea that calcium and cadmium bind to identical sites. Since the assessed values of m are very similar, a prediction of competitive binding of calcium on the basis of Eq. (6) seems a reasonable (first order) approach.

Although the experimental binding data show that calcium binding is smaller than the cadmium binding, the assessed log $\tilde{K}_{Ca}$ is larger than log $\tilde{K}_{Cd}$. This somewhat surprising result is caused by the differences in x_{Ca} and x_{Cd}. According to Eq. (3) the binding constant is related to the ratio M_s/H_s^x, hence, the effective binding constant at a given concentration M_s is determined by the ratio $\tilde{K}_M/H_s^x$. As long as the $pH_s>\pm3.0$ the effective constant for cadmium is larger than that for calcium, and the calculated cadmium binding is larger than the calcium binding, which corresponds with the experimental data.

Figure 4 shows that the assessed LF equation and x_{Ca} in combination with the description of the protonation results in a fairly good description of the experimental binding data. The best description of the experimental data is obtained for pH=10. At pH=6 the description slightly overestimates the binding, and at pH=8 the binding is somewhat underestimated.

176

Table 2. The parameters obtained for the description of the pH dependent cadmium binding to the PPHA humic acid in a 0.1 M KNO_3 electrolyte with the uncoupled binding model. For the parameters for the electrostatic model and the proton binding reference is made to table 1.

parameter	Langmuir Freundlich	Tóth
x	0.50	0.50
$\log \tilde{K}_{Cd}$	-0.03	0.65
m	0.73	0.23
$\Gamma_{Cd,Max}$ (mmol/g)	1.56	6.88
r^2	0.98	0.98
RMSE	0.13	0.13

$$r^2 = 1 - \frac{\sum_{i=1}^{np}(n_i - \bar{n}_i)^2}{\sum_{i=1}^{np}(n_i - \bar{n}_i)^2}$$

$$RMSE = \left(\frac{\sum_{i=1}^{np}(n_i - \hat{n})^2}{m - np}\right)^{0.5}$$

- n_i measured value for datapoint i
- $\hat{n}_i$ fitted value for datapoint i
- np number of datapoints
- p number of parameters
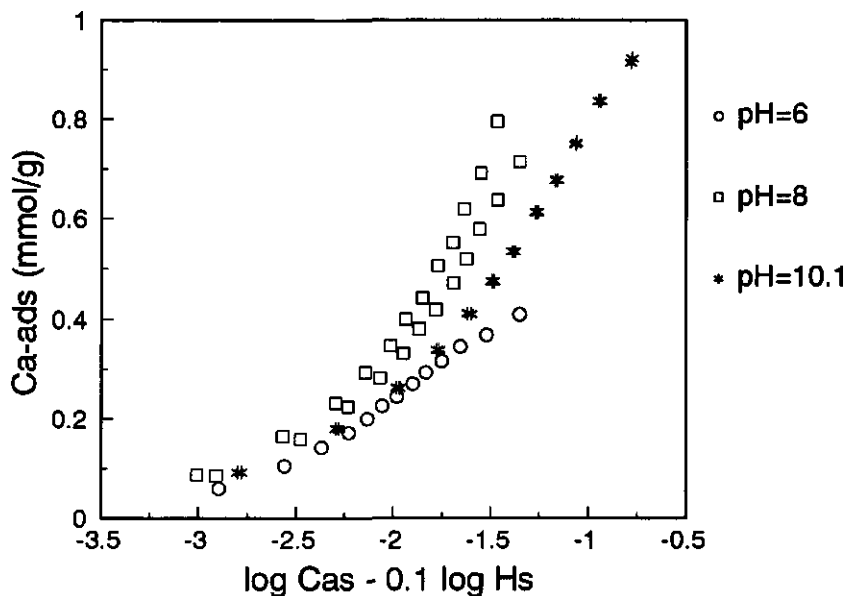- $\bar{n}$ average value of measured datapoints

Figure 3. The calcium binding to the PPHA replotted as a function of $\log Ca_S - 0.1 \log H_S$ for three pH values.
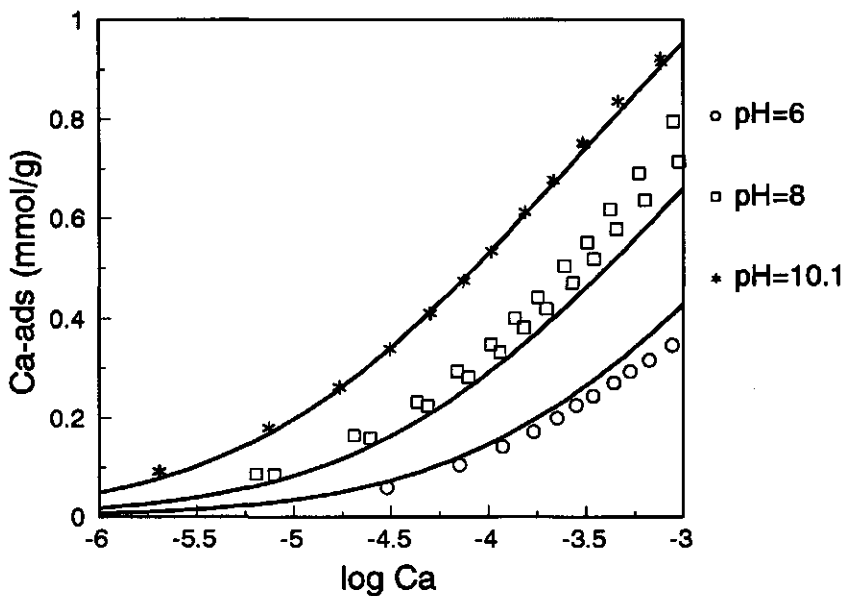
Figure 4. The calculated calcium binding for the uncoupled model, compared with the experimental data. For the parameter values reference is made to tables 1 and 2.

Model Calculations

Cadmium binding in the Presence of Calcium

Because the obtained values for m_{Ca} and $\Gamma_{max,Ca}$ corresponds with the values of m_{Cd} and $\Gamma_{max,Ca}$, Eq. (6), in combination with the description of the protonation, seems a sound basis to predict the effect of calcium on the cadmium binding. In figure 5 the cadmium binding is calculated for pH=4 (fig 5a), pH=6 (fig 5b) and pH=8 (fig 5c) at four different electrolyte situations:

1. I=0.1 M indifferent 1:1 electrolyte

2. I=0.01 M indifferent 1:1 electrolyte

3. I=0.01 M mixed electrolyte, containing 0.001 M calcium, 0.007 M of an indifferent monovalent cation and 0.009 M of an indifferent anion.
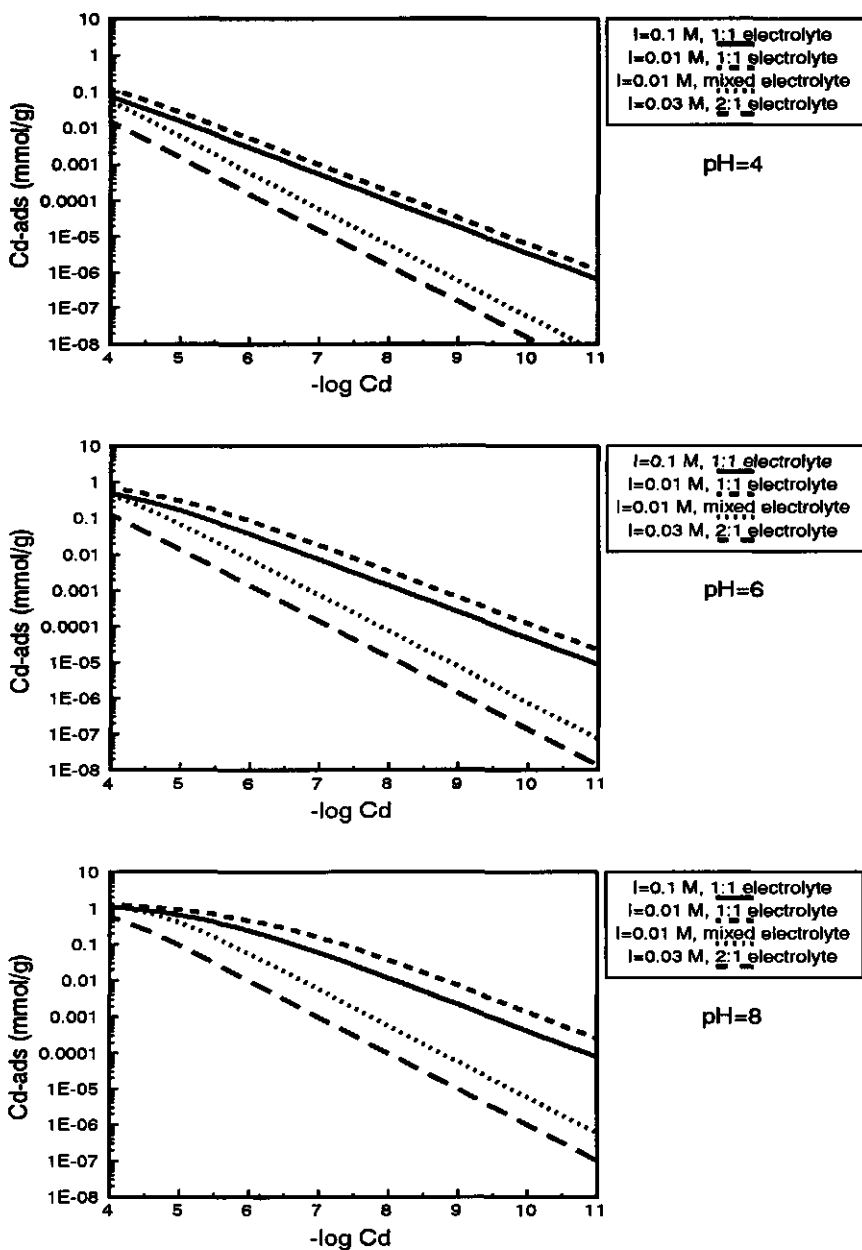
178

Figure 5. The calculated cadmium binding for 4 different electrolytes and three different pH values. For the parameter values reference is made to tables 1 and 2.

179

4. I=0.03 M 2:1 electrolyte with 0.01 M calcium as the divalent ion and 0.02 M monovalent indifferent anion

Note that the median cadmium and calcium constants, given in table 1 and 2, hold for an ionic strength of 0.1 M. For the calculation of the median constants at different ionic strengths, use is made of activity coefficients calculated from the extended Debye Hückel equation.

Electrolyte solution 1 corresponds with the conditions used to obtain the experimental data which were used to calibrate the model description for cadmium and the calcium binding. In non saline soils and freshwater systems, however, the ionic strength of the soil solution is much smaller than 0.1 M. The value of 0.01 M of the second and the third electrolyte is a more realistic value. The ionic strength of the fourth electrolyte corresponds to that of a 0.01 M $CaCl_2$ electrolyte.

The curves for the first two electrolytes illustrate the magnitude of the ionic strength effects on the metal ion binding. The lower the ionic strength, the smaller the screening of the charge and the larger the electrostatic effects. As can be seen in figure 5 this results in a larger cadmium binding.

For low cadmium concentrations (in the absence of calcium) the denominator of Eq. (4) is approximately equal to one. Under these conditions Eq. (4) can be simplified to:

$$\Gamma_{Cd} = K'([Cd^{2+}])^m \tag{7}$$

with

$$K' = \Gamma_{Cd,max} \left(\frac{\tilde{K}_{Cd}}{(H^+)} \gamma^{2-x} \right)^m \tag{8}$$

Equation (7) is known as the ordinary Freundlich equation, an empirical relation which is widely used in soil and environmental sciences. When equation (7) holds, the adsorption isotherm in a log-log format should have a constant slope m. The log Cd range for which this constraint is met depends on pH and ionic strength.

When calcium is present in solution the binding of cadmium strongly decreases. As long as the cadmium binding is much smaller than the calcium binding, the competitive binding equation (Eq. (6)) reduces to:

$$\Gamma_{Cd}=\Gamma_{max}\frac{\tilde{K}_{Cd}\dfrac{Cd_S}{H_S^{x_{Cd}}}}{\tilde{K}_{Ca}\dfrac{Ca_S}{H_S^{x_{Ca}}}} \cdot \frac{\left(\tilde{K}_{Ca}\dfrac{Ca_S}{H_S^{x_{Ca}}}\right)^m}{1+\left(\tilde{K}_{Ca}\dfrac{Ca_S}{H_S^{x_{Ca}}}\right)^m} \qquad (9)$$

which can also be written as:

$$\Gamma_{Cd}=\Gamma_{max}\frac{\tilde{K}_{Cd}(Cd^{2+})}{\tilde{K}_{Ca}(Ca^{2+})(H^+)^{x_{Cd}-x_{Ca}} \ Y^{x_{Cd}-x_{Ca}}} \cdot \theta_{Ca} \qquad (10)$$

or:

$$\Gamma_{Cd}=K''(Cd^{2+}) \qquad (11)$$

The equations (9-11) show that as long as calcium is in excess, the cadmium binding is essentially given by a linear binding relation with a rather complicated conditional constant which depends on the calcium concentration, the pH and the electrostatics. For the electrolytes used calcium dominates up to log Cd=-5, and the resulting binding equations are linear.

The fact that the addition of calcium reduces the cadmium binding is the basis for the use of 0.01 M CaCl$_2$ as an extractant. In the case of a CaCl$_2$ electrolyte the desorption is further promoted by the formation of cadmium chloride complexes in solution, which leads to an extra increase of the total dissolved cadmium concentration in solution.

The curves in figure 5 show that the fraction of the bound cadmium that can be extracted with an 0.01 M CaCl$_2$ electrolyte depends strongly on the pH and composition of the soil solution. When the initial soil solution is indifferent almost all of the bound cadmium can be extracted from the organic adsorption complex. When there is already some calcium present the

181

extractable fraction or the efficiency of the 0.01 M CaCl$_2$ electrolyte is much smaller. Other factors that determine the efficiency of CaCl$_2$ are the presence of other specifically adsorbing ions and the experimental conditions during the extraction. Think for instance of the solid solution ratio and of the variation of the pH during the extraction. The conditional efficiency makes that the extractable fraction is not more than an operational quantity, which from a chemical point of view is hard interpret, unless additional information is available.

Cadmium Binding to Solid Soil Organic Matter

It should be realized that the model calculations are speculative since the Cd/Ca competition are not yet verified by experimental data. The parameters of the model have been assessed on the basis of binding data to a purified humic acid extracted from a peaty soil. Even when the soil organic matter dominates adsorption behaviour it is unlikely that the binding properties of a soil are identical to that of the purified humic acid. In soil the organic matter is partly associated with the mineral phase, which at least will influence the conformation of the organic matter, and the presence of ions like Fe^{3+} and Al^{3+} further complicates the binding behaviour.

Despite all complications the calculations learn that as long as cadmium is at trace level, the binding of cadmium will hardly influence the state of the functional groups and the complex binding equations reduce to simple binding expression. Since the cadmium concentration in the soil solution and in aquatic ecosystems rarely exceeds pCd=6, the application of simple Freundlich type or even linear binding equations should result in good description of the binding behaviour. Note however that the constants of these equations (Eqs (8-10)) are complicated expressions which highly depend on environmental conditions like pH, ionic strength and the concentration of other specifically adsorbing ions. The dependence of the constants on the environmental conditions is often described on the basis of empirical regression functions, which only for a limited variation of environmental conditions results in attractive expressions. The major advantage of a more mechanistic approach, as presented in this paper, is that it provides a sound

basis to describe the dependency of the binding on the environmental conditions. The mechanistic model can be used to predict the effect of the variation in environmental conditions on cadmium binding.

Cadmium Binding to the Dissolved Organic Matter

Because the purified humic substances are in general dissolved, their binding properties will correspond closer to the properties of the dissolved organic matter in natural systems than with the solid organic matter. Therefore the derived model may be used to evaluate the significance of cadmium binding to dissolved organic matter.

Figure 6 gives the dissolved organic matter concentration for which 20 % of the cadmium present in solution is bound to dissolved organic matter as a function of the total cadmium concentration in solution, $Cd_{T,dis}$. This $DOC_{20\%}$ is calculated for the binding curves presented in figure 5 and is expressed as mg C/l. In the calculation it is assumed that carbon makes up 50% of the dissolved organic matter on weight basis and that all of the dissolved carbon is present as the purified humic acid. It is further assumed that Cd^{2+} is the only inorganic cadmium species in the solution. Under these constraints the $DOC_{20\%}$ is given by the following simple expression:

$$DOC_{20\%} = \frac{0.25}{2 \times 10^{-6}} \cdot \frac{Cd_{T,dis}}{\Gamma_{Cd}} \tag{12}$$

with $Cd_{T,dis}$ in mol/l and Γ_{Cd} in mmol/g.

The negligence of a 20 % cadmium binding to the dissolved organic carbon results in an error in the calculated *free* cadmium concentration. When cadmium does not form any inorganic complexes, the calculated free concentration will be equal to the total dissolved cadmium, which is 1.25 the free cadmium concentration. This factor correspond to a calculated cadmium concentration which is 0.1 log unit larger than the free cadmium concentration.

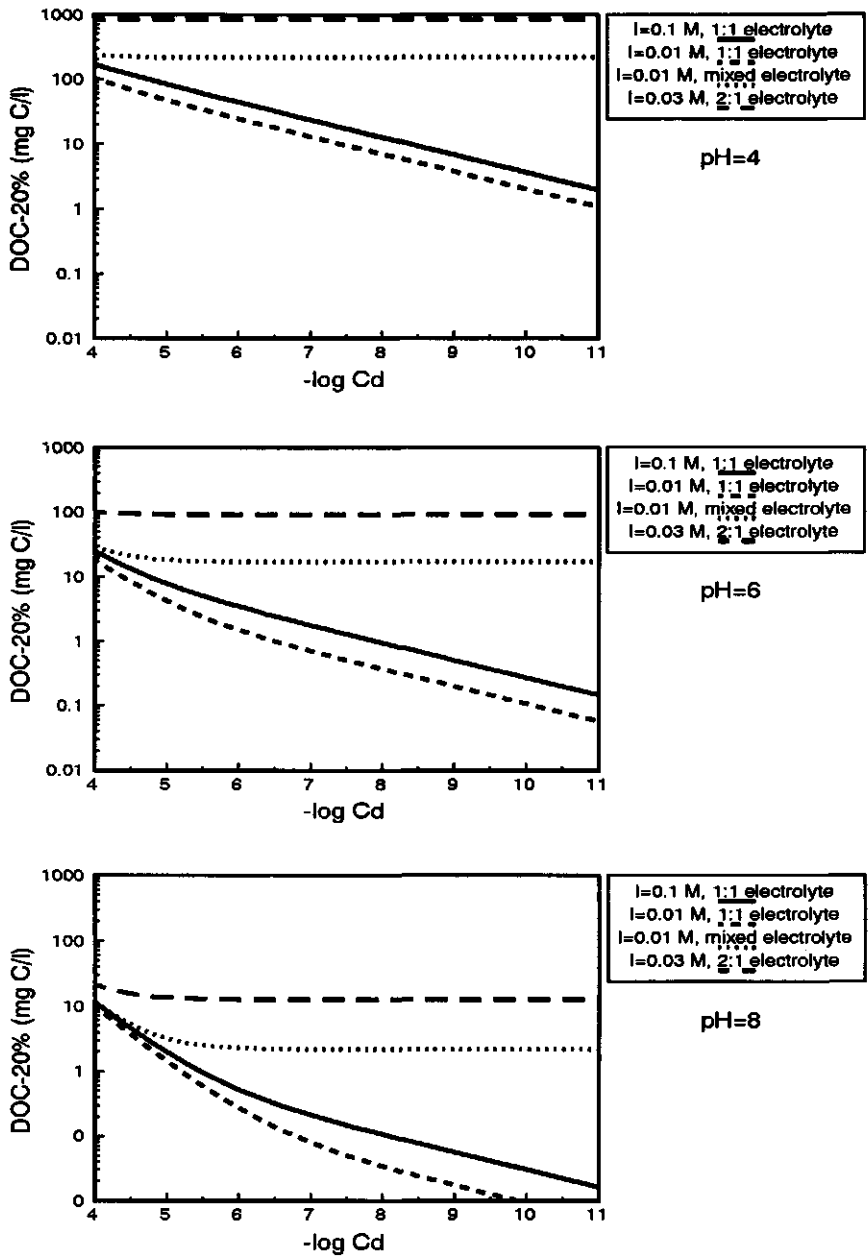The calculated $DOC_{20\%}$ is proportional to the ratio of the total dissolved

Figure 6. The calculated $DOC_{20\%}$ for the binding curves presented in fig. 5.

cadmium concentration over the bound cadmium. For the calcium containing electrolyte the bound cadmium is given by a linear binding equation for a large cadmium concentration range (figure 5, Eq. (11)), and as a consequence the calculated $DOC_{20\%}$ is constant. At low cadmium concentration the cadmium binding in an indifferent electrolyte is given by a Freundlich type equation. This makes that the ratio is also a Freundlich isotherm with a slope equal to 1-m.

Because the cadmium binding depends strongly on the pH and on the composition of the electrolyte, also the $DOC_{20\%}$ depends on these conditions as is shown clearly in figure 6. In most soils the DOC ranges from 0-20 mg C/l. For the calcium electrolytes the calculated $DOC_{20\%}$ lines at pH=4 are far beyond this value, indicating that at these conditions cadmium binding to the DOC is not significant. At higher pH's values, especially at pH=8 binding to the DOC can, however, be very relevant.

For the indifferent electrolyte (curves 1 and 2) the $DOC_{20\%}$ is not constant but depends on the cadmium concentration. For low Cd concentrations (log Cd<-6) binding to DOC plays a significant role in the speciation of cadmium for all three pH values. At high pH the binding is that strong that binding to the DOC is important at low DOC (DOC<1 mg C/l).

Conclusions

-      Calcium binding to the PPHA can be described well with an uncoupled binding model.

-      Model calculations show that the cadmium binding at trace metal levels is given by simple Freundlich or even linear binding equations. The coefficients of these equations however are complicated expressions, which depend strongly on pH and solution composition and follow from the mechanistic model.

-       In general the cadmium concentration will be much smaller than the calcium concentration. Although the experimental binding curves show that cadmium binds more strongly to the humic material, the excess of the calcium concentration makes that calcium highly suppresses the cadmium

185

binding.

Cadmium binding to the dissolved organic carbon is especially important when the pH is high and the concentration of other specifically adsorbing metal ions is low. For a 0.01 M $CaCl_2$ electrolyte the binding to the DOC can be neglected in most systems and the inorganic species dominate the speciation in solution.

Acknowledgement

References

1. Van Riemsdijk, W.H.; De Wit J.C.M.; Nederlof, M.M.; Koopal, L.K. In *Contaminated Soil'90*, Arendt, F.; Hinsenveld, M.; Van Den Brink, W.J. (eds.), Kluwer Academic Publishers: Dordrecht, 1990 359-366.

2. Bolt, G.H.; Bruggenwert, M.G.M. *Soil Chemistry. A. Basic Elements.* Elsevier: Amsterdam, 1978.

3. Sposito, G. *The Surface Chemistry of Soils*, Oxford University Press: New York, 1984.

4. Stevenson, F.J., *Humus Chemistry. Genesis, Composition, Reactions*; Wiley Interscience: New York, 1982.

5. Buffle, J. In *Metal Ions in Biological Systems*. Vol 18. Dekker: New York, 1984, Ch. 6.

6. Aiken, G.R., D.M. McKnight, R.L.Wershaw and P. MacCarthy (Eds.) *Humic Substances in Soil, Sediment, and Water*; Wiley Interscience: New York, 1985

7. Sposito, G., *CRC Crit. Rev. Environ. Control* 1986, *16*, 193-229.

8. Buffle, J. *Complexation Reactions in Aquatic Systems: An Analytical Approach*; Ellis Horwood Limited: Chichester, 1988.

9. Hayes, M.H.B.; MacCarthy, P.; Malcolm, R.L.; Swift, R.S. (Eds.), *Humic Substances II: In Search of Structure*; Wiley Interscience: New York, 1989.

10.   Livens, F.R., *Environ. Pollution* 1991, *70*, 183-208.

11.   MacCarthy, P.; Perdue, E.M., 1991, In *Interactions at the Soil Colloid - Soil Solution Interface*; Bolt, G.H.; De Boodt, M.F.; Hayes, M.H.B.; McBride M.B. (Eds.); NATO ASI Series Series E: Applied Sciences-Vol. 190, Kluwer Academic Publishers, Dordrecht, 469-489.

12.   Thurman, E.M. In *Humic Substances in Soil, Sediment, and Water*; Aiken, G.R., D.M. McKnight, R.L.Wershaw and P. MacCarthy (Eds.) Wiley Interscience: New York, 1985. Ch. 4.

13.   De Wit, J.C.M.; Van Riemsdijk, W.H.; Nederlof, M.M.; Kinniburgh, D.G.; Koopal, L.K. *Analytica Chim. Acta* 1990, *232*, 189-207.

14.   De Wit, J.C.M.; Van Riemsdijk, W.H.; Koopal, L.K.; Milne, C.J.; Kinniburgh, D.G. The Description of Cadmium Binding to a Purified Peat Humic Acid, Submitted to *Environ. Sci. Technol.*

15.   De Wit, J.C.M.; Nederlof, M.M.; Van Riemsdijk, W.H.; Koopal, L.K. *Water, Air and Soil Pollution* 1991, *57-58*, 339-349.

16.   De Wit, J.C.M.; Van Riemsdijk, W.H.; and Koopal, L.K.; *Finnish Humus News* 1991, *3*, 139-144.

17.   De Wit, J.C.M., W.H. Van Riemsdijk and L.K. Koopal, *Proton Binding to Humic Substances. A. Electrostatic Effects.* Submitted to *Environ Sci. Technol.*

18.   De Wit, J.C.M., W.H. Van Riemsdijk and L.K. Koopal, *Proton Binding to Humic Substances. B. Chemical Heterogeneity and Adsorption Models.* Submitted to *Environ Sci. Technol.*

19.   De Wit, J.C.M.; Koopal, L.K; Van Riemsdijk, W.H.; Kinniburgh, D.G.; Milne, C.J. *Analysis of Proton Binding by a Peat Humic Acid,* in preparation, (to be submitted to Analytica Chimica Acta).

20.   Häni, H.; Gupta, S. *Landwirtsch. Forsch. Sh.* 1980, *37*, 267-274.

21.   Sauerbeck, D.R.; Styperek, B. In: *Chemical Methods for Assessing Bio-available Metals in Sludges and Soils*, Leschber, R.; Davis, R.D.; L'Hermite, P. (Eds.), Elsevier Applied Science Publishers: London, 1985, pp.49-66.

22.   Houba, V.J.G.; Novozamsky, I.; Huybregts, A.W.M.; Van der Lee, J.J. *Plant and Soil* 1986, *96*, 433-437.

23.   Eriksson, J.E., *Water Air Soil Pollut.* 1990, *53*, 69-81.

24.   Boekhold, A.E.; Temminghoff, E.J.M.; Van der Zee, S.E.A.T.M.; Influence of Electrolyte Composition and pH on Cadmium Sorption by an Acid Sandy Soil

J. Soil Sci. In press.

25.   Sips, R. *J. Chem. Phys.* **1948**, *16*, 490.

26.   Jaroniec, M.; Madey, R. *Physical Adsorption on Heterogeneous Solids*, Elsevier: Amsterdam, 1988.

27.   Jaroniec, M. *Adv. Colloid Interface Sci.* **1983**, *18*, 149-225.

28.   Van Riemsdijk, W.H., J.C.M. de Wit, L.K. Koopal and G.H. Bolt, 1986, *J. Colloid Interface Sci.* 116:511-522.

29   De Wit, J.C.M.; Van Riemsdijk, W.H.; Koopal, L.K., *Analytical Isotherms Equations for Multicomponent Adsorption to Heterogeneous Surfaces.* submitted to *J.Colloid Interface Sci.*

30   De Wit, J.C.M.; Van Riemsdijk, W.H.; Koopal, L.K., *Analytical Isotherms Equations for Multicomponent Adsorption to Heterogeneous Surfaces. Part II. Consecutive Reactions.* submitted to *J.Colloid Interface Sci.*

31.   Thurman, E.M. and Malcolm, R.L. 1981. Preparative isolation of aquatic humic substances. *Environmental Science and Technology.* **15**, 463.

32.   Kinniburgh, D.G. and Milne, C.J. 1992. Guide to the Wallingford Titrator. *British Geological Survey Technical Report* WD/92/14, 160pp.

33.   Keizer, M.G.; De Wit; J.C.M.; Meeussen, J.C.L.; Bosma, W.J.P., Nederlof, M.M.; Van Riemsdijk; W.H.; Van der Zee, S.E.A.T.M. *ECOSAT;* Technical Note of the Department of Soil Science and Plant Nutrition, Wageningen Agricultural University, Wageningen, 1992.

Chapter 7

Analytical Isotherm Equations for Multicomponent Adsorption to Heterogeneous Surfaces

Abstract

In this paper analytical expressions are presented that allow to describe multicomponent binding to chemical heterogeneous surfaces. The equations are derived under the constraint that the affinity distributions for the different species can be rescaled to one common distribution by means of a mathematical transformation. The features of the derived equations are illustrated on the basis of model calculations.

.

This paper is submitted for publication in *Journal of Colloid and Interface Science*: J.C.M. de Wit, W.H. van Riemsdijk, L.K. Koopal, Analytical Isotherm Equations for Multicomponent Adsorption to heterogeneous Surfaces.

Introduction

On most natural surfaces a variety of different types of functional groups or imperfections are present, which makes such surfaces chemically heterogeneous (1-2). The chemical heterogeneity influences the adsorption behaviour. In the most simple case of adsorption to a homogeneous surface the adsorption of a certain species can be described with only one surface-adsorbate interaction parameter or affinity constant. For adsorption to a heterogeneous surface a distribution of affinity constants is necessary. This distribution is discrete when there are a distinct number of different groups present, or continuous when there are a very large number of different groups. In this paper we concentrate on continuous heterogeneity.

The overall adsorption on a continuous heterogenous surface is given by the adsorption per group of identical sites, the so called local adsorption, integrated over the affinity distribution. In general the integration can only be solved numerically, however, for certain distribution functions in combination with the Langmuir equation as the local isotherm, analytical solutions are known. Three of these analytical overall isotherms are the Langmuir Freundlich (LF) equation (3), the Generalized Freundlich (GF) equation (4) and the Tóth equation (5).

All three adsorption equations are originally derived for mono-component adsorption. Jaroniec and Van Riemsdijk et al (1,6-9) have shown that the analytical equations for mono-component adsorption can be extended to multi-component adsorption under the assumption that the shape of the affinity distribution for different components are identical. However, this condition is clearly a simplification (10). In this paper we present analytical isotherm equations for competitive adsorption in which the affinity distribution of the different components may differ in shape, width and position on the log K axis. Although all three monocomponent equations (LF, GF, Tóth) can be extended, we will only discuss the extensions of the Langmuir Freundlich equation.

The characteristic features of the derived relations will be illustrated with some model calculations.

Monocomponent Adsorption

In general the overall adsorption of a component i, $\theta_{i,t}$, on a continuous heterogeneous surface is given by an integral equation:

$$\theta_{i,t} = \int_{\Delta \log K_i} \theta_{i,L} \, f(\log K_i) \, d \, (\log K_i) \qquad (1)$$

where $f(\log K_i)$ is the distribution function of the affinity constants and $\theta_{i,L}$ is the local adsorption isotherm which holds for parts of the surface with a certain local affinity $K_{i,L}$. In the case of a Langmuir isotherm the local adsorption is expressed as a function of $K_{i,L}$ and the concentration (or activity) of the species i in the solution phase according to:

$$\theta_{i,L} = \frac{K_{i,L} c_i}{1 + K_{i,L} c_i} \qquad (2)$$

In absence of lateral interactions c_i is simply the concentration, $c_i^\#$. In the presence of lateral interactions the Langmuir equation can still be used, provided that the product of the solution concentration $c_i^\#$ and a factor γ_i, expressing the interactions, is used as the expression for c_i. In such a case the adsorption as a function of the solution concentration itself may deviate strongly from the Langmuir isotherm, but the adsorption expressed as a function of c_i ($= c_i^\# \gamma_i$) is of the Langmuir type.

For a random heterogeneous surface the interaction factor γ_i is independent of the site type L and Eq. (1) with (2) as local isotherm and the LF distribution function can be solved analytically. This results in the Langmuir Freundlich or LF adsorption equation:

$$\theta_{i,t} = \frac{(\bar{K}_i c_i)^{m_i}}{1 + (\bar{K}_i c_i)^{m_i}} \qquad (3)$$

where $\theta_{i,t}$ is the overall coverage of the surface with i, $\bar{K}_i$ is the median value of the affinity distribution for i and m_i, which has a value between 0 and 1, determines the width of the distribution

192

Multi-component Competitive Adsorption - Congruent Heterogeneity

In a multi-component system different components are present which can form complexes with the surface sites. Binding of component i to a surface site of type L can now be given by the Langmuir equation for multicomponent adsorption:

$$\theta_{i,L} = \frac{K_{i,L}c_i}{1 + \sum_i K_{i,L}c_i} \tag{4}$$

The summation of $\theta_{i,L}$ for all components i results in:

$$\theta_{T,L} = \frac{\sum_i K_{i,L}c_i}{1 + \sum_i K_{i,L}c_i} \tag{5}$$

We call $\theta_{T,L}$ the total local adsorption. Note that $\theta_{T,L} = 1 - \theta_{ref,L}$, where $\theta_{ref,L}$ is the fraction of the reference surface species (unoccupied) for the sites of type L.

Following Jaroniec (6-7) and Van Riemsdijk et al (8-9) we assume that the affinity constant $K_{i,L}$ is composed of two contributions:

$$K_{i,L} = k_i K_L \tag{6}$$

with k_i the component specific part, which is not influenced by the chemical heterogeneity and K_L is the part which is subject to the chemical heterogeneity, independent of the type of component. The assumption that K_L is only dependent on the type of polyfunctional ligand or surface is of course an idealization.

Equation (6) implies that the shape of the affinity distribution is the same for all components, while the location of the affinity distribution on the log K axis may differ. We will call this type of distributions *congruent*. The introduction of Eq. (6) into Eq. (5) results in:

$$\theta_{T,L} = \frac{K_L c^*}{1 + K_L c^*} \tag{7}$$

with:

$$c^* = \sum_i k_i c_i = \sum_i k_i c_i^* \gamma_i \tag{8}$$

Since only K_L is subject to chemical heterogeneity and $\theta_{T,L}$ as a function of c^* is mathematically equivalent to the monocomponent Langmuir relation, the overall fraction of sites covered with any of the components, $\theta_{T,t}$, follows from an integration analogous to Eq. (1). For the LF distribution this results in:

$$\theta_{T,t} = \frac{\left(\sum_i \tilde{K}_i c_i\right)^m}{1 + \left(\sum_j \tilde{K}_i c_i\right)^m} \tag{9}$$

Note that again $\theta_{T,t} = 1 - \theta_{ref,t}$, where $\theta_{ref,t}$ is the overall fraction of all unoccupied sites.

The overall binding of a certain component i, $\theta_{i,t}$ is given by the product of the fraction $\tilde{K}_i c_i$ over $\Sigma \tilde{K}_i c_i$ times θ_T:

$$\theta_{i,t} = \frac{\tilde{K}_i c_i}{\sum_i \tilde{K}_i c_i} \theta_{T,t} \tag{10a}$$

By combining Eq. (9) and (10a) $\theta_{i,t}$ can also be written as:

$$\theta_{i,t} = \frac{\tilde{K}_i c_i}{\left[1 + \left(\sum_i \tilde{K}_i c_i\right)^m\right] \left(\sum_i \tilde{K}_i c_i\right)^{1-m}}$$

(10b)

Equation (9) or (10) is the multicomponent LF equation for a certain component i (8,9).

Multicomponent Adsorption - Non Congruent Heterogeneity

Transformation of affinity distributions

Although the multicomponent LF equation (Eq. (9) or (10)) is an elegant expression its main restriction is that all components should conform to one identically shaped or congruent distribution. When the monocomponent adsorption of various components to the same surface as described by Eq. (3) does not result in the same value of m_i, Eq. (10) cannot be used to describe the competitive adsorption.

Here we address a more general approach that combines the advantage of analytical binding equations with a more realistic variation in distribution functions for various adsorbing species. This approach is based on the idea that different individual monocomponent distributions can be rescaled to one distribution that is the same for all components by using a mathematical transformation.

Monocomponent Binding

The overall adsorption as a function of the solution concentration can be obtained directly from adsorption experiments. The mono-component binding equation, Eq. (1) implies that the observed binding results from a combination of a local isotherm and an affinity distribution. Since the overall binding is experimentally determined, the choice of a certain local isotherm directly affects the affinity distribution. This implies

195

that a transformation of the distribution functions can be obtained by transforming the local isotherm under the constraint that the resulting expression leads to the same overall binding.

If we call the transformed affinity distribution $f(\log K_L)$ and if the transformed local isotherm is assumed to be still of a Langmuir type function, Eq. (1) can be written as:

$$\theta_i t = \int_{\Delta \log K_L} \frac{K_L X_i}{1 + K_L X_i} f(\log K_L) \, d\log K_L \tag{11a}$$

where X_i is a function of c_i and k_i:

$$X_i = g(k_i, c_i) \tag{11b}$$

When the function $g(k_i c_i) = k_i c_i$ and $f(\log K_L)$ is a LF distribution, integration of Eq. (11) results in Eq. (3), with $\log \tilde{K}$ as median and p as width.

We will now show how the width of a LF distribution can be adjusted by adjusting the expression for the local isotherm. To do so we use the following expression:

$$g(k_i, c_i) = (k_i' c_i)^{n_i} \tag{12}$$

Using Eq. (11) with $f(\log K_L)$ as a LF distribution with width p, in combination with Eq. (12) results in a LF type of adsorption equation for i:

$$\theta_{i,t} = \frac{\left(\tilde{K}(k_i' c_i)^{n_i}\right)^P}{1 + \left(\tilde{K}(k_i' c_i)^{n_i}\right)^P} \tag{13}$$

Equation (13) can be written as a LF equation with $n_i p$ as the heterogeneity parameter and $\tilde{K}_i'$ as the median value:

$$\theta_{i,t} = \frac{(\bar{K}_i' c_i)^{n_i p}}{1 + (\bar{K}_i' c_i)^{n_i p}} \tag{14}$$

with

$$\tilde{K}_i' = \bar{K}^{1/n_i} k_i \tag{15}$$

Of course Eq. (13) could also have been obtained directly when Eq. (1) had been integrated over a LF distribution with $\bar{K}_i'$ as the median and $n_i p$ as the width. We therefore may conclude that any monocomponent LF equation can be rescaled to a LF type of equation with a different width and median by making the local isotherm equation a function of $(k_i c_i)^m$

Multicomponent Binding

The possibility to rescale LF distributions to any specific width can be used to derive an analytical equation for multicomponent binding for cases where the monocomponent isotherms are LF equations with different widths. Before the integration can be performed all individual monocomponent distributions have to be rescaled to one common log K distribution which is a characteristic of the surface. This rescaling corresponds to the following expression for the total local adsorption:

$$\theta_{T,L} = \frac{K_L \sum_i X_i}{1 + K_L \sum_i X_i} \tag{16a}$$

with

$$X_i = (k_i c_i)^{n_i} \tag{16b}$$

The value of n_i follows from the values of m_i obtained for the monocomponent adsorption and from the width of the common log K distribution, p, which is a priori not known:

197

$$n_i p = m_i \tag{17}$$

Using Eq. (16) as the local isotherm equation and the LF distribution with width p as the affinity distribution, results in the following competitive binding equation:

$$\theta_{i,t} = \frac{(\tilde{K}_i c_i)^{n_i}}{\sum_i (\tilde{K}_i c_i)^{n_i}} \cdot \frac{\left(\sum_i (\tilde{K}_i c_i)^{n_i}\right)^P}{1 + \left(\sum_i (\tilde{K}_i c_i)^{n_i}\right)^P} \tag{18}$$

An interesting situation arises when p=1. This value implies that all distributions are transformed into a Dirac delta function, meaning a homogeneous common distribution. Note that when p=1, Eq. (18) is identical to the transformed local isotherm equation which implies that $\theta_{i,t} = \theta_{i,L}$.

A relatively wide common distribution, i.e. a relatively small value of p, will result in $n_i > 1$ for components with $m_i > p$. This can be avoided by choosing p larger than any of the m_i, which implies that the width of the mono component LF equation is equal or larger than the width of the common distribution. When we consider that the common distribution corresponds to the heterogeneity of the adsorbate, the constraint $m_i > p$ implicates that the component specific part of the affinity may not reduce the heterogeneity, but results in an extra heterogeneity.

In general the value of p is unknown and cannot be obtained from monocomponent binding data, which makes it impossible to predict the competitive adsorption based on information from mono component adsorption to heterogeneous surfaces, only. In principle p can be assessed on the basis of binding data for multicomponent systems. In the next section we will analyze the effect of the chosen values of p for some simple cases.

Model Calculations

In the model calculations we will consider the binding of a component A to a continuous heterogeneous surface in the presence of a constant concentration of component B. The monocomponent binding of A to the surface can be described by a LF equation with a width m=a and $\tilde{K}_A$ as the median affinity constant, the monocomponent binding of B is described by a LF equation with the width m=b and median $\tilde{K}_B$. We further assume that binding of A can be given by the multicomponent expression Eq. (18). For the two component system this expression reads:

$$\theta_A = \frac{(\tilde{K}_A c_A)^\alpha}{(\tilde{K}_A c_A)^\alpha + (\tilde{K}_B c_B)^\beta} \cdot \frac{\left[(K_A c_A)^\alpha + (K_B c_B)^\beta\right]^p}{1 + \left[(K_A c_A)^\alpha + (K_B c_B)^\beta\right]^p} \tag{19}$$

with $\alpha = a/p$ and $\beta = b/p$.

The second term of the RHS of Eq. (19) is equals to the sum of θ_A and θ_B. When $\theta_A + \theta_B \approx 1$ the binding of A is essentially an A/B exchange process. In this limiting case θ_A is fully determined by the first term of the RHS. This first term corresponds with the following overall exchange stoichiometry:

$$SB_\beta + \alpha A \rightleftharpoons SA_\alpha + \beta B \tag{20}$$

Equation (20) clearly shows that surface heterogeneity influences the observed stoichiometry. Due to the heterogeneity, A/B exchange ratios unequal to one can be obtained, although both A and B bind to the same sites and only monodentate SA and SB surface species are assumed to be formed.

Homogeneous Surface

The most simple case is the homogeneous surface (a=b=p=1). The binding of A is now given by the two component Langmuir isotherm equation. In figure 1 the binding of component A is given as a function of $\log c_A$ for three values of $\log c_B$, for a surface with $\tilde{K}_B = \tilde{K}_A = 1$. If different

values for $\tilde{K}_A$ and $\tilde{K}_B$ are chosen, the figures can still be used, provided that the product $\tilde{K}_i c_i$ result to the same values as used in the examples.

All three curves in figure 1 have a shape identical to the homogeneous monocomponent Langmuir Equation, and at low θ_A the binding is linear. The position of the curves depends on c_B. At a high c_B, B is a strong competitor and a high c_A is necessary in order to obtain a considerable binding.

Congruent Heterogeneous Surface

In the first heterogeneous case we use the "classical" assumption (6-9) that the shape of both affinity distributions is the same. This corresponds with a=b=p and $\alpha=\beta=1$. In figure 2 we have calculated the binding curves for A for p=0.4. The values of the mean affinity constants and the c_B values are identical to the values used in figure 1. We will use those values in all model calculations.

The curves given in figure 2 look very similar to those in figure 1. The curve for the highest c_B is even identical to that of figure 1. At high c_B the second fraction of the RHS of Eq. (19) equals one and the first fraction of the RHS determines the binding, irrespective c_A. For $\alpha=\beta=1$ the first fraction is not influenced by the heterogeneity and the calculated binding curve is identical to those for homogeneous surfaces. This limiting situation is observed for the curve with highest c_B.

The second fraction at the RHS of Eq. (19), remains also constant as long as $c_A \ll c_B$. The course of the binding of A is then fully determined by the numerator of the first fraction, which is a linear adsorption relation. The slope of one in the log-log plot shows that up to $\theta=0.1$ (log $\theta=-1$) $c_A \ll c_B$ and that the binding is given by a linear adsorption relation. The heterogeneity does only influence the binding when $\theta_A > 0.1$.

When the RHS of Eq. (19) is initially not equal to one and log $(\tilde{K}_A A)$ becomes of the same order of log $(\tilde{K}_B B)$ the second fraction is no longer constant. From that point on the heterogeneity will influence the binding and the curves will deviate from the homogeneous curves.
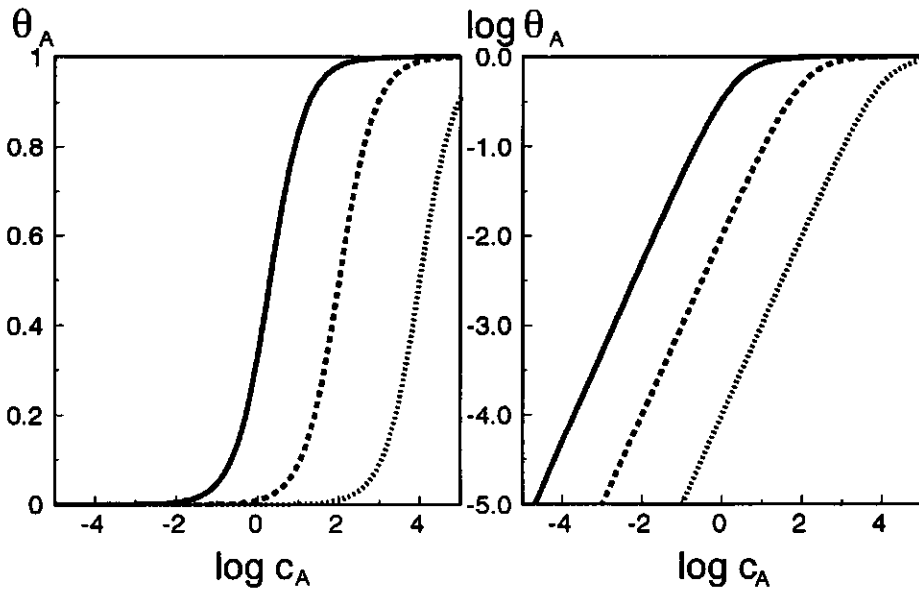
Figure 1. The binding of component A to a homogeneous surface as a function of $\log c_A$ in a lin-log and a log-log format for three values of c_B. $\log \check{K}_A = \log \check{K}_B = 0$, $p=a=b=1$, ——— $\log c_B = 0$, ----------- $\log c_B = 2$, ·················· $\log c_B = 4$.
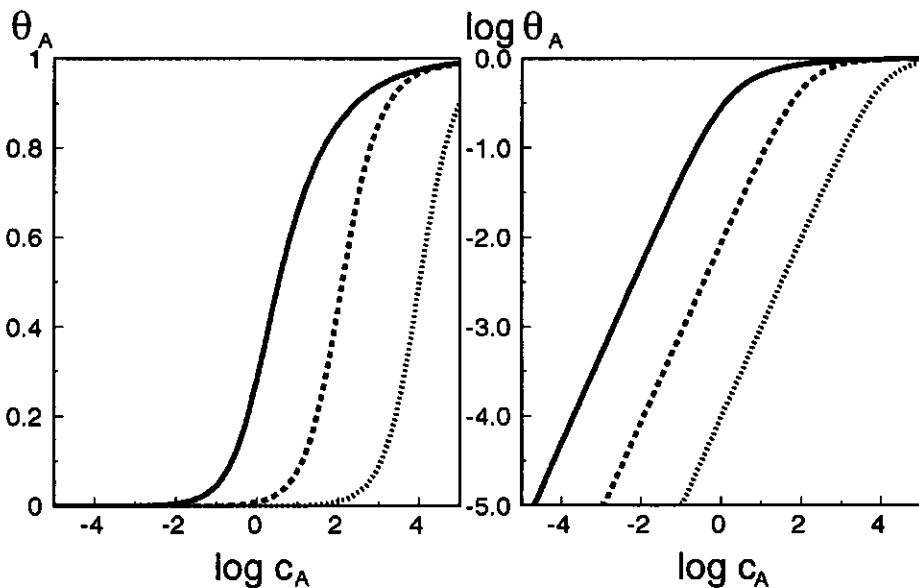

Figure 2. The binding of component A to a congruent heterogeneous surface as a function of $\log c_A$ in a lin-log and a log-log format for three values of c_B. $\log \check{K}_A = \log \check{K}_B = 0$, $p=a=b=0.4$, ——————— $\log c_B = 0$, ----------- $\log c_B = 2$, ·················· $\log c_B = 4$.

Non Congruent Heterogeneous Surface: p=1

Instead of choosing p equal to a or b, we may also chose different values for p, a and b. An interesting case is obtained for p=1, which results in the following binding equation:

$$\theta_A = \frac{(\tilde{K}_A c_A)^a}{(\tilde{K}_A c_A)^a + (\tilde{K}_B c_B)^b} \cdot \frac{(K_A c_A)^a + (K_B c_B)^b}{1 + (K_A c_A)^a + (K_B c_B)^b} \tag{21}$$

which equals:

$$\theta_A = \frac{(\tilde{K}_A c_A)^a}{1 + (K_A c_A)^a + (K_B c_B)^b} \tag{22}$$

According to Eq. (22) the binding at low concentration of A is not longer given by a linear relation but by a non linear Freundlich equation. This illustrated in figure 3, where θ_A is calculated for p=1 and a=b=0.4. A comparison of the curves of figure 3 with those of figure 2 shows that not only the shape of the θ_A curves has changed, but also its dependence on the concentration of B.

Non Congruent Heterogeneous Surface: p=a or p=b and a≠b

In the following cases we assume that a is either somewhat smaller than b (a=0.3 and b=0.4) or that a is somewhat larger (a=0.4 and b=0.3). This implies that the monocomponent binding curve of A is somewhat more heterogeneous than that of B (a=0.3, b=0.4, fig. 4) or somewhat less heterogeneous (a=0.4, b=0.3, fig 5). The monocomponent binding curves are given in figure 6. We will further assume that p equals the largest value of a or b, which for b>a and p=b (β=1) results in the following binding equation:
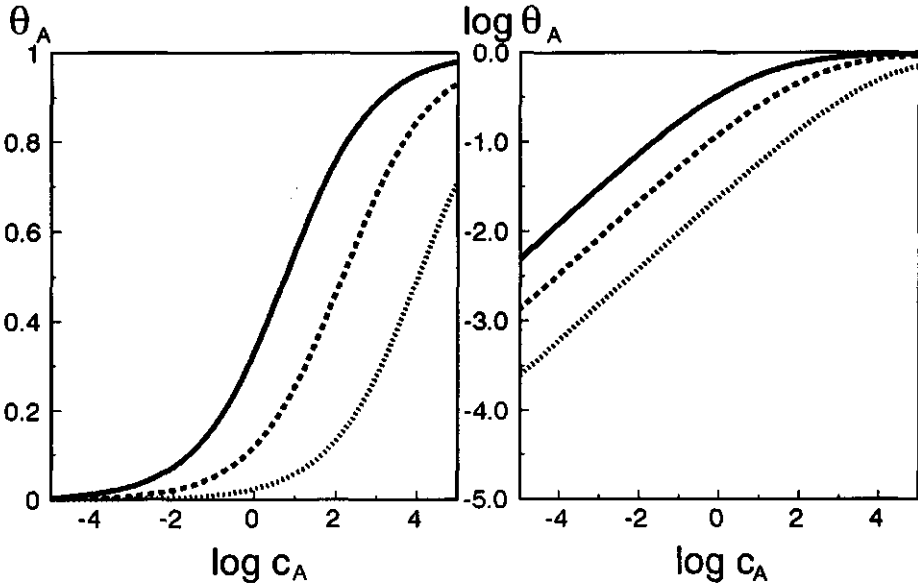
202

Figure 3. The binding of component A to a non congruent heterogeneous surface as a function of log c_A in a lin-log and a log-log format for three values of c_B. log $\bar{K}_A$=log $\bar{K}_B$=0, p=1, a=b=0.4, ———— log c_B=0, ----------- log c_B=2, ················· log c_B=4.
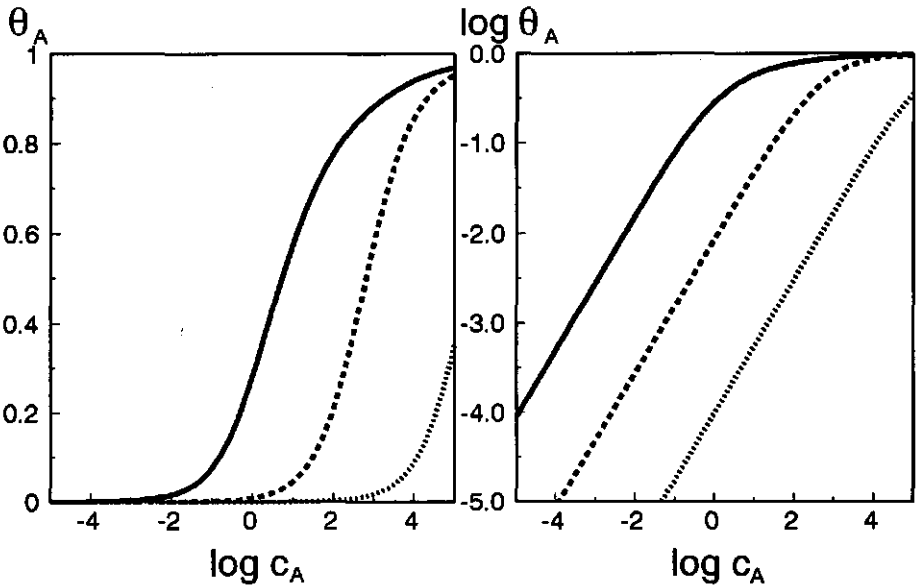

Figure 4. The binding of component A to a non congruent heterogeneous surface as a function of log c_A in a lin-log and a log-log format for three values of c_B. log $\bar{K}_A$=log $\bar{K}_B$=0, p=0.4, a=0.3, b=0.4, ———— log c_B=0, ----------- log c_B=2, ················· log c_B=4.

203

$$\theta_A = \frac{(\bar{K}_A c_A)^\alpha}{(\bar{K}_A c_A)^\alpha + \bar{K}_B c_B} \cdot \frac{\left[(K_A c_A)^\alpha + K_B c_B\right]^b}{1 + \left[(K_A c_A)^\alpha + K_B c_B\right]^b} \qquad (23)$$

and for a>b and p=a (α=1) in:

$$\theta_A = \frac{\bar{K}_A c_A}{\bar{K}_A c_A + (\bar{K}_B c_B)^\beta} \cdot \frac{\left[K_A c_A + (K_B c_B)^\beta\right]^a}{1 + \left[K_A c_A + (K_B c_B)^\beta\right]^a} \qquad (24)$$

These two equations result in a different behaviour, which can be illustrated for the limiting case that the concentration of A is very low. In this case the course of the θ_A depends solely on the numerator of the first fraction of the binding equations (Eq. (23) and Eq. (24)). For p=b the binding equation (Eq. (23)) reduces to a non linear Freundlich adsorption equation, while for p=a the binding equation (Eq. (24)) reduces to a linear binding equation. The differences in binding behaviour at low c_A is shown in the log-log plots of figs. 4 and 5. In the curves of fig. 4, (p=b) up to θ_A=0.1 the slope equals 0.75, in fig. 5 (p=a) the slope is 1.

When $\theta_A + \theta_B$=1 the exchange equation (20) holds. If α=β an exchange ratio equal to one is obtained. This is the case in figs (1-3). In fig. 4, p=b, α<β and 1.33 molecules of B are released upon binding of 1 molecule of A. The large exchange ratio makes B a strong competitor and, as a consequence, the curves of A are far apart. In fig. 5 p=a, α>β and 0.8 molecules of B are released, which results to a relative small dependence of θ_A on B.

As is illustrated in figure 6, the differences in the monocomponent binding curves for the different values of a and b used to calculate the curves of the figs. 4 and 5 are rather small. Nevertheless the curves for the two component systems show that a different heterogeneity for a and b has already pronounced effects even when the difference between a and b is small.
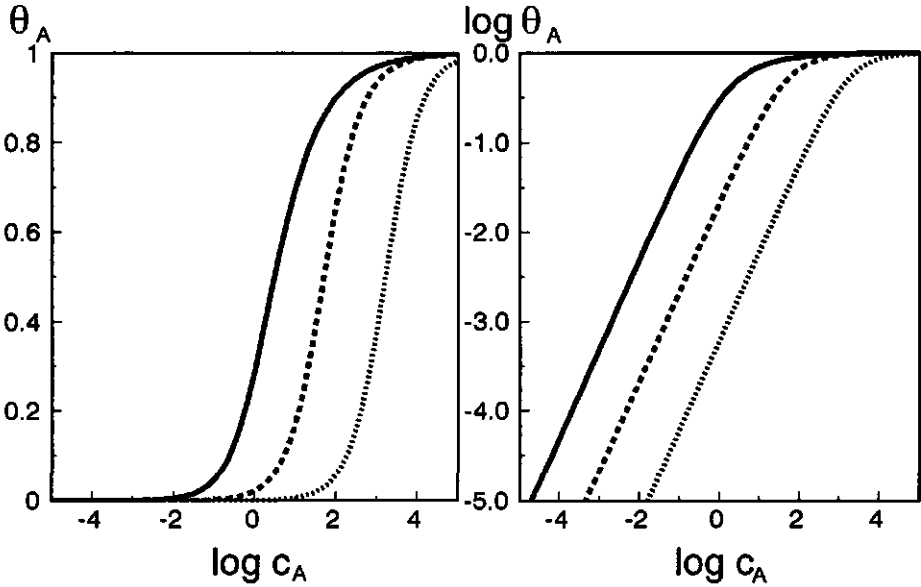
Figure 5. The binding of component A to a non congruent heterogeneous surface as a function of log c_A in a lin-log and a log-log format for three values of c_B. log $\tilde{K}_A$=log $\tilde{K}_B$=0, p=0.5, a=0.5, b=0.4, ——— log c_B=0, ----------- log c_B=2, ·················· log c_B=4.

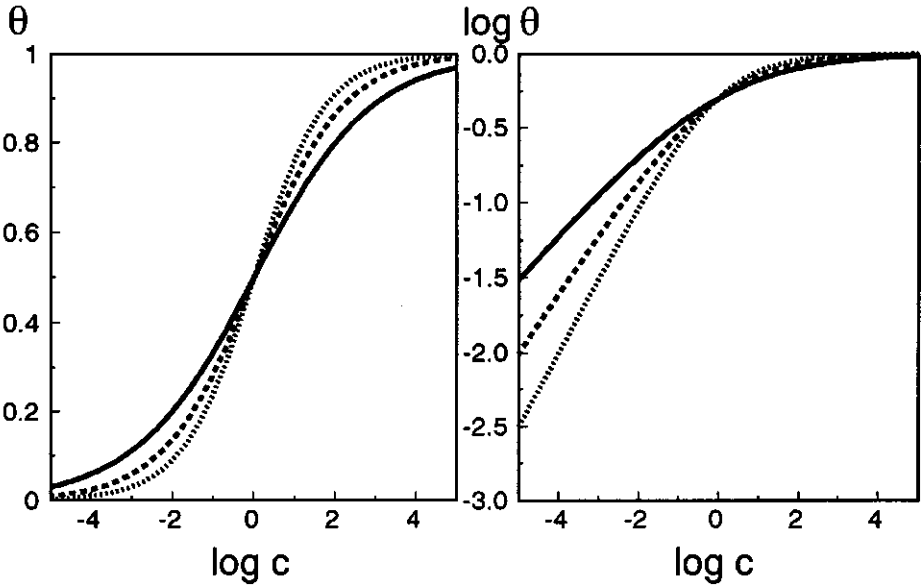**Figure 6.** The monocomponent binding curves as a function of log c_A in a lin-log and a log-log format for three values of the heterogeneity parameter m. log $\tilde{K}$=0——— m=0.3, ------------ m=0.4, ·················· m=0.5.

Concluding Remarks

- Surface heterogeneity may strongly influence metal ion and proton binding. Since in general the affinity distribution for a certain type of ion will be characterized by its own shape, its own mean affinity constant and its own width, it seems logical to take these differences explicitly into account in modelling ion binding. The presented analytical multi-component binding equations to heterogeneous ligands allow in principle to do this.

- For every component considered the derived equation based on non-congruent distributions has one extra parameter compared to the heterogeneous multicomponent binding equation in which it is assumed that all distributions are congruent. The major problem in the application of the derived equations to experimental data is the determination of the width p of the common distribution. The value of p can only be assessed on the basis of the binding data for multicomponent systems.

- The examples for the two component system showed that a different heterogeneity for different components can have profound and intriguing effects on the binding of those component and on the competition. To our opinion the obtained equations provide a basis for a description of multi-component competitive binding to natural colloids and may help to understand the competitive nature of the differences in binding behaviour between different metal ions.

Acknowledgement

References

1.   Buffle, J. *Complexation Reactions in Aquatic Systems: An Analytical Approach*; Ellis Horwood Limited: Chichester, 1988.

2.   Van Riemsdijk, W.H.; Koopal, L.K. In *Environmental Particles*; Buffle, J.; Van Leeuwen, H.P. Lewis Publishers: Chelsea, Michigan, 1992, Chapter 12.

3.   Sips, R. *J. Chem. Phys.* **1948**, *16*, 490.

4.   Sips, R. *J. Chem. Phys.* **1950**, *18*, 1024.

5.   Tóth, J.; Rudziňsky, W.; Waksmundsku, A.; Jaroniec, M.; Sokolowsky, S. *Acta Chim. Hungar.* **1974**, *82*, 11.

6.   Jaroniec, M.; Madey, R. *Physical Adsorption on Heterogeneous Solids*, Elsevier: Amsterdam, 1988.

7.   Jaroniec, M. *Adv. Colloid Interface Sci.* **1983**, *18*, 149-225.

8.   Van Riemsdijk W.H., G.H. Bolt, L.K. Koopal and J. Blaakmeer, 1986, J. Colloid Interface Sci. 109:219-228.

9.   Van Riemsdijk, W.H., J.C.M. de Wit, L.K. Koopal and G.H. Bolt, 1986, J. Colloid Interface Sci. 116:511-522.

10.   Kinniburgh, D.G. *J. Soil Sci.* **1983**, *34*, 759-769.

Chapter 8

Analytical Isotherm Equations for Multicomponent Adsorption to Heterogeneous Surfaces.

Part II. Consecutive Reactions.

Abstract

In this paper analytical expressions are presented that allow to take into account the effect of the chemical hetereogeneous nature of a ligand in the description of consecutive binding reactions. Features of the derived expressions are illustrated with calculations for a two step protonation reaction of a heterogeneous ligand. A discussion of this 2pK model to describe the protonation of naturally occurring ligands such as hydrous oxides and humic substances is given.

210

Introduction

Naturally occurring ligands are often chemically heterogeneous, which complicates the description of the adsorption behaviour. In general the binding to hetereogeneous ligands is given by complex expressions that can only be solved numerically. Fortunately for specific conditions three analytical solutions are known. These adsorption equations are the Langmuir Freundlich (LF) equation (1), the Generalized Freundlich equation (2) and the Tóth equation (3).

All three adsorption equations are originally derived for mono-component adsorption. The analytical equations for mono-component adsorption can be extended to multi-component adsorption under the assumption that the shape of the affinity distribution for different components is identical (4-7). Unfortunately the assumption that all components must confirm to one identically shaped distribution is not very satisfactory nor very realistic.

In a previous paper we have presented an approach that combines the advantage of analytical binding equations with a more realistic variation in distribution functions (8). In that approach a multicomponent LF isotherm expression was obtained under the assumption that the different monocomponent LF distributions can be rescaled to one identically shaped LF distribution by using a mathematical transformation.

In this paper analytical expressions will be derived for cases that the multi-component binding process can be described as a set of consecutive binding or exchange reactions, and that every consecutive reaction may be characterized by a certain heterogeneity. In principle the type of heterogeneity may differ from one step of the consecutive reactions to another. Although analytical expressions can be derived for all three equations or for combinations of them, we will only give a derivation on the basis of the Langmuir Freundlich equation. The features of the derived expressions will be illustrated on the basis of model calculations for heterogeneous ligands that protonate in two consecutive steps. This is followed by a discussion of the prospects of the derived model to describe the protonation of naturally occurring ligands such as (hydrous) oxides

and humic substances.

Theory

In this section we will derive a general expression for the following type of consecutive reactions occurring at a heterogeneous ligand:

$$S+A \rightleftharpoons SA \qquad (1)$$

$$SA+B \rightleftharpoons SAB \qquad (2)$$

For a homogeneous ligand, in the absence of lateral interactions, each of these equations is characterized by a single affinity constant for instance K_1 for equation (1) and K_2 for equation (2).

The combination of Eqs. (1) and (2) results in the equation:

$$S+A+B \rightleftharpoons SAB \qquad (3)$$
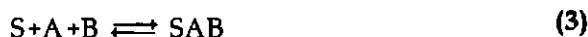
with, for a homogeneous ligand, an overall affinity constant equal to the product of K_1 and K_2.

For a heterogeneous ligand the binding to each site type is given by a homogeneous binding equation, the local binding equation. The total binding is given by a weighted summation of the local contributions and, as a consequence, for a heterogeneous ligand the affinity is no longer given by a single affinity constant but by a distribution of affinity constants. In this paper we assume that (1) the affinity distributions are continuous, (2) the distribution of K_1 for Eq. (1) and K_2 for Eq. (2) are independent and (3) both distributions are given by Langmuir Freundlich distributions. In view of the independence, the width and the mean log K value for the affinity distributions may be different.

The overall binding equation for the formation of SAB, given by Eq. (3), is influenced by the distributions of both K_1 and K_2. So if S is the reference species onto which binding occurs, the distribution of K_1 influences both the formation of the SA and the SAB species, while the distribution of

K_2 influences only the formation of the SAB species.

Let's first concentrate on the way the distribution of K_2 influences the adsorption. For a certain site type, present at the heterogeneous ligand, characterized by a certain K_1 and K_2 we can define a fraction $\theta'_{L,SAB}$:

$$\left[\quad \theta'_{L,SAB} \equiv \frac{\{SAB\}}{\{SA\}+\{SAB\}} \quad \right]_{K_1} \tag{4}$$

where the subscript K_1 and the subscript L (from local) indicate respectively that the expression holds for sites with a certain K_1 and a certain K_2.

Note that the fraction defined by Eq. (4) does not equal the fraction of SAB species of one sites type relative to all sites, since the reference species S is not taken into account in the denominator.

Equation (4) can be combined with the expression for the equilibrium constants related to Eq. (2), which results in a Langmuir type of local binding equation:

$$\left[\quad \theta'_{L,SAB} = \frac{K_2 B}{1+K_2 B} \quad \right]_{K_1} \tag{5}$$

where B is the concentration of B (or a related quantity).

Although a particular site type is of course characterized by a particular value of K_1 and K_2, Eq. (5) shows that the defined fraction does only depend on K_2.

The total fraction of the SAB species with respect to the sum of the SAB and the SA species for all sites with the same K_1, but a different K_2 can be defined by:

$$\theta'_{t,SAB} \equiv \frac{\{SAB\}_{T,K_1}}{\{SA\}_{T,K_1}+\{SAB\}_{T,K_1}} \tag{6}$$

An expression for $\theta'_{t,SAB}$ can be obtained by integrating Eq. (5) over the

213

affinity distribution of $\log K_2$, $f(\log K_2)$:

$$\theta'_{t,SAB} = \left[\int_{\Delta \log K_2} \theta'_{L,SAB} f(\log K_2) d \log K_2 \right]_{K_1} \tag{7}$$

Integration with the LF affinity distribution and Eq. (5) as the local isotherm gives:

$$\left[\theta'_{t,SAB} = \frac{\left(\bar{K}_2 B\right)^{m_2}}{1 + \left(\bar{K}_2 B\right)^{m_2}} \right]_{K_1} \tag{8a}$$

This equation is a monocomponent Langmuir Freundlich equation, with m_2 as the width of the LF distribution and $\log \bar{K}_2$ as its median $\log K$ value.

The fraction $\theta'_{t,SAB}$ is defined for sites with a certain K_1. A corresponding fraction, expressing the overall fraction of the SAB species relative to the SA plus the SAB species for all sites, is given by a weighted summation of the $\theta'_{t,SAB}$ for all K_1.

Under the assumption that the distribution of K_2 is the same for every site type, irrespective the value of K_1, the weighted summation of $\theta'_{t,SAB}$ is identical to $\theta'_{t,SAB}$ for a group of sites with a certain K_1. As a consequence Eq. (8) does not only hold for a certain group of sites, but also for the entire surface, and we may write Eq. (8a) also as:

$$\theta'_{t,SAB} = \frac{\left(\bar{K}_2 B\right)^{m_2}}{1 + \left(\bar{K}_2 B\right)^{m_2}} \tag{8b}$$

From the combination of the Eqs. (6) and (8) an expression for $\{SAB\}_{T,K_1}$ as a function of $\{SA\}_{T,K_1}$ for all sites characterized by the same K_1:

$$\{SAB\}_{T,K_1} = \left(\bar{K}_2 B\right)^{m_2} \{SA\}_{T,K_1} \tag{9}$$

With the help of Eq. (8) an expression can be obtained for the

214

fraction of the sites with a certain K_1 which are not in the reference state S, $\theta_{L,SA+SAB}$:

$$\theta_{L,SA+SAB} = \frac{\{SA\}_{T,K_1} + \{SAB\}_{T,K_1}}{\{S\}_{T,K_1} + \{SA\}_{T,K_1} + \{SAB\}_{T,K_1}} = \frac{\{SA\}_{T,K_1} + (\bar{K}_2 B)^{m_2}\{SA\}_{T,K_1}}{\{S\}_{T,K_1} + \{SA\}_{T,K_1} + (K_2 B)^{m_2}\{SA\}_{T,K_1}} \quad (10)$$

Note that in this case the subscript L indicates that Eq. (10) does only hold for sites with a certain K_1.

With the help of the expression for the equilibrium constant K_1 for Eq. (1), Equation (10) can be rearranged to:

$$\theta_{L,SA+SAB} = \frac{K_1 X}{1 + K_1 X} \quad (11)$$

where

$$X = A\left[1 + (\bar{K}_2 B)^{m_2}\right] \quad (12)$$

Eq. (11) is mathematically identical to the Langmuir equation and can be seen as a pseudo homogeneous local isotherm equation. If we assume that the distribution of K_2 is the same irrespective the value of K_1, the fraction of all sites which are not in the reference state S, $\theta_{t,SA+SAB}$ is given by the following integral equation:

$$\theta_{t,SA+SAB} = \int_{\Delta \log K_1} \theta_{L,SA+SAB} f(\log K_1) d\log K_1 \quad (13)$$

For the LF distribution, the integration of Eq. (13) results in the following LF type of equation:

$$\theta_{t,SA+SAB} = \frac{(\bar{K}_1 X)^{m_1}}{1 + (\bar{K}_1 X)^{m_1}} \quad (14)$$

where $\log \bar{K}_1$ is the median of the log K_1 affinity distribution and m_1 is its

215

width.

The fraction of the SAB species relative to all sites, $\theta_{t,SAB}$ is given by the product of Eq.(8) and Eq.(14):

$$\theta_{t,SAB}=\theta'_{t,SAB}\theta_{t,SA+SB} \tag{15}$$

which is a product of two LF equations. The fraction of the SA species relative to all sites, $\theta_{t,SA}$, is given by:

$$\theta_{t,SA}=\left(1-\theta'_{t,SAB}\right)\theta_{t,SA+SAB} \tag{16}$$

and the fraction of the reference species, $\theta_{t,ref}$ by:

$$\theta_{t,ref}=1-\theta_{t,SA+SAB} \tag{17}$$

The procedure of defining pseudo homogeneous local isotherms, such as Eqs (5) and (10), followed by integration over the distribution function is not restricted to two reactions, it can also be used for a series of consecutive binding reactions.

A 2 pK Model for the Protonation of Heterogeneous Ligands

The protonation of a ligand in a 2 pK model is described as a two step protonation of a surface species S^z:

$$S^z+H^+ \rightleftharpoons SH^{z+1} \tag{18}$$

$$SH^{z+1}+H^+ \rightleftharpoons SH_2^{z+2} \tag{19}$$

with z the charge number of the chosen reference species S.

The total proton binding to the polyfunctional ligand, Γ_H, is given by:

$$\Gamma_H = N_S(\theta_{T,1} + 2\theta_{T,2}) \tag{20}$$

where θ_1 corresponds with the total fraction of SH^{z+1} species, θ_2 corresponds with the total fraction of the SH_2^{z+2} species and N_S is the total site density.

If we work out the appropriate expressions for $\theta_{T,1}$ and $\theta_{T,2}$ following the procedure given in the previous section, the next expression for Γ_H is obtained:

$$\Gamma_H = N_S \cdot \frac{1 + 2\left(\tilde{K}_2 H\right)^{m_2}}{1 + \left(\tilde{K}_2 H\right)^{m_2}} \cdot \frac{\left(\tilde{K}_1 H \left[1 + \left(\tilde{K}_2 H\right)^{m_2}\right]\right)^{m_1}}{1 + \left(\tilde{K}_1 H \left[1 + \left(\tilde{K}_2 H\right)^{m_2}\right]\right)^{m_1}} \tag{21}$$

where $\log \tilde{K}_1$ and m_1 are respectively the mean value and the width of the distributions of the first protonation reaction, and $\log \tilde{K}_2$ and m_2 are the mean value and the width for the second protonation reaction. Lateral interactions can be taken into account in Eq (21) by considering H as the product of the proton concentration in solution and a factor which accounts for the interactions. We will illustrate the effect of heterogeneity on the binding behaviour using some example calculations, neglecting lateral interactions. In that case H is simply the proton concentration.

For sake of comparison, we consider first a homogeneous colloid ($m_1=m_2=1$). In fig. 1a the protonation of a homogeneous colloid with log $K_1=8$ and log $K_2=4$ and $N_S=1$ is given. The curve clearly shows 2 consecutive protonation steps, and is identical to the protonation curve of a simple diprotic ligand such as phthalic acid. The dotted line in fig. 1a shows the fraction of the SH species, θ_1, as a function of the pH. At pH>10 the surface is fully deprotonated and $\theta_1=0$. At lower pH value reaction (18) will start to become important and θ_1 will increase. At pH=6 all sites bind one proton and $\theta_1=1$. The second reaction starts to become significant at pH<6. Due to this reaction θ_1 decreases and the fraction of the SH_2^{z+2} species, θ_2 increases.

217

Figure 1. (a) the proton binding $\Gamma_H(pH)$ and (b) its first derivative $f'(pH)$ for a homogeneous colloid according to the two pK model (eg. Eq. 20). $\log \bar{K}_1=8$, $\log \bar{K}_2=4$, $m_1=m_2=1$.

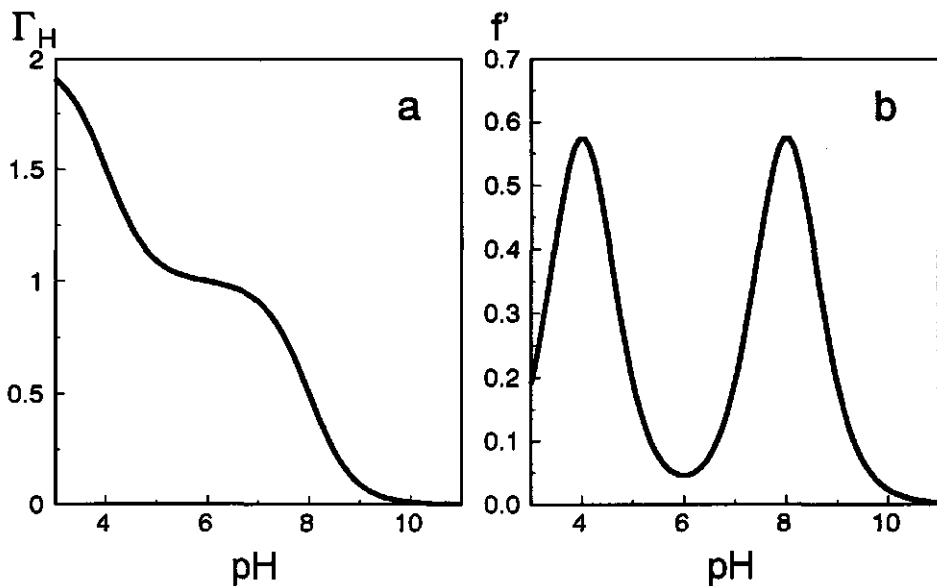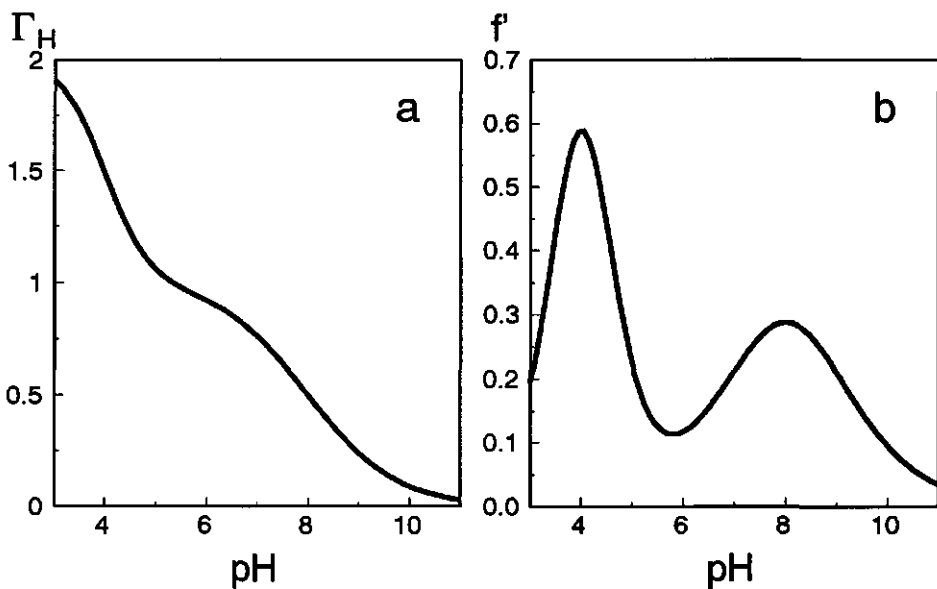Figure 2. (a) the proton binding $\Gamma_H(pH)$ and (b) its first derivative $f'(pH)$ for a heterogeneous colloid according to the two pK model (eg. Eq. 20). $\log \bar{K}_1=8$, $\log \bar{K}_2=4$, $m_1=0.5$, $m_2=1$.

In figure 1b the first derivative of the $\Gamma_H(pH)$ curve with respect to pH of fig 1a is plotted as function of the pH. This derivative can be interpreted as an approximation of the affinity distribution using the condensation approximation (8-9). The pH scale in that case can be interpreted as a log K scale. For wide distributions the condensation approximation and the true distribution correspond very well. For rather homogeneous surfaces with narrow distributions the CA approximation is poor, and results in a considerable broadening of the peaks. For the homogeneous ligand of fig. 1a, the true affinity distribution should show two discrete spikes located at log K_H=4 and 8. The CA distribution shows much wider peaks. Nevertheless the position of the peaks on the pH or log K_{CA} axis correspond to the intrinsic values.

In fig 2 the binding and the first derivative are given for the case that only the first protonation constant is distributed, while the second protonation constant is not distributed. A consequence of heterogeneity is the presence of a certain number of high affinity sites and of low affinity sites. The high affinity sites do already protonate at high pH whereas the low affinity sites do not protonate until the pH is rather low. The more heterogeneous the surface is, the higher is the pH for which a considerable protonation of the surface occurs, and the lower the pH for which the surface becomes fully protonated. As a consequence, the larger the heterogeneity is, the lower is the slope of the binding curve. The heterogeneity of the first protonation step makes the slope of the proton binding curve at high pH smaller, and the distribution around pH=8 wider.

The heterogeneity of the first protonation step does not influence the second protonation step; both the binding curve at low pH and the peak at pH=4 are the same as for the homogeneous case. For the parameters chosen, the second protonation step starts when the first protonation step is almost fully elapsed. At the pH values where the second protonation step starts, the second fraction of the RHS of Eq. (21) is already very close to one and the second protonation step is fully determined by the first fraction of the RHS. Because m_2=1, this fraction is identical to the expression for the homogeneous ligand.

If $m_1 \neq 1$ and $m_2 \neq 1$, both protonation steps will be influenced by the heterogeneity. In figure 3 and 4 two examples for of such systems are given. In fig. 3 the protonation and the corresponding CA affinity distribution is given for $m_1 = m_2 = 0.5$ in fig. 4 for $m_1 = 0.3$ and $m_2 = 0.5$. In both cases $\log \tilde{K}_1 = 4$ and $\log \tilde{K}_2 = 8$.

The heterogeneity results in protonation curves that are very smooth, and have a small slope. Both the distributions in figs 3b and 4b shows two wide peaks, with the peak positions at $pH = \log \tilde{K}_i$. Because $m_1 = m_2$ the distribution curve of fig 3b is symmetrical. The distribution of fig 4b shows an asymmetrical distribution that corresponds to the different m_1 and m_2 used in the example.

Amphoteric Hydrous Oxides

Although a description on the basis of the simple so called "one pK model" may be preferred on theoretical grounds (11-14) and results to a very good description of the amphoteric behaviour of hydrous oxides, many authors use the more classical homogeneous 2 pK model (15-19). In this 2 pK model $z = -1$ and $n = 0$. The curves given in figure 1 give an example of such a model, neglecting the electrostatic effects.

Although many authors have mentioned the chemical heterogeneous nature of oxides only Van Riemsdijk et al (6-7) have considered a heterogeneous 2pK model. In their approach only the constant for the first protonation equation was distributed ($m_1 \neq 1$) while the second step was not distributed ($m_2 = 1$). Calculation for this case were shown in fig. 2. A consequence of using $m_2 = 1$ is that the overall proton affinity distribution is asymmetrical. It is a combination of the broad peak for the first protonation step and the spike of the second. For oxides heterogeneous 2 pK models in which the constants for both steps are assumed to be distributed (eg. figs. 3 and 4) have not yet been considered.

For the curves presented in figs. 1-4 the difference in $\log K_1$ and $\log K_2$ was 4 log K units. For many oxides the difference is smaller than 4 log K units. When the difference becomes smaller than 2 log K units

Figure 3. (a) the proton binding $\Gamma_H(pH)$ and (b) its first derivative $f'(pH)$ for a heterogeneous colloid according to the two pK model (eg. Eq. 20). $\log \tilde{K}_1=8$, $\log \tilde{K}_2=4$, $m_1=0.5$, $m_2=0.5$

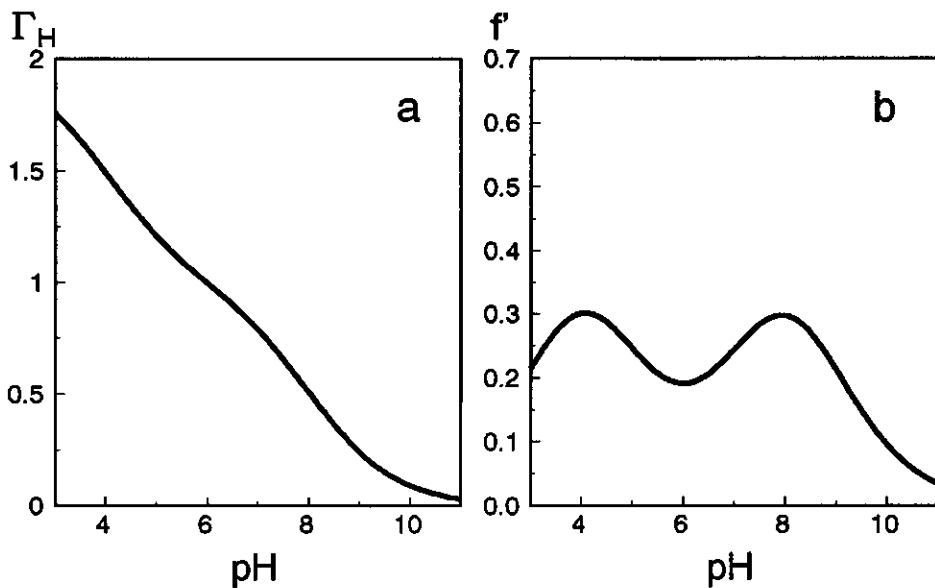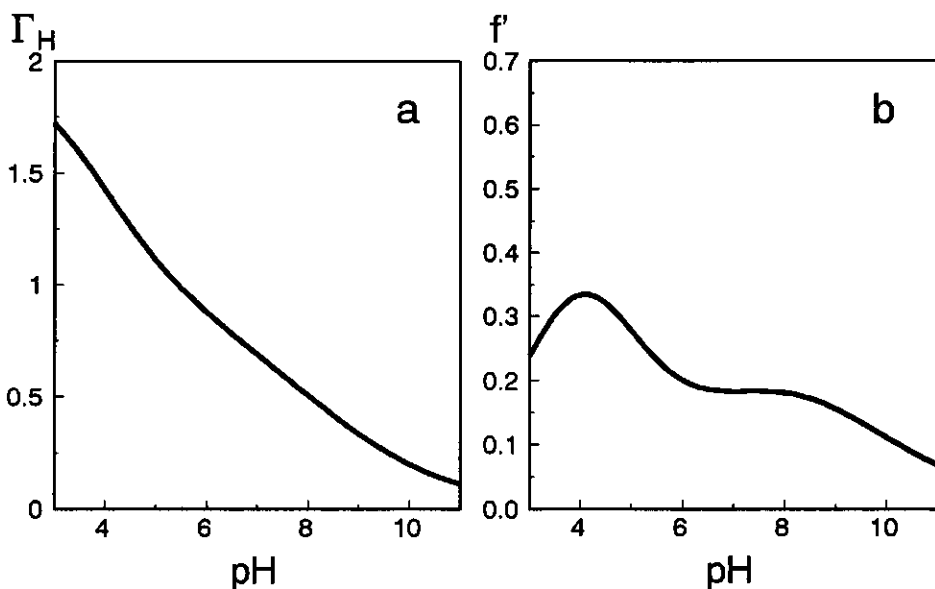**Figure 4.** (a) the proton binding $\Gamma_H(pH)$ and (b) its first derivative $f'(pH)$ for a heterogeneous colloid according to the two pK model (eg. Eq. 20). $\log \tilde{K}_1=8$, $\log \tilde{K}_2=4$, $m_1=0.3$, $m_2=.5$

221

reaction (19) will already start while reaction (18) is not yet fully elapsed.

The formulation of the binding equations is only one part of the models that describe the protonation of oxides. Since oxides are variably charged colloids, the binding equations are combined with a double layer model that accounts for the electrostatic effects. Due to the pronounced electrostatic effects only a small number of the sites are titrated upon charging (often no more then 20 %), and only a small part of the binding curve can be established on the basis of titration data. This fact makes that a homogeneous model can describe the proton binding. The incorporation of heterogeneity does in general not result to a better description.

Humic Substances

Humic substances are naturally occurring heterogeneous organic ligands which have a pH dependent negative charge (19-24). Humic substances are non Nernstian. The electrostatic effects are distinct but much smaller than for oxides, which makes that upon charging a large fraction of the total number of sites are titrated and that the intrinsic heterogeneity can be clearly observed in the binding curves.

The intrinsic proton affinity distribution of the humic substances is characterized by a large broad peak with its peak position in the log K range 3 to 4, and by a second broad peak with a peak position at $\log K_H > 8$ (25-29). De Wit et al (29) assumed that the two peaks are two different classes of sites. The sites of each class were assumed to protonate in one step and for the distribution of the protonation constants two Langmuir Freundlich distributions were used. With these assumptions experimental proton binding curves could be described well by a weighted summation of two Langmuir Freundlich equations, in combination with a double layer model to account for the electrostatic effects.

Since a 2 pK model results in a bimodal affinity distribution (figs 1-4), a two step protonation according to Eqs. (18) and (19) with z=-2 is an alternative description of the observed proton binding. Such a 2 pK model for humic substances is physically realistic when most of the sites are

present in coordinated structures like for instance in phthalic acid and salicylic acid. Structures which are believed to play an important role in the binding of metals ions by humic substances (19-25).

The extension of the 2 pK model to describe metal ion binding can be made by specifying a metal ion binding equation, for instance the formation of the SM species from the S^{2-} species. The chemical heterogeneity for the metal binding can for instance be described by using analytical expression for non congruent affinity distributions as derived by De Wit et al (8) in combination with the heterogeneous 2pK model. This model may provide a sound basis for a description of competitive metal ion binding to humic substances.

Concluding Remarks

-    Ion binding to heterogeneous colloids is of complex nature. The derived analytical binding equations for consecutive binding are relatively simple and flexible and are more realistic than the heterogeneous binding equations that have been used before.

-    The multicomponent binding equations are essentially products of Langmuir Freundlich type of equations. For every consecutive binding step two parameters have to be specified: the mean log K value, which determines the location of the affinity distribution on the log K axis and a parameter which determines the width of the distribution, or the degree of heterogeneity.

-    The derived 2 pK model for the protonation of heterogeneous ligands may be of interest for the description of proton binding to natural heterogeneous colloids like humic and fulvic acids.

Acknowledgement

References

1.   Sips, R. *J. Chem. Phys.* **1948**, *16*, 490.

2.   Sips, R. *J. Chem. Phys.* **1950**, *18*, 1024.

3.   Tóth, J.; Rudziński, W.; Waksmundsku, A.; Jaroniec, M.; Sokolowsky, S. *Acta Chim. Hungar.* **1974**, *82*,11.

4.   Jaroniec, M.; Madey, R. *Physical Adsorption on Heterogeneous Solids*, Elsevier: Amsterdam, 1988.

5.   Jaroniec, M. *Adv. Colloid Interface Sci.* **1983**, *18*, 149-225.

6.   Van Riemsdijk W.H., G.H. Bolt, L.K. Koopal and J. Blaakmeer, 1986, J. Colloid Interface Sci. 109:219-228.

7.   Van Riemsdijk, W.H., J.C.M. de Wit, L.K. Koopal and G.H. Bolt, 1986, J. Colloid Interface Sci. 116:511-522.

8.   De Wit, J.C.M.; Van Riemsdijk, W.H.; Koopal, L.K.; *Analytical Isotherms Equations for Multicomponent Adsorption Surfaces*, submitted to *J. Colloid Interface Sci.*.

9.   Nederlof, M.M.; Van Riemsdijk, W.H.; Koopal, L.K.; *J. Colloid Interface Sci.* **1990**, *135*, 410-426.

10.   Nederlof, M.M., Van Riemsdijk, W.H.; Koopal, L.K.; *Environ. Sci. Technol.* **1992**, *26*, 763-771.

11.   Hiemstra, T.; Van Riemsdijk, W.H.; Bolt, G.H. *J.Colloid Interface Sci.* **1989**, *133*, 91-104.

12.   Hiemstra, T.; Van Riemsdijk, W.H.; De Wit, J.C.M. *J.Colloid Interface Sci.* **1989**, *133*, 105-117.

13.   Hiemstra, T.; Van Riemsdijk, W.H.; Bolt, G.H. *Colloid Surf.* **1991**, *59*, 7-25.

14.   Van Riemsdijk, W.H.; Koopal, L.K. In *Environmental Particles*; Buffle, J.; Van Leeuwen, H.P. Lewis Publishers: Chelsea, Michigan, 1992, Chapter 12.

15.   Hohl, H.; Stumm, W. *J. Colloid Interface Sci.* **1976**, *55*, 281.

16.   Westall, J.; Hohl, H.; *Adv. Colloid Interface Sci.* **1980**, *12*, 265.

17.   James, R.O.; Parks, G.A. In: Matijevic, E. (Ed.) *Surface and Colloid Science. Vol 12.*, Plenum: New York, 1982, p. 119.

18.   Dzombak, D.A.; Morel, F.M.M. *Surface Complexation Modelling. Hydrous Ferric Oxide.* Wiley: New York, 1990.

19.   Stevenson, F.J., *Humus Chemistry. Genesis, Composition, Reactions*; Wiley Interscience: New York, 1982.

20.   Buffle, J. In *Metal Ions in Biological Systems*. Vol 18. Dekker: New York, 1984, Ch. 6.

21.   Aiken, G.R., D.M. McKnight, R.L.Wershaw and P. MacCarthy (Eds.) *Humic Substances in Soil, Sediment, and Water*; Wiley Interscience: New York, 1985

22.   Sposito, G., *CRC Crit. Rev. Environ. Control* **1986**, *16*, 193-229.

23.   Buffle, J. *Complexation Reactions in Aquatic Systems: An Analytical Approach*; Ellis Horwood Limited: Chichester, 1988.

24.   Hayes, M.H.B.; MacCarthy, P.; Malcolm, R.L.; Swift, R.S. (Eds.), *Humic Substances II: In Search of Structure*; Wiley Interscience: New York, 1989.

25.   De Wit, J.C.M.; Van Riemsdijk, W.H.; Nederlof, M.M.; Kinniburgh, D.G.; Koopal, L.K. *Analytica Chim. Acta* **1990**, *232*, 189-207.

26.   De Wit, J.C.M.; Nederlof, M.M.; Van Riemsdijk, W.H.; Koopal, L.K. *Water, Air and Soil Pollution* **1991**, *57-58*, 339-349.

27.   De Wit, J.C.M.; Van Riemsdijk, W.H.; and Koopal, L.K.; *Finnish Humus News* **1991**, *3*, 139-144.

28.   De Wit, J.C.M., W.H. Van Riemsdijk and L.K. Koopal, *Proton Binding to Humic Substances. A. Electrostatic Effects*. Submitted to *Environ Sci. Technol.*

29.   De Wit, J.C.M., W.H. Van Riemsdijk and L.K. Koopal, *Proton Binding to Humic Substances. B. Chemical Heterogeneity and Adsorption Models*. Submitted to *Environ Sci. Technol.*

225

Summary

Humic substances are polydisperse mixtures of organic molecules which, at least to some extent, determine the mobility and bio-availability of heavy metals in soils, sediments and aquatic ecosystems. In order to be able to make a sound risk assessment of the fate of trace metals a good conception and preferably a sound model description of the metal ion binding to humics is essential, but not yet realized. This observation was the motive for the research presented in this thesis.

Metal ions are believed to bind to the functional groups of humic substances. Important functional groups are carboxylic groups and phenolic groups. Each type of functional group will have its own affinity constant, which value depends on the type of functional groups and on its direct chemical environment in the organic molecule. Due to the complex structure of humic substances there is a large variation in different classes of functional groups and, as a consequence, humic substances are heterogeneous ligands. The chemical heterogeneity makes that ion binding to humics is not characterized by a single affinity constant, but by a whole distribution of affinity constants. Unfortunately the affinity distribution for humic substances is a priori unknown. Spectroscopic techniques can be helpful to quantify the total number of certain types of functional groups present in the organic molecules, at present, however, these techniques do not allow for the determination of the chemical affinity distribution.

The state of the functional groups is strongly determined by the pH. The pH determines the dissociation of the functional groups and mainly controls the negative charge of the humic substance. Below pH=2 the functional groups are almost fully protonated, and the negative charge of the humic substance is low. Under natural conditions the pH is always larger than 2 and a considerable fraction of the functional groups is dissociated and the humics have a negative pH dependent charge. Due to the attraction by the electric field around the negative humic particles, the concentration of metal ions near the functional groups is increased which promotes metal ion binding. The magnitude of the attraction is determined by the strength of the electric field or the electric potential. In general, the strength of the electric field of humic substances is unknown and cannot be obtained directly from experimental results.

229

Because the chemical heterogeneity, the pH and the electrostatic effects strongly influence metal ion binding it is essential to characterize humic substance with respect to these factors and to understand first the proton binding behaviour, in absence of metal ions. In order to do this we have developed the so called master curve procedure, which is presented in the chapters 2-4 of this thesis. These chapters are preceded by an introductive first chapter in which the geochemistry and the properties of humic substances are discussed in a broader perspective.

The master curve procedure is essentially an analysis of a set of proton binding curves expressed as charge versus pH measured at different, but constant ionic strength. It is a general procedure which is not restricted to humic substances only, it can in principle be used to analyze proton binding data for many different systems such as, for instance, hydrous oxides, latices, and even bacteria and plant roots.

In absence of other specifically binding ions, proton binding is a monocomponent process. The protonation of the humic substances is determined by the chemical heterogeneity and by the pH near the functional groups at the location of binding, pH_s. The pH_s depends on the pH in the bulk solution and on the electric potential at the location of binding. This potential depend on the charge Q of the humics, on the properties of the humic particles like geometry, rigidity and permeability and on the ionic strength and the type of electrolyte. At a high ionic strength the concentration of the electrolyte ions is large and the electric field can be screened effectively. The electrostatic effects are then rather small and the double layer, i.e. the layer in which the concentration of the ions differs from that in the bulk due to the electric field of the humics, is thin. The opposite holds at a low ionic strength. In that case the electrostatic effects are large and the double layer is relatively thick. The ionic strength dependency of the electrostatic interactions results in an ionic strength dependency of the proton binding curves.

As the electric potential is not experimentally accessible we have to rely on double layer models to calculate the potential. In the master curve procedure double layer models can be used that allow for the calculation of

the electric potential from the charge Q and the ionic strength without making assumptions on the chemical heterogeneity.

With the help of the double layer model pH_s can be calculated and the experimental data can be replotted as a function of this pH at the location of binding. Because in pH_s we have accounted for the electrostatics and, hence, for the ionic strength effects, the $Q(pH_s)$ curve should merge into one single master curve. When there remains a considerable salt effect in the $Q(pH_s)$ curves the double layer model is not appropriate and should be adjusted.

For 11 different humic substances the ionic strength dependency of the proton binding curves could be described well by using a spherical or a cylindrical double layer model. In both double layer models humic substances were treated as rigid and impermeable particles all characterized by the same radius. The radius determines the curvature of the surface, which influences the strength of the electric field. The larger the radius the smaller the curvature, but the larger the electrostatic effects.

The double layer models used relate the potential to the charge per particle expressed per unit surface area. The experimental charge, is measured as a function of the charge per unit mass. For the conversion of the experimental quantities to charge per surface area, the specific surface area is needed. For spheres and cylinders the specific surface area is related to the density of the humics and the radius of the particles. When humics are considered to be rigid impermeable particles it seems logical to assume that the water content of the humic particle is limited. We consider the case that water makes up 50 % of the volume of the humic particle an upper limit. Under this constraint the density expressed as unit mass of the *dry* material per hydrated volume of the humic particles ranges from 700-1700 kg/m³. Because the master curves obtained for this density range do only differ slightly, we use a density of 1000 kg/m³ as a convenient value. In that case the radius is the single adjustable parameter in the master curve procedure.

For the spherical double layer model the optimal radius for the 11 different humic substances ranges from 0.6 to 4.4 with r=0.85 nm as the median value. The size and volume of a sphere is fully determined by its radius. From the combination of radius with the density the molecular weight

231

of the humics can be calculated. For the humics samples analyzed this *electrostatic* molecular weight ranges from 545 to 215000 with a median value of 1550. The obtained values are not irrealistic, but are in most cases somewhat lower than the values obtained with other techniques.

The size of a cylinder is determined by both its radius and length. In the electrostatic model the end effects of the cylinder are neglected, and only the radius is the parameter that determines the electrostatic interactions. In principle in the cylindrical double layer model the length may differ strongly for one particle to another and we do not have to assume that the particles are equally sized. This is an advantage of the cylindrical model over the spherical model.

The obtained optimal values of the cylinder radius ranges from 0.19 to 2.5 with r=0.32 nm as the median value. These values are significantly smaller than the radii for the spherical model, which is due to the more strongly curved surface of a sphere than that of a cylinder. For identical radii the smaller curvature of the cylinder makes that the electrostatic effects for the cylinder are larger than that of the sphere. Since the electrostatic effects are fixed by the experiment, the radius of the cylinder should be smaller than that of sphere in order to obtain the same electrostatic effects.

The dimensions obtained from the double layer model indicate that purified humic substances of originating from aquatic systems, are small molecules, with a limited number of functional groups. They should be considered oligo electrolytes rather than poly electrolytes. On the basis of the proton titration data only, no preference for the cylindrical or the spherical model could be obtained. The cylindrical model does fit somewhat better with the picture of a chain molecule which is supported by many research groups. The spherical model allows for the assessment of a molecular weight.

Since humic substances are poly disperse mixtures of different organic compounds the treatment of humic substances as impermeable and rigid particles with a simple geometry, characterized by one average radius seems crude. Nevertheless this first order approach results in a surprisingly good description of the ionic strength dependency of the proton binding. Polydispersity and other effects like changes of the conformation of the humic

particles and aggregation seem to be of second order in relation to the proton binding behaviour of humics.

Because the electrostatic effects are filtered, the shape of the $Q(pH_s)$ curves is directly related to the chemical heterogeneity or to the affinity distribution. Several techniques are available to obtain the affinity distribution from binding curves. Each technique has its pros and contras and the technique to be used depends to a large extent on the quality of the experimental data. When a non optimal technique is used, the experimental errors will have a large effect on the obtained affinity distribution. A well suited and relatively simple method is the condensation approximation (CA) in combination with a recently developed smoothing spline technique. In this smoothing spline technique the smoothing parameter is selected using the generalised cross validation (GCV) technique in combination with some (physical) constraints. The GCV-smoothing spline procedure is used to obtain a representation of the most likely master curves through the $Q(pH_s)$ data points. The CA distribution is obtained by taking the first derivative of the spline representation of the data.

The obtained CA affinity distributions for humic substances are very similar. They are all characterized by a large and rather broad peak with a peak position in the log K range 3-4. In general, the peaks obtained for the spherical double layer model are somewhat smaller and their peak position is shifted to a slightly lower log K value than those for the cylindrical double layer model. The affinity distributions obtained for samples which were titrated over a large pH range up to pH 11 indicate the presence of a second broader peak with a peak position with log K>8.

The obtained affinity distributions are used to select a site binding model for the description of the proton binding. The affinity distribution show a continuous change of the affinity instead of a series of narrow nicely separate peaks. For this reason we prefer a description based on a continuous heterogeneity above that on a discrete heterogeneity.

There are only a few analytical binding equations for continuous heterogeneous ligands. Three of these equations are the Langmuir Freundlich (LF) equation, the Generalised Freundlich (GF) equation and the Tóth

233

equation. The affinity distributions underlying these equations are different. The LF distribution is a semi Gaussian symmetrical distribution. The GF distribution is an exponential distribution with a high affinity tail. The Tóth equation is asymmetrical and has a low affinity tail. All three distributions are characterized by only one peak. In the case the distributions show two peaks, a combination of two equations is used in the description of the data. Although the description of the $Q(pH_s)$ was fairly good for all three equations, the LF and the Tóth equation gave somewhat better results than the GF equation.

The combination of the assessed binding equation with the double layer model results in a model for the experimental proton binding data. Because we could describe both the electrostatic effects and the $Q(pH_s)$ rather well, it is not surprising that the combined model resulted in a good description of the experimental results.

In natural systems the proton is by definition present. Because protons bind specifically to the functional groups of the humic substances, metal ion binding to humics is at least a two component process. In order to describe competitive binding the stoichiometry of the metal ion binding must be established and assumptions have to be made about the relation between metal ion binding and the proton binding.

A sound model for metal ion binding should explicitly take into account the heterogeneous nature of the humics and the electrostatic effects, the model should have a small number of adjustable parameter and should be able to describe binding for a wide range of conditions with respect to pH and solution composition. Unfortunately it is not possible to derive the binding stoichiometry and the relation between the binding of different components fully from first principles. Therefore the choices that have to be made are always to some extent arbitrary. As a consequence many different model descriptions have been proposed, none of which yet can be considered as a unified model for metal ion binding to humic substances.

In our approach the description of the proton binding forms the basis for the model for the metal ion binding. In the proton binding model the electrostatic effects are taken into account by using a spherical or a cylindrical

double layer model and the chemical heterogeneity by using analytical binding equations for continuous heterogeneous ligands. The advantage of these type of equations is that they are characterized by only a few adjustable parameters, and account for the heterogeneity in a simple and elegant way. For the description of metal ion binding we have examined whether the proton binding model could be extended in a simple fashion. In this thesis we mainly use the Langmuir Freundlich equations in combination with the spherical double layer model, but the trends in the obtained results are also observed for the cylindrical double layer model and the Tóth or the GF equation. Like with the description of the proton data, the application of the LF and the Tóth equation give an almost equally good description. The description based on the GF equation is less good.

In order to describe metal ion binding we used an approximate binding stoichiometry in which upon the binding of one metal ion x protons are released in the solution. The parameter x may have a non integer value.

With respect to the relation between the proton and the metal ion binding we distinguish between uncoupled adsorption and fully coupled adsorption, which are two limiting cases. In the fully coupled model protons and metal ion compete for the same surface sites and have a congruent affinity distribution (i.e. the distributions have an identical shape but may have a different position on the log K axis). Under this constraint analytical expression for the multicomponent binding to continuous heterogeneous ligands are known that can be used to describe the binding.

In the uncoupled model there is no site competition, metal ions and protons each have their own type of binding sites. As a consequence metal ion binding can be described with a monocomponent binding equation for continuous heterogeneous ligands. The competition between protons and metal ion binding in the uncoupled model is determined by the magnitude of the average stoichiometry factor x and by electrostatic effects. Initially, in the absence of metal ions, the humics have a certain pH dependent negative charge. When the parameter x is smaller than the charge number of the metal ion, the binding of metal ion reduces the negative charge of the humics. This in turn will reduce the potential, which results in an extra release of protons

in addition to the x protons released according to the binding stoichiometry. The binding stoichiometry and the electrostatics play also an important role in the determination of the proton release in the fully coupled case. An extra factor is the release due to the site competition.

In chapter 5 the fully coupled model and the uncoupled model have been used for the description of cadmium binding to a purified humic substance extracted from a peaty soil. The cadmium binding was measured at three constant pH values and over up to 7 decades of cadmium concentrations.

In order to describe the cadmium binding over the whole cadmium concentration range with the fully coupled model, the presence of a small number of sites (around 1 %) has to be assumed which have a higher affinity for cadmium than the bulk of the sites. This group of sites determines the binding at the low concentration end of the cadmium concentration range. Although the concept of a small number of high affinity sites, which behave different from the bulk of the sites, is well accepted, it is not an elegant model concept since it results to a considerable increase in the number of adjustable parameters.

With the uncoupled model we were able to describe the pH dependent binding over the whole cadmium concentration range with only four parameters. These parameters are the stoichiometry parameter x, the total number of available metal ion binding sites, the median log K value and the width of affinity distribution underlying the binding equation. For the determination of the parameter x a master curve type of procedure has been developed. Because the protons and the metal ions bind to different type of functional groups the metal ion binding can be described by a monocomponent type of binding equation. If the uncoupled binding model with an average stoichiometry is appropriate, the metal ion binding curves for the different pH values should merge into a master curve when they are replotted as a function of M_s/H_s^x. M_s and H_s are respectively the metal ion and the proton concentration near the functional groups at the location of binding. These concentrations can be calculated when the potential is known, which follows from the charge of the humics and the double layer model.

236

The charge at a certain degree of metal ion binding can be calculated form the initial charge of the humics (in absence of metal ions), the degree of metal ion binding and the experimentally measured release of the protons. The remaining three parameters follow from fitting the binding equation to the master curve of metal ion binding.

In addition to protons, in natural and in polluted systems there are other ions present that bind specifically to humic substances and will influence the cadmium binding. One of these ions is calcium. In order to be able to analyze the effect of calcium on the cadmium binding the calcium binding to the humic substance should be understood first. In chapter 6 calcium binding data are presented for the humic acid extracted from a peaty soil. The same humic acid is used to study the cadmium binding as reported in chapter 5.

A comparison of the binding data shows that cadmium binds more strongly to the humic acid than calcium and that the pH dependency of the cadmium binding is larger. For the description of the calcium data we have used the uncoupled binding model only, and again this model gave a good description of the pH dependent binding for the whole calcium concentration range.

Calcium and cadmium ions have rather similar properties, it seems therefore logical to assume that both ions bind to the same type of sites. This picture is supported by the fitted parameters of the binding equations which are very similar. Moreover, a fairly good description of the calcium binding could be obtained when the maximum number sites and the width of the affinity distribution are chosen according to the values obtained for the cadmium binding. Hence, a model of the calcium and cadmium competition on the basis of a multicomponent binding equation for congruent affinity distributions is a logical first order approach.

The validity of the model for the competitive Ca-Cd binding could not yet tested on competitive binding data, as these data are not (yet) available for the investigated material. Instead, the model was used for some model calculations.

Even in many polluted situations cadmium is present at trace levels.

The calculations show that at trace level concentrations the cadmium binding at constant pH, both in absence and in presence of calcium, can be described by a simple Freundlich or even a linear binding equation. The parameters of these relations are, however, conditional, and depend on the conditions in a complicated way.

Although calcium binds less strongly then cadmium, the calcium concentration is, in general, several orders of magnitude higher then the cadmium concentration, which makes calcium a relatively strong competitor for the cadmium binding. Due to this competition the presence of 0.01 M $CaCl_2$ highly reduces the cadmium binding. Because the presence of chloride further promotes the desorption of cadmium by the formation of cadmium chloride complexes in solution, a solution of 0.01 M $CaCl_2$ is an effective extractant for cadmium adsorbed to humic material. The model calculations show further that the efficiency of this extractant is not constant, it depends on the condition of the system (pCd, pH, other electrolytes present). This illustrates that in soil systems the fraction that can be extracted with 0.01 M $CaCl_2$ is an operationally defined fraction. Although the extracted fraction may give an indication for the readily exchangeable fraction of metal ions, and thereby of their bio availability, the variable efficiency of the extraction makes a sound and mechanistic interpretation of the extracted fraction rather complicated.

The major part of soil organic matter belongs to the solid phase. A small fraction is dissolved in the soil solution. Binding to this dissolved organic matter complicates the interpretation of batch experiments in which the binding isotherm of a metal ion to the solid phase of the soil system is determined. In general, in batch experiments it is assumed that cadmium in the solution phase is present as the "free" cadmium ion and as inorganic complexes. The binding to the dissolved organic matter is neglected and the "free" cadmium concentration in the solution phase is calculated with simple chemical equilibrium calculations. The derived competitive binding model provides a good basis to estimate the magnitude of the error in the calculated free cadmium concentration due to neglect of the binding to the dissolved organic matter. The model predicts that in the absence of calcium and at high pH and low ionic strength only a small concentration of dissolved organic

matter result in a considerable error. In the presence of 0.01 M $CaCl_2$ and especially at low pH the error is negligible, even at the high end of the range of natural values of the dissolved organic matter.

Despite their ability, especially of the uncoupled model, to describe pH dependent ion binding over a large concentration and pH range with only a few adjustable parameters, the assumptions underlying the fully coupled and the uncoupled adsorption models are somewhat too simplistic and not fully physical sound. In our opinion a sound model for competitive metal ion binding should combine site competition with continuous, but non congruent affinity distributions and should take into account electrostatic effects. Thus far only analytical multi component binding equations for continuous heterogeneous ligand were known (to us) that were based on congruent affinity distributions. In the chapters 7 and 8 we go beyond the assumption of identical distributions and derive analytical equations that allow to take into account non congruent affinity distributions. In these chapters it is shown on the basis of model calculations that a non congruent heterogeneity highly influences the shape of the adsorption isotherms and the competition between different components. The intriguing results makes the application of the equations to experimental competitive binding data for humics an interesting future challenge.

Samenvatting

Eeuwenlang is het voorspellen van het eind der tijden voorbehouden geweest aan religieuze sekten. Thans zijn de milieuprofeten op dit werkterrein actief. Hoewel een deel van de milieuprofeten qua vreemde ideeën, uiterlijk en afwijkende leefgewoonten direct afkomstig lijken te zijn uit een archaïsche sekte, bevinden zich onder de profeten ook "fatsoenlijke" mensen zoals gerespecteerde wetenschappers en (veelal gepensioneerde) politici. Door het schrijven van rapporten en het voeren van acties en met steun van radio en tv, werd een ieder, eind jaren zestig en begin jaren zeventig, bewust gemaakt van het gevaar van pesticiden als DDT, van de beperkte energievoorraad, van luchtverontreiniging en van de slechte oppervlaktewaterkwaliteit. Gedurende de economische malaise van de eind zeventiger en begin tachtiger jaren nam de aandacht voor de milieuproblematiek wat af. Gifwijken, mest, zure regen en meer recent de CO_2 problematiek en het gat in de ozonlaag hebben er voor gezorgd dat thans de schrik er weer goed in zit.

Elk type samenleving produceert afval en beïnvloedt het leefmilieu, bijvoorbeeld door het bouwen van huizen en het beoefenen van landbouw, en heeft daarom te maken met milieuproblemen. Grote, en zeker de supra-nationale milieuproblemen kunnen niet los worden gezien van de maatschappelijke organisatie en duurzame oplossingen moeten vooraleer gevonden worden via politieke en diplomatieke wegen, dan via de wetenschap en technologie.

Uiteindelijk is er bij milieuverontreiniging altijd sprake van een verandering van de fysische en chemische eigenschappen van stoffen. Zowel om de risico's van stoffen in het milieu op verantwoorde wijze te kunnen analyseren als om nieuwe reinigingstechnieken te kunnen ontwikkelen, moet het gedrag van de stoffen in het natuurlijk milieu voldoende goed bekend zijn. Hoewel het onderzoek beschreven in dit proefschrift een fundamenteel karakter heeft en daarom niet direct gekoppeld is aan een bepaald milieuprobleem, poogt het bij te dragen aan het inzicht in het gedrag van verontreinigende stoffen en met name van zware metalen.

Zware metalen zoals bijvoorbeeld koper, cadmium, lood en zink komen in een groot aantal verontreinigde situaties voor. Denk hierbij aan

243

bodemverontreiniging en waterverontreiniging en aan haven- en zuiverings-slib. Een belangrijk aspect dat het gedrag van zware metalen bepaald, is de regulatie van de concentratie in de waterfase. In het algemeen zal een hoge concentratie in oplossing leiden tot een verhoogde mobiliteit van een stof en een verhoogde biologische beschikbaarheid.

De concentratie in oplossing wordt in hoge mate gereguleerd door bindingsprocessen aan vaste en colloïdale bestanddelen van het systeem. Tot deze bestanddelen behoren de humeuze verbindingen. Simpel gesteld zijn humeuze verbindingen organische verbindingen die na rottingsprocessen en secundaire synthese ontstaan zijn uit dierlijke en plantaardige materialen en die niet overeenkomen met uit de organische of biochemie bekende organische verbindingen. Humeuze verbindingen komen in allerlei type ecosystemen voor, variërend van bodems tot zoetwater- en zoutwatersystemen.

Vaak wordt een onderscheid gemaakt tussen verschillende fracties van de humeuze verbindingen. Deze fracties zijn operationeel gedefinieerd als fracties die na een bepaalde stap in een extractie schema overblijven. Zo lost bijvoorbeeld de fulvozuurfractie zowel op in loog als in zuur, terwijl de humuszuurfractie oplost in loog, doch neerslaat na aanzuren.

In dit proefschrift is onderzoek gedaan naar de binding van protonen en zware metaalionen aan humuszuren en fulvozuren. Ondanks een verschillend oplosgedrag wordt er in het algemeen vanuit gegaan dat de wijze waarop humus- en fulvozuren metaalionen binden sterk overeenkomen. Het vermogen van humuszuren[1] om metaalionen te binden ontstaat door de aanwezigheid van zogenaamde functionele groepen. Belangrijke functionele groepen zijn de zure carbonzuurgroepen en de fenolische groepen. De bindingseigenschappen van een functionele groep hangen af van het type groep en van de nabije chemische omgeving in het humusmolecuul. Iedere functionele groep heeft een eigen, intrinsieke affiniteitsconstante voor een bepaald ion. In humeuze verbindingen zijn verschillende type functionele groepen aanwezig en kan de chemische structuur sterk verschillen. Dit maakt

---

[1] voor het gemak spreken we van nu af aan slechts van humuszuren, in plaats van humus- en fulvozuren.

244

humuszuren heterogene liganden.

Door de chemische heterogeniteit kan de binding van een ion niet gekarakteriseerd worden door één bepaalde constante, maar moet een verdeling van affiniteitsconstanten gebruikt worden. Helaas is deze verdeling niet a priori bekend. Hoewel met behulp van spectroscopische technieken wellicht een indruk verkregen kan worden van het totaal aantal van de verschillende type groepen, geven deze technieken geen informatie over de chemische affiniteitsverdeling.

Doordat de meeste functionele groepen een zuur/base gedrag vertonen wordt de toestand van de functionele groepen sterk door de pH bepaald. Bij lage pH, pH<2, zijn functionele groepen vrijwel volledig geprotoneerd en is de negatieve lading van de humuszuren klein. In natuurlijke systemen is de pH hoger dan twee en zijn een groot aantal groepen gedissocieerd waardoor de humuszuren een pH afhankelijke negatieve lading hebben. Doordat positieve ionen door het negatieve elektrische veld aangetrokken worden is de concentratie van de positieve metaalionen vlakbij de functionele lading groter dan in de bulk van de oplossing. De metaalbinding wordt hierdoor bevorderd. De mate waarin de binding beïnvloed wordt, hangt af van de sterkte van het elektrische veld.

Evenals de chemische heterogeniteit zijn de electrostatische effecten onbekend, kunnen ze per humuszuurmonster sterk verschillen en zijn ze niet direct experimenteel te bepalen. Omdat de chemische heterogeniteit en de electrostatische effecten van belang zijn voor metaalion-binding is in dit proefschrift een methode ontwikkeld om humuszuren ten aanzien van deze factoren te karakteriseren. Deze methode is de zogenaamde *mastercurve*-methode, die in de hoofdstukken 2-4 besproken wordt. In het introducerende hoofdstuk dat hieraan vooraf gaat worden de geochemie en de eigenschappen van humuszuren in een breder perspectief gezet.

Feitelijk is de mastercurve methode een analyse van een reeks protonbindingscurven gemeten bij verschillende zoutsterkten, elk uitgedrukt als lading Q als functie van de pH. Als er naast protonen geen andere ionen aanwezig zijn die specifiek aan de functionele groepen binden, dan is protonbinding een monocomponent bindingsproces. De mate van protonering

wordt bepaald door de chemische heterogeniteit en de pH vlakbij de functionele groepen, op de plaats waar de binding plaats vindt. Deze pH noemen we pH_S. De pH_S hangt af van de pH in de bulk van de oplossing en van de elektrische potentiaal op de plaats van binding. De elektrische potentiaal is een maat voor de sterkte van het elektrische veld, en zijn waarde hangt af van de lading Q van de humuszuren, van eigenschappen van humusmoleculen zoals vorm, rigiditeit, en permeabiliteit en van de zoutsterkte en samenstelling van de oplossing.

Bij een hoge zoutsterkte is de concentratie van de ionen in oplossing hoog en wordt het elektrisch veld goed afgeschermd. De electrostatische effecten zijn dan klein en de dubbellaag, de laag waarin de concentratie van de ionen afwijkt van die in de bulk, is dun. Bij lage zoutsterkte geldt het tegenovergestelde, de electrostatische effecten zijn groot en de dubbellaag is dik. De afhankelijkheid van de electrostatische effecten van de zoutsterkte heeft een zoutsterkte afhankelijke protonbinding als gevolg.

Doordat de elektrische potentiaal niet experimenteel bepaald kan worden moet er gebruikt gemaakt worden van dubbellaagmodellen om deze potentiaal te berekenen. In de mastercurve methode kan in principe elk dubbellaagmodel gebruikt worden dat de potentiaal kan berekenen uit de lading Q en de zoutsterkte, zonder dat er aannames nodig zijn ten aanzien van de chemische heterogeniteit.

Met behulp van een gekozen dubbellaagmodel kan pH_S berekend worden en kunnen de experimentele data weergegeven worden als functie van deze pH op de plaats waar de binding plaats vindt. Doordat in pH_S gecorrigeerd is voor de electrostatische effecten mogen de $Q(pH_S)$ curven geen zoutafhankelijkheid meer vertonen en moeten ze samenvallen in een mastercurve. Indien de $Q(pH_S)$ curven nog steeds een duidelijke zout-afhankelijkheid vertonen, dan voldoet het gekozen dubbellaagmodel kennelijk niet en moet het aangepast worden.

De zoutafhankelijkheid van 11 verschillende humus- en fulvozuren bleek redelijk goed beschreven te kunnen worden door gebruik te maken van een dubbellaagmodel voor harde bollen of cilinders. In beide modellen worden humus deeltjes beschouwd als rigide en niet permeabele deeltjes die

246

gekarakteriseerd worden door een bepaalde gemiddelde straal. Deze straal bepaald de kromming van het oppervlak, en de kromming bepaald mede de sterkte van het elektrische veld. Des te groter de straal, des te kleiner de kromming, en des te groter de electrostatische effecten.

In de gebruikte dubbellaagmodellen wordt de elektrische potentiaal gerelateerd aan de lading van het deeltje, uitgedrukt per m^2 deeltjes oppervlak. De experimenteel gemeten lading, Q is uitgedrukt per gram humuszuur. Om Q om te rekenen in een oppervlakte ladingsdichtheid is het specifiek oppervlak nodig. Voor bolletjes en cilinders is het specifiek oppervlak gerelateerd aan de dichtheid van de humuszuren en de straal van de deeltjes. Omdat humuszuren beschouwd worden als rigide en niet permeabele deeltjes, is het logisch om aan te nemen dat de hoeveelheid water in het molecuul beperkt is. We beschouwen de situatie dat er op gewichtsbasis evenveel water als humuszuur in het volume van een humus-deeltje aanwezig is als een uiterste limiet. Onder deze aanname varieert de dichtheid van humuszuren, uitgedrukt als massa van het humusmateriaal per volume van de deeltjes van 700 tot 1700 kg/m^3. Doordat de mastercurven die voor deze dichtheden gevonden niet sterk verschillen, gebruiken we een dichtheid van 1000 kg/m^3 als een gemiddelde waarde. De straal is dan dus de enige overgebleven aanpasbare parameter in de mastercurve methode.

Voor het dubbellaagmodel voor de harde bollen varieert de gevonden straal voor de 11 onderzochte humus- en fulvozuren van 0.6 tot 4.4 nm, met r=0.85 nm als mediaan. De grootte en het volume van een bolletje wordt volledig door de grootte van de straal bepaald. Met behulp van de straal en de dichtheid kan het moleculgewicht van de humuszuren berekend worden. Voor de geanalyseerde humuszuren varieerde dit zogenaamde electro-statische moleculgewicht van 545 tot 215000, met 1550 als mediaan. De gevonden waarden zijn niet irrealistisch, doch wat kleiner dan de waarden die met behulp van andere technieken gevonden worden.

De grootte van een cilinder wordt bepaald door zijn straal en lengte. In het electrostatische model worden de effecten van de uiteinden van de cilinders verwaarloosd en enkel de straal is de parameter die de grootte van de electrostatische interacties bepaald. In principe mag de lengte van de

cilinders dus sterk verschillen voor de verschillende humusdeeltjes en is het niet noodzakelijk om aan te nemen dat de deeltjes een identieke grootte hebben.

De gevonden stralen voor het cilindrisch dubbellaagmodel variëren van 0.19 tot 2.5 nm, met r=0.32 nm als mediaan. Dat deze stralen kleiner zijn dan die voor het harde bol model komt door het verschil in kromming van het deeltjes oppervlak. Bij een gelijke straal is de kromming van het oppervlak van een cilinder kleiner dan die van een bol. Hierdoor zijn de electrostatische effecten voor de cilinder groter. Doordat echter de grootte van de electrostatische effecten vastgelegd zijn door het experiment, moet de straal van een cilinder kleiner zijn dan de straal van een bol om het benodigde van electrostatische effect te verkrijgen.

De dimensies van de humusdeeltjes die volgen uit het toepassen van de dubbellaagmodellen wijzen erop dat gezuiverde humuszuren redelijk kleine moleculen zijn met een beperkt aantal functionele groepen. Het zijn eerder oligo-electrolieten dan poly-electrolieten. Uit de analyse van protonbindingsgegevens volgt geen voorkeur voor het harde bolletje of cilindermodel. Het cilindermodel komt iets beter overeen met het beeld dat humuszuren flexibele lineaire (poly)electrolieten zijn, een beeld dat aangehangen wordt door vele onderzoeksgroepen. Het harde bolletjesmodel heeft als voordeel dat het berekenen van een molecuulgewicht mogelijk is.

Doordat humuszuren polydisperse mengsels zijn van verschillende organische verbindingen is het beschouwen van humuszuren als rigide en niet permeabele deeltjes met een simpele geometrie die gekarakteriseerd wordt door 1 gemiddelde straal een grove benadering. Desalniettemin geeft deze eerste orde benadering een verrassend goede beschrijving van het zoutsterkte effect van protonbindingscurven. Polydispersiteit en andere effecten zoals veranderingen van de conformatie van humusdeeltjes en aggregatieverschijnselen blijken bij protonbinding slechts tweede orde effecten te zijn.

Doordat de electrostatische effecten weggefiltreerd zijn is de vorm van de $Q(pH_s)$ mastercurven direct gerelateerd aan de chemische heterogeniteit ofwel de intrinsieke affiniteitsverdeling. Er zijn verschillende technieken

beschikbaar waarmee de affiniteitsverdeling verkregen kan worden uit een bindingscurve. Iedere techniek heeft zijn voor- en nadelen. De techniek die gebruikt kan worden hangt in grote mate af van de kwaliteit van de experimentele gegevens. Experimentele fouten kunnen namelijk een groot effect hebben op de gevonden affiniteitsverdeling. De methode die het minst gevoelig is voor de experimentele fouten is de condensatie approximatie (CA) methode in combinatie met een smoothing spline techniek waarin de smoothingsparameter bepaald wordt door gebruikt te maken van de "generalised cross validation" (GCV) techniek in combinatie met enkele (fysische) randvoorwaarden. De smoothing spline procedure wordt gebruikt om de meest waarschijnlijke mastercurve door de $Q(pH_s)$ datapunten te bepalen. De affiniteitsverdeling die volgt uit de CA methode is evenredig met de eerste afgeleide van de met de spline bepaalde mastercurve.

De voor de 11 verschillende humus- en fulvozuren gevonden affini- teitsverdelingen vertonen veel overeenkomsten. Allen worden ze gekarakteriseerd door een grote en relatief brede piek met een piek positie tussen log K=3 en 4. In het algemeen zijn de pieken die verkregen worden voor de mastercurven voor het harde bolletjes dubbellaagmodel iets smaller en is de piek iets verschoven naar lagere log K waarden, dan de verdelingen die verkregen worden voor de cilinders. De affiniteitsverdelingen van monsters die getitreerd zijn over een groter pH traject (tot aan pH=11) wijzen op de aanwezigheid van een tweede bredere piek met een piekpositie voor log K>8.

De gevonden affiniteitsverdelingen kunnen gebruikt worden bij het kiezen van een geschikt model voor de beschrijving van de protonbinding. De verdelingen illustreren duidelijk dat humuszuren heterogene liganden zijn. In plaats van smalle en goed gescheiden pieken vertonen de verdelingen een geleidelijke en continue verandering van de affiniteit. Vanwege deze resultaten verkiezen we een beschrijving waarin uitgegaan wordt van een continue heterogeniteit boven een beschrijving die uitgaat van een discrete heterogeniteit.

Slechts een beperkt aantal analytische vergelijkingen voor continue heterogene liganden zijn bekend. Drie bekende vergelijkingen zijn de

Langmuir-Freundlich-vergelijking (LF), de Generalised-Freundlich-vergelijking (GF) en de Tóth-vergelijking. De onderliggende affiniteitsverdelingen van deze drie vergelijkingen verschillen sterk. De LF verdeling is een pseudo Gaussische, symmetrische verdeling, de GF verdeling is een exponentiële verdeling met een hoge-affiniteitsstaart en de Tóth verdeling is asymmetrisch en heeft een lage-affiniteitsstaart. Alle drie verdelingen worden gekarakteriseerd door één piek. Als de CA verdeling twee pieken vertoond, dan wordt in de beschrijving van de $Q(pH_s)$ gebruikt gemaakt van een sommatie van twee bindingsvergelijkingen. Ondanks het feit dat alle drie de vergelijking de $Q(pH_s)$ data redelijk goed beschrijven geven de LF- en de Tóth-vergelijking een iets beter resultaat dan de GF-vergelijking.

Een combinatie van de gevonden bindingsvergelijking met het dubbellaagmodel geeft een model voor de experimentele protonbinding. Doordat we in staat zijn zowel de electrostatische effecten als de $Q(pH_s)$ data redelijk goed te beschrijven, is het niet verwonderlijk dat het gecombineerde model een goede beschrijving van de experimentele gegevens geeft.

Doordat protonen in waterige systemen per definitie aanwezig zijn en doordat protonen specifiek aan de humuszuren binden is metaalbinding minimaal een twee component bindingsproces. Naast de reeds genoemde electrostatische effecten en de chemische heterogeniteit zal in modellen die metaalbinding beschrijven voor een reeks verschillende condities met betrekking tot pH, zoutsterkte en samenstelling van de oplossing, expliciet rekening moeten worden gehouden met de wijze waarop de protonbinding en de metaalbinding elkaar wederzijds beïnvloeden. Helaas is het niet mogelijk om metaalbinding te beschrijven zonder min of meer arbitraire aannamen ten aanzien van de formulering van de metaalbindingsvergelijking en de wijze waarop de verschillende ionen met elkaar in competitie zijn. Als gevolg hiervan zijn er een groot aantal verschillende modelbeschrijvingen voorgesteld in de literatuur. Geen enkele benadering kan vooralsnog beschouwd worden als het goede model voor de beschrijving voor metaalbinding aan humuszuren.

In onze benadering vormt het model voor de protonbinding de basis voor de beschrijving van de metaalbinding. In het protonmodel worden de

electrostatische effecten beschreven met behulp van een dubbellaagmodel voor harde bollen en cilinders, terwijl de chemische heterogeniteit wordt meegenomen door gebruik te maken van analytische bindingsvergelijkingen voor liganden met een continue heterogeniteit. Een belangrijk voordeel van deze vergelijkingen is dat ze slechts weinig aanpasbare parameters hebben en dat de heterogeniteit op elegante wijze in rekening wordt gebracht.

In de modelbeschrijving voor de metaalbinding is nagegaan in hoeverre het model voor de protonbinding op eenvoudige wijze kon worden uitgebreid. We hebben hierbij zowel gebruik gemaakt van de Langmuir-Freundlich-vergelijking en de Tóth-vergelijking in combinatie met het dubbellaagmodel voor harde bollen. Het blijkt dat beide vergelijkingen de binding even goed kunnen beschrijven, en dat de resultaten sterk overeen-komen met de resultaten die gevonden worden als de vergelijkingen gecombineerd worden met het dubbellaagmodel voor cilinders. De resultaten voor het cilindrische dubbellaagmodel worden echter niet gepresenteerd. De GF-vergelijking is buiten beschouwing gelaten, omdat deze vergelijking een iets minder goede beschrijving van de protonbinding geeft.

Om de metaalbinding te kunnen beschrijven kiezen we een benaderende metaalbindingsvergelijking waar bij binding van 1 metaalion x protonen vrijkomen. Deze parameter x kan een gebroken waarde hebben.

Met betrekking tot de relatie tussen het proton en de metaalionen maken we onderscheid tussen *ontkoppelde* adsorptie en *volledig gekoppelde* adsorptie, twee uitersten. Bij het volledig gekoppelde model binden protonen en metaalionen aan dezelfde groepen en hebben ze een congruente affiniteitsverdeling. Dit houdt in dat de verdelingen exact dezelfde vorm hebben. De positie van de verdeling op de affiniteits-as kan echter verschillen. Onder deze randvoorwaarden zijn er analytische vergelijkingen voor multi-componentbinding aan liganden met een continue heterogeniteit bekend.

In het ontkoppelde model hebben metaalionen en protonen hun eigen bindingsplaatsen, die kwa aantal groepen als kwa chemische heterogeniteit mogen verschillen. Doordat er verschillende bindingsplaatsen zijn is er geen directe "site"-competitie en kan zowel protonbinding als metaalbinding

beschreven worden met monocomponent bindingsvergelijkingen voor liganden met een continue heterogeniteit. De competitie tussen de protonbinding en de metaalbinding wordt bepaald door de waarde van de parameter x en de electrostatische effecten. In afwezigheid van metaalionen hebben de humuszuren een pH afhankelijke negatieve lading. Als de waarde van x kleiner is dan de valentie van het metaalion, dan leidt metaalbinding tot een afname van de negatieve lading. Dit leidt tot daling van de potentiaal, hetgeen een extra vrijkomen van protonen als gevolg heeft. Naast het vrijkomen van protonen door de bindingsvergelijking en de electrostatica komen in het volledig gekoppelde model ook nog protonen vrij als gevolg van de competitie.

In hoofdstuk 5 worden het volledig gekoppelde en het ontkoppelde model gebruikt om cadmiumbinding aan een humuszuur, afkomstig uit een veengrond, te beschrijven. De cadmiumbinding is gemeten bij drie pH waarden en voor cadmiumconcentraties die varieerden tussen $\log Cd=-10$ tot $\log Cd=-3$.

In het volledig gekoppelde model kon de cadmiumbinding over het gehele cadmiumconcentratietraject slechts beschreven worden door aan te nemen dat een klein aantal groepen (circa 1 %) een hogere affiniteit heeft dan de bulk van de groepen. Deze hoge-affiniteitsgroepen bepalen de binding voor de zeer lage cadmiumconcentraties. Hoewel het concept van een klein aantal groepen met een hoge affiniteit niet irrealistisch is en door velen geaccepteerd wordt, is het geen elegante model aanpak, daar het leidt tot een relatief sterke toename in het aantal aanpasbare parameters.

Met het ontkoppelde model zijn we in staat de pH afhankelijke binding te beschrijven voor het gehele cadmiumconcentratie traject met slechts vier aanpasbare parameters. Deze parameters zijn respectievelijk: de parameter x, het adsorptiemaximum voor de cadmiumbinding, de mediane log K waarde en de breedte van de affiniteitsverdeling, alle horende bij de gebruikte adsorptievergelijking.

In de monocomponent-vergelijkingen is de metaalbinding slechts een functie van de verhouding M_s/H_s^x, hetgeen inhoudt dat in het ontkoppelde model de metaalbindingscurven samenvallen in een mastercurve als ze

252

uitgezet worden als functie van deze verhouding $M_S/H_S{}^x$. De variabelen M_S en H_S zijn respectievelijk de metaalion en de protonconcentratie nabij de functionele groepen op de plaats van de metaalbinding, en kunnen berekend worden als de potentiaal nabij de groepen bekend is. Deze potentiaal volgt uit de lading en het dubbellaagmodel. De lading volgt uit de initiële lading (in afwezigheid van metaalionen), de mate van de metaalbinding en het gemeten aantal protonen dat vrijkomt door metaalbinding. Door een mastercurve voor metaalbinding te construeren wordt de waarde van x direct gevonden, terwijl de andere 3 parameters verkregen worden door het aanpassen van de bindingsvergelijking aan de mastercurve.

Naast de protonen zijn er zowel in natuurlijke als in verontreinigde ecosystemen, andere ionen aanwezig die specifiek aan de humuszuren binden. De cadmiumbinding wordt hierdoor beïnvloed. Een belangrijk ion in dit opzicht is calcium. Om het effect van calcium op de cadmiumbinding te kunnen beschrijven moet eerst de binding van calcium bekend zijn. In hoofdstuk 6 worden calciumbindingsgegevens aan een humuszuur afkomstig uit de veengrond gepresenteerd en geanalyseerd. Het gebruikte humuszuur is identiek aan het humuszuur dat in hoofdstuk 5 is gebruikt om de cadmiumbinding te bestuderen.

Een vergelijking van de bindingsgegevens laat zien dat cadmium sterker aan het humuszuur bindt dan calcium en dat de pH-afhankelijkheid van de cadmiumbinding groter is. Voor het beschrijven van de calciumbinding hebben we alleen gebruikt gemaakt van het ontkoppelde model en de LF-vergelijking. Dit resulteerde wederom in een goede beschrijving van de pH-afhankelijke binding voor het gehele concentratiegebied.

Omdat de eigenschappen van calcium- en cadmiumionen sterk overeenkomen ligt het voor de hand om aan te nemen dat beide ionen binden aan dezelfde bindingsplaatsen. Het feit dat de gevonden adsorptie maxima en de breedte van de affiniteitsverdeling voor beide ionen sterk overeenkomen ondersteunt dit idee. Doordat de calciumgegevens redelijk goed beschreven kunnen worden indien de breedte en het adsorptiemaximum voor de cadmiumgegevens gebruikt worden, lijkt een

beschrijving van de competitie tussen calcium en cadmium op basis van multi-component-vergelijkingen voor congruente verdelingen een goede eerste benadering. Helaas is de bruikbaarheid van dit model nog niet getoetst aan experimentele bindingsgegevens, en is het slechts gebruikt voor enkele modelberekeningen.

Over het algemeen is cadmium, zelfs in verontreinigde situaties, in zeer lage concentraties aanwezig in de bodemoplossing. Uit de modelberekeningen blijkt dat bij deze lage concentraties de cadmiumbinding beschreven kan worden met simpele Freundlich- of zelfs met lineaire bindingsvergelijkingen. Dit geldt zowel in systemen waar geen calcium aanwezig is, als in systemen waar wel calcium aanwezig is. Tevens blijkt uit de berekeningen dat de coëfficiënten van deze vergelijkingen sterk conditioneel zijn en op een gecompliceerde wijze afhangen van milieucondities als pH, zoutsterkte en calciumconcentratie.

Hoewel calcium veel minder sterk bindt dan cadmium, is de calciumconcentratie in het algemeen veel groter dan de cadmiumconcentratie. Als gevolg hiervan is calcium een relatief sterke competitor voor cadmiumbinding en neemt de cadmiumbinding als gevolg van deze competitie sterk af na toevoeging van 0.01 M $CaCl_2$. Doordat de afname van cadmiumbinding verder versterkt wordt door de vorming van cadmium-chloride-complexen in oplossing is een 0.01 M $CaCl_2$ oplossing een effectief extractiemiddel voor cadmium. De berekeningen illustreren tevens dat de fractie die met een 0.01 M $CaCl_2$ oplossing geëxtraheerd kan worden niet constant is, maar afhangt van de condities van het systeem. Hoewel de extraheerbare fractie een indicatie kan geven van het deel van de geadsorbeerde metaalionen dat eenvoudig omgewisseld kan worden, en daardoor een beeld geeft van de biologische beschikbaarheid, maakt de conditionele efficiëntie een gedetailleerde en mechanistische interpretatie zeer complex.

Het grootste deel van de organische stof in de bodem behoort tot de vaste fase. Een klein deel is echter opgelost in de waterfase. De binding aan deze opgeloste organische stof bemoeilijkt de interpretatie van experimenten waarmee de adsorptie-isotherm van een metaalion aan de vaste fase van de

bodem bepaald wordt. Over het algemeen wordt in schudexperimenten aangenomen dat de cadmium in de vloeistoffase aanwezig is als het *vrije* cadmiumion en als anorganische complexen. De binding aan de opgeloste organische stof wordt verwaarloosd en de vrije cadmiumconcentratie wordt uitgerekend met behulp van chemische evenwichtsberekeningen. Het ontwikkelde model voor competitieve binding vormt een goede basis om de grootte van de fout in de vrije cadmiumconcentratie die ontstaat door het verwaarlozen van de binding aan de opgeloste organische stof af te schatten. Het model voorspelt dat, als calcium niet aanwezig is, de binding aan de opgeloste organische stof leidt tot een significante fout, zelfs bij relatief lage gehaltes aan opgeloste organische stof. In de aanwezigheid van 0.01 M CaCl$_2$ daarentegen is de binding zelfs bij hoge concentraties onbelangrijk.

Ondanks de mogelijkheid, met name van het ontkoppelde model, om de pH-afhankelijke ionbinding te beschrijven voor een groot concentratietraject met slechts weinig parameters, zijn de aannamen van zowel het ontkoppelde als het volledig gekoppelde model te simplistisch. In een, naar onze mening, beter en meer realistisch model voor competitieve ionbinding zou uitgegaan moeten worden van "site"-competitie in combinatie met niet-congruente verdelingen. Tot nu toe waren (ons) slechts analytische vergelijkingen bekend waarin uitgegaan werd van congruente verdelingen. In de hoofdstukken 7 en 8 gaan we een stap verder en leiden we analytische multi-componentvergelijkingen af voor niet-congruente verdelingen. In genoemde hoofdstukken wordt op basis van modelberekeningen aangetoond dat de niet-congruente verdelingen sterk de vorm van de isothermen en de competitie tussen de verschillende componenten beïnvloeden. De intrigerende resultaten maken het toepassen van deze vergelijken op experimentele gegevens een interessante uitdaging voor de nabije toekomst.

Levensloop

Han de Wit werd geboren op 30 september 1962 in Gouda. Na het doorlopen van het VWO aan het Christelijk Lyceum-Havo te Gouda begon hij in 1980 met een studie milieuhygiëne aan de Landbouwuniversiteit te Wageningen. In 1987 rondde hij deze studie af met als afstudeervakken bodemverontreiniging, bodemscheikunde, en natuurbeheer.

Vanaf april 1987 tot september 1992 werkte hij bij de vakgroep Bodemkunde en Plantevoeding van de Landbouwuniversiteit. Gedurende deze periode deed hij onderzoek naar de binding van metaalionen aan bodembestanddelen, zoals de bodem organische stof. De belangrijkste resultaten van dit onderzoek zijn in dit proefschrift weergegeven.

Sinds september 1992 is hij werkzaam bij TAUW Infraconsult, een ingenieursbureau te Deventer.